ABSTRACT

BALTZEGAR, DAVID ANDREW. Investigation of Novel Paracellular and Endocrine Mechanisms Governing Osmotic Balance in Teleost Fishes (Actinopterygii: Teleostei). (Under the direction of Dr. Russell J Borski).

Hydromineral balance is critical to survival of all organisms. Euryhaline teleosts are capable of surviving wide fluctuations in salinity by rapidly altering the abundance and direction of ion transport within the gill epithelium to achieve a balance of osmotic forces. While the Mitochondrion-Rich Cell (MRC) or cloride cell, is a well-studied system, supporting elements critical to proper MRC function and restoration to homeostasis remain to be identified. Here we describe research into two novel areas governing osmoregulatory physiology in teleost fishes: the claudin gene family, involved in the paracellular movement of water and ions, and leptin, a 16kD cytokine that mobilizes carbohydrate energy during acute periods of osmotic stress.

Claudins, a family of tight junction proteins, are the principal determinants of ion and water permeability between cells via paracellular transport. We investigated three claudins in the euryhaline tilapia (*Oreochromis mossambicus*) during both acute and long-term salinity transfer: Claudin 3c (*Omcldn3c*), Claudin 28a (*Omcldn28a*) and Claudin 30 (*Omcldn30*). In both short and long-term salinity acclimation, gill *Omcldn3c* mRNA expression was significantly higher in FW-acclimated fish. Gill *Omcldn28a* and *Omcldn30* were significantly higher in FW-acclimated fish after 7 days, but not in long-term acclimated fish. Tilapia claudin mRNA expression was localized to pavement cells of the gill epithelium using *in situ* hybridization, but expression was not prevalent in MRC-rich regions. These

studies are the first to show gill claudin mRNA is regulated by environmental salinity, and may act to decrease water and ion permeability during FW adaptation.

Claudin gene diversity remains poorly described in teleost fishes, and comparative studies are hindered by poor descriptions of homology. Despite the prominence of the zebrafish (*Danio rerio*) as a vertebrate developmental model, the full complement of claudins for this species remains unknown. Using the current genomic assembly along with predicted gene sequences (NCBI), we describe 54 zebrafish claudins, of which 24 were previously uncharacterized. Seven zebrafish claudins appear unique, possibly the result of gene duplication or loss in other lineages. Using large-scale phylogenetic analysis, supported with evidence of genomic synteny, we inferred the homology of these claudins to those of other vertebrate groups. The mRNA of these claudins was examined in cDNA from 8 tissues, with nearly all claudin paralogs possessing unique expression profiles.

Leptin is a 16kD cytokine hormone inducing anorexigenic effects on feeding in mammals. As an *adipostat*, leptin acts with insulin to regulate glucose and triglyceride metabolism in mammals. Here, we describe the molecular sequence of a leptin ortholog (*lepa*) and its putative receptor (*lepr*) in the Mozambique tilapia, and examine mRNA expression (in the gill and liver) during salinity transfer. Gill *lepa* mRNA expression appears consistent with pleitropic actions as a local growth factor. Hepatic mRNA expression of *lepa* and *lepr* were significantly upregulated within 4 hours of transfer to 2/3 seawater (25 ppt), but were not

responsive to freshwater challenge. We hypothesized leptin may function to mobilize energy reserves during periods of acute hyperosmotic stress.

We then examined the effects of acute SW transfer, along with exogenous administration of recombinant leptin(s) or cortisol, upon key blood metabolites and hepatic energy reserves in tilapia. Our combined findings suggest two mechanisms of glucose mobilization occur during acute hyperosmotic stress: (1) hepatic glycogenolysis induced by the actions of leptin, and (2) cortisol-mediated gluconeogenesis of amino acids in the liver. We proposed a unified model of energy mobilization linking both new and historical observations of carbohydrate and lipid metabolism during salinity adaptation. These studies were the first to show leptin is sensitive to osmotic perturbations, and may act to mobilize glucose during periods of acute hyperosmotic stress.

Investigation of Novel Paracellular and Endocrine Mechanisms Governing Osmotic Balance in Teleost Fishes (Actinopterygii: Teleostei)

by
David Andrew Baltzegar

A dissertation submitted to the Graduate Faculty of
North Carolina State University
in partial fulfillment of the
requirements for the degree of
Doctor of Philosophy

Zoology

Raleigh, North Carolina

2013

APPROVED BY:

_____	_____
Dr. Russell J. Borski Committee Chair	Dr. Craig V. Sullivan
_____	_____
Dr. John Godwin	Dr. Christopher Ashwell

DEDICATION

I dedicate this dissertation to my wife Jennifer, who above all else, was the most determined to see it to fruition. *Babe, we did it.*

BIOGRAPHY

David Andrew Baltzegar was born in Augusta, GA in 1977, the only son of Russell Baltzegar and Marta Bradford. He grew up in Edgefield County, SC and attended high school in North Augusta, SC. He attended the College of Charleston in 1995, and graduated with a Bachelor of Science in Marine Biology in 2000. In 2002, he returned to Charleston and received a Master of Science (Marine Biology) in 2006 under the direction of Dr. Robert Chapman. While working on his Master's thesis, he met both his wife (Jennifer Fountain Baltzegar) and his current advisor, Dr. Russell Borski, who was there on sabbatical. Following completion of his degree, he joined the lab of Dr. Borski at NC State. Upon completion of his PhD, David will explore career options through the North Carolina Biotechnology Center Industrial Fellowship Program.

ACKNOWLEDGMENTS

I wish to thank my committee members for their help and constructive advice, both in the development of this work, and also for the mentorship and training in practice of scientific methodology. I especially wish to thank my major advisor, Dr. Russell Borski, in this endeavor. Under his tutelage, I had the privilege to attend the Pawley Summer Research Program in Hawaii, and present elements of this work in national and international meetings. Above all else, he has shown me that being a successful scientist is much like owning and operating a small business, for one must wear all hats. After many years as a student, this was the final lesson.

I wish to thank present and past members of the Borski, Sullivan, and Godwin labs for their help and advice: Dr. Matthew Picha, Dr. Benjamin Reading, Dr. Miller Johnstone III, Dr. Eugene Won, Jonathon Douros, Jamie Mankiewicz, Melissa Slane, Scott Salger, and Valerie Williams. I wish you the best in all things to come.

I also wish to thank those who are responsible for the maintenance and care of our research animals: Brad Ring, John Davis, and Dr. Andrew McGinty. Without your help and diligence, none of this work would be possible.

Last, I wish to thank my wife Jennifer, and my parents Russell and Marty, for their enduring love and support.

TABLE OF CONTENTS

LIST OF TABLES

Page

APPENDIX B.

APPENDIX C.

LIST OF FIGURES

Page

CHAPTER I.

CHAPTER II.

CHAPTER III.

CHAPTER IV.

APPENDIX A.

APPENDIX B.

APPENDIX C.

CHAPTER I

Regulation of Claudin mRNA During Salinity Adaptation in the Euryhaline Mozambique Tilapia (*Oreochromis mossambicus*)[1]

[1] This chapter is being prepared for submission as the following publication: Baltzegar, D.A., Ozden, O., Brune, E.S., and R.J. Borski (2013). Regulation of claudin mRNA during salinity adaptation in the euryhaline Mozambique tilapia (*Oreochromis mossambicus*). (Manuscript in Preparation)

Abstract

The aim of this study was assess the function of teleost claudin 3 and claudin 4-related proteins during salinity adaptation in euryhaline tilapia (*Oreochromis mossambicus*). The expression of 3 claudins, *Omcldn3c*, *Omcldn28a*, and *Omcldn30* were examined during salinity transfer and localized within the gill epithelium. Evolutionary homology was determined by Bayesian phylogeny: *Omcldn3c* is likely homologous to mammalian claudin 3, while *Omcldn28a* and *Omcldn30* are identifiable homologs of claudin 4. Gene expression was examined in tissues after long-term acclimation to freshwater (FW) or 2/3 seawater (SW). Acute regulation was examined in the gill and posterior intestine during 1, 4, and 7 days of FW and SW challenge. *Omcldn3c* mRNA was significantly lower in the gill of long-term SW fish, and expression decreased in gill and posterior intestine of SW-challenged fish. *Omcldn28a* mRNA was significantly higher in gills of long-term acclimated SW fish, but did not change with SW challenge. Gill expression of *Omcldn28a* increased at day 7 of FW challenge and differed little from sham fish at other time points of challenge. Expression of *Omcldn28a* was not detected in the posterior intestine. Gill *Omcldn30* mRNA expression was higher in FW-challenged fish (7 days), but not different between long-term FW or SW acclimated fish. No effect of salinity was observed on *Omcldn30* transcript levels in the posterior intestine. Claudin mRNA in the gill was examined by *in situ* hybridization and colocalized to Na^+, K^+–ATPase immunostaining. All claudins were expressed abundantly in intermediate or pavement cell layers, but not to populations of ionocytes. Our results suggest *Omcldn3c* and *Omcldn28a* do not form leaky tight junctions characteristic of seawater adaptation, but instead act to confer reduced permeability in the FW environment.

Introduction

The reversal of ion transport modes to achieve hydromineral balance is a critical factor in the survival of euryhaline fishes (Evans *et al.*, 2005). Traditionally, osmoregulatory studies have largely focused upon dynamic mechanisms of transcellular transport in gill Mitochondrial Rich Cells (MRCs), which are dispersed on the filament and lamellae surface (Evans *et al.*, 2005). Recent studies have shown that paracellular transport, the movement of water and small solutes between cells, may also contribute significantly to the permeability of gill epithelia, particularly in pavement cells (PVC), which comprise 90% of the gill surface epithelium (McCormick, 2001; Tipsmark *et al.*, 2008a). Paracellular transport is largely regulated by the diversity of claudin proteins, the dominant constituent of epithelial tight junctions (Angelow and Yu, 2007; Van Itallie and Anderson, 2006).

Marine teleosts must actively drink seawater (SW) to counter passive water loss, acquiring an obligatory salt load that is then extruded from the gill (McCormick, 2001). This excretion occurs in gill MRCs, and also through leaky tight junctions associated with Accessory Cells (AC). Monovalent ion transport is driven by abundant Na^+-K^+-ATPase, which is colocalized with K^+ channels and Na^+-K^+-$2Cl^-$ cotransporters in the basolateral membrane of the MRC (Evans *et al.*, 2005). This generates localized concentrations of Cl^- and Na^+ within the MRC and the MRC-AC paracellular space, respectively. By the prevailing model, chloride ions exit the MRC through apical channels, and sodium is excreted by electrochemical diffusion across leaky MRC-AC tight junctions (Evans, 1999; Evans *et al.*, 2005). In contrast, freshwater teleosts must actively acquire sodium and chloride ions through the gill to counter

diffusional ion loss in hypo-osmotic environments (McCormick, 2001). Active uptake is thought to be coupled with H^+/HCO_3^- exchange through apical channels of a freshwater-type MRC (for review, see Evans *et al.*, 2005).

Although less studied, evidence suggests that paracellular permeability within the gill integument may play a significant role in hydromineral balance. In the euryhaline eel (*Anguilla anguilla*), SW-acclimated fish exhibit greater levels of water influx when placed in FW than do FW-acclimated fish, yet water loss (serosal to mucosal) is reduced (Isaia and Hirano, 1976). This polarization could be explained, in part, by changes in aquaporin levels within discrete cells or layers of the gill epithelium, or from changes in paracellular permeability (Chasiotis *et al.*, 2012a; Cutler and Cramb, 2002; Cutler *et al.*, 2007; Evans, 1999). In *Fundulus heteroclitus*, rapid changes in the formation of MRC-PVC and PVC-PVC tight junctions were observed with changes in the salinity of the membrane-bathing medium (Karnaky, 1991; Marshall *et al.*, 1997).

The thickness or relative "tightness" of epithelial tight junctions are governed by the constituent transmembrane proteins. Claudins, a diverse protein family containing two extracellular loops (ECL1 and ECL2), are the main determinants of barrier formation in tight junctions (Angelow and Yu, 2007; Van Itallie and Anderson, 2006). The ECL1 domain interacts across the extracellular space with claudins of an opposing cell to form a hydrophobic barrier or semi-selective ion pore (Krause *et al.*, 2008; Krause *et al.*, 2009; Van Itallie and Anderson, 2006).

As different claudins possess unique properties, both the abundance and *species* of claudin proteins present may influence the permeability of cellular tight junctions (Angelow *et al.*, 2008). Claudin proteins exhibit relatively short-half lives (hours; Van Itallie *et al.*, 2004), which is consistent with dynamic regulation of gill tight junctions that occur with salinity adaptation in *F. heteroclitus*. This suggests that claudins within gill epithelial tight junctions are dynamically responsive to fluctuations in environmental salinity and may form part of the adaptive response. Recent examination of teleost genomes has revealed a large expansion of the claudin gene family, with 56 proteins described in Fugu (*Takifugu rubripes*; Loh *et al.* 2004). Despite recent investigations, the physiological function of these claudins, particularly in the regulation of hydromineral balance, remain largely unknown, although previous studies in our laboratory and others indicate that they may be regulated in a tissue-specific and salinity-dependent manner in teleost fishes (Bui and Kelly, 2011; Loh *et al.*, 2004; Tipsmark *et al.*, 2008a-b; Tipsmark *et al.*, 2009).

Here, we examine the response of three claudins in the euryhaline tilapia (*Oreochromis mossambicus*): *Omcldn3c, Omcldn28a, Omcldn30* and assess their regulation in the gill and posterior intestine during both long-term and acute salinity adaptation. Additionally, we assessed whether these claudins were colocalized to MRC populations or other cell types within the teleost gill to ascertain whether they may augment transcellular pathways of ion transport or perhaps regulate paracellular water permeability through other means.

Materials and Methods

Animals

Two separate salinity experiments were performed. For the tissue expression profile and claudin localization, male tilapia (N = 20; 100-150 g) were acclimated for 8 weeks in FW (salinity 0-2 ppt; hardness 244-475 mg/L; alkalinity 105-110 mg/ L; pH 8.0) or SW (2/3 full-strength; Crystal Sea salt mix, Marine Enterprises, Baltimore, MD; salinity 22-25 ppt; pH 8.0). Animals were held at constant temperature (24 ± 1°C), photoperiod (12: 12 h light-dark cycle), and feeding regime (2 % body weight per day; 40% protein, 10% fat; Ziegler Brothers, Gardner, PA). The fish were fed daily except for 24 hours prior to sampling.

To examine acute regulation, FW and SW salinity challenges were simultaneously performed. Prior to salinity transfer, fish were acclimated for 3 weeks in FW (salinity 0-2 ppt; hardness, 350 mg/L; alkalinity, 110 mg/L; pH 8.0) or SW (25 ppt; pH 8.0). The temperature, photoperiod and feeding regimes were identical to the previous study. To perform the challenges, FW-acclimated fish were transferred to SW (FW to SW) or sham transferred (FW to FW), and SW-acclimated fish were transferred to FW (SW to FW) or sham transferred (SW to SW). Fish from all groups were sampled at 0, 1, 4, and 7 days post-transfer. Fish were not fed for 24 hours prior to sampling.

Sampling

Fish were anesthetized in buffered Tricaine methanesulfonate (MS-222; Sigma-Aldrich, St. Louis, MO) before blood collection using heparinized syringes. The animals were then

decapitated and kept on ice during tissue sampling. For the tissue expression profile, the following tissues (50-100 mg) were collected: gill (left second arch), heart, kidney (whole), testes, pituitary, brain (including hypothalamus), skin, stomach, esophagus, anterior intestine (1 cm below pyloric sphincter), and posterior intestine (1 cm anterior of the anus). For the salinity challenge, only gill and posterior intestine were collected. Tissues were stored in RNA later (Ambion-Applied Biosystems, Austin, TX) overnight (4°C) and then frozen at –80 °C until use. Plasma was collected from blood samples by centrifugation (3,000 x *g*) and stored at -20°C. All procedures were performed in accordance with husbandry and sampling protocols approved by the North Carolina State University *Institutional Animal Care and Use Committee*.

Plasma osmolality

Plasma osmolality (mOsmol/kg) was measured in duplicate using a VAPRO vapor pressure osmometer (WesCor, Logan, UT).

RNA isolation and cDNA preparation

Total RNA was collected from sample tissues using TRI reagent (Molecular Research Center, Cincinnati, OH). Isolations were performed according to manufacturer's protocol except for skin tissue, where an additional phase separation was performed to remove pigment. RNA quality was assessed by 18S and 28S ribosomal band integrity in gel electrophoresis, and by $OD_{260:280}$ ratio (range 1.8-2.0) using a Nanodrop 1000 spectrophotometer (Thermo Scientific, Wilmington, DE). The RNA was then DNAse-treated

(Turbo DNA-free, Ambion) and requantified before 1 µg was reversed transcribed (High Capacity cDNA Synthesis kit, Applied Biosystems).

Molecular cloning

The cloning of *Omcldn28a* and *Omcldn30* was described previously (Tipsmark *et al.*, 2008a). For *Omcldn3c*, a partial sequence was obtained by amplification using degenerate primers designed from *Paralibidochromis chilotes* expressed sequence tag (Genbank Accession *BJ676291*; primers in Table 1). The full coding sequence was obtained by successful Rapid Amplification of cDNA Ends (RACE) PCR using a FirstChoice RNA ligase-mediated RACE kit (Ambion) with gene specific primers designed from the partial sequence (Table 1). Sanger di-deoxy sequencing of PCR amplicons was performed at the University of Chicago Comprehensive Cancer Center (Chicago, IL). RACE-PCR sequences were assembled into a 1,128 bp sequence contig using Vector NTI Contig Express (*v10.3*, Invitrogen, Carlsbad, CA). The assembly was then validated by additional PCR of the full coding sequence, which spanned connecting regions of the assembly (primers; Table 1). GoTaq DNA polymerase (Promega) and provided buffers were used for all PCR reactions, with 200 µM dNTP mix and 400 µM primer concentrations.

Phylogenetic analysis

Bayesian phylogenetic analysis of the tilapia claudins was performed using MrBayes (*v3.1*) on a teragrid computing platform available online at http://www.phylo.org (Huelsenbeck and Ronquist, 2001; Miller *et al.* 2010). The analysis was performed using the WAG (Whelan and Goldman, 2001) substitution model with gamma distributed among-site rate variation

(generations = 250,000, sample frequency = 100, burnin = 1000). The unrooted 50% majority rule consensus tree was visualized in TreeView (Page, 1996) with additional illustration performed using CorelDraw (*v12*). Putative teleost *cldn3* and *cldn4* homologs (claudins 3c, 27a and 27c, 28a-b, 29a-b, 30a-d; and claudins *a-e*, and *h* in zebrafish) from the Atlantic salmon (*Salmo salar*), Fugu (*Takifugu rubripes*), and zebrafish (*Danio rerio*) were included in the analysis with human claudins 3, 4, 8, and 10. Predicted claudin sequences from the Nile tilapia (*Oreochromis niloticus*) and zebrafish genomic assemblies were included in the analyses; available online at NCBI *Gene* (http://www.ncbi.nlm.nih.gov/gene). A distant sequence, human Claudin Domain Containing 1 (*CLDND1*) was also included. Protein accession numbers for all sequences used are provided as Supplemental Information (Table A1; Appendix A).

Quantitative gene expression

Tilapia claudin mRNA was measured by quantitative real-time PCR (qPCR) using the SYBR green absolute quantification method. Gene primers were developed using ABI Primer Express (*v3.0*) (Table 1). The PCR was performed using 20 ng of cDNA template and 75 nM primer concentrations with Brilliant II SYBR Green master mix (Agilent, Santa Clara, CA). Triplicate runs for all samples were performed using an ABI 7900HT sequence detection system. The cycling parameters were as follows: 1 cycle—95°C for 10 minutes; 40 cycles—95°C for 30 s, 60°C for 60 s, and 72°C for a 60 s extension. Raw fluorescence values were analyzed by *LinRegPCR* software to verify equal amplification efficiency (Ramakers *et al.* 2003). Cycle threshold (Ct) values were transformed using a copy number standard curve

derived from 10-fold diluted plasmids containing the gene coding sequence (R^2 = 0.98-0.99). Correct amplification of gene targets were verified by melt-curve analysis and select sequencing of qPCR products. All data were normalized to total RNA concentration and natural log transformed for statistical analysis (Picha *et al.* 2006; Tipsmark *et al.* 2008a). For the tissue expression profile, values are expressed as mRNA copy per nanogram total RNA. Values below the range of the standard curve were considered undetected (ND). For the salinity challenges, values are expressed as relative fold change compared to the group mean for initial FW-acclimated fish (FW_0).

RNA probe synthesis

Partial sequences of the tilapia claudins and elongation factor 1 alpha subunit (*ef1α*; Genbank *HE608771*) were subcloned into a pSPT18 vector (Roche, Penzberg, Germany). Extracted plasmids were used as template for PCR amplification (primers: forward, 5'–ATA ACC TTA TGT ATC ATA CAC ATA CGA TTT AGG TGA—3'; reverse, 5'—GCT TAT CGA AAT TAA TAC GAC TCA CT—3'). The cycling parameters were as follows: one cycle—95°C for 2 minutes; 30 cycles—95°C for 30 seconds, 52°C for 30 seconds, 72°C for 1 minute; one cycle—72°C for 5 minutes. These amplicons were then used as template for *in vitro* transcription of DIG-labeled antisense (T7) or sense (Sp6) riboprobes. Synthesis reactions were as follows: 20 U of T7 or Sp6 RNA polymerase with provided buffers (Promega), 8 U of RNAse inhibitor (Promega), 2.3 µL of 10X DIG RNA labeling mix (Roche), and 200 ng of DNA template. These reactions were incubated at 37°C for 3 hours, followed by addition

of 4 U of DNAse I (Ambion) and another 30 minute incubation. RNA probes were cleaned with NucAway spin columns (Ambion) and stored in 1 µg aliquots at -80°C.

Northern blotting

Ten micrograms of gill total RNA was electrophoresed in a denaturing 1% agarose gel using NorthernMax (Ambion) reagents and protocol. The RNA was transferred to Nylon membrane by overnight capillary transfer with 20X SSC, UV crosslinked at 254 nm, and rinsed in 2X SSC. After drying, the membrane was cut into lengthwise strips (by lane) and prehybridized at 68°C for 30 minutes with 10 mL of DIG EasyHyb hybridization buffer (Roche). Membranes were hybridized overnight at 68°C with 200 ng/mL antisense probe in 5 mL of preheated hybridization buffer. Membranes were washed twice in 2X SSC / 0.1% SDS at room temperature for 5 minutes, followed by two washes in 0.2X SSC / 0.1 % SDS at 68°C for 15 minutes. The membranes were equilibrated in 1X MABT (150 mM NaCl, 100 mM Maleic acid, 0.1% Tween-20) for 5 minutes, and blocked (1% Roche blocking reagent in 1X MABT) for 30 minutes. This was replaced with fresh solution containing Anti-DIG/ AP (Roche; 1:10,000 dilution) and incubated for 45 minutes. Membranes were washed twice in 1X MABT for 15 minutes, and equilibrated in 1X AP (10 mM NaCl, 10 mM Tris-HCl; pH 9.5) for 5 minutes. Membranes were covered in NBT/BCIP solution (Roche, tablet form) and allowed to develop overnight at 37°C. Afterward, membranes were rinsed in distilled water, then 70% ethanol, and dried before imaging (Syngene Gene Genius).

RNA *in situ* hybridization

Collected gill tissue was rinsed in cold 1X PBS, and stored overnight (4°C) in 4% paraformaldehyde (*w/v* in 1X PBS). The tissues were rinsed and equilibrated in 30% sucrose (*w/v* in 1X PBS), then serially in 60, 80, 90 and 100% OCT compound (v/v in 1X PBS) for 1-hour intervals at 4°C. The tissues were frozen in fresh, 100% OCT at –80°C. Tissues were sectioned in sagittal and transverse planes (10-20 µM) using an UltraPro5000 cryostat (Vibratome). The sections were briefly dried on Superfrost Plus slides (Fisher) and stored at –80°C until use. Slides were defrosted (RT, 15 min), rehydrated in 1X PBS (15 min), acetylated (0.1 M Triethanolamine + 0.025% acetic anhydride; 10 min), and rinsed again (1X PBS, 10 min) before hybridization. The slides were then incubated in PreHyb buffer (50% deionized formamide, 200 mM NaCl, 9 mM Tris-HCl pH 7.5, 1 mM Trizma, 7 mM NaH_2PO_4, 6 mM Na_2HPO_4, 5 mM EDTA) for 30 minutes at 65°C. The hybridization conditions were as follows: 100 µL of Hyb buffer (PreHyb + dextran sulfate (10% w/v), 1 mg/ml yeast tRNA (Life Technologies), and 1X Denhardt's reagent) containing 2.5-5 ng/µL probe was incubated (70°C, 10 min) before application to tissue sections, followed by a coverslip. Slides were hybridized overnight at 65°C in a humidified chamber. Afterwards, slides were washed three times in Wash buffer (50% deionized formamide, 1X SSC, 0.1% Tween-20) at 65°C for 30 minutes, followed by twice in 1X MABT (150 mM NaCl, 100 mM Maleic acid, 0.1% Tween-20: pH 7.5) at RT for 30 minutes. The slides were blocked for 90 minutes (20% sheep serum, *v/v* in 1X MABT) before overnight incubation with anti-DIG/AP (Roche, 1:4000 in blocking solution) at 4°C. The slides were washed four times in 1X MABT (30 min, RT) and equilibrated in AP buffer (10 mM NaCl, 10 mM Tris-HCl; pH 9.5)

for 15 minutes before overnight staining in NBT/BCIP (Roche; 1 tablet in 10 mL distilled H_2O) at 4°C. After staining, the slides were washed twice in 1X PBS.

Immunocytochemistry

After *in situ* hybridization, adjacent paraffin wells were made on the slides for positive and negative (control) detection of $Na^{(+)}$-$K^{(+)}$-ATPase (NKA) using the *a5* monoclonal antibody (mouse anti-chicken NKA α/β; Hybridoma Bank, University of Iowa), whose specificity has been demonstrated in multiple fish species (Tipsmark *et al.*, 2008c; Tipsmark *et al.*, 2004; Tipsmark *et al.*, 2002). Immunoreactivity was detected by a goat anti-mouse DAB kit (Invitrogen) according to provided protocol with the following modifications: the peroxide quenching step was omitted as hybridization removes endogenous peroxidase activity, the primary antibody incubated overnight at 4°C in a humidified chamber (1:1000 dilution in 1% block; 35 µg/mL Ig), and DAB staining (500 µg/mL diaminobenzidine, 0.015% H_2O_2 in 1X PBS) proceeded for 20 seconds. After, slides were washed twice in 1X PBS for 5 minutes. Slides were dehydrated serially in ethanol (50%, 70 %, 90%, 100%, 100%) for 5 minutes, and immersed in CitriSolv (Fisher) for 5 minutes. Slides were mounted with Permount (Fisher) and dried overnight before photographing (*Olympus* BH-2 microscope with *Sony* Digital DFW-X710 camera). Post-hoc image analysis was limited to whole-figure contrast adjustment (Corel *v12*). No other modifications were performed.

Statistical Procedures

All statistical procedures were performed using JMP (*v8*, SAS, Cary, NC). For the tissue expression profile, mRNA values were compared by unpaired t-tests to examine the effect of long-term FW or SW exposure. For the salinity challenge, a 2-way factorial ANOVA was employed to examine the effects of treatment (FW to FW, FW to SW, SW to SW, and SW to FW), time (0, 1, 4, and 7 days post-transfer), and their interaction. If the whole model was significant, treatment groups were compared using Tukey's HSD post-hoc test. For statistical purposes, the 0 time point (for each acclimation) was treated as both a FW and SW exposure group. All mRNA values were natural log transformed to meet the assumption of homogeneity of variance. Group means were accepted as significant when $p < 0.05$.

Results

Molecular cloning

The molecular sequence of *Omcldn28a* and *Omcldn30* were previously described (Tipsmark *et al.*, 2008a). For *Omcldn3c*, the RACE sequences produced a 1,128 bp contig having 4-fold or greater sequence coverage. The coding sequence was then verified by additional PCR of the open reading frame (651 bp), which spanned connecting regions of the assembly. The translated coding sequence of *Omcldn3c* is 91% similar and 80% identical to pufferfish (*T. rubripes*) claudin 3c. The full sequence of *Omcldn3c* was submitted to Genbank (*JQ412916*).

Phylogenetic analysis of claudin proteins

Bayesian phylogenetic analysis identified the tilapia claudins as orthologous to teleost Claudin 3c (*Omcldn3c*), Claudin 28a (*Omcldn28a*), and Claudin 30 (*Omcldn30*), respectively (Fig. 1; 89-100% clade-credibility score, ccs). These proteins were also identified in Nile tilapia (*O. niloticus*), as predicted claudin loci were included in our analysis: claudin 3c, *LOC100700473*; claudin 28a, *LOC100692042*; and claudin 30, *LOC100692852* (100% ccs; Fig. 1). These predicted proteins were 88-99 % identical to the Mozambique tilapia sequences. The phylogeny contained human claudins (Claudins 3, 4, 8, and 10), along with a distant protein, Claudin Domain Containing 1, which was used for tree polarization (Fig. 1; Table A1, Appendix A). All putative homologs of Claudin 3 and Claudin 4 (teleost + human) formed a unified clade (87 % ccs), which was sister to human Claudin 8 (Fig. 1). Teleost claudins 27, 28, 29, and 30 formed a unified clade with human Claudin 4 (98% ccs). A monophyletic origin for all claudin 3-like proteins was not observed (Fig. 1).

Tissue expression profile of tilapia claudins

The mRNA expression of *Omcldn3c*, *Omcldn28a*, and *Omcldn30* were examined in tissues from fish acclimated long-term to FW and to SW (25 ppt). Claudin mRNA expression was highest in tissues with direct contact to the external environment (gill, skin, esophagus), and were often two orders of magnitude higher than that of internal tissues (Fig. 2). *Omcldn3c* was present in all tissues except the pituitary, with greatest abundance in the gill, kidney, esophagus, and posterior intestine (Fig. 2A). In the gill, *Omcldn3c* was significantly higher in

FW fish compared to SW fish (Fig. 2A; $p < 0.001$). *Omcldn28a* mRNA expression was highest in the gill, skin, and esophagus (Fig. 2B). Gene expression was significantly higher in the gills of SW-acclimated fish ($p = 0.005$), and in the stomach of FW-acclimated fish (Fig 2B; $p = 0.019$). *Omcldn28a* mRNA expression was below detection limits in the posterior intestine. Gene expression of *Omcldn30* was predominant in the gill, skin, and esophagus, however no differences were observed between FW and SW-acclimated fish in these tissues (Fig. 2C). Significantly higher *Omcldn30* mRNA was present in the kidney of SW fish ($p = 0.014$) and in the brain of FW fish (Fig. 2C; $p = 0.035$). Gene expression of *Omcldn30* mRNA was not detected in the pituitary (Fig. 2C).

Salinity challenges

Claudin mRNA expression was examined in the gill and posterior intestine, major organs for monovalent ion transport and water reabsorption, respectively, during simultaneous SW and FW challenges (Fig. 3). Freshwater-acclimated tilapia were transferred to SW (FW to SW) or sham transferred (FW to FW). Seawater-acclimated fish were transferred to FW (SW to FW) or sham-transferred (SW to SW). Plasma osmolality was measured for each group to assess osmotic perturbation. In the SW-transferred fish plasma osmolality significantly increased after 24 hours relative to sham fish ($p < 0.001$), and then declined after day 4 (Fig. 3A). In FW-transferred fish, no differences in plasma osmolality were observed relative to sham, however plasma osmolality was generally lower after 24 hours (Fig. 3B).

Claudin mRNA expression was examined in the gill during the salinity transfer. Tilapia *Omcldn3c* mRNA was significantly higher in FW- than in SW-acclimated fish prior to transfer ($p < 0.01$; FW_0 vs SW_0; Fig. 3C). Gill *Omcldn3c* mRNA was significantly lower in fish transferred to SW at 24 hours ($p < 0.001$) and thereafter (Fig. 3C). Gill *Omcldn3c* mRNA expression was significantly higher in FW-challenged fish at 7 days relative to sham fish ($p < 0.001$). However, mRNA expression in both groups declined after 4 days (Fig. 3D). For *Omcldn28a*, no significant changes in gill mRNA expression were observed during the SW challenge (Fig. 3E). In SW fish transferred to FW, *Omcldn28a* mRNA expression was significantly higher than sham fish at day 7 ($p < 0.001$; Fig. 3F). Gill *Omcldn30* mRNA expression was significantly higher in SW-challenged tilapia, relative to sham fish, at day 4 ($p < 0.01$), but levels declined afterwards (Fig. 3G). In FW-challenged fish, gill *Omcldn30* were significantly higher at day 7, relative to sham fish ($p < 0.001$; Fig. 3H).

The mRNA expression of *Omcldn3c* and *Omcldn30* was examined in the posterior intestine of challenged fish (Fig. 3I-L). The mRNA expression of *Omcldn28a* was below qPCR detection limits for this tissue (Fig. 2B). In FW fish transferred to SW, *Omcldn3c* mRNA expression in the posterior intestine declined significantly at 24 hours relative to sham fish ($p < 0.001$), and then returned to sham levels afterwards (Fig. 3I). In SW-fish transferred to FW, *Omcldn3c* mRNA expression was not significantly different from sham fish (Fig. 3J). For Omcldn30, mRNA expression in the posterior intestine was lower in SW-challenged fish, relative to sham fish at day 7 ($p < 0.05$; Fig. 3K). No difference in *Omcldn30* mRNA expression was observed during the FW challenge (Fig. 3L).

Localization of claudin mRNA in tilapia gill

Claudin mRNA expression was localized in the gill using *in situ* hybridization coupled with Na^+, K^+-ATPase immunostaining. The hybridization specificity of claudin riboprobes were established by Northern blotting (Fig. 4A). As related claudins may have similar molecular weights, riboprobe specificity was also verified by hybridization to endonuclease digested DNA (Fig. A1; Appendix A). As these claudins lack intron regions (Loh *et al.*, 2004), restriction sites within the mRNA also exist within the genomic sequence (Fig. A1; Appendix A). Control tests for background were performed using both saggital and transverse sections (10 µM) of gill filament (Fig. 4B). Antisense and sense probes were tested in conjunction with positive and negative Na^+,K^+-ATPase immunostaining (α5 antibody; Fig. 4C-F).

Tilapia claudin mRNA was localized in both FW and SW acclimated gill tissue (Fig. 5). Although 10 µm sections give better resolution (Fig. 4C-F), 20 µm sections were used in the salinity comparisons to provided better detection of mRNA (Fig. 5). Ionocytes (MRCs) were localized to the interlamellar space of the gill filament, however they appear asymmetrically distributed towards the trailing edge of the gill filament (Fig. 5B, D, F, H, J, L). *Omcldn3c* mRNA expression was observed within gill pavement cells and intermediate cells of the interlamellar space, where Na^+, K^+-ATPase positive cells were occasionally dispersed (Fig. 4C, E and Fig. 5A, C). The prominent region *Omcldn3c* mRNA expression was in the leading (efferent) edge of the filament (Fig. 5B,D). *Omcldn3c* mRNA was not detected in cells of the trailing edge, which are heavily populated with Na^+, K^+-ATPase positive cells (Fig. 5B). *Omcldn28a* mRNA expression was located in the interlamellar space and restricted

to the first cell layers of the epithelium, expression appeared slightly deeper in the gill of SW fish, suggesting additional mRNA expression within intermediate cells (Fig. 5E,G). As with *Omcldn3c*, the *Omcldn28a* mRNA expression was prominent in the leading edge, away from abundant α5 cell populations (Fig. 5F,H). *Omcldn30* mRNA expression was detected in deeper tissue layers (intermediate cells) of the interlamellar region, and was more prominent within the leading edge (Fig. 5J,L). The mRNA expression of *ef1α*, used as a positive control, was detected within interlamellar regions of both the leading and trailing edge (Fig. 5M-P).

Discussion

Gene or genome duplication has given rise to an unprecedented diversity of claudins within the genomes of teleost fish, with up to 56 claudins currently described in Fugu (Loh *et al.*, 2004). The largest expansion of genes occurred for claudin 3,4-like proteins, with 17 teleost claudins that were likely homologous to mammalian *cldn3* and *cldn4* (Loh *et al.*, 2004; Tipsmark *et al.*, 2008b). Using Bayesian phylogenetic analysis of protein sequences, we evaluated homology of *Omcldn28a* and *Omcldn30*, previously described in our laboratory (Tipsmark *et al.* 2008a), as well as for claudin 3c (*Omcldn3c*) identified in this study. We confirm orthology of the tilapia claudins to those of other teleosts, and confirm that fish claudin groups 27, 28, 29, and 30 appear related to mammalian *cldn4* (Fig. 1). Orthologs of *Omcldn3c*, *Omcldn28a*, and *Omcldn30* were also identified for a related tilapia species, *Oreochromis niloticus*, using predicted loci identified from genome annotation (Fig. 1). Currently, we were not able to show direct homology for all claudin 3-like proteins in

vertebrates as no unified clade was resolved for this group (Fig. 1), however phylogenetic resolution will likely improve in future with additional evidence from genomic assemblies (Chapter 2).

Recent studies have shown that claudin 3,4-related proteins are particularly abundant within the gill epithelium and are responsive to osmotic perturbation (Bui and Kelly, 2011; Chasiotis *et al*., 2012a-b; Tipsmark *et al*., 2008a-c). To further investigate the role of these claudins during salinity adaptation, we examined mRNA expression in multiple tissues using long-term acclimated FW or SW fish (Fig. 2). For all claudins (*Omcldn3c*, *Omcldn28a*, and *Omcldn30*), mRNA expression was most prevalent in tissues with direct contact to the external environment or in those possessing osmoregulatory functions (e.g. skin, esophagus, gill, posterior intestine; Fig. 2). We then assessed mRNA expression of these claudins within the gill and posterior intestine during acute salinity transfer using simultaneous SW and FW challenges (Fig. 3).

During long-term salinity acclimation, gill *Omcldn3c* mRNA expression was significantly lower in SW fish, compared to those in FW ($p < 0.001$; Fig. 2A), and was also observed in acclimated fish prior to salinity transfer ($p < 0.05$; Fig. 3C,D). Previous studies have shown *cldn3c* mRNA expression is regulated by changes in external salinity. In pufferfish (*Tetraodon sp*.), *cldn3c* mRNA expression was significantly lower in the gill after 3 weeks of acclimation to full-strength SW, compared to FW fish (Bagherie-Lachidan *et al.*, 2008, Duffy *et al.*, 2011). In the stenohaline goldfish (*Carassius auratus*), transfer of fish from FW to ion-

poorer water significantly increased gill mRNA expression of *cldnh* (*cldn3c* ortholog [see Fig. 1]; Chasiotis *et al.*, 2012b). Acute regulation of this claudin by salinity has yet to addressed in a naturally euryhaline species. In this study, transfer of FW-acclimated tilapia to SW reduced gill *Omcldn3c* mRNA expression within 24 hours, and expression remained significantly lower thereafter ($p < 0.001$; Fig. 3C). In contrast, gill *Omcldn3c* mRNA expression increased after day 4 and remained elevated by day 7 of FW challenge (Fig. 3D). These results, along with that observed for goldfish (Chasiotis *et al.* 2012b) strongly support a role for this claudin during FW adaptation. Interestingly, reductions in gill *Omcldn3c* mRNA, observed in SW-challenged fish (1 day), occur more rapidly than increases in gill *Omcldn3c* mRNA during FW-challenge (4-7 days). This finding could support previous hypotheses that reductions in *Omcldn3c* in SW fish are associated with reducing Na^+ permeability within "leaky" tight junctions (Bagherie-Lachidan *et al.*, 2008). However, it may also suggest this claudin is rapidly replaced during reorganization of the gill epithelia.

For *Omcldn28a*, we previously reported no significant differences in gill mRNA abundance after SW transfer, however gill mRNA expression was strongly upregulated beginning after 24 hours and extending through 7 days in FW-challenged fish (Tipsmark *et al.*, 2008a; Fig. A2, Appendix A). A similar, albeit less pronounced response was observed in the present study, where *Omcldn28a* transcript levels were significantly higher at day 7 in FW challenged fish ($p < 0.001$; Fig. 3F), and little response occurred with SW challenge (Fig. 3E). The muted response observed here with FW challenge may be associated with the limited perturbation in blood osmolality measured in our FW transferred fish (Fig 3B),

relative to that of the previous study (Tipsmark *et al.*, 2008a). A similar lack of effect on gill *cldn28a* with SW challenge was observed in Atlantic salmon (*S. salar*, Tipsmark *et al.* 2008b), although changes with FW challenge were not investigated in this species. We did observe an increase in *Omcldn28a* mRNA expression in the gill of long-term SW than FW-acclimated tilapia (Fig. 2B). Although this result is difficult to reconcile it suggests a strong temporal component to the regulation of this claudin. Nonetheless, collective studies in tilapia and limited work from salmonids point to a more prominent role for *Omcldn28a* in FW, rather than SW osmoregulation. Consistent with this hypothesis, the administration of prolactin, a key FW adapting hormone in teleosts, increased gill *cldn28a* transcript levels in Atlantic salmon (Tipsmark *et al.*, 2009), while treatment with cortisol and growth hormone, endocrine factors linked to hyperosmoregulatory processes, had little effect on *cldn28a* mRNA expression.

Similar to previous findings, we found no consistent pattern in *Omcldn30* gene expression with salinity. No differences in gill *Omcldn30* mRNA were observed between longterm FW and SW acclimated fish, although higher transcript levels were seen in the kidney and brain of SW and FW fish, respectively (Fig. 2C). Expression was elevated by 7 days in FW transferred fish (Fig. 3H) and in Atlantic salmon gill *cldn30* mRNA expression significantly declined over a similar time-course in SW challenged fish (Tipsmark *et al.*, 2009). However, we found *Omcldn30* transcripts paradoxically increased after 4 days in SW challenged animals (Fig. 3G). The results suggest that *Omcldn30* mRNA is not under strong influence by a particular salinity, but may be temporally regulated by other factors influencing gill

function. Although previous work raised the possibility of a function of *Omcldn30* in FW adaptation (Tipsmark *et al.* 2008a; Fig A2, Appendix A), additional studies are clearly warranted in other teleosts to better identify how salinity or other factors might regulate this claudin. Evidence suggests cortisol, a stress hormone known to act permissively in FW adaptation but plays a dominant role in salt excretion, may enhance the expression of this protein (Tipsmark *et al.*, 2009).

In fishes, the gastrointestinal tract is critical to maintaining proper hydration in a hyperosmotic environment. Marine teleosts actively drink seawater, which is removed of excess sodium and chloride ions through active transport in the esophageal and upper regions of the gastrointestinal tract (Jobling, 1995; Parmalee and Renfro, 1983). Water is then absorbed in the posterior regions of the intestine, coupled to HCO_3^- and Ca^{2+} transport from the intestinal lumen (Jobling, 1995; Whittamore *et al*., 2010). Despite the importance of the gastrointestinal tract in regulating hydromineral balance, examination of claudins within these tissues under different salinities has yet to be reported. We evaluated the mRNA expression of *Omcldn3c* and *Omcldn30* in the posterior intestine during salinity transfer (Fig. 3I-L). We found *Omcldn3c* mRNA expression is reduced in the posterior intestine by 24 hours after SW challenge (Fig. 3I). By contrast, transcript levels showed elevated levels after 24 hours following transfer of SW fish to FW. Expression of *Omcldn30* did not significantly differ with salinity and *Omcldn28a* appears to show expression in the posterior intestine. The acute rise in *Omcldn3c* with FW and decline with SW acclimation suggests this claudin may

be involved in reducing paracellular water permeability in the intestine of FW fish and promotes water reabsorption in SW adapted tilapia.

A focus of this study was to determine if tilapia claudins described here are localized near ionocyte (Mitochondria Rich Cells, MRCs) populations within the gill epithelium. Previous studies suggested that reductions in gill *cldn3c* mRNA expression with SW acclimation may contribute to the formation of leaky MRC-Accessory Cell tight junctions which form the principal site for Na^+ ion excretion during SW adaptation (Bagherie-Lachidan *et al.*, 2008; Evans *et al.*, 2005). Although we observe some claudin mRNA expression in cells adjacent to MRCs (Fig. 4C, 5G), on the whole colocalization with ionocytes was rare. Transverse sections of the gill epithelium show mRNA expression of all three claudins (*Omcldn3c*, *Omcldn28a*, and *Omcldn30*) as more prominent in the leading (efferent) edge of the gill filament. Putative MRCs, commonly identified by Na^+, K^+-ATPase immunoreactivity, were typically restricted to the trailing (afferent) edge of the gill filament (See Fig. 4B for orientation). This asymmetric pattern of ionocyte distribution has been previously reported in tilapia (Evans *et al.*, 2005; Heijden *et al.*, 1997). This absence of colocalization suggest these claudins are not restricted to leaky MRC-AC tight junctions, but instead are general constituents of tight junctions between pavement cells (PVC) and intermediate cells within the gill epithelium. This finding contradicts observations from cultured goldfish gill epithelial cells, where *cldnh* (*cldn3c*, Fig 1) mRNA expression was higher in MRCs compared to PVCs (Chasiotis *et al.*, 2012b). This discordance may reflect insufficient purity of isolated cell fractions (gradient centrifugation) from harvest epithelial cells, but also could underlie

functional differences in claudin orthologs across distant fish groups. Recent evidence points to teleost *cldn10e* as a key component of "leaky" Na^+ tight junctions associated with SW adaptation, as gill mRNA expression of this claudin increases after hyperosmotic transfer and may be restricted to MRC cell populations within the gill (Tipsmark *et al.*, 2008b; Bui *et al.*, 2010).

In this study, we characterize the regulation of mRNA expression for three claudins (*Omcldn3c*, *Omcldn28a*, and *Omcldn30*) in the gill and posterior intestine of the euryhaline tilapia (*O. mossambicus*) during salinity transfer. To our knowledge, this is the first study to describe the regulation of teleost claudins in the posterior intestine, as well as direct localization of *cldn3c* within the gill epithelium. Changes in gill mRNA expression of *Omcldn3c* and *Omcldn28a* were consistent with a role in FW adaptation, where increased tight junction thickness may decrease water permeability and offset passive ion loss. *Omcldn3c* expression in the gill and posterior intestine was acutely down-regulated in SW challenged fish, yet like *Omcldn28a* and *Omcldn30*, was not colocalized to MRC populations in the gill. Thus, this claudin does not appear to be a primary component of leaky MRC-AC tight junctions associated with SW adaptation. Rather, *Omcldn3c* may be transiently down-regulated during salinity-induced epithelial remodulation (Kammerer *et al.*, 2009), or simply replaced by increases in abundance of other claudins types. While future studies demonstrating ion permeability properties for novel teleost claudins are clearly needed, the sheer diversity of this protein family along with its potential to form complex heterophilic interactions (Angelow *et al.*, 2008) suggest a coordinated response of multiple claudins occur

with osmoregulation. Transcriptomic studies (*e.g.*, *RNAseq*) examining claudin regulation may be more beneficial than the current single gene approach in evaluating their function in salinity adaptation.

Acknowledgements

We gratefully acknowledge Andy McGinty, Brad Ring, and members of the Pamilco Aquaculture Field Laboratory (Aurora, NC) for the production and maintenance of the fish used in this study. Additionally we thank Drs. H. Patisaul, E. Black, B. J. Reading, and M. Weiser (NCSU, Raleigh, NC) for their assistance and constructive advice. We also gratefully acknowledge Dr. Ozkan Ozden (Vanderbilt University, Nashville, TN) for his contributions of expression work on the gastrointestinal tract (Figures 3I-L in this manuscript are reproduced from Ozden, 2009).

REFERENCES

Angelow, S., Yu, A.S., 2007. Claudins and paracellular transport: an update. *Curr Opin Nephrol Hypertens* 16, 459-464.

Angelow, S., Ahlstrom, R., Yu, A.S., 2008. Biology of claudins. *Am J Physiol Renal Physiol* 295, F867-876.

Bagherie-Lachidan, M., Wright, S.I., Kelly, S.P., 2008. Claudin-3 tight junction proteins in *Tetraodon nigroviridis*: cloning, tissue-specific expression, and a role in hydromineral balance. *Am J Physiol Regul Integr Comp Physiol* 294, R1638-1647.

Bui, P., Bagherie-Lachidan, M., Kelly, S.P., 2010. Cortisol differentially alters claudin isoform mRNA abundance in a cultured gill epithelium from puffer fish (*Tetraodon nigroviridis*). *Mol Cell Endocrinol* 317, 120-126.

Bui, P., Kelly, S.P., 2011. Claudins in a primary cultured puffer fish (*Tetraodon nigroviridis*) gill epithelium. pp.179-194 *In*: Kursad, T. (*ed*), Methods in Molecular Biology, Vol. 762, Claudins: Methods and Protocols. Humana Press, Springer, NY, 447 p.

Chasiotis, H., Kolosov, D., Bui, P., Kelly, S.P, 2012a. Tight junctions, tight junction proteins and paracellular permeability across the gill epithelium of fishes: a review. *Resp Physiol Neurobiol* 184, 269-281.

Chasiotis, H., Kolosov, D., Kelly, S.P., 2012b. Permeability properties of the teleost gill epithelium under ion-poor conditions. *Am J Physiol Regul Integr Comp Physiol* 302, R727-R739.

Cutler, C.P., Cramb, G., 2002. Branchial expression of an aquaporin 3 (AQP-3) homologue is downregulated in the European eel *Anguilla anguilla* following seawater acclimation. *J Exp Biol* 205, 2643-2651.

Cutler, C.P., Martinez, A.S., Cramb, G., 2007. The role of aquaporin 3 in teleost fish. *Comp Biochem Physiol A Mol Integr Physiol* 148, 82-91.

Duffy, N.M., Bui, P., Bagherie-Lachidan, M., Kelly, S.P., 2011. Epithelial remodeling and claudin mRNA abundance in the gill and kidney of pufferfish (*Tetraodon biocellatus*) acclimated to altered environmental ion levels. *J Comp Physiol B* 181, 219-238.

Evans, D.H., 1999. Ionic transport in the fish gill epithelium. *J Exp Zool* 283, 641.

Evans, D.H., Piermarini, P.M., Choe, K.P., 2005. The multifunctional fish gill: dominant site of gas exchange, osmoregulation, acid-base regulation, and excretion of nitrogenous waste. *Physiol Rev* 85, 97-177.

Heijden, A., Verbost, P., Eygensteyn, J., Li, J., Bonga, S., Flik, G., 1997. Mitochondria-rich cells in gills of tilapia (*Oreochromis mossambicus*) adapted to fresh water or seawater: quantification by confocal laser scanning microscopy. *J Exp Biol* 200, 55-64.

Huelsenbeck, J.P., Ronquist, F., 2001. MRBAYES: Bayesian inference of phylogenetic trees. *Bioinformatics* 17, 754-755.

Isaia, J., Hirano, T., 1976. Effect of environmental salinity change on osmotic permeability of the isolated gill of the eel, *Anguilla anguilla* L. *J Physiol* (Paris) 70, 737-747.

Jobling, M., 1995. Environmental biology of fishes. Chapman and Hall, London, U.K.

Kammerer, B.D., Sardella, B.A., Kultz, D., 2009. Salinity stress results in rapid cell cycle changes of tilapia (*Oreochromis mossambicus*) gill epithelial cells. *J Exp Zool A Ecol Genet Physiol* 311, 80-90.

Karnaky, K., 1991. Teleost osmoregulation: Changes in the tight junction in response to the salinity of the environment. pp 175-185 *in*: Cereijido, M., Anderson, J. (*eds*.), The Tight Junction. C.R.C. Press, Boca Raton.

Krause, G., Winkler, L., Mueller, S.L., Haseloff, R.F., Piontek, J., Blasig, I.E., 2008. Structure and function of claudins. *Biochim Biophys Acta* 1778, 631-645.

Krause, G., Winkler, L., Piehl, C., Blasig, I., Piontek, J., Muller, S.L., 2009. Structure and function of extracellular claudin domains. *Ann N Y Acad Sci* 1165, 34-43.

Loh, Y.H., Christoffels, A., Brenner, S., Hunziker, W., Venkatesh, B., 2004. Extensive expansion of the claudin gene family in the teleost fish, *Fugu rubripes*. *Genome Res* 14, 1248-1257.

Marshall, W.S., Bryson, S.E., Darling, P., Whitten, C., Patrick, M., Wilkie, M., Wood, C.M., Buckland-Nicks, J., 1997. NaCl transport and ultrastructure of opercular epithelium from a freshwater-adapted euryhaline teleost, *Fundulus heteroclitus*. *J Exp Zool* 277, 23-37.

McCormick, S.D., 2001. Endocrine control of osmoregulation in teleost fish. *Amer. Zool*. 41, 781-794.

Miller, M.A., Pfeiffer, W., Schwartz, T., 2010. Creating the CIPRES Science Gateway for inference of large phylogenetic trees, Gateway Computing Environments Workshop (GCE), New Orleans, LA, pp. 1-8.

Ozden, O., 2009. Expression of claudin tight junction proteins in response to varying environmental and physiological conditions. Doctoral Dissertation, North Carolina State University. 154 p

Page, R.D.M., 1996. Tree View: An application to display phylogenetic trees on personal computers. *CABIOS* 12, 357-358.

Parmelee, J.T., Renfro, J.L., 1983. Esophageal desalination of seawater in flounder: role of active sodium transport. *Am J Physiol Regul Integr Comp Physiol* 245, R888-R893.

Picha, M.E., Silverstein, J.T., Borski, R.J., 2006. Discordant regulation of hepatic IGF-I mRNA and circulating IGF-I during compensatory growth in a teleost, the hybrid striped bass (*Morone chrysops* x *Morone saxatilis*). *Gen Comp Endocrinol* 147, 196-205.

Ramakers, C., Ruijter, J.M., Deprez, R.H., Moorman, A.F., 2003. Assumption-free analysis of quantitative real-time polymerase chain reaction (PCR) data. *Neurosci Lett* 339, 62-66.

Tipsmark, C.K., Madsen, S.S., Seidelin, M., Christensen, A.S., Cutler, C.P., Cramb, G., 2002. Dynamics of $Na^{(+)}$,$K^{(+)}$,$2Cl^{(-)}$ cotransporter and $Na^{(+)}$,$K^{(+)}$-ATPase expression in the branchial epithelium of brown trout (*Salmo trutta*) and Atlantic salmon (*Salmo salar*). *J Exp Zool* 293, 106-118.

Tipsmark, C.K., Madsen, S.S., Borski, R.J., 2004. Effect of salinity on expression of branchial ion transporters in striped bass (*Morone saxatilis*). *J Exp Zool A Comp Exp Biol* 301, 979-991.

Tipsmark, C.K., Baltzegar, D.A., Ozden, O., Grubb, B.J., Borski, R.J., 2008a. Salinity regulates claudin mRNA and protein expression in the teleost gill. *Am J Physiol Regul Integr Comp Physiol* 294, R1004-1014.

Tipsmark, C.K., Kiilerich, P., Nilsen, T.O., Ebbesson, L.O., Stefansson, S.O., Madsen, S.S., 2008b. Branchial expression patterns of claudin isoforms in Atlantic salmon during seawater acclimation and smoltification. *Am J Physiol Regul Integr Comp Physiol* 294, R1563-1574.

Tipsmark, C.K., Luckenbach, J.A., Madsen, S.S., Kiilerich, P., Borski, R.J., 2008c. Osmoregulation and expression of ion transport proteins and putative claudins in the gill of Southern Flounder (*Paralichthys lethostigma*). *Comp Biochem Physiol A Mol Integr Physiol* 150, 265-273.

Tipsmark, C.K., Jorgensen, C., Brande-Lavridsen, N., Engelund, M., Olesen, J.H., Madsen, S.S., 2009. Effects of cortisol, growth hormone and prolactin on gill claudin expression in Atlantic salmon. *Gen Comp Endocrinol* 163, 270-277.

Van Itallie, C.M., Colegio, O.R., Anderson, J.M., 2004. The cytoplasmic tails of claudins can influence tight junction barrier properties through effects on protein stability. *Journal of Membrane Biology* 199, 29-38.

Van Itallie, C.M., Anderson, J.M., 2006. Claudins and epithelial paracellular transport. *Annu Rev Physiol* 68, 403-429.

Whelan, S., Goldman, N., 2001. A general empirical model of protein evolution derived from multiple protein families using a maximum-likelihood approach. *Mol Biol Evol* 18, 691-699.

Whittamore, J.M., Cooper, C.A., Wilson, R.W., 2010. HCO_3^- secretion and $CaCO_3$ precipitation play major roles in intestinal water absorption in marine teleost fish *in vivo*. *Am J Physiol Regul Integr Comp Physiol* 298, R877-86.

Table 1. Primer sequences used in the cloning and mRNA expression analysis of tilapia claudins *Omcldn3c*, *Omcldn28a*, *Omcldn30, and ef1α.* Abbreviations: TA, the annealing temperature (°C) used during PCR amplification; F, forward primer; R, reverse primer; CDS, coding sequence; qPCR, quantitative reverse transcription – polymerase chain reaction; RACE, rapid amplification of cDNA ends. Restriction sites in primer sequences, used for cloning, are underlined.

Gene / Primer Name	Sequence (5' to 3')	T_A (°C)	Application
Omcldn3c			
3c-F	GAT GGG TTT GGA GAT CGT GGG C	58	initial fragment
3c-R	GCC CCT AGC TCC ATC TTC TGA GA		
3c-5R1	GGT AGG GCA CAT GAT AAT ATG GCT A	53	5' RACE-PCR 1°
3c-5R2	CCC ACG ATC TCC AAA CCC A	51	5' RACE-PCR 2°
3c-3F1	GCA CCA ACT GCA TTG AAG AGG A	53	3' RACE-PCR 1°
3c-3F2	CGC TGG AGT CTT CTT CAT CCT TAG TGG C	56	3' RACE-PCR 2°
3cCDS-F	ATG TCG ATG GGT TTG GAG AT	56	***contig verification***
3cCDS-R	TCA GAC GTA GTC TTT CTT GTC GT		
3cISH-F	AGC TGA AAG CTT TAC AAC CCT ACT CTG CTC TCT TCT	55	*in situ* probe
3cISH-R	AGC TGA GAA TTC TCA AGC TCT GAA AAT CTA AGT CTA		
3cQ-F	TGG GTG TCA TGA TCT CCG TAG TC	60	qPCR
3cQ-R	TCA CTT TGG CTT TAC TTC CTT CCT		
Omcldn28a			
28a-F	GCY YTG CCC ATG TGG A	50	initial fragment
28a-R	SGT GTK KGC TGA CCA		
28a-5R1	GCT CTG CAT GAC ACA GTT CAT CCA	56	5' RACE-PCR 1°
28a-5R2	CCG TCA CAA TGT TGG CTC CAA T	58	5' RACE-PCR 2°
28a-3F1	CTA TGA TTC TCT GCT GGC TCT TCC	56	3' RACE-PCR 1°
28a-3F2	TAT GGG AGT TAT CCT GGG CAT TGC	58	3' RACE-PCR 2°
28aCDS-F	ATG GTG TCA ATG GGA CGA CA	57	***contig verification***
28aCDS-R	TCA AAC ATA GGC TCG GCT GG		
28aISH-F	AGC TGA AAG CTT ATT GTT GCT TTT ATG GGA GTT ATC	57	*in situ* probe
28aISH-R	AGC TGA GAA TTC AAA ATC ATT TAT AGT CCT TC		
28aQ-F	CTC CTG CCC ACC CAA AGA	60	qPCR
28aQ-R	CTG GCA CCG CCG TAC TTC		

Table 1. Continued

Gene / Primer Name	Sequence (5' to 3')	T_A (°C)	Application
Omcldn30			
30-F	**CTG KGC ATY ATT GG**	47	initial fragment
30-R	**CCW GCR ATG ATG AAG A**		
30-5R1	**GGT CAT CCA GAT GCC TTC CC**	55	5' RACE-PCR 1°
30-5R2	**GCC AGC AGG ATG CCA ATG ATA C**	52	5' RACE-PCR 2°
30-3F1	**TAC ATG GGA AGG CAT CTG GA**	55	3' RACE-PCR 1°
30-3F2	**GCT GCT CGA GCC CTT ACT AT**	54	3' RACE-PCR 2°
30CDS-F	ATG GTT TCA GCT GCT TTG CA	55	***contig verification***
30CDS-R	TCA AAC ATA GCC CTT GTT TG		
30ISH-F	**AGC TGA AAG CTT ACA ATC CAA TGT TCA ATG CCT CTC**	56	**in situ *probe***
30ISH-R	**AGC TGA GAA TTC ATT TTG TGA CTC CAC AGT GTG GCA**		
30Q-F	**GGG AGC TTC ACT GTT CAT TGG**	60	qPCR
30Q-R	**GGA GCT GAG TAC TTG GCA GAG TAG T**		
Ef1α			
EF1a-F	**ATT GAT GCC CCT GGA CAC A**	58	partial CDS
EF1a-R	**AGT TCC GAT ACC GCC AAT C**		
EF1aIS-F	**AGC TGA AAG CTT AAG AAC ATG ATC ACT GGT AC**	60	**in situ *probe***
EF1aIS-R	**AGC TGA GAA TTC TTC CGA TAC CGC CAA TCT TGT AGA**		

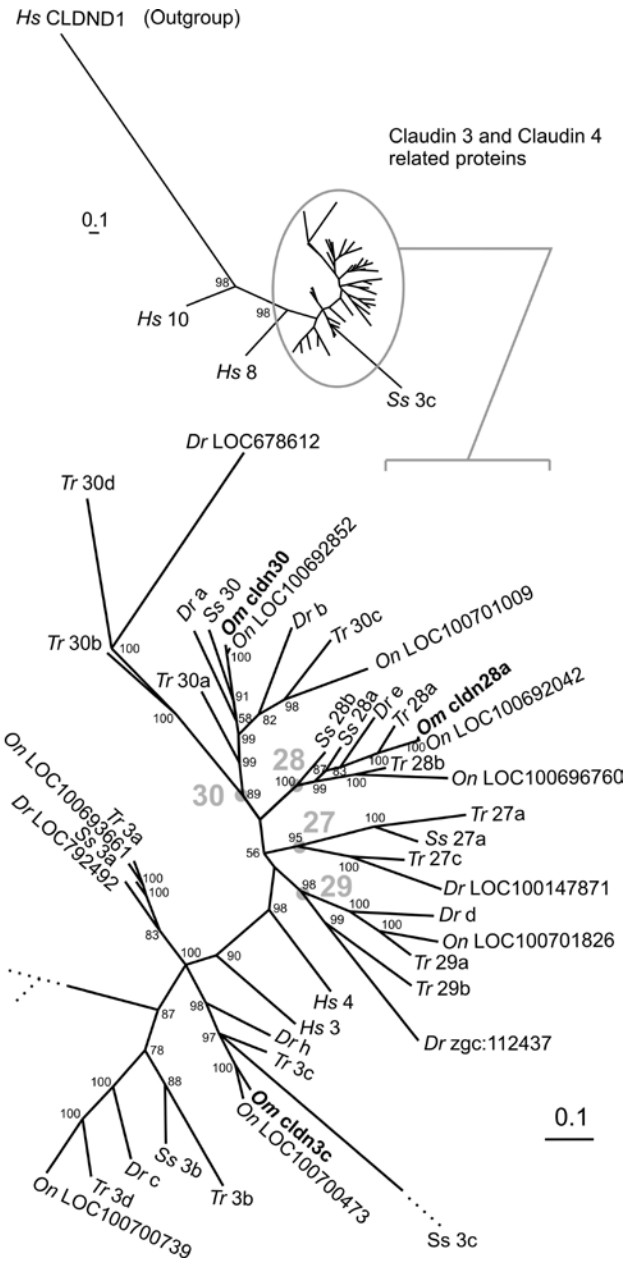

Figure 1. Unrooted consensus tree of teleost claudin 3 and claudin 4-related proteins. The grey dots and numerals within the tree indicate monophyletic origin for claudin groups. The node values represent clade-credibility scores (percentage of supporting trees). The branch-length scale indicates 0.1 amino acid substitutions per site. *Notations*: outgroup, distant member used for tree polarization; *cldnd1*; claudin domain containing 1. Taxonomic abbreviations: Dr, *Danio rerio*; Hs, *Homo sapiens*; Om, *Oreochromis mossambicus*; On, *Oreochromis niloticus*; Ss, *Salmo salar*; Tr, *Takifugu rubripes*. Accession numbers for all reference sequences are listed in Table A1 (Appendix A).

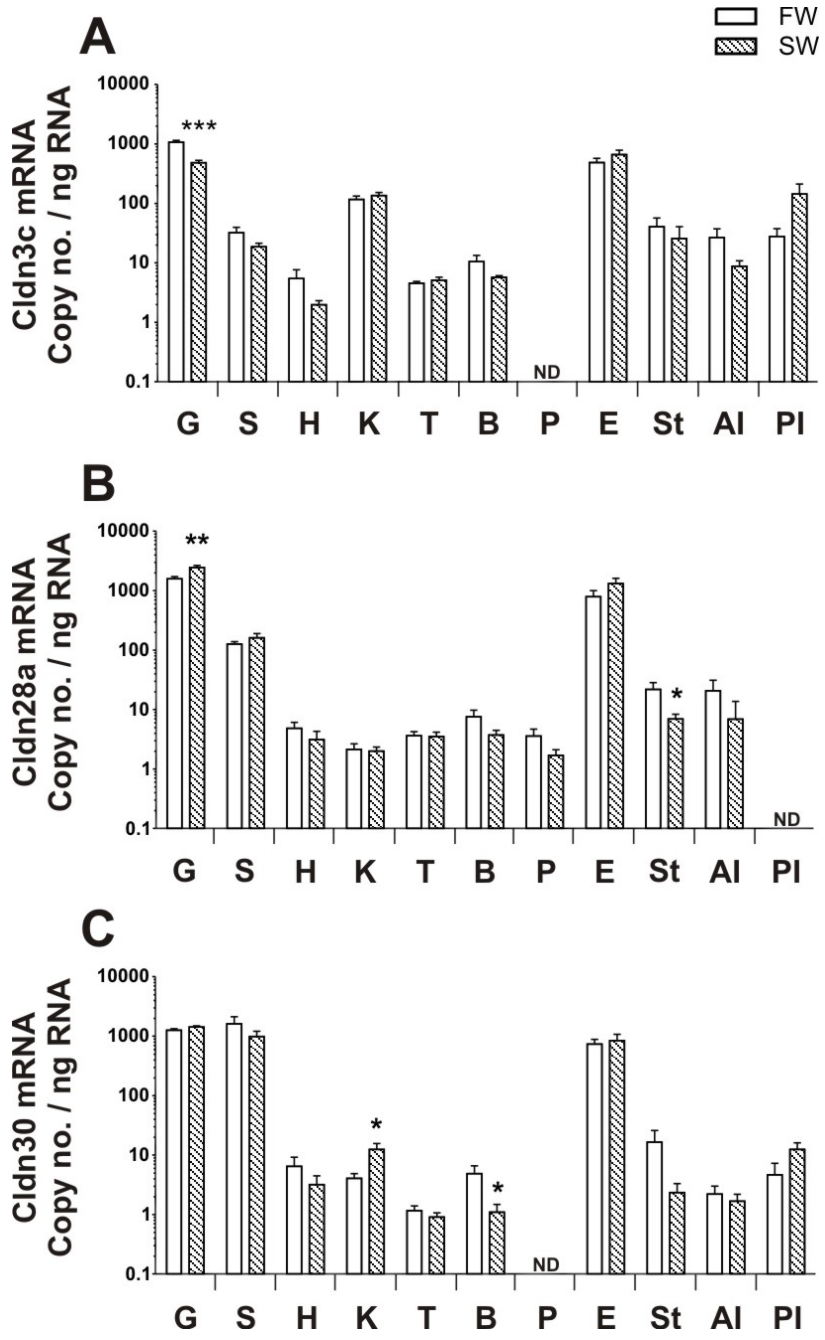

Figure 2. Tissue mRNA expression profile of tilapia claudins after long-term acclimation to FW or 2/3 SW. (**A**) *Omcldn3c*. (**B**) *Omcldn28a*. (**C**) *Omcldn30*. Tissue abbreviations: G, gill tissue; S, skin; H, heart; K, kidney; T, testes; B, brain; P, pituitary; E, esophagus; St, stomach; AI, anterior intestine; PI, posterior intestine. Expression values were normalized to total RNA. Notations: ND, not detected; *** $P < 0.001$; ** $P < 0.01$; *$P < 0.05$. Values represent means ± SE (n = 5-6).

Figure 3. Effect of salinity transfer on plasma osmolality and claudin mRNA expression in tilapia. Data in **A**, **C**, **E**, **G**, **I**, and **K** represent FW-acclimated fish transferred to 2/3 SW (FW to SW) or sham-transferred (FW to FW). Data in **B**, **D**, **F**, **H**, **J**, and **L** represent SW-acclimated fish (25 ppt) transferred FW (SW to FW) or sham transferred (SW to SW). (**A**-**B**) Plasma osmolality (mOsmol/ kg solute). (**C**-**D**) *Omcldn3c* gill mRNA expression. (**E**-**F**) *Omcldn28a* gill mRNA expression. (**G**-**H**) *Omcldn30* gill mRNA expression. (**I**-**J**) *Omcldn3c* mRNA expression in the posterior intestine. (**K**-**L**) *Omcldn30* mRNA expression in posterior intestine. Figures 3I-L are reproduced from Ozden (2009). All expression data were normalized to total RNA, and are expressed as relative fold change to the mean of the time zero group. Values represent means ± SE (n = 6-8); ***$P < 0.001$, **$P < 0.01$, *$P < 0.05$; significant effects are compared against the sham group. Different letters indicate values between initial fish (FW_0, SW_0) are significantly different; $P < 0.05$.

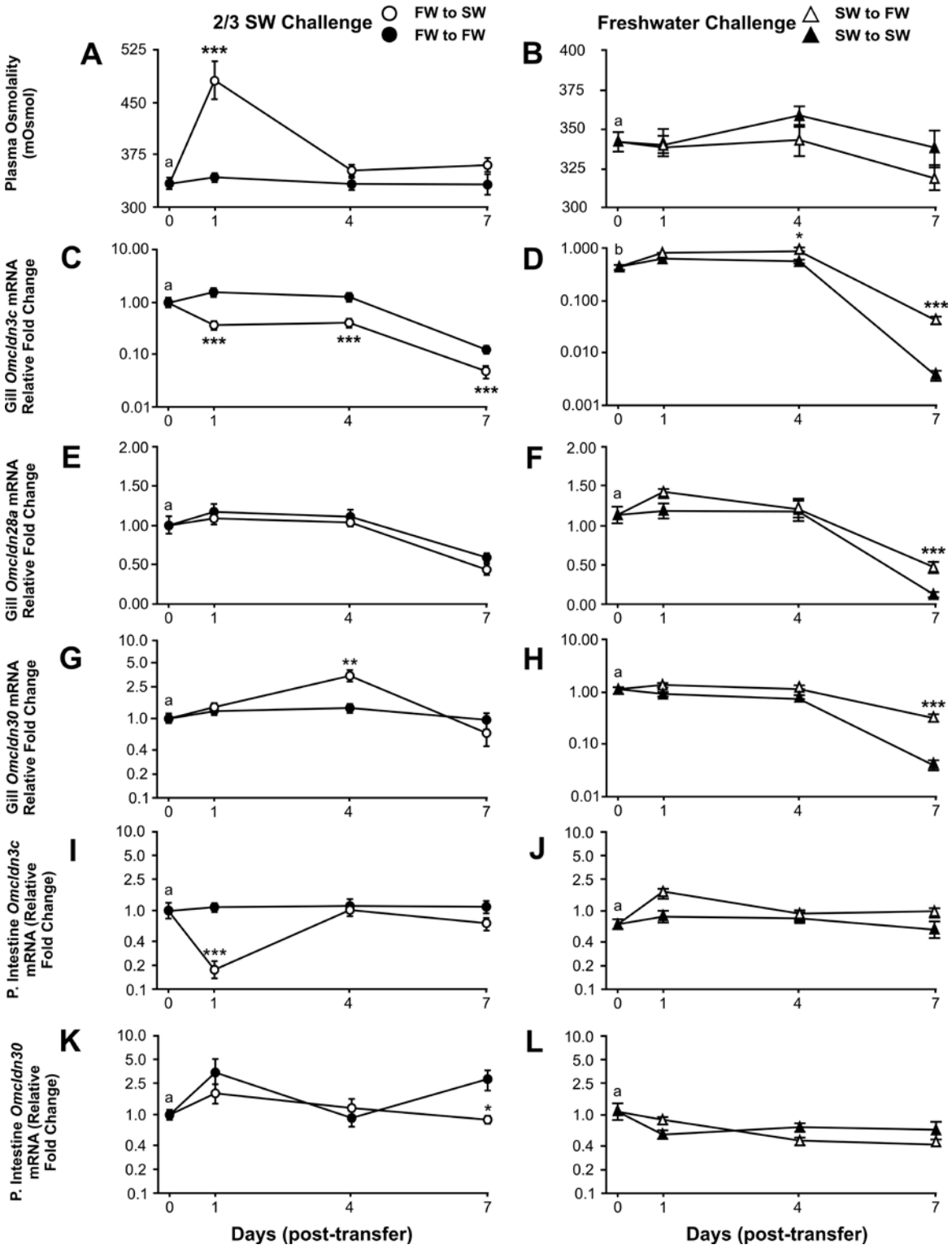
2/3 SW Challenge
FW to SW
FW to FW
Freshwater Challenge
SW to FW
SW to SW
A
B
C
D
E
F
G
H
I
J
K
L
Plasma Osmolality (mOsmol)
Gill Omcldn3c mRNA Relative Fold Change
Gill Omcldn28a mRNA Relative Fold Change
Gill Omcldn30 mRNA Relative Fold Change
P. Intestine Omcldn3c mRNA (Relative Fold Change)
P. Intestine Omcldn30 mRNA (Relative Fold Change)
Days (post-transfer)
Days (post-transfer)

Figure 4. Detection of tilapia claudin mRNA by RNA probe hybridization. (**A**) Northern blot containing 10µg of gill total RNA hybridized to antisense probes for *Omcldn3c*, *Omcldn28a*, *Omcldn30*, and *ef1-α*. The scale indicates electrophoretic movement of a molecular standard (1-4 kb). The original blot was cut into strips for separate probe hybridizations. (**B**) Illustration of tilapia gill filament for histological orientation. (**C**-**F**) *Omcldn3c* mRNA expression (blue stain, black arrowhead) colocalized with $Na^{(+)}$-$K^{(+)}$-ATPase (NKA) immunoreactivity (brown stain, red arrowhead) in 10µm frozen gill sections. In photos in **C** and **E**, the *Omcldn3c* antisense mRNA probe was used; photos **D** and **F** the *Omcldn3c* sense probe was used as a negative control. In photos **C** and **D**, the *a5* (anti- NKA) antibody was used; photos **E** and **F** the α5 antibody was absent (negative control). *Omcldn3c* sense and antisense probes were used on adjacent gill sections. Positive and negative NKA staining was performed on the same slide (paraffin wells). Arrows indicate dorsal orientation. Scale bar = 10µm. Photographs are at 400X magnification.

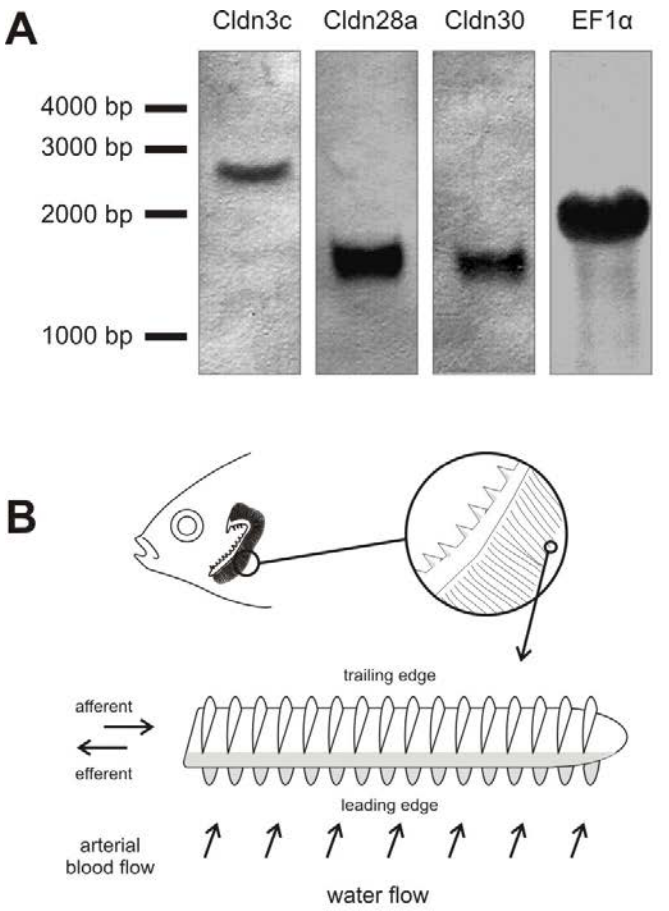
A
Cldn3c
Cldn28a
Cldn30
EF1α
4000 bp
3000 bp
2000 bp
1000 bp
B
trailing edge
afferent
efferent
leading edge
arterial
blood flow
water flow
C-F
Cldn3c Antisense
Cldn3c Sense
NKA (+)
NKA (-)
C
D
E
F
Dorsal
10

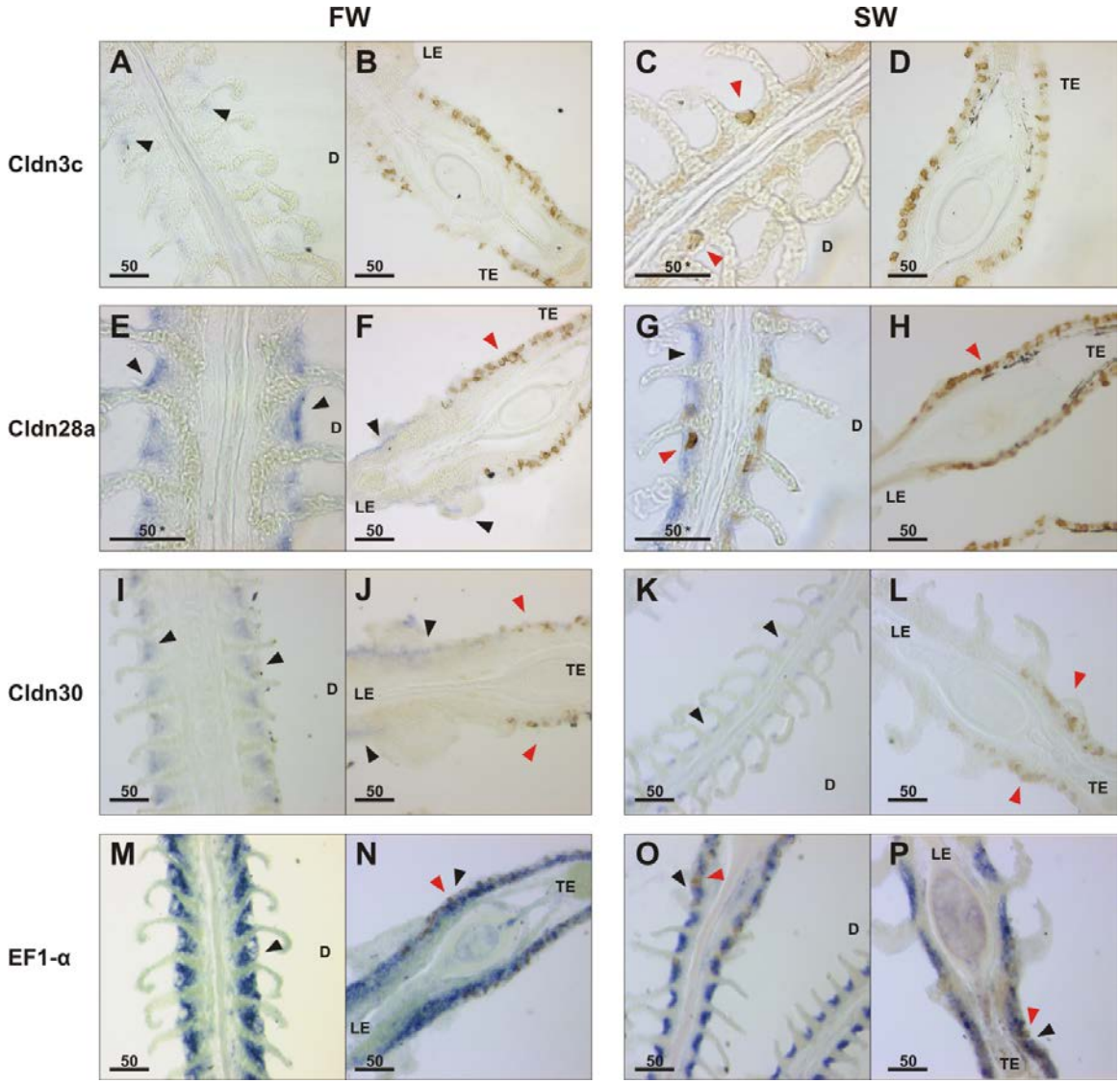

Figure 5. Detection of tilapia claudin mRNA coupled with Na^+, K^+-ATPase (NKA) staining in the gill filament of FW and SW acclimated tilapia. All photos show positive mRNA detection by *in situ* hybridization of frozen tissue sections using antisense probe RNA (black arrowhead), and positive NKA staining (red arrowhead) with the α5 antibody (**A-D**) *Omcldn3c* mRNA detection in FW (**A-B**) and SW (**C-D**) fish. (**E-H**) *Omcldn28a* mRNA detection in FW (**E-F**) and SW (**G-H**) fish. (**I-L**) *Omcldn30* mRNA detection in FW (**I-J**) and SW (**K-L**) fish. (**M-P**) Detection of *ef1α* in FW (**M-N**) and SW (**O-P**) fish. Photos **A**, **C**, **E**, **G**, **I**, **K**, **M,** and **O** are of 20µm saggital sections through the gill filament, and show individual gill lamellae. Photos **B**, **D**, **F**, **H**, **J**, **L**, **N**, and **P** are of 20µm transverse sections through the filament. *Abbreviations*: D, dorsal; le, leading edge; te, trailing edge. Scale bar denotes 50µm in width with photo taken at 200X magnification, except where noted by asterisk (400X).

CHAPTER II

Phylogenetic Revision of the Vertebrate Claudin Gene Family[1]

[1] This chapter has been submitted for publication as the following manuscript: Baltzegar, D.A., Reading, B.J., Brune, E.S., and R.J. Borski (2013) Phylogenetic revision of the vertebrate claudin gene family. *Marine Genomics* (manuscript under review).

Abstract

Claudins are the dominant constituents of cellular tight junctions and both their abundance and composition confer selective properties of paracellular ion fluxes across vertebrate tissues. Despite the prominence of zebrafish (*Danio rerio*) as a developmental model and the existence of an annotated genome, the diversity and homology of claudins to other vertebrate groups are poorly described. In this study, we identify 54 zebrafish claudins, including 24 that are previously undescribed, and infer homology of the encoded polypeptide sequences to other vertebrate claudin groups by Bayesian phylogenetic analysis. In this analysis, 197 vertebrate claudin and claudin-like proteins were classified into discrete 'superclades' of related proteins. Based on these groupings, an interim reclassification is proposed, which will resolve ambiguity in the present nomenclature for major vertebrate groups. Fifty-two of the 54 identified claudins were detected in cDNA preparations from whole, adult zebrafish, and 43 exhibited distinct tissue expression profiles. Despite prolific expansion of the claudin gene family in teleost genomes, these claudins can still be broadly separated into two functional groups: (1) "classic" claudins that characteristically contain an equal number of opposing, charged residues in the first extracellular loop (ECL1) and (2) "non-classic" claudins that typically have an ECL1 containing a variable number of charged residues. Functional analysis of these groups indicates that ‘classic’ claudins may act to reduce total paracellular permeability, whereas ‘non-classic’ claudins may constitute pores that facilitate paracellular ion permeability.

Introduction

Claudins are transmembrane proteins governing the formation of cellular tight junctions. In the extracellular matrix, claudins interact with other claudins or occludens to regulate paracellular permeability. The specific permeability properties are conferred both by the type and abundance of constituent claudins that span the paracellular space (Krause *et al.*, 2008; Van Itallie *et al.*, 2006). As compartmentalization into microenvironments of distinct ionic composition is critical to biological systems, it is not surprising that claudins are now identified as vital to normal vertebrate development and homeostasis: embryonic (Hardison *et al.*, 2005; Münzel *et al.*, 2011; Siddiqui *et al.*, 2010), lumens and blood-brain barrier (Abdelilah-Seyfried 2010; Cheung *et al.*, 2011; Jeong *et al.*, 2008; Zhang *et al.*, 2010), ion and osmoregulation (Bagherie-Lachidan *et al.*, 2008; Le Moellic *et al.*, 2005; Nilsson *et al.*, 2007; Ohta *et al.*, 2006; Tipsmark *et al.*, 2008a), and carcinoma and disease (D'Souza *et al.*, 2005; Hewitt *et al.*, 2006; Satake *et al.*, 2008; Winkler *et al.*, 2009).

Zebrafish (*Danio rerio*) is a prominent vertebrate model, particularly in the fields of developmental biology and physiology. However, its full complement of claudins is unknown. Ongoing genome assembly and annotation revisions have created spurious or redundant records, thus making transcriptomic profile analysis difficult despite availability of high-density array platforms. Additionally, the current nomenclature for zebrafish claudins is ambiguous, comprising both alphabetical and numerical designations, which only partially reflect homology to claudins in other taxa. This ambiguity is compounded by erroneous classifications in other groups. For example, zebrafish claudin j (*cldnj*) is essential to the

formation of the otolith (hearing) during development (Hardison *et al.*, 2005). This gene is clearly an ortholog of pufferfish (*Takifugu rubripes*) claudin 6 (*cldn6*), yet neither is homologous to human claudin 6 (*CLDN6*; GenBank UGID:1293154).

Conventionality of gene nomenclature is essential, albeit dynamic and rooted on the persistent accumulation of data (Povey *et al.*, 2001). The same safeguards that prevent variability and confusion of gene nomenclature, however, also promote obsolescence. As examples, Kollmar and colleagues (2001) identified 11 claudins with no homology to mammalian proteins, described as claudins *a-k*. In 2004, genome analysis of the pufferfish yielded a staggering 56 claudins, presumably the result of gene and genome-wide duplication. Those with no direct mammalian homolog(s) were classified within new numeric groups (Loh *et al.*, 2004). The largest expansion occurred at the claudin 4 loci: human *CLDN4* putatively shares a common ancestor to 13 discrete fish claudins (*cldn27a-d, cldn28a-c, cldn29a-b, cldn30a-d*) (Loh *et al.*, 2004). Currently, the same theoretical ortholog from a "non-model" fish could be classified as *cldn4, cldnd,* or *cldn29a*. From an evolutionary perspective, the expansion of the claudin gene family provides a unique opportunity to model the possible fates of duplicated genes. Yet, this task remains difficult without comprehensive reclassification of vertebrate claudins.

In this study, we identified 54 zebrafish claudins, of which 24 were previously undescribed (novel) in the annotated assembly (*Zv9*). Homology by shared evolutionary history is inferred using human, mouse (*Mus muscul*us), frog (*Xenopus tropicalis*), and pufferfish claudins by

Bayesian phylogenetic inference and genome synteny. The mRNA expression of identified claudins was verified in preparations from whole zebrafish. Tissue specific expression of claudin genes in zebrafish is also reported. Since standardization of gene nomenclature is requisite to a unified knowledge base derived from both model and non-model organisms, we propose an interim reclassification scheme for all major claudin groups, reflective of common evolutionary descent. This reclassification provides a much needed reference for the study of claudin function across taxa.

Methods and Materials

Identification of putative claudins

Candidate zebrafish claudins were identified by review of accessioned records available through NCBI *Gene* (www.ncbi.nlm.nih.gov/gene; search criteria: *Danio rerio* claudin, in March of 2010). These records contained both validated and provisional claudins, hypothetical loci containing *claudin-like* domains (*pfam00822*: PMP22_Claudin; PMP-22/EMP/MP20/Claudin family), and other closely related genes (claudin domain containing 1 [*cldnd1*], peripheral myelin protein 22 [*pmp22*], lens intrinsic membrane protein [*lim*], calcium channel voltage-dependent gamma subunits 1-8 [*cacng*]). Our preliminary search was refined by BLASTp search (of the translated peptide sequences) to the *Takifugu rubripes* and *Mus musculus* non-redundant protein databases (NCBI). Sequences with a Claudin BLASTp match *or* containing the *pfam00822* PMP/Claudin domain were selected for further study. Final candidate genes were selected by peptide sequence alignment using *ClustalX*

(Thompson *et al.*, 1997) and by preliminary phylogeny analysis with human, mouse, *Xenopus tropicalis,* and *Takifugu rubripes* claudin, *cldnd1*, *pmp22*, and *cacng2* sequences (parameters: generations = 2 million, sample frequency = 2,000, among-site variation = equal (fixed), amino acid rate matrix = Poisson, burnin = 950). The complete list of sequences selected for analysis (total = 197) is provided as Table B2 (Appendix B).

Phylogeny and genomic synteny comparisons

Bayesian phylogenetic analysis was performed using four models for amino acid substitution: *Poisson* (Bishop *et al.*, 1987), *Blosum62* (Henikoff *et al.*, 1992), *WAG* (Whelan *et al.*, 2001), and the *Equalin* model, an F81 model variant (Felsenstein 1981). All other analysis parameters were held constant (generations = 50 million, sample frequency = 10,000, among-site rate variation = equal [fixed], burnin = 1250). Analysis was performed using MrBayes (v3.1.2) on TeraGrid computing accessible through the Cyberinfrastructure for Phylogenetic Research (CIPRES) Portal, available online at http://www.phylo.org/portal2/home.action (Huelsenbeck *et al.*, 2001, Miller *et al.*, 2010). Consensus trees from the Bayesian analysis were tested as "user trees" for significant differences in log likelihood using the Shimodaira-Hasegawa (S-H) test for alternate evolutionary hypotheses in TREE-PUZZLE (Schmidt *et al.*, 2002; Shimodaira *et al.*, 1999). The S-H test for log likelihood testing was performed with the following models: *Blosum62*, *WAG*, *Dayhoff* (Dayhoff *et al.*, 1978), and *JTT* (Jones *et al.*, 1992).

Genomic synteny comparisons were performed using the following assemblies available through *Ensembl* (collaboration of *EMBL - EBI* and the Wellcome Trust Sanger Institute, available at http://www.ensembl.org : Fugu [*Takifugu rubripes*] – International Fugu Genome Consortium version 4 [June, 2005]; human [*Homo sapiens*] – Genome Reference Consortium assembly version 37 [February, 2009]; mouse [*Mus musculus*] – Mouse Genome Sequencing Consortium version 37 [April, 2007]; Western clawed frog [*Xenopus tropicalis*] – Joint Genome Institute version 4.2 [November, 2009]; zebrafish [*Danio rerio*] – Sanger Institute assembly version 9 [*Zv9*; April 2010]. Orthology of non-claudin genes were determined using the *Ensembl* annotated "orthologues" database and by local alignment search tools (BLAST/BLAT) available through NCBI and *Ensembl*.

RNA extraction and tissue expression

Zebrafish males (Tuebingen longfin strain) were used to examine mRNA expression of identified claudins. The following tissues were collected from 5 fish: eye, whole brain, gill, heart, kidney (whole), intestine (whole), spleen, skin, and testes. Additional males were used for preparation of whole fish total RNA. Collected tissue was preserved in RNAlater (Ambion) at 4°C overnight before bead homogenization with RNAzol RT (Molecular Research Center) buffer. Total RNA was extracted by manufacturer's protocol (MRC). Following extraction, DNA contamination was removed by DNAse-I treatment using a Turbo DNA-free kit (Ambion). Before cDNA synthesis, total RNA from all tissues was quantified by A_{260} absorbance using a NanoDrop (ND1000) spectrophotometer. RNA quality was assessed by 18S and 28S ribosomal band integrity after gel electrophoresis. One

microgram of total RNA for each tissue (or from whole fish) was reverse-transcribed with random primers using a High Capacity cDNA Reverse Transcription Kit (Applied Biosystems). The cDNA reactions were diluted 1:6 prior to PCR amplification.

Primer pairs for 54 putative *D. rerio* claudins were designed from accessioned NCBI *Gene* sequences using Vector NTI software (Lu *et al.*, 2004). Additionally, the housekeeping gene β-actin 1 (*bactin1*) was amplified as a positive control. A complete list of primers and annealing temperatures are provided in Table B3 (Appendix B): amplicon size range = 400-500 bp, annealing temperature range = 54 - 63 °C. All PCR reactions were performed using *Taq* DNA polymerase and 10X buffer (Fisher Scientific). Reactions (25 µL) contained the following: 1X Buffer A, 0.2 mM dNTP mix, forward and reverse primers (0.4 µM each), DNA polymerase (0.3 U/µL), 1.3 µL of diluted cDNA (~ 11 ng), and nuclease-free water (Sigma-Aldrich; to volume). The PCR cycling parameters were as follows: (1 cycle) 95 °C for 2 minutes; (40 cycles) 95 °C for 30 seconds, 54-63 °C for 30 seconds, 72 °C for 45 seconds; (1 cycle) 72 °C for 5 minutes, 4 °C holding.

To validate successful PCR of the targeted claudin, amplification was first performed using whole-fish cDNA and these were submitted for sequencing. All PCR reactions were cleaned by Qiaquick PCR purification columns (Qiagen) and concentrated as a 2X elution. Samples were submitted to the University of Chicago CRC-DNA sequencing facility with the forward primer (Applied Biosystems 3730XL 96-capillary sequencer). Sequence chromatograms were identified by BLASTn search to accessioned *D. rerio* claudins (non-redundant database;

Organism = *Danio rerio* [txid7955]; August 20th, 2010; e-values: 0.0 – $7e^{-35}$; % identity = 76-100). Two poor-quality sequences, LOC557209 and LOC794676, were identified by alignment using Blast2align (NCBI; 77-82 % identity).

For the tissue expression profile, amplification was performed simultaneously with cDNA derived from discrete tissue preparations. All templates were normalized by starting total RNA concentration (1 µg) and verified by *bactin1* amplification. The reaction and cycling parameters were as stated previously. After amplification, the PCR products were gel electrophoresed with a 1 kb DNA marker (Promega) (1% agarose in 1X TAE buffer, 4 µg/mL ethidium bromide). The agarose gels were imaged using a digital Gene Genius system (Syngene), with post-hoc image analysis restricted to whole-figure cropping and reverse-contrast enhancement, using CorelDraw (*v12*). No other modifications were performed.

Functional analysis of major claudin groups

Zebrafish claudins were assigned designations as 'classic' (superclades in Figs. 1C, 1D, 2B, 2C, 2D, and 2E) or 'non-classic' (superclades in Figs. 1B, 1E, 1F, 1G, and 1H) by sequence similarity to human orthologs (Lal-Nag and Morin, 2009). Claudin domain demarcations were predicted using SMART (Schultz *et al.*, 1998) and protein sequence alignments were performed using MacVector *ClustalW* (Thompson *et al.*, 1994). Consensus peptide sequences of claudin extracellular loops were generated using the HCV Sequence Database of the Los Alamos National Laboratory (available online at: http://hcv.lanl.gov).

Results

Phylogenetic analysis

A revised list of 197 claudin sequences from human, mouse, Fugu, *Xenopus*, and zebrafish were obtained from available NCBI and *Ensembl* gene records. Consensus trees derived from phylogenetic analysis under different model assumptions were tested for significant differences in log-likelihood using the S-H test available in TREE-PUZZLE (Schmidt *et al.*, 2002; Shimodaira *et al.*, 1999). The WAG model yielded the best scoring consensus tree (log-likelihood -64230.25), and was significantly better than the *Poisson* or *Equalin* trees, regardless of the substitution model used in the S-H test (*Blosum62*, *WAG*, *Dayhoff*, or *JTT*; $p < 0.05$). Although it possessed a higher log likelihood score, the WAG model tree was not significantly better than the *Blosum62* consensus tree ($p = 0.371$ to 0.528). The WAG model was the best-scoring consensus tree of these two and hence is reported here (Figs. 1 and 2). Tree topology for the 2nd best-scoring tree (*Blosum62*) is identical except for the following cases: mouse and human claudin 7 are grouped with claudin 1 (compare with Fig. 1C; WAG model); zebrafish *LOC793915* is not grouped with claudin 16 but is sister to claudins 11 + 16 (Fig. 1E, both monophyletic); zebrafish *zgc:63990* is not united with claudin 12 and is unresolved (Fig. 1G); all vertebrate claudin 3 form a unified clade, sister to claudin 8 and claudin 8-like (Fig. 2C), zebrafish *cldna* and *cldnb* form a clade with pufferfish *cldn30c* (Fig. 2D), and mouse *Cldn4* forms a discrete clade with mouse *Cldn13* (Fig. 2D). Raw consensus treefiles for all models analyzed are available as Supplemental Information (Fig. B1; Appendix B).

Identification of zebrafish claudins

Of the 54 zebrafish claudins identified in our analysis, 47 were identified as putative orthologs of claudins previously described in pufferfish (Loh *et al.*, 2004). To avoid ambiguity, all claudins are listed (Table B1; Appendix B) both by accepted (current) gene names as well as those proposed using the interim reclassification scheme (see Section 2.3). In cases where ortholog assignment was ambiguous or conflicted with accepted nomenclature, genomic synteny was used as additional evidence for homology (Figs. 3 and S2-S5). Final assignment was determined by sum of evidence: *cldn7a* and *cldn7b* – current paralog designation (NCBI) was not supported by our phylogeny or genomic synteny (Fig. 1C, Fig. 3A); *cldn15a* and *cldn15b* – genomic synteny supported current paralog assignment (Fig. 3B); *cldn11a* and *cldn11b* – phylogeny supported by synteny (Fig. B2.C; Appendix B); *cldn18* – undetermined due to chromosomal rearrangement at zebrafish loci (Fig. B2.D; Appendix B); *cldn8a-d* – phylogeny supported (Fig. B3.B; Appendix B); *cldn10a-e* – genomic synteny supports orthology of *cldn10a* and *cldn10e*, others equivocal due to chromosomal rearrangement (Fig. B3.B; Appendix B); *cldn33a-b* and *cldn34* – orthology supported by synteny (Fig. B4; Appendix B); claudins 3a, 3c-d, 5c, 8-like, 28a-c, 28d, 29a-b, 30a, 30c-d, 37b – orthology to Fugu claudins supported by genomic synteny (Fig. B5; Appendix B). Gene orthologs to the following Fugu claudins were not identified in our zebrafish analyses: *cldn3b*, *cldn13* (renamed here as *cldn36*), *cldn14a* (renamed *cldn14*), *cldn27a* (renamed *cldn37a*), *cldn27d* (renamed *cldn28e*), *cldn28b*, and *cldn30b*.

Seven zebrafish claudins have no direct ortholog in the pufferfish, presumably due to gene loss in the Fugu genome or lineage-specific gene duplication in zebrafish: *LOC567620* and *si:ch211-95j8.2* are both homologous to pufferfish *cldn23a*, and are described here as *cldn23a1* and *cldn23a2*, respectively (Fig. 1G); *cldnk* and *LOC100334365* are paralogs of pufferfish *cldn31* and designated as *cldn31a* and *cldn31b*, respectively (Fig. 2B); zebrafish *LOC793915* (designated as *cldn16*) forms a monophyletic group with tetrapod claudin 16, but currently has no pufferfish ortholog (Fig. 1E); zebrafish *zgc:63990* aligns as basal to vertebrate claudin 12 in a weakly supported clade (52% ccs, Fig. 1G) and is designated as *cldn12-like*; no vertebrate homolog was identified for zebrafish *cldng*, however it groups most closely to vertebrate claudin 5 (designated as *cldn5-like*; Fig. 1B). A complete list of all sequences used in our analysis is available as Supplemental Information (Table B2; Appendix B).

Proposed interim reclassification of major claudin groups

Bayesian phylogenetic analysis identified eight claudin "superclades", as grouped by shared homology of amino acid sequence: claudins 10, 15, and 15-like (Fig. 1B); claudins 1, 7, and 19 (Fig. 1C); claudins 2, 14, 20, and 34 (Fig. 1D); claudins 11 and 16 (Fig. 1E), claudins 22, 25 (excluding teleost *cldn25*), and 33 (Fig. 1F); claudins 23 and 12 (Fig. 1G), claudin 18 (Fig. 1H), and claudins 3, 4, 5, 6, 8, 8-like, 9, 13, 27, 28, 29, 30, 31, 32, and 35 (Fig. 2A-D). The claudin groups below were identified as monophyletic, where all designated members form a unified clade of homology, in our phylogeny: claudins 1, 2, 5, 10, 11, 12, 15, 16, 19, 20, 23, 29, 30, and 31 (Figs. 1, 2).

Monophyly could not be easily assigned to the remaining claudin groups, due to poor tree resolution or more often, these groups are paraphyletic as currently described. Each of these groups is discussed within a proposed interim reclassification scheme where necessary. A revised list of proposed changes to major claudin groups are provided as Supplemental Information (Table B3; Appendix B). *Claudin 3* – homology of all claudin 3 genes is supported by genomic synteny (Fig. B5; Appendix B), but not in our consensus tree (Fig. 2C). Tetrapod *Cldn3* groups with *Cldn8* and *Cldn8-like* sequences with a poor clade credibility score (ccs, 59%). Therefore, no reclassification is proposed. *Claudin 4*– claudin 4 is not present in teleost fishes, but is likely ancestral to claudins 27, 28, 29, and 30 (Fig. 2D, ccs 84%). Homology of these fish claudins to tetrapod claudin 4 is also supported by genomic synteny (Fig. B5; Appendix B). Claudin 4 is only monophyletic in tetrapods with the inclusion of mouse *Cldn13*, a gene with no identifiable homolog in humans or *Xenopus*, but is adjacent to *Cldn4* in the murine genome (Fig. B5; Appendix B). Our analysis supports the paralog reclassification of mouse *Cldn4* to *Cldn4α* and mouse *Cldn13* to *Cldn4β* (Fig. 2D). *Claudin 6 and 9* – mammalian claudin 6 is monophyletic and a paralog of claudin 9 (100% ccs, Fig. 2B). Pufferfish *cldn6* and zebrafish *cldnj* are homologous, but not to tetrapod claudin 6 or 9, but rather to tetrapod claudin 8, see Fig. 2C). Synteny indicates the lack of presence of claudin 6 and claudin 9 in teleost fishes, thus these claudins are specific to tetrapods (Fig. B2.B; Appendix B). We propose that mouse and human claudin 6 and claudin 9 be reclassified as claudin 6α and claudin 6β paralogs, respectively, while *T. rubripes cldn6* and *D. rerio cldnj* be reclassified as claudin 8-like. *Claudin 7* – an unresolved node supports monophyly of tetrapod and teleost claudin 7 only with the inclusion of claudin 1 (72% ccs,

Fig. 1C). Genomic synteny shows no clear homology at the claudin 7 loci between tetrapods and teleosts. Therefore, no reclassification is proposed. *Claudin 8 and 17* – vertebrate claudin 8 is monophyletic only with the inclusion of claudin 17, which is present only in tetrapods (86% ccs, Fig. 2C). Homology was supported by genomic synteny, suggesting mammal claudin 8 and claudin 17 are paralogs (Fig. B3.A; Appendix B). A reclassification of tetrapod claudin 8 to claudin 8α, and claudin 17 to claudin 8β, is proposed. Zebrafish *cldn17* is an ortholog of pufferfish *cldn8c* (100% ccs). *Claudin 13* – no homology was observed between mouse and pufferfish claudin 13 (Fig. 2D,E) despite both genes being in relative proximity to claudin 4-related genes (Fig. B5; Appendix B). Our inference suggests teleost claudin 13 is ancestral to the expansion of the largest claudin superclade (Fig. 2A,E). Reclassifying *T. rubripes cldn13* to a new group, claudin 36, is proposed. *Claudin 14* – with the exclusion of teleost *cldn14b*, all vertebrate claudin 14's form a monophyletic group (100% ccs, Fig. 1D). Reclassification of pufferfish *cldn14b* and zebrafish *LOC568833* to claudin 34 is proposed. *Claudin 18* – a unified clade of all vertebrate claudin 18 sequences also includes the outgroup sequences (*CldnD1*, *CldnD2*, *Pmp22*, and *TMEM204*) used for polarization of the unrooted tree (86% ccs, Fig. 1H). Genomic synteny suggests homology for mammal and Fugu claudin 18, however chromosomal rearrangement has yielded equivocal evidence for homology of this gene in the zebrafish (Fig. B2.D; Appendix B). No revision is currently proposed. *Claudin 21* – Currently there are no genes with the designation claudin 21. Human *CLDN21* was described by Katoh and Katoh (2003) at locus *4q35.1*, but this gene was reclassified as *CLDN24* in later assemblies (GRCh37; Genome Reference Consortium Build 37, April 2009). In the mouse, *Cldn21* is annotated in GRC assembly 37 (April 2007, current *Ensembl*

version) at chromosome 9, but was reclassified as *Cldn25* in GRC assembly 37.2 (March 2011, current NCBI version). The *Cldn25* identified in the earlier assembly was then reclassified as claudin domain containing 1 (*CldnD1*, chromosome 16, v37.2). No teleost claudin 21 has been described. The closing of this group to avoid further ambiguity is proposed. *Claudins 22 and 24* – mammal claudin 22 is monophyletic only with the inclusion of claudin 24, a paralog gene in our analysis (83% ccs, Fig. 1F, and Fig. B2.A; Appendix B). No identifiable homolog has been found in teleost fishes. Redesignation of mammal *Cldn22* and *Cldn24* to *Cldn22α* and *Cldn22β* (respectively) is proposed. *Claudin 25* and *26* – mammal claudin 25 is not homologous to teleost claudin 25. Human and mouse claudin 25 are monophyletic and ancestral to claudins 22 and 24 (100% ccs, Fig. 1F), while pufferfish *cldn25* and *cldn26* are homologs of *D. rerio* claudin 15-like (100% ccs, Fig. 1B). Reclassification of *T. rubripes cldn25* and *cldn26* to *cldn15la* and *cldn15lb*, respectively, is proposed. The group designation claudin 26 should be closed to avoid future ambiguity. *Claudins 27* and *28*—claudin 27 is paraphyletic as currently described. Claudins 27a and 27c form a monophyletic clade ancestral to claudin 28 (100% ccs), while *cldn27b* and *cldn27d* group within claudin 28 (97% ccs, Fig. 2D). Reclassification of *cldn27b* and *cldn27d* to *cldn28d* and *cldn28e*, respectively, is proposed. To avoid future ambiguity, *cldn27a* and *cldn27c* should be assigned to a new group, claudin 37 (*cldn37a* and *cldn37b*, respectively). *Claudin 32* – claudin 32a is not homologous to claudin 32b (Fig 2D,E). Reclassification of *T. rubripes cldn32b* and *D. rerio LOC570842* to a new group, claudin 35, is proposed (Fig. 2E). This would accompany reclassification of orthologs *T. rubripes cldn32a* and *D. rerio cldni* to claudin 32, proper. *Claudin 33*—claudins 33a and 33b are monophyletic, however claudin

33c forms an ancestral clade to claudins 22, 24 and 25 (Fig. 1F, 100% ccs, and Fig. B4; Appendix B). Reclassification of claudin 33c to claudin 25-like is proposed.

mRNA expression of zebrafish claudins

As duplicate genes could be nonfunctional (pseudogenes), another objective was to determine the proportion of the identified claudins expressed as mRNA. Forty-three claudins were detected in a panel of 8 discrete tissue cDNA preparations. Zebrafish *cldn7a* was expressed ubiquitously, while *cldn5b*, *cldn5a,* and *cldn11a* were detected in all but one tissue type (Fig. 4). Other claudins were expressed only in a single tissue: *cldn8l* (brain), *cldn10c* and *cldn10e* (gill), *cldn10d* (spleen), *cldn18* (kidney), and *cldn33a* (testes). With the exception of *cldn10c* and *cldn10e,* all claudin group paralogs exhibited unique expression patterns (Fig 4). Nine zebrafish claudins were not detected in our tissue profile but were detected in cDNA preparations obtained from whole (homogenized) fish: *cldn5c*, *cldn8a, cldn15b, cldn15la, cldn5lb, cldn16, cldn29a, cldn31b,* and *cldn34* (data not shown). All amplicons were sequenced and validated against the targeted claudin sequence by BLASTn search or by pair-wise BLAST sequence alignment (*Blast2align*) (Table B5; Appendix B).

Two zebrafish claudins, *cldn10a* and *cldn23a2*, were not detected in our expression analysis (tissue profile or whole fish cDNA). A search of the NCBI zebrafish EST database identified an available embryonic cDNA clone (Agencourt) for *cldn23a2* GenBank: CN0248601.1, suggesting the expression of this claudin may be ontogenetically regulated (MegaBLAST

search, 98% sequence identity, e value = 0.0). A similar search for zebrafish *cldn10a* yielded no significant results.

Functional analysis of major claudin groups

The nucleotide sequences reported here (Table B1; Appendix B) encode claudin proteins with an average length of 240 amino acids and a predicted molecular weight of 26 kDa. The zebrafish claudins exhibited typical tetraspan transmembrane structure with two conserved extracellular loops, one intracellular loop, a short internal amino terminal sequence and a carboxy terminal cytoplasmic domain of variable length (Fig. 5). One exceptional claudin (*cldn10c*) is considerably longer than the others (440 amino acids), has a predicted molecular weight of 48.3 kDa, and contains five predicted transmembrane domains.

The first claudin extracellular loop (ECL1) contains the signature residues tryptophan, glycine, and leucine [W-GLW] (Van Itallie and Anderson, 2006) followed by two cysteine residues [C-C] involved in the barrier function (Wen *et al.*, 2004). The [W-GLW] motif is conserved in all zebrafish claudins except 'non-classic' claudins from the superclade shown in Fig. 1B, which have a [W-NLW] motif (Fig. 5). The [C-C] motif is conserved in the ECL1 of all zebrafish claudins (Fig. 5).

In addition to these two characteristic motifs, the ECL1 contains several acidic and basic residues that determine charge- and size-selectivity of channels or pores formed between claudins, allowing for paracellular permeability of select ions and small molecules (Colegio

et al., 2002, 2003; Krause *et al.*, 2008; Angelow and Yu, 2009; Lal-Nag and Morin, 2009). The ECL1 sequences of 'classic' zebrafish claudins are conserved, whereas those of 'non-classic' claudins are less so (Fig. 5) as similarly observed in mouse (Krause *et al.*, 2008) and human (Lal-Nag and Morin, 2009). The ECL1 of 'classic' claudins typically contain a combination of three positive residues (lysines [K] and/or arginines [R]) and three negative residues (glutamic acids [E] and/or aspartic acids [D]) imparting a net neutral charge to the loop (Fig. 5). Ordering of these residues is as follows: [K/R-E/D-K-D-D-R]. Although the locations of these residues are conserved in claudins depicted in Figs. 2E, 2D, 2C, and 2B, they appear in slightly different positions (by alignment) in claudins from superclades shown in Figs. 1C and 1D (see Fig. 5). A notable exception among the 'classic' claudins includes the four claudin 8 isoforms (Fig. 2C), which contain an additional 2 [D/E] and 1 or 3 [R] residues. Multiple copies of claudin 8 in fishes and their grouping in relation to mammalian claudin 8 orthologs (Fig. 2C) suggest gene duplication followed by possible neofunctionalization. In contrast, the ECL1 of 'non-classic' claudins have a greater number of charged residues and the positions of such residues appear less conserved (not shown).

Claudins of opposing cell membranes dimerize (i.e., *trans*-interact) through hydrophobic association of aromatic residues in the second extracellular loop (ECL2) (Angelow *et al.*, 2008) and all of the zebrafish claudins contain conserved [W], tyrosine [Y], and phenylalanine [F] residues required for such interactions (Fig. 5). The ECL2 of mammalian claudins typically consists of a helix-turn-helix motif (Krause *et al.*, 2009), however alignment of zebrafish ECL2 regions clearly resolve four distinct functional groupings and

the consensus sequences of three of these groups are shown in Fig. 5. ‘Classic’ claudins belonging to the superclades depicted in Figs. 2B, 2C, 2D, and 2E contain an ECL2 with a predicted sheet-turn-helix motif, whereas that of the remaining two ‘classic’ claudin superclades (Figs. 1C and 1D) are predicted to have a sheet-turn motif. This indicates that the ECL2 of these two groups of ‘classic’ claudins form hairpins, albeit of different secondary structures and suggestive of different *trans*-interacting characteristics.

The ‘non-classic’ claudins resolve into one group with an ECL2 helix-turn motif (Fig. 1B) and another group that has low consensus (superclades Figs. 1E, 1F, 1G, and 1H). Interestingly, ‘non-classic’ zebrafish claudins typically lack a second proline [P] in the ECL2 that is present in the ‘classic’ claudins (Fig. 5) and this may influence hairpin formation.

Discussion

Claudins are the dominant constituents of cellular tight junctions and both their abundance and composition confer selective properties of paracellular ion flux across vertebrate tissues (Krause *et al.*, 2009; Van Itallie *et al.*, 2006). The zebrafish, despite its status as one of the five major vertebrate models, is poorly annotated with respect to the diversity of the claudin members present in this species. In this study, our objectives were to review accessioned sequence records currently available through NCBI *Gene* and *Ensembl*, and identify both known and unknown zebrafish claudins based on their homology to known claudins from other well-studied vertebrate genomes: human, mouse, Fugu, and *Xenopus tropicalis*. To promote better comparative inference across taxa, the zebrafish claudins were then

reclassified under a proposed interim scheme, designed to create a unified framework for all vertebrate groups, reflective of shared evolutionary descent. Additionally, we report zebrafish claudin mRNA expression by tissue profiles and functionally examine select features in the polypeptide sequences of claudin groups. This work was undertaken to aid future investigations of claudin function in the zebrafish developmental model, and to facilitate further hypothesis testing in other vertebrate groups.

From a comprehensive review of 88 claudin and *claudin-related* sequences, 54 claudins were identified in the zebrafish (Table B1; Appendix B). These sequences were used with other vertebrate claudins (197 sequences, Table B2; Appendix B) in an unrooted Bayesian phylogenetic analysis, which was then tested using four prominent model assumptions in the literature (substitution probability matrices: *Poisson, Equalin, Blosum62,* and *WAG*). The consensus trees were then tested together for significant differences in log-likelihood score by the S-H test for alternate evolutionary hypotheses (Shimodaira *et al.,* 1999). Homology of all vertebrate claudin groups was determined by the inclusion of outgroup sequences. To date, this work comprises the most comprehensive dataset, and one of the most computationally difficult methods of analysis, ever used to infer the evolutionary history of vertebrate claudins (Kollmar *et al.,* 2001; Krause, *et al.* 2009; Loh, *et al.* 2004; Tipsmark *et al.,* 2008b). At its core, evolutionary inference is merely a hypothesis, and we sought to support our findings when needed by additional evidence gathered from genomic synteny (Fig. 3, S1-5). Fifty-one zebrafish claudins were homologous to at least one claudin previously described by Loh and colleagues (2004) in the pufferfish, *T. rubripes*. Orthologs

of three zebrafish claudins, *LOC793915* (*cldn16*), *zgc:63990* (*cldn12l*), and cldng (*cldn5l*) have yet to be identified in pufferfish. Additionally, subsequent to our analysis, two putative claudins were discovered in the zebrafish genomic assembly (Zv9, *Ensembl*): *ENSDART 00000126328* and *ENSDART 00000076524.* Identified tentatively as zebrafish *cldn36* and *cldn34b* respectively, their appearance illustrates that gene discovery is ongoing; as accessioned sequence records and assemblies are continuously updated and revised.

Gene names are discovery based, and reflect observed phenotypes, function, or esoteric whims of the discoverer (e.g., *cheap date*, *kryptonite*), yet these names are essentially meaningless if orthologs cannot easily be identified in other groups. Our analysis provided the opportunity to infer evolutionary relationships of claudins across vertebrates, and assess how well accepted gene names identify homology in other groups. Zebrafish claudins containing alphabetical names (*cldna-k*) have clear orthologs in pufferfish, which have numerical designations (Fig. 1, 2). In mammals, lineage-specific gene duplicates (paralogs) are not identified as such, and these names have been erroneously assigned to genes in fishes (claudin 6 and claudin 9, claudin 8 and 17, claudin 22 and 24; Fig. 1-2, S2-3). To address this problem, we have proposed a reclassification for major claudin groups based upon our analysis of six commonly studied vertebrate models: human, mouse, zebrafish, Fugu, and *Xenopus tropicalis*. Nomenclature commissions strictly regulate the use of gene names. However, our goal is to provide a comprehensive tool for investigators in the interim. The closing of claudin groups 9, 13, 17, 21, 24, 26 and 27 is recommended to avoid future ambiguity. New, provisional groups are also proposed where homology could not be

assigned or is contradictory to previous designations: 4-like, 5-like, 8-like, 25-like, 34, 35, 36, and 37 (Table B3; Appendix B). These changes are designed to minimally affect current usage, yet convey needed evidence for common descent.

The mRNA expression of 43 zebrafish claudins were observed in a panel of eight discrete tissue types (Fig. 4), with an additional 9 claudins detected from whole fish cDNA. Only one claudin, zebrafish *cldn10a*, had no evidence for expression, either in our analysis or by searches of accessioned Expressed Sequence Tags (EST). Additionally, paralog claudins nearly always possessed distinct tissue expressional profiles, which may suggest sub-functionalization for teleost claudins. Some paralogs, such as *cldn10c*, *cldn10d*, and *cldn10e*, were restricted to expression by single tissue types (Fig. 4). These findings are significant to the study of gene and genome duplication events, where gene duplicates have the theoretical potential to neofunctionalize, due to relaxation of selection pressures (Conant *et al.*, 2008; Ohno 1970). Expansion of the claudin gene family in teleost fishes, paired with unique gain of function/loss of function techniques available in the zebrafish model, could provide an interesting case study for assessing the link between duplication and the development of evolutionary novelty.

It is postulated that a net excess of positively or negatively charged residues in the ECL1 of claudins promotes formation of paracellular anion or cation pores, respectively, between trans-interacting caudins (Krause *et al.*, 2008). Various studies in mouse and human collectively suggest that ‘classic’ claudins are involved in processes that reduce paracellular

permeability (Krause *et al.*, 2008). The overall conservation of six charged residues in the ECL1 of 'classic' zebrafish claudins (Fig. 5) may impart a similar functional property as an equal proportion of unequally charged residues leads to a tight interaction (Krause *et al.*, 2009). Additionally, Colegio *et al.* (2002) have reported that offsetting the net charge by substituting a negative for a positive residue at one of these conserved sites in ECL1 of human *CLDN4* increases paracellular Na^+ permeability. Therefore, 'classic' zebrafish claudins consisting of those belonging to superclades depicted in Figs. 1C, 1D, 2B, 2C, 2D, and 2E may function in tight junctions characteristic of low paracellular permeability to water.

Since 'non-classic' claudins typically appear to increase paracellular permeability to various ions and claudin composition within tight junctions is thought to influence paracellular permeability properties (review: Krause *et al.*, 2008), structural variation in this particular class of claudins is not surprising. Comparatively less is known of the functional properties of basic and acidic residues in the ECL1 of 'non-classic' claudins, thus they pose interesting targets for future investigations that employ site directed mutagenesis (see: Wen *et al.*, 2004; Piontek *et al.*, 2008; Angelow and Yu, 2009). For example, Colegio *et al.* (2002) reported that substituting all of the acidic with basic residues in the ECL1 of human *CLDN15* reverses paracellular permeability from cations to anions. These findings collectively suggest that 'non-classic' claudins may participate in formation of leaky junctions and variation in their composition at tight junction sites influences paracellular permeability characteristics (e.g., anion, cation, etc.). Finally, future investigations of *trans*-interactions will be required to

elucidate the significance of structural differences in the ECL2 of 'non-classic' zebrafish claudins, which may relate to cell-matrix interactions that regulate cell differentiation or proliferation in addition to that of tight junction formation (see: Angelow *et al.*, 2008; Heiskala *et al.*, 2001).

Here, we describe the molecular structures, homology, and mRNA expressions of 54 unique zebrafish claudins in the most recent annotated zebrafish genome (*Zv9*). In order to resolve ambiguity and promote future gene discovery with correct classification, we propose a unified interim nomenclature based upon shared evolutionary history of vertebrate claudins. Additionally, we classify zebrafish claudins into broad functional groups based upon the structures and features of the ECL1 and ECL2. This work was undertaken to provide investigators with better insight into the evolutionary relationships and functionality of vertebrate claudins, and to facilitate future hypothesis testing from a comparative approach.

Acknowledgements

The authors would like to thank Dr. John Godwin (NC State University, Raleigh) for providing the zebrafish (Tuebingen) used in this study. This study was funded by the National Science Foundation and the United States Department of Agriculture.

REFERENCES

Abdelilah-Seyfried, S., 2010. Claudin-5a in developing zebrafish brain barriers: another brick in the wall. *BioEssays* 32, 768-776.

Angelow, S., Yu, A.S.L., 2009. Structure-function studies of claudin extracellular domains by cysteine-scanning mutagenesis. *J Biol Chem* 284, 29205-29217.

Angelow, S., *et al.*, 2008. Biology of claudins. *Am J Physiol Renal Physiol* 295, F867-876.

Bagherie-Lachidan, *et al.*, 2008. Claudin-3 tight junction proteins in *Tetraodon nigroviridis*: cloning, tissue-specific expression, and a role in hydromineral balance. *Am J Physiol Regul Integr Comp Physiol* 294, R1638-1647.

Bishop, M.J., Friday, A.E., 1987. Tetrapod relationships: the molecular evidence, in: Patterson, C. (Ed.) Molecules and morphology in evolution. Cambridge University Press, Cambridge (UK), pp 123-139

Cheung, I.D., *et al.*, 2011. Regulation of intrahepatic biliary duct morphogenesis by Claudin 15-like b. *Dev Biol* 361, 68-78.

Colegio, O.R., *et al.*, 2002. Claudins create charge-selective channels in the paracellular pathway between epithelial cells. *Am J Cell Physiol* 283, C142-147.

Colegio, O.R., *et al.*, 2003. Claudin extracellular domains determine paracellular charge selectivity and resistance but not tight junction fibril architecture. *Am J Physiol Cell Physiol* 284:C1346-1354.

Conant, G.C., Wolfe, K.H., 2008. Turning a hobby into a job: How duplicated genes find new functions. *Nat Rev Genet* 9, 938-950.

D'Souza, T., *et al.*, 2005. Phosphorylation of claudin-3 at threonine 192 by cAMP-dependent protein kinase regulates tight junction barrier function in ovarian cancer cells. *J Biol Chem* 280, 26233-26240.

Dayhoff, M.O., *et al.*, 1978. A model of evolutionary change in proteins. pp 345-352 in: Atlas of protein sequence and structure. Vol. 5(S3). National Biomedical Research Foundation, Washington, D.C.

Felsenstein, J., 1981. Evolutionary trees from DNA sequences: A maximum likelihood approach. *J Mol Evolution* 17, 368-376.

Hardison, A.L., *et al.*, 2005. The zebrafish gene claudinj is essential for normal ear function and important for the formation of the otoliths. *Mech Dev* 122, 949-958.

Heiskala, M., *et al.*, 2001. The roles of claudin superfamily proteins in paracellular transport. *Traffic* 2:92-98.

Henikoff, S., Henikoff, J.G., 1992. Amino acid substitution matrices from protein blocks. *Proc Nat Acad Sci USA* 89, 10915-10919.

Hewitt, K.J., *et al.*, 2006. The claudin gene family: expression in normal and neoplastic tissues. *BMC Cancer* 6, 186.

Huelsenbeck, J.P., Ronquist, F., 2001. MRBAYES: Bayesian inference of phylogenetic trees. *Bioinformatics* 17, 754-755.

Jeong, J.Y., *et al.*, 2008. Functional and developmental analysis of the blood-brain barrier in zebrafish. *Brain Res Bull* 75, 619-628.

Jones, D.T., *et al.*, 1992. The rapid generation of mutation data matrices from protein sequences. *Comput. Appl. Biosci*. 8, 275-282.

Katoh, M., Katoh, M., 2003. CLDN23 gene, frequently down-regulated in intestinal-type gastric cancer, is a novel member of CLAUDIN gene family. *Int J Mol Med* 11, 683-689.

Kollmar, R., *et al.*, 2001. Expression and phylogeny of claudins in vertebrate primordia. *Proc Natl Acad Sci USA* 98, 10196-10201.

Krause, G., *et al.*, 2008. Structure and function of claudins. *Biochim Biophys Acta* 1778, 631-645.

Krause, G., *et al.*, 2009. Structure and function of extracellular claudin domains. *Ann N Y Acad Sci* 1165, 34-43.

Lal-Nag, M., Morin, P.J., 2009. The claudins. *Genome Biol* 10, 235 doi:10.1186/gb-2009-10-8-235.

Le Moellic, C., *et al.*, 2005. Aldosterone and tight junctions: modulation of claudin-4 phosphorylation in renal collecting duct cells. *Am J Physiol Cell Physiol* 289, C1513-1521.

Loh, Y.H., *et al.*, 2004. Extensive expansion of the claudin gene family in the teleost fish, *Fugu rubripes*. *Genome Res* 14, 1248-1257.

Lu, G., Moriyama, E.N., 2004. Vector NTI, a balanced all-in-one sequence analysis suite. *Brief Bioinform* 5, 378-388.

Miller, M.A., *et al.*, 2010. Creating the CIPRES Science Gateway for inference of large phylogenetic trees, Gateway Computing Environments Workshop (GCE), New Orleans, LA.

Münzel, E.J., *et al.*, 2011. Claudin k is specifically expressed in cells that form myelin during development of the nervous system and regeneration of the optic nerve in adult zebrafish. *Glia* 60, 253-70

Nilsson, H., *et al.*, 2007. Effects of hyperosmotic stress on cultured airway epithelial cells. *Cell Tissue Res* 330, 257-269.

Ohno, S., 1970. Evolution by gene duplication. Springer-Verlag, Heidelberg.

Ohta, H., *et al.*, 2006. Restricted localization of claudin-16 at the tight junction in the thick ascending limb of Henle's loop together with claudins 3, 4, and 10 in bovine nephrons. *J Vet Med Sci* 68, 453-463.

Piontek, J., *et al.*, 2008. Formation of tight junction: determinants of homophilic interaction between classic claudins. *FASEB* J 22, 146-158.

Povey S., *et al.*, 2001. The HUGO Gene Nomenclature Committee (HGNC). *Hum Genet* 109:678-680.

Satake, S., *et al.*, 2008. Cdx2 transcription factor regulates claudin-3 and claudin-4 expression during intestinal differentiation of gastric carcinoma. *Pathol Int* 58, 156-163.

Schmidt, H.A., *et al.*, 2002. TREE-PUZZLE: maximum likelihood phylogenetic analysis using quartets and parallel computing. *Bioinformatics* 18, 502-504.

Schultz, J., *et al.*, 1998. SMART, a simple modular architecture research tool: Identification of signaling domains. *Proc Natl Acad Sci USA* 95, 5857-5864.

Shimodaira, H., Hasegawa, M., 1999. Multiple comparisons of log-likelihoods with applications to phylogenetic inference. *Mol Biol Evol* 16, 1114-1116.

Siddiqui, M., *et al.*, 2010. The tight junction component Claudin E is required for zebrafish epiboly. *Dev Dynamics* 239, 715-722.

Thompson, J.D., *et al.*, 1994. CLUSTALW: improving the sensitivity of progressive multiple sequence alignment through sequence weighting, position-specific gap penalties and weight matrix choice. *Nucleic Acids Res* 22, 4673-4680.

Thompson, J.D., *et al.*, 1997. The CLUSTAL_X windows interface: flexible strategies for multiple sequence alignment aided by quality analysis tools. *Nucleic Acids Res* 25, 4876-4882.

Tipsmark, C.K., *et al.*, 2008a. Salinity regulates claudin mRNA and protein expression in the teleost gill. *Am J Physiol Regul Integr Comp Physiol* 294, R1004-1014.

Tipsmark, C.K., *et al.*, 2008b. Branchial expression patterns of claudin isoforms in Atlantic salmon during seawater acclimation and smoltification. *Am J Physiol Regul Integr Comp Physiol* 294, R1563-1574.

Van Itallie, C.M., Anderson, J.M., 2006. Claudins and epithelial paracellular transport. *Annu Rev Physiol* 68, 403-429.

Wen, H., *et al.*, 2004. Selective decrease in paracellular conductance of tight junctions: role of the first extracellular domain of claudin-5. *Mol Cell Biol* 24, 8408-17

Whelan, S., Goldman, N., 2001. A general empirical model of protein evolution derived from multiple protein families using a maximum-likelihood approach. *Mol Biol Evol* 18, 691-699.

Winkler, L., *et al.*, 2009. Molecular determinants of the interaction between *Clostridium perfringens* enterotoxin fragments and Claudin-3. *J Biol Chem* 284, 18863-18872.

Zhang, J., *et al.*, 2010. Establishment of a neuroepithelial barrier by Claudin5a is essential for zebrafish brain ventricular lumen expansion. *Proc Natl Acad Sci USA* 107, 1425-1430.

Figure 1. Bayesian phylogeny of vertebrate claudin protein sequences. **(A)** Unrooted radial consensus tree from analysis using the WAG substitution model (best log-likelihood score). Taxa sequences were "pruned" from the tree, with the major branches circled for better depiction in cladogram format (B-H). The largest branch of claudins (shaded) is depicted in Figure 2. The relative position of outgroups *CldnD1*, *CldnD2*, *Pmp22*, and *TMEM204* are shown but not depicted (treefile available in Supplemental Information). Branch length scale represents 0.1 amino acid substitutions per site (**B**) vertebrate claudin groups 10, 15, and 15-like (*15-l*). (**C**) claudin groups 1, 7, and 19. (**D**) claudin groups 2, 14, and 20. (**E**) claudin groups 11 and 16. (**F**) claudin groups 22, 25, 25-like (*25-l*), 33, and 34. (**G**) claudin groups 12, 12-like (*12-l*), and 23. (**H**) claudin 18. Taxon labels denote the abbreviated scientific name (Dr, *Danio rerio*; Hs, *Homo sapiens*; Mm, *Mus musculus*; Tr, *Takifugu rubripes*; Xt, *Xenopus tropicalis*) followed by the current (accepted) claudin group designation. Proposed changes to nomenclature are shown in parentheses. Large grey numerals and dots on the tree indicate the monophyletic origin of a major claudin group. Small font numerals at each node represent clade-credibility values (percent of total Bayesian trees supporting each node in the consensus tree). Zebrafish claudin sequences are in bold font. Mouse *Cldn24* and *LOC100045502* are identical sequences (double asterisks; see F).

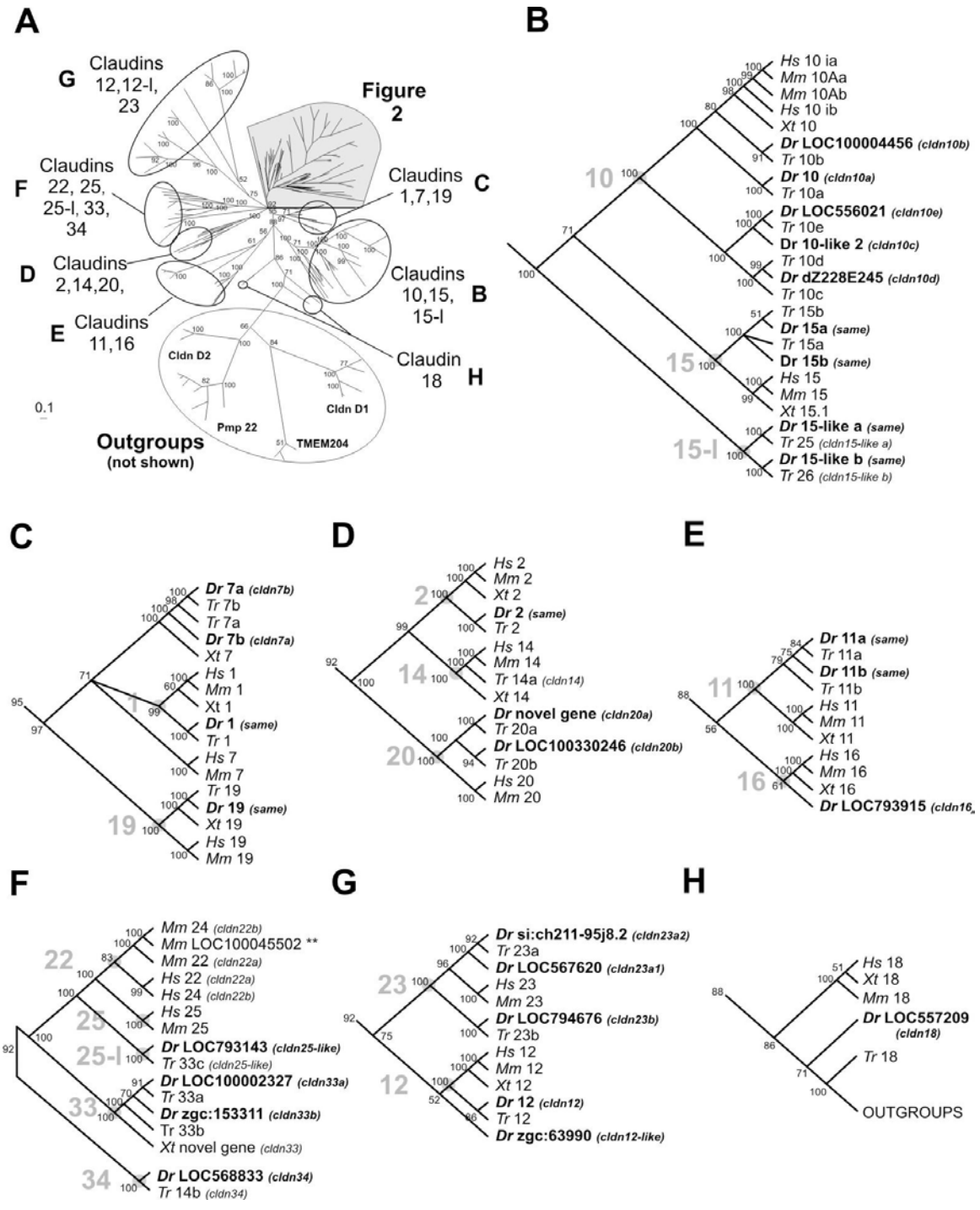
A
G
Claudins
12,12-l,
23
Figure
2
Claudins
22, 25,
25-l, 33,
34
F
Claudins
1,7,19
C
D
Claudins
2,14,20,
Claudins
10,15,
15-l
B
E
Claudins
11,16
Cldn D2
Claudin
18
H
0.1
Cldn D1
Pmp 22
TMEM204
Outgroups
(not shown)
B
Hs 10 ia
Mm 10Aa
Mm 10Ab
Hs 10 ib
Xt 10
Dr LOC100004456 (cldn10b)
Tr 10b
Dr 10 (cldn10a)
Tr 10a
Dr LOC556021 (cldn10e)
Tr 10e
Dr 10-like 2 (cldn10c)
Tr 10d
Dr dZ228E245 (cldn10d)
Tr 10c
Tr 15b
Dr 15a (same)
Tr 15a
Dr 15b (same)
Hs 15
Mm 15
Xt 15.1
Dr 15-like a (same)
Tr 25 (cldn15-like a)
Dr 15-like b (same)
Tr 26 (cldn15-like b)
10
15
15-l
C
Dr 7a (cldn7b)
Tr 7b
Tr 7a
Dr 7b (cldn7a)
Xt 7
Hs 1
Mm 1
Xt 1
Dr 1 (same)
Tr 1
Hs 7
Mm 7
Tr 19
Dr 19 (same)
Xt 19
Hs 19
Mm 19
1
19
D
Hs 2
Mm 2
Xt 2
Dr 2 (same)
Tr 2
Hs 14
Mm 14
Tr 14a (cldn14)
Xt 14
Dr novel gene (cldn20a)
Tr 20a
Dr LOC100330246 (cldn20b)
Tr 20b
Hs 20
Mm 20
2
14
20
E
Dr 11a (same)
Tr 11a
Dr 11b (same)
Tr 11b
Hs 11
Mm 11
Xt 11
Hs 16
Mm 16
Xt 16
Dr LOC793915 (cldn16
11
16
F
Mm 24 (cldn22b)
Mm LOC100045502 **
Mm 22 (cldn22a)
Hs 22 (cldn22a)
Hs 24 (cldn22b)
Hs 25
Mm 25
Dr LOC793143 (cldn25-like)
Tr 33c (cldn25-like)
Dr LOC100002327 (cldn33a)
Tr 33a
Dr zgc:153311 (cldn33b)
Tr 33b
Xt novel gene (cldn33)
Dr LOC568833 (cldn34)
Tr 14b (cldn34)
22
25
25-l
33
34
G
Dr si:ch211-95j8.2 (cldn23a2)
Tr 23a
Dr LOC567620 (cldn23a1)
Hs 23
Mm 23
Dr LOC794676 (cldn23b)
Tr 23b
Hs 12
Mm 12
Xt 12
Dr 12 (cldn12)
Tr 12
Dr zgc:63990 (cldn12-like)
23
12
H
Hs 18
Xt 18
Mm 18
Dr LOC557209
(cldn18)
Tr 18
OUTGROUPS

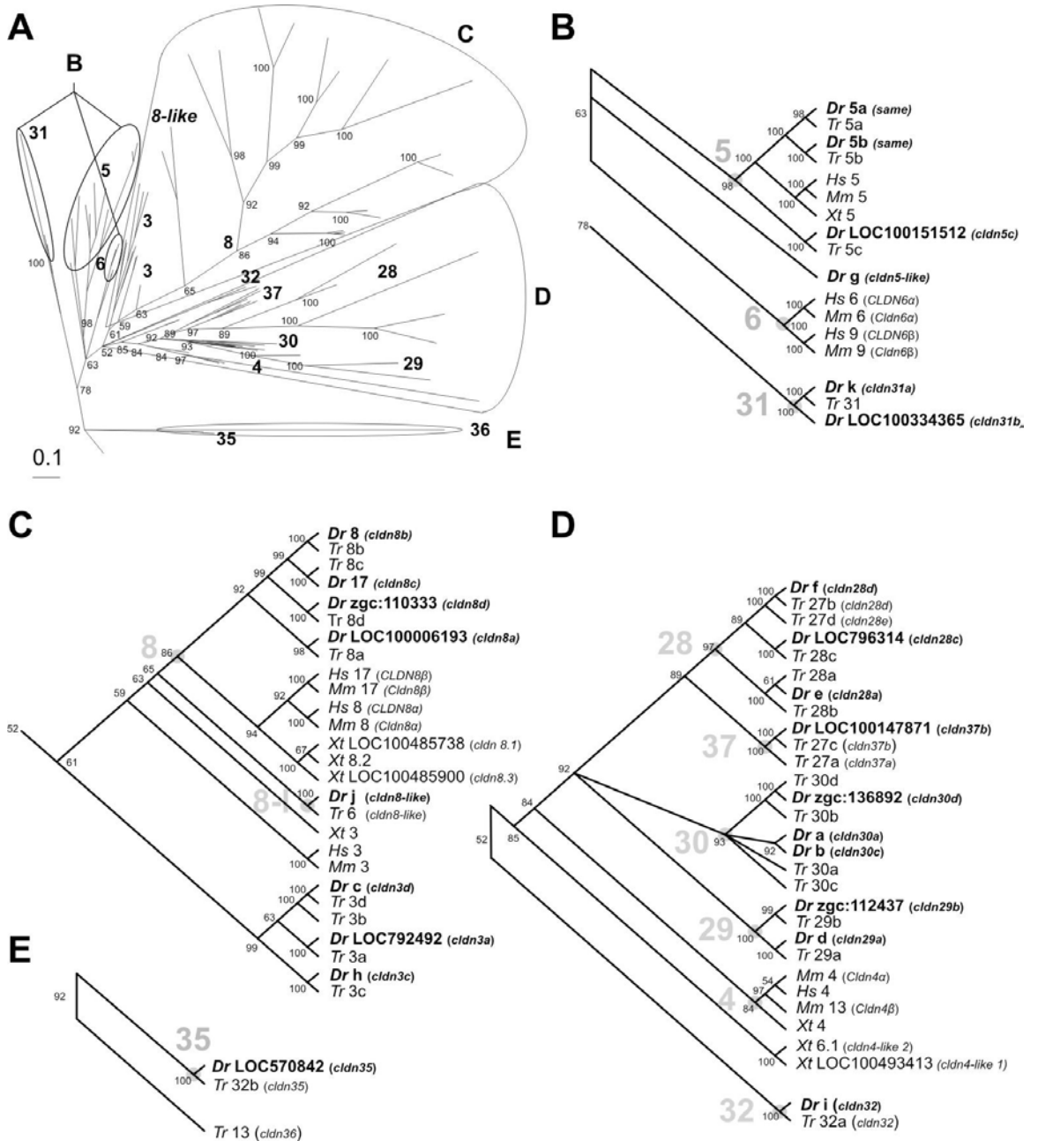

Figure 2. Phylogeny of vertebrate claudins (continued)**. (A)** Unrooted radial consensus tree of the largest claudin superclade (from Figure 1). Taxa sequences are pruned and depicted as subgroups in cladogram format (B-E). The position of claudin groups on the radial tree are indicated with bold font. Branch length scale represents 0.1 amino acid substitutions per site. (**B**) claudin groups 5, 5-like, 6, and 31. (**C**) claudin groups 3, 8, and 8-like. (**D**) claudin groups 4, 4-like, 28, 29, 30, 32, and 37. (**E**) claudin groups 35 and 36. Taxon labels and symbols are as described in Figure 1.

Figure 3. Homologous loci containing claudin 7 and claudin 15 homologs in Fugu and zebrafish genomic assemblies. (**A**) claudin 7a and claudin 7b. (**B**) claudin 15a and claudin 15b. The orthology of zebrafish claudins, when unresolved by phylogeny (Figures 1, 2), were identified by genomic synteny. The existing nomenclature incorrectly assigns orthology to zebrafish *cldn7a* (now reclassified as *cldn7b*) and *cldn7b* (now reclassified as *cldn7a*), but is correctly assigned for zebrafish *cldn15a* and *cldn15b*. Gene and inter-gene distances depicted are for illustrative purposes only and are not to relative scale. *Symbols*: empty box, claudin gene (group ortholog); hatched box, genes with no observable ortholog in compared regions; black box, orthologous genes across loci; shaded box, homologous genes giving alternate evidence for paralog identity; rc, reverse complemented sequence. *Gene abbreviations*: *chrnb1*, cholinergic receptor, nicotinic, beta 1; *fgf11*, fibroblast growth factor 11; *fis1*, fission 1; *gpr65*, G protein coupled receptor 65; *grk1b*, G protein-coupled receptor kinase 1 b; *kcnip1*, Kv channel interacting protein 1; *lsmd1*, LSM domain containing 1; *npm1*, nucleophosmin 1; *prki*, protein-kinase, interferon-inducible; *sat2*, spermine N1-acetyltransferase family member 2; *ugt5g1*, UDP glucuronosyltransferase 5 family, polypeptide G1. *Genome assembly regions* (Ensembl): Fugu (*v4*)—(*cldn7a*) scaffold_6: 271,571-323,547 (nt); (*cldn7b*) scaffold_276: 193,528-320,757; (*cldn15a*) scaffold_63: 1,148,610-1,161,616; (*cldn15b*) scaffold_6: 1,983,619-1,995,310; zebrafish (*Zv9*)—(*cldn7a*) Chromosome 7: 23,566,760-23,876,679; (*cldn7b*) Chromosome 10: 22,203,960-22,449,654 (reverse complement); (*cldn15a*) Chromosome 7: 21,949,415-22,003,543; (*cldn15b*) Chromosome 5: 63,250,685-63,622,810.

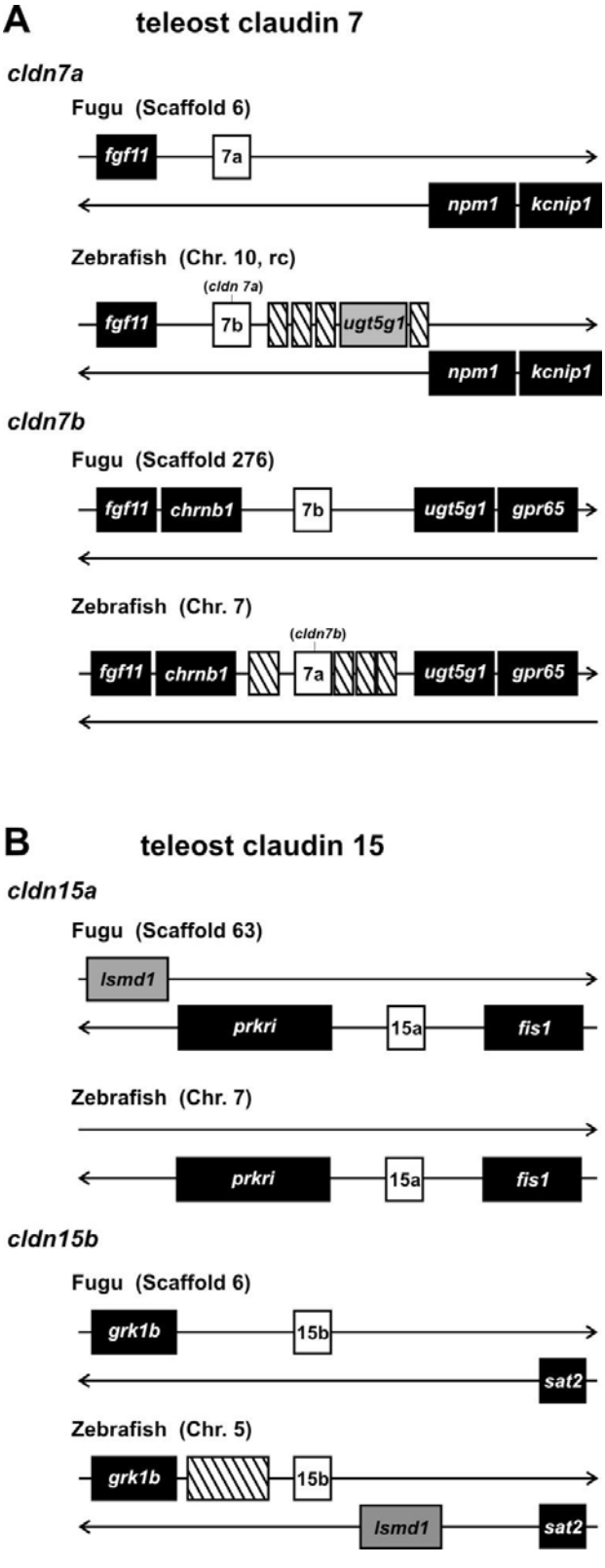
A
teleost claudin 7
cldn7a
Fugu (Scaffold 6)
fgf11
7a
npm1
kcnip1
Zebrafish (Chr. 10, rc)
(cldn 7a)
fgf11
7b
ugt5g1
npm1
kcnip1
cldn7b
Fugu (Scaffold 276)
fgf11
chrnb1
7b
ugt5g1
gpr65
Zebrafish (Chr. 7)
(cldn7b)
fgf11
chrnb1
7a
ugt5g1
gpr65
B
teleost claudin 15
cldn15a
Fugu (Scaffold 63)
lsmd1
prkri
15a
fis1
Zebrafish (Chr. 7)
prkri
15a
fis1
cldn15b
Fugu (Scaffold 6)
grk1b
15b
sat2
Zebrafish (Chr. 5)
grk1b
15b
lsmd1
sat2

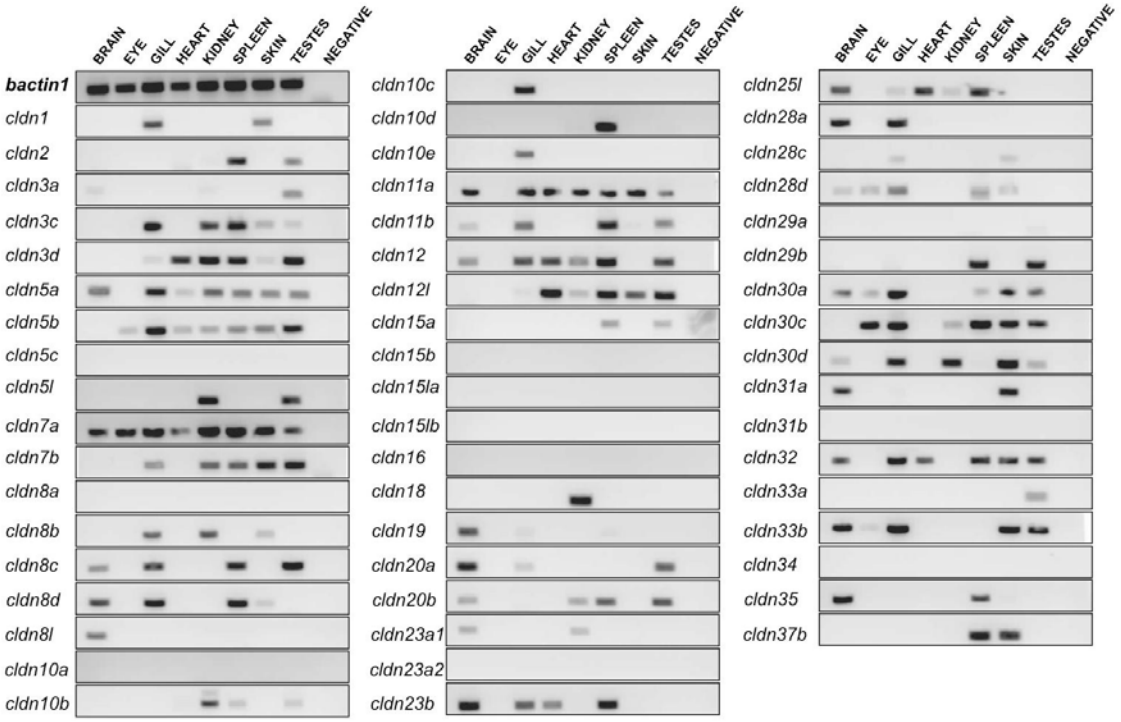

Figure 4. Tissue expression profile of zebrafish claudins**.** Endpoint (plus/minus) PCR assay of identified zebrafish claudins using prepared cDNA derived from the following tissues: brain (whole), eye, gill, heart, kidney (whole), spleen, skin, and testes. *Controls*: zebrafish beta actin (*bactin1*) was used as a positive control for all tissues, sterile water as a negative control. One microgram of total RNA was used as template for all cDNA preparations. All claudin gene symbols reflect proposed claudin nomenclature in the interim reclassification scheme (listed in Table B1; Appendix B). The photographed gel images were reverse contrasted for better band visualization and printing efficiency.

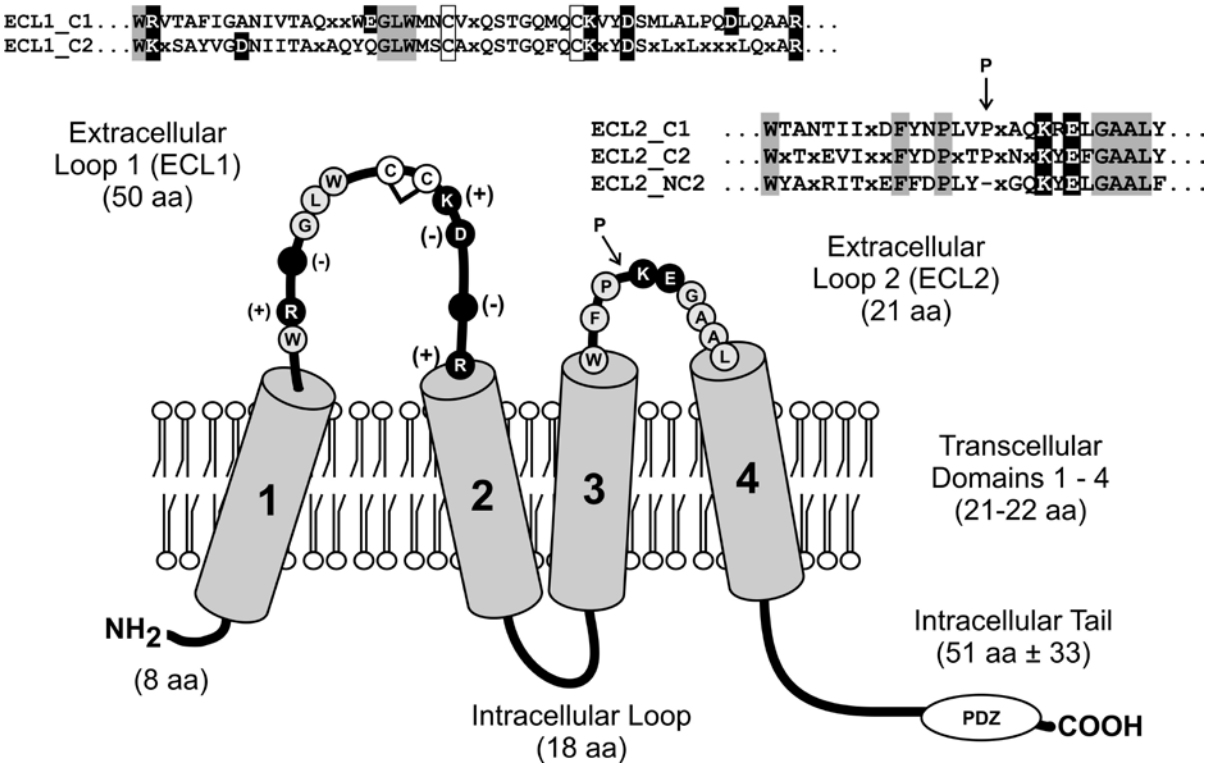

Figure 5. Domain model of a representative zebrafish claudin. Consensus peptide sequence alignments corresponding to the first extracellular loop (prefix ECL1) and second extracellular loop (prefix ECL2) of zebrafish claudins are shown above the corresponding structures depicted in the cartoon. The consensus sequences are defined as follows: suffix _C1 are 'classic' claudins from superclades in Figs. 2B, 2C, 2D, and 2E; suffix _C2 are 'classic' claudin superclades shown in Figs. 1C and 1D; suffix _NC1 are 'non-classic' claudins from superclade 1B. Conserved uncharged residues (including the [W-GLW] motif of ECL1) are indicated by the gray shading and conserved charged residues are indicated by black shapes and white text. Two cysteine [C] residues conserved in all claudins are indicated in white boxes within the ECL1 alignment and white circles in the cartoon. An 'x' in the sequence alignment designates a non-conserved residue position. The second proline [P] residue present in the ECL2 of 'classic' claudins, but absent in 'non-classic' claudins is indicated by the arrow. The cylinders numbered 1 through 4 depict transmembrane domains. A putative PDZ domain interacting motif at the carboxy-terminus of the intracellular tail also is depicted in the cartoon. This motif is largely conserved in 'classic' claudins, however it is not conserved in 'non-classic' claudins. Average lengths for each domain are given in amino acids (aa).

CHAPTER III

Cloning of Leptin A (*lepa*), and its Putative Receptor (*lepr*) in Mozambique Tilapia: Molecular Characterization and Response During Osmotic Challenge

Abstract

The aim of the present study was to assess whether regulation of leptin, a cytokine hormone best characterized for its function in controlling energy homeostasis, is influenced by salinity in the euryhaline Mozambique tilapia. The molecular sequence of leptin A (*lepa*) and leptin receptor (*lepr*) were characterized, and mRNA expression was measured in the gill and liver during seawater (SW; 25ppt) and freshwater (FW) challenge. The *lepa* transcript levels were most abundant in the liver and fat with lower expression in other tissues, including the gill, kidney, skin, brain, hypothalamus, and pituitary. Tilapia *lepr* was ubiquitously expressed. In the gill, little change was observed in *lepa* expression during the initial phases of acclimation to either FW or SW. However, *lepa* transcript was reduced at 96 hours in SW-challenged fish, and subsequently returned to sham levels by 14 days ($p < 0.05$). Expression of *lepr* diverged during the first 24 hours, declining in FW sham-transferred and increasing in SW-transferred fish. By day 4, gill *lepr* mRNA levels in SW challenged fish declined significantly and then returned to sham levels by 14 days ($p < 0.05$). Little change in gill *lepa* or *lepr* transcript levels was observed when fish were transferred from SW to FW, although *lepr* levels increased FW transferred fish at day 4. The discordance in gill *lepa* and *lepr* regulation in FW versus SW challenged fish at 4 days suggest the cytokine may function as a local growth factor and changes in mRNA expression may reflect periods of gill epithelial reorganization. In the liver, *lepa* and *lepr* mRNA expression were acutely upregulated during the seawater challenge (*lepa*, 25-fold increase after 4 hours), but little change occurred during freshwater challenge. Hepatic *lepa* mRNA expression correlated significantly to plasma osmolality in seawater-challenged fish ($p < 0.001$). These findings indicate that

hepatic leptin production and sensitivity are increased during acute periods of seawater acclimation, and point to a possible function for the hormone in mobilizing energy reserves or the regulation of hydromineral balance.

Introduction

Leptin is 16kD cytokine hormone most known for its role in regulating appetite and energy balance in mammals (Ahima and Flier, 2000; Copeland *et al.*, 2011). In teleost fishes, multiple leptins have been characterized to date, however their function is poorly understood (Gorissen *et al.*, 2009; Kling *et al.*, 2009; Kurokawa and Murashita, 2009; Rønnestad *et al.*, 2010; Zhang *et al.*, 2012). In mammals, circulating leptin is secreted from adipose tissue and circulates in proportion to total fat stores. Acting via its membrane-bound cytokine receptor (*lepr*), leptin promotes satiety in the hypothalamic feeding center (see Ahima and Flier, 2000 for review). High levels of circulating leptin induce lipolysis in liver and fat tissue, which is consistent with an adipostatic function (Huang *et al.*, 2006; Wang *et al.*, 1999). In many fishes, the liver is the primary source of circulating hormone (Kurokawa and Murashita, 2009; Kurokawa *et al.*, 2005; Won *et al.*, 2012). In contrast to mammals, increases in leptin are reported for many, but not all, fish species during periods of fasting when appetite suppression is unlikely to occur (Frøiland *et al.*, 2012; Fuentes *et al.*, 2012; Kling *et al.*, 2012; Trombley *et al.*, 2012; Zhang *et al.*, 2012). Yet, a characteristic decline in feeding behavior is commonly reported (Li *et al.*, 2010; Murashita *et al.*, 2008; Won *et al.*, 2012). Although these observations remain unresolved, leptin is consistently identified as a key regulator of metabolic energy (Aguilar *et al.*, 2010; Gambardella *et al.*, 2012; Kling *et al.*, 2012; Liu *et al.*, 2012).

Osmoregulation is critical to survival in teleost fishes, particularly for euryhaline species where movement across broad salinity ranges forms a vital component to their life history

(Evans, 1999; Martino and Able, 2003). Historically, endocrine control of osmoregulation is largely understood to be achieved through the actions of prolactin, cortisol, and growth hormone (Borski *et al.*, 2001; Dean *et al.*, 2003; McCormick, 2001; Sakamoto and McCormick, 2006). Recent studies have also identified hepatic IGF-I as an important mediator of seawater adaptation (Evans *et al.*, 2005; Tipsmark *et al.*, 2007). These hormones act directly upon the gill to stimulate the activity and abundance of ion transporters (e.g., Na^+, K^+ - ATPase, Na^+, K^+ , Cl^- cotransporters), and induce proliferation of appropriate ionocytes (Auperin *et al.*, 1994; Evans *et al.*, 2005; Heijden *et al.*, 1997; McCormick, 2001; Pelis and McCormick, 2001). Salinity tolerance may confer both ecological and long-term metabolic benefits to euryhaline fishes. However, rapid increases in active transport likely require extensive use of metabolic resources in the short term (Bashamohideen and Parvatheswararao, 1972; Morgan *et al.*, 1997; Ron *et al.*, 1995; Tseng and Hwang, 2008).

Studies have identified significant regulatory interactions between leptin and prominent osmoregulatory hormones in teleosts (Copeland *et al.*, 2011). In mammals, rising levels of cortisol stimulate leptin secretion from adipocytes, and elevated levels of circulating leptin in turn inhibit both basal and ACTH-mediated glucocorticoid secretion (Szucs *et al.*, 2001; Wabitsch *et al.*, 1996). Leptin also directly stimulates secretion of prominent pituitary hormones, including growth hormone and prolactin (Gonzalez *et al.*, 1999; Saleri *et al.*, 2004). In fishes, observations are consistent with of conservation for these interactions. Treatment with recombinant human leptin (rhLeptin) attenuated both adrenocorticotropin (ACTH) secretion and interrenal production of cortisol in the common carp (*Cyprinus*

carpio) (Gorissen *et al.*, 2012). In tilapia, treatment with rhLeptin increased prolactin secretion in a dose dependent manner in cultured pituitary cells (Tipsmark *et al.*, 2008). Additionally, possible feedback interactions with growth hormone were observed: in rainbow trout (*Oncorhynchus mykiss*), hepatic leptin mRNA expression decreased following GH treatment (Kling *et al*., 2012), and rhLeptin stimulated mRNA expression of growth hormone receptors (GHR1, GHR2) in cultured striped bass (*Morone saxatilis*) hepatocytes (Borski *et al.*, 2011). Despite growing evidence for interactions with prominent osmoregulatory hormones and the extensive energy requirements for maintaining hydromineral balance, the response of leptin during salinity adaptation has yet to be explored.

In this study, we describe the molecular sequence of a leptin A ortholog (*lepa*) and its putative receptor (*lepr*) in the Mozambique tilapia (*Oreochromis mossambicus*), and assess the mRNA expression of these genes in the gill and liver during osmotic challenge.

Methods and Materials

Husbandry and salinity challenges

Male tilapia (N = 216; 50 g mean body weight) were acclimated for 4 weeks in freshwater (FW; salinity, 0-1 ppt; alkalinity, 240-350 mg/L; hardness, 105-110 mg/L; pH 8.0) or 2/3 seawater (SW; Crystal Sea ® salt mix, Marine Enterprises, Baltimore, MD; salinity, 25 ppt; pH 8.0). Fish were held at constant temperature (24-26 °C) and photoperiod (12: 12 h light-

dark cycle) and fed floating feed pellets daily (2 % body weight; Finfish Silver Formula, 40% protein / 10% fat, Ziegler Brothers, Gardner, PA), except 24 hours before sampling.

Two separate salinity challenges were sequentially performed. For the SW challenge, fish acclimated to FW were transferred to SW or FW (sham). After sampling, the cages were restocked with fish for acclimation to SW (4 weeks). A freshwater challenge was then performed, with SW acclimated fish transferred to FW or SW (sham). The sampling times were identical for both challenges: 0 (initial acclimated fish), 4, 24, 96, and 336 hours (14 days) post-transfer. Sampled fish were anesthetized in buffered Tricaine methanesulfonate (MS-222; Sigma-Aldrich, St. Louis, MO) and blood was collected from the caudal vein using heparinized syringes. Animals were subsequently decapitated, and kept on ice during tissue sampling. One hundred milligrams of gill (2nd arch) and liver tissue were collected for RNA isolation and were stored in 1 mL of RNAlater (Ambion-Applied Biosystems, Austin, TX) overnight at 4°C and then frozen at -80°C until use. Blood was centrifuged (3,000 x *g*) for 10 min and plasma was collected and stored at -20° C until use. All procedures were performed in accordance with husbandry and sampling protocols approved by the North Carolina State University *Institutional Animal Care* and *Use Committee*.

Plasma osmolality

Plasma osmolality (mOsmol/kg) was measured in duplicate using a VAPRO vapor pressure osmometer (WesCor, Logan, UT).

Total RNA isolation and cDNA synthesis

Total RNA from collected tissues was isolated using TRI Reagent (Molecular Research Center, Cincinnati, OH). These isolations were performed according to supplied protocol except for skin, and liver tissue. For skin, an additional phase separation was performed to remove excessive pigment. For liver, samples homogenized in TRI Reagent were then cleaned using Direct-zol™ RNA purification columns (Zymo Research, Irvine, CA) to remove excessive glycogen content. RNA quality was assessed by OD 260:280 ratio (range 1.8 to 2.0) using a Nanodrop ND1000 spectrophotometer (Thermo Scientific, Wilmington, DE). Total RNA was DNAse-treated using Turbo DNA-free reagents and protocol (Life Technologies). Total RNA was requantified before 1 µg was reverse-transcribed (High Capacity cDNA Synthesis Kit, Life Technologies).

Molecular cloning and sequencing

Primer sequences used in the molecular cloning and gene expression of tilapia leptin A (*lepa*) and leptin receptor (*lepr*) are provided in Table 1. Partial sequences were obtained by PCR of genomic DNA to design gene-specific primers for use in 5' and 3' RACE-PCR (Rapid Amplification of cDNA Ends). For leptin, a 211 bp gene fragment was amplified with degenerate primers designed from a multiple sequence alignment of known fish leptins. For leptin receptor, two amplicons were obtained, 230 and 190 bp, respectively from the 3' end (Supplemental Table 1). These PCR reactions were performed for 35 cycles using GoTaq® polymerase and buffers (Promega, Madison, WI), 10mM dNTP mix and 10 µM primer

concentrations. Amplicons were ligated into pGEM™ T-easy cloning vector (Promega, Madison, WI) for transformation into JM109 series competent cells. Selected clones for each amplicon were submitted to the University of Chicago Cancer Research Center for forward and reverse sequencing with M13 universal primers.

From these sequences, gene specific primers were developed for RACE-PCR using the SMARTer™ RACE cDNA amplification kit (Clontech, Mountain View, CA). Both 5' and 3' cDNA libraries were prepared from 1 µg of total RNA, isolated from tilapia liver tissue, according to manufacturer's protocol. Primers were developed specifically for use in conjunction with kit-supplied adaptor primers (Table 1). Two rounds of 5' and 3' RACE-PCR were performed, with a 1:50 dilution of the primary PCR used as template in a nested PCR reaction. Cycling parameters for the PCR reactions were as follows: primary (5 cycles) – 94°C for 30 seconds, 72°C for 3 minutes, (5 cycles) – 94°C for 30 seconds, 70°C for 30 seconds, 72°C for 3 minutes, (25 cycles) – 94°C for 30 seconds, 68°C for 30 seconds, 72°C for 3 minutes; and nested (1 cycle) – 94°C for 3 minutes, (20 cycles) – 94°C for 30 seconds, 68°C for 30 seconds, 72°C for 3 minutes. An additional nested PCR was performed for *lepr* to extend into the 5' UTR. PCR reactions were performed using Advantage 2® polymerase mix and reagents (Clontech). Cloning and sequencing of all RACE amplicons were performed as before.

The full cDNA coding sequence of tilapia *lepa* and *lepr* were assembled from clone sequences using Contig Express (Vector NTI, Invitrogen) software. For *lepa*, an additional

PCR was performed of the coding sequences to verify the *in silico* assembly (primers; Table 1). The full *lepr* coding sequence was too large for TA cloning (3.4 kb), and the assembly was instead fortified by additional sequencing of RACE-PCR clones. Alignments of translated protein sequences for tilapia *lepa* and *lepr* were performed using NCBI *Blast2align* and *ClustalX* (Tatusova and Madden, 1999; Thompson *et al*., 1997).

Phylogenetic analysis

Bayesian phylogenetic analysis of protein sequences was performed separately for leptin and leptin receptor using MrBayes (*v 3.1.2*), available with TeraGrid computer usage through Cyberinfrastucture for Phylogenetic Research (CIPRES) Portal (Huelsenbeck and Ronquist, 2001; Miller *et al*., 2010). Analyses were performed using the WAG amino acid substitution model with gamma distributed among-site rate variation (generations = 250,000 (leptin) – 290,000 (leptin receptor), sample frequency = 100, burnin = 1000). Unrooted 50% majority rule consensus trees were visualized in TreeView (Page, 1996). Sequences of two related cytokines, interleukin-6 (*il6*) and granulocyte colony stimulating factor (*gcsf*), were used as outgroups in the leptin analysis, and their receptors (*il6r*, *gcsfr*) for leptin receptor. All protein sequences used for the phylogenetic analyses are provided in Table 2.

Tissue expression

The following tissues were collected for a tissue expression profile of tilapia *lepa* and *lepr*: brain (telencephalon, optic lobe, cerebrum, and the anterior region of the myelencephalon),

the hypothalamus, pituitary, skin, gill, head kidney, liver, white muscle, fat, stomach, and both anterior and posterior regions of the intestine. One microgram of total RNA for each tissue was transcribed into cDNA as described above, and each RT reaction was diluted 1:2 for PCR amplification. Sterile, nuclease-free water was used as template for a negative control. The housekeeping gene beta-actin (*bactin1*) was amplified for all reactions for use as a positive control (Table 1). PCR reactions were performed using GoTaq® polymerase and reagents (Promega), using 10mM dNTP mix and 10 μM primers, with the following cycling procedure: (1 cycle) – 95°C for 2 minutes; (40 cycles) – 95°C for 30 seconds, 57-64°C for 30 seconds, 72°C for 30 seconds; (1 cycle) – 72°C for 5 minutes, 4°C holding.

Northern blotting

Primers used to develop antisense RNA probes for *lepa* and *lepr* (both 5' and 3') are provided in Table 1. This procedure entailed the secondary amplification of a PCR amplicon with primers containing a T7 (forward primer) and Sp6 (reverse primer) promoter regions (Table 1). Secondary amplicons were cut from an agarose gel and cleaned using PCR purification columns (Qiagen) before *in vitro* transcription with DIG-dUTP labeling (Roche). Synthesis reactions were as follows: 20 U of T7 or Sp6 RNA polymerase with provided buffers (Promega), 8 U of RNAse inhibitor (Promega), 2.3 μL of 10X DIG RNA labeling mix (Roche), and 200 ng of PCR template. The housekeeping gene, elongation factor 1 alpha subunit (*ef1a*), was used as a control. This probe was developed by direct transcription of a partial gene sequence (*CCE45928*) cloned into pSPT18 expression vector (Roche). Reactions were incubated for 3 hours at 37 °C followed by DNAse treatment. RNA probes were

cleaned of non-incorporated DIG nucleotides by use of RNeasy miniprep columns (Qiagen) and stored in 1µg aliquots at -80°C.

Total RNA was isolated from tilapia liver, fat, gill, and white muscle tissue. A total of 1.2 mg of total RNA was then enriched for polyA-encoding RNA (mRNA) using a Dynabead® mRNA purification kit (Invitrogen; 4.9% yield). Enriched RNA (0.5-12 µg) was then electrophoresed in a 1% denaturing agarose gel using NorthernMax reagents and protocol (Life Technologies). Gel RNA was transferred to a Nylon membrane by overnight capillary transfer with 20X SSC, UV cross-linked at 254 nm, and then briefly rinsed in 2X SSC. After drying, the membranes were cut into lengthwise strips and prehybridized for 1 hour with 10 mL of UltraHyb® hybridization buffer (Life Technologies). The pre-hybridization buffer was replaced with 5 mL of fresh, preheated buffer containing 200 ng/mL of DIG-labeled riboprobe and hybridized overnight at 68°C. After hybridization, membranes were washed twice in 2X SSC/ 0.1% SDS at room temperature for 5 minutes, followed by two washes in 0.2X SSC/ 0.1 % SDS at 68°C for 15 minutes. The membranes were equilibrated in 1X MABT (150 mM NaCl, 100 mM maleic acid, 0.1% Tween-20) for 5 minutes, and blocked (1% Roche blocking reagent in 1X MABT) for 30 minutes. The blocking buffer was replaced with a fresh solution containing Anti-DIG/ AP (Roche; 1:10,000 dilution) and incubated for 45 minutes. Membranes were then washed twice in 1X MABT for 15 minutes, and equilibrated in 1X Alkaline Phosphatase buffer (10 mM NaCl, 10 mM Tris-HCl; pH 9.5) for 5 minutes. Membranes were covered in NBT/BCIP substrate solution (Thermo-Scientific)

and allowed to develop overnight at 37°C. Afterward, the membranes were rinsed in distilled water, then 70% ethanol, and dried before digital imaging (Syngene Gene Genius).

Quantitative RT-PCR

Messenger RNA (mRNA) expression of target genes were measured by SYBR Green Quantitative Real-Time PCR (qPCR). Gene-specific primers for *lepa, lepr*, and *bactin1* were developed using ABI Primer Express (v 3.0) software (Table 1). Primer sequences for the mRNA detection of Na^+, K^+-ATPase, α-1a and α-1b subunits, were developed by Tipsmark and colleagues (2011). Assays were performed with 25 ng of cDNA template and 75 nM primer concentrations using Brilliant II SYBR Green master mix (Stratagene, La Jolla, CA). Triplicate runs for all samples, standards, and negative controls were performed on an ABI 7900HT sequence detection system. The cycling parameters were as follows: 1 cycle—95°C for 10 minutes; 40 cycles—95°C for 30 s, 60°C for 60 s, and 72°C for a 60 s extension. Pooled cDNA samples were used to account for assays using multiple plates (across-plate normalization), with negative controls run on each plate. Cycle threshold (Ct) values for experimental samples were analyzed by absolute quantification, using standard curves derived from 2-fold serially diluted cDNA pools for each tissue (R^2 = 0.98-0.99). Data for target genes were then normalized to the mRNA expression of the housekeeping gene beta-actin (*bactin1*). Normalized values are expressed as relative fold changes to the mean of the Time 0 group. Primer specificity was determined by melt curve analysis and sequencing of qPCR amplicons.

Statistical procedures

All statistical procedures were performed using JMP 9 (SAS Institute, Cary, NC). A two-way factorial ANOVA was employed to examine the effects of treatment (challenge or sham transfer), time (0, 4, 24, 96 and 336 hours post transfer), and their interaction. If the whole model effects were significant, the treatment groups were compared using the Tukey-Kramer's Highly Significant Difference post-hoc test. For statistical purposes, the 0 time point (for each challenge) was treated as both a FW and SW exposure group. All mRNA values were natural log transformed to meet the assumption of homogeneity of variance. Group means were accepted as significant when $p < 0.05$. Linear correlations of leptin mRNA to plasma osmolality were performed separately for each treatment group after preliminary step-wise analysis in JMP (SAS Institute, Cary, NC).

Results

Characterization of tilapia *lepa* and *lepr*

A full assembly of 5' and 3' RACE-PCR clones identified the coding sequence of *O. mossambicus* leptin A (*lepa*) with 4X or greater sequence coverage. The contig assembly produced a 1,224 bp mRNA sequence containing a 486 bp open-reading frame (*Genbank Acc. No.* KC354702). A comparison of both genomic and cDNA coding sequences revealed a single, 95 bp intron demarcated by a canonical AG: GT mRNA splicing signal at the 225th nucleotide position. The translated peptide sequence is 74-82% identical to other perciform leptin A sequences, but shares only 12% identity to the human leptin homolog (Fig. 1).

Additionally, a predicted gene sequence in the genomic assembly of the Nile tilapia was identified (*O. niloticus*, LOC100704227), which is 99 % identical to Mozambique tilapia *lepa*. A putative 20-residue signal peptide, four helical domain regions (helix A-D), and a common disulfide bond are identified based upon conserved regions within the perciform leptins (Fig. 1).

For leptin receptor, the RACE-PCR assembly (4X coverage) produced a 3,836 bp mRNA sequence containing a 3,423 bp open-reading frame (*Genbank:* KC354703). The deduced peptide sequence is poorly conserved with other fish and vertebrate leptin receptor sequences, however conserved structural domains were identified (Fig. 2). Tilapia *lepr* shares 56% sequence identity to *Takifugu rubripes* leptin receptor (NP_001124341), and 28% identity to the human ortholog (NP_002294) (Fig. 2). The following domain regions were identified based on sequence conservation with medaka (*Oryzias latipes*, NP_001153915), salmon (*Salmo salar*, NP_001158237), and Fugu (*T. rubripes*) leptin receptor: signal peptide, three fibronectin type III (*FN3*) domains with two containing a WSxWS motif, an immuglobin-like (*Ig-like*) C-2 type domain, and JAK/STAT signaling boxes within the intracellular region (Fig. 2).

Phylogenetic analysis of tilapia *lepa* and *lepr*

Homology of the putative tilapia *lepa* and *lepr* sequences was assessed by Bayesian phylogenetic inference of protein sequences (Fig. 3). In an unrooted consensus tree containing related clades of the cytokines interleukin-6 (*il6*) and granulocyte colony

stimulating factor (*gcsf*), all putative leptin homologs formed a unified clade with poor consensus support (54% clade credibility score; Fig. 3A). The leptin sequences of higher teleosts (Acanthomorpha) formed two distinct clades, consistent with gene duplication (leptin A and B paralogs; 96-100 % support). The *O. mossambicus* leptin sequence grouped with percomorph (Perciformes + Tetraodontiformes) leptin A orthologs, with medaka (*Oryzias latipes*) as sister taxa (86%). Within the phylogeny, tetrapod (Sarcopterygii) leptins also formed a monophyletic clade (100%); the leptins of less-derived teleosts (e.g. Salmoniformes, Ostariophysi) were not resolved (Fig. 3A). Phylogenetic analysis of *lepr*, *il6r*, and *gcsfr* produced a monophyletic clade uniting all putative leptin receptor proteins (Fig. 3B; 100%). This grouping was further divided into tetrapod and teleost subclades (100 %). Mozambique tilapia *lepr* aligned most closely to Fugu (*Takifugu rubripes*) leptin receptor (98 %; Fig. 3B).

Tissue expression profile and Northern Blotting

The presence or absence of tilapia *lepa* and *lepr* mRNA expression was examined in discrete tissues by endpoint RT-PCR amplification and Northern Blotting (Fig. 4). Tilapia *lepa* mRNA is prominently expressed in cDNA from both liver and fat (white adipose) tissue, but lower mRNA levels were also detected in brain, hypothalamus, pituitary, skin, gill, and kidney tissue. Leptin receptor mRNA expression was detected in all tissues examined (Fig. 4A). The mRNA of tilapia *lepa* and *lepr* were examined using polyA-enriched mRNA from select tissues by Northern blots (Fig. 4B,C). For *lepa*, a 1.2 kb mRNA transcript was faintly detected in a membrane containing 12 µg of enriched RNA from liver tissue, but not from fat

(Fig. 4B). The housekeeping gene elongation factor 1-alpha (*ef1a*) was detected in both tissues, using 0.5 µg of the same RNA, however lower band intensity was also observed in fat (Fig. 4B). For leptin receptor, riboprobes from both the 5' and 3' end of the mRNA were used to detect transcript or splicing variants. A single, 5.1 kb band was observed in RNA from muscle and gill tissue using either probe (Fig. 4C). Relative band intensities for muscle and gill tissue were assessed by additional *ef1a* probe hybridization to the same RNA (0.5 µg; Fig. 4C).

Response of *lepa* and *lepr* mRNA during salinity transfer

Sequential challenges were performed using fish acclimated to freshwater (FW, 0 ppt) and 2/3 seawater (SW, 25 ppt), respectively. Plasma osmolality and changes in gill mRNA expression of Na^+, K^+ -ATPase α-1a and α-1b subunits (*atpa1a* and *atpa1b*) were measured as markers of osmotic stress (Fig. 5A-C). In the SW challenge, plasma osmolality was significantly elevated at 4 and 24 hours following SW transfer, relative to levels observed prior (FW_0; $p < 0.05$). Although osmolality was higher in SW challenged fish, values were did not differ significantly compared with sham-transferred FW fish (Fig. 5A). For the FW challenge, SW-acclimated fish transferred to FW, mean plasma osmolality was not significantly different from control (Fig. 5A). The gill mRNA expression of the Na^+, K^+ -ATPase FW isoform (α-1a, *atpa1a*) was reduced five-fold in SW-challenged fish at 4 hours, and was also significantly lower by 336 hours post-transfer ($p < 0.001$, Fig. 5B). An opposite response was observed in FW-challenged fish, where a five-fold increase in gill *atpa1a* mRNA occurred 24 hours after transfer, and remained significantly higher at 96 hours ($p <$

0.001, Fig. 5B). The gill mRNA expression of the SW isoform of Na^+, K^+ -ATPase (α-1b, *atpa1b*) was significantly higher in SW-challenged fish at 4, 96, and 336 hours, relative to sham fish ($p < 0.05$; Fig. 5C). In FW-challenged fish, gill *atpa1b* mRNA was significantly lower than sham fish after 24 hours (Fig. 5C; $p < 0.001$).

Gill mRNA expression of tilapia *lepa* and *lepr* was examined in challenged fish (Fig. 5D and Fig. 6A). In SW-challenged tilapia, gill *lepa* mRNA was significantly lower at 96 hours relative sham fish ($p < 0.01$), but expression levels were restored to initial (F_0) and sham levels after 336 hours (Fig. 5D). Freshwater challenged fish showed a trends towards higher, but insignificant, *lepa* gill mRNA expression following 96 hours of transfer (Fig. 5D). In contrast, gill *lepr* mRNA expression was initially higher in SW-challenged tilapia, relative to sham fish, for the first 24 hours (Fig. 6A; $p < 0.001$). This difference resulted from both an increase of gill *lepr* mRNA expression in SW challenged and reduction in sham fish (4 hours; $p < 0.05$). By 96 hours, SW-challenged fish had lower gill *lepr* transcript levels, which subsequently returned to sham levels by 336 h ($p < 0.05$). In FW-challenged tilapia, gill *lepr* mRNA expression was higher than sham fish at 96 hours ($p < 0.05$), but not at earlier or later times (0, 4, 24, or 336 hours; Fig. 6A).

Tilapia *lepa* and *lepr* mRNA expression were examined in the liver of challenged fish (Fig. 6B-D). The SW challenged fish had elevated levels of *lepa* mRNA over the first 24 h of transfer. Hepatic *lepa* mRNA increased 25-fold by 4 hours post-transfer ($p < 0.001$; relative to F_0), and then declined by 24 hours, returning to initial mRNA levels thereafter (24-336

hours; Fig. 6B). In sham fish, *lepa* mRNA expression significantly decreased at 4 hours ($p < 0.05$; relative to F_0), but was not significantly different at later times (Fig. 6B). In FW-challenged fish, *lepa* mRNA levels did not change during transfer, however mRNA expression in sham fish was significantly higher at 24 hours post-transfer (Fig. 6B; $p < 0.001$).). Linear correlations of hepatic *lepa* mRNA expression to plasma osmolality were performed for both challenges (Fig. 6C). In SW-challenged fish, a positive correlation between plasma osmolality and *lepa* mRNA was observed (slope $\neq 0$, $p < 0.001$, $R^2 = 0.290$). No significant correlation was observed in sham-transfer groups or from FW-challenged fish (Fig. 6C). Tilapia *lepr* mRNA expression was also significantly higher in SW-challenged fish at 4 hours ($p < 0.001$), but not at later times (Fig. 6D). In the FW challenge, no significant differences in *lepr* mRNA were observed, however both groups were significantly reduced from initial (SW_0) levels by 336 hours ($p < 0.05$, Fig. 6D).

Discussion

Phylogenetic analysis identified our leptin sequence as an ortholog of teleost leptin A, and is similar in sequence to other perciform leptin A proteins (Fig. 1, 3A). Characteristic of fish leptins, tilapia leptin shares poor sequence identity to mammalian homologs (12%; H. sapiens; Fig. 1). In fishes, multiple leptin genes have been reported for several species: medaka (*O. latipes*), zebrafish (*D. rerio*), Atlantic salmon (*S. salar*), and carp (*C. carpio*) (Gorissen *et al.*, 2009; Huising *et al.*, 2006; Kurokawa and Murashita, 2009; Rønnestad *et al.*, 2010). In others, only a single leptin is present (Kurokawa *et al.*, 2005). This diversity has been explained by events of whole-genome duplication, gene loss, and further

duplication in tetraploid species (Kurokawa and Murashita, 2009; Rønnestad *et al.*, 2010; Won *et al.*, 2012). Our phylogeny supports independent duplication for both carp (leptin I and II) and salmon (*lepa1* and *lepa2*) sequences (Fig. 3A). A putative whole genome duplication event (3R hypothesis), occurring earlier in teleost evolution (Neopterygii), may explain distinct leptin clades (*lepa* and *lepb*) observed for higher teleosts (Acanthomorpha) (Fig. 3A) (Taylor *et al.*, 2003). In the pufferfishes (Tetraodontiformes), secondary loss of a *lepb* ortholog was proposed (Kurokawa *et al.*, 2008; Kurokawa *et al.*, 2005; Won *et al.*, 2012). This agrees with our findings, as known pufferfish leptins (*T. rubripes* and *T. nigroviridis*) are both orthologs of perciform *lepa* (Fig. 3A). Using genome synteny, Won and colleagues (2012) hypothesized that perciform fishes may also lack the *lepb* ortholog. Recently however, both *lepa* and *lepb* were reported in the Orange-spotted grouper (*Epinephelus coioides*) (Zhang *et al.*, 2012). Based on these new sequences, we identified predicted orthologs of both *lepa* and *lepb* in the genome assembly of the Nile tilapia (*Oreochromis niloticus*), and have included these in our sequence alignment and phylogeny (Table 2; Fig. 1, 3A). Further characterization of the *lepb* ortholog will be addressed in future studies.

Leptin is expressed locally by many tissues in mammals, but adipose tissue is considered the source of circulating hormone (Ahima and Flier, 2000; Ahima and Osei, 2004). In contrast, mRNA detection of leptin was restricted to the liver in Fugu (*T. rubripes*) and in striped bass (*M. saxatilis*), suggesting hepatic origin for circulating leptin in fishes (Kurokawa *et al.*, 2005; Won *et al.*, 2012). Tilapia *lepa* mRNA levels are abundant in cDNA derived from both

liver and fat tissue, but lower (relative) levels of expression were also observed from brain (telencephalon), hypothalamus, pituitary, skin, and gill cDNA preparations (Fig. 4A). Using Northern blotting, we examined *lepa* mRNA expression in liver and fat to determine relative abundance in these tissues (Fig. 4B). Using 12 µg of polyA-enriched RNA, a faint band of correct size (1.2 kb) was detected in liver, but not fat tissue, suggesting higher levels in the liver. These observations require further validation by quantitative amplification methods (qPCR), as Northern detection barely exceeded threshold limits, and mRNA levels for the control gene (ef1α) were also lower in fat samples (Fig. 4B). Expression of leptin in both liver and fat tissue are reported in salmon (*S. salar*), and also for broiler chickens (*Gallus gallus*), suggesting the source of circulating leptin may reflect differential reliance upon adipose tissue as a source of mobilizable lipids (Ashwell *et al.*, 1999; Rønnestad *et al.*, 2010). Nevertheless, it appears that in addition to fat, the liver is a primary organ for leptin production in tilapia.

Physiological actions of leptin are mediated through binding of a membrane bound receptor (*lepr*; Mancour *et al.*, 2012). Using iterative rounds of RACE-PCR, we identified a putative long form variant of tilapia *lepr*, which contained both the transmembrane and intracellular domain regions (Fig. 2). Although monophyletic with other leptin receptor proteins, tilapia *lepr* shares poor sequence identity (≤ 56 %) with other fish homologs, despite the presence of common domain features (*e.g.* FN3, Ig-like domain; Fig. 2,3). Within the intracellular region, both Janus kinase 2 (Jak2) and STAT motifs are identifiable, suggesting cellular signaling pathways are conserved across vertebrate groups (Fig. 2). Multiple forms of leptin receptor

have been described in mammals and some fish species, but not in others (Cao *et al.*, 2011; Gong *et al.*, 2012; Kurokawa *et al.*, 2008; Zabeau *et al.*, 2003). Recently, three *lepr* isoforms were identified in Crucian carp (*Carassius carassius*), with two isoforms present in the gill (Cao *et al.*, 2011). Using Northern blot, we tested both 5' and 3' riboprobes in hybridization with tilapia gill and muscle tissue to identify potential *lepr* splice variants, however no additional bands were observed (Fig. 4C). Therefore, we observe only the long-form variant of *lepr* in tilapia. Whether additional isoforms are present in higher teleost groups (Acanthomorpha) remains to be described.

Plasma osmolality and Na^+, K^+-ATPase alpha subunit mRNA expression were measured to assess the degree of osmotic stress achieved during SW and FW osmotic challenge (Fig. 5A-C). After transfer of freshwater fish to 2/3 SW, plasma osmolality increased significantly from initial (T_0) levels, and significant changes in gill Na^+, K^+-ATPase mRNA were observed relative to sham fish ($p < 0.05$; Fig. 5A-C). Gill mRNA expression of the seawater isoform (α1b; *atpa1b*) increased while the freshwater isoform (α1a; *atpa1a*) declined in SW acclimated relative to sham fish (Fig. 5B,C). During transfer of SW-fish to freshwater, plasma osmolality was not significantly different (Fig. 5A), however the mRNA response of gill Na^+, K^+-ATPase was opposite to that for the SW-challenge; significant increase in *atpa1a* accompanied by a decrease in *atpa1b* ($p < 0.001$; Fig. 5 B,C). The discordant regulation of the salinity-dependent gill Na^+, K^+-ATPase isoforms (Tipsmark *et al.*, 2011), along with changes in osmolality (SW challenge), demonstrates that osmotic perturbation and ion imbalance were established during the salinity transfer experiments.

Studies identify leptin as both an endocrine and paracrine/autocrine growth factor in mammals, promoting the proliferation and differentiation of epithelial cells (Attoub *et al.*, 2000; Bouloumie *et al.*, 1998; Torday *et al.*, 2002). In the gill, *lepa* mRNA expression was significantly lower in SW-challenged fish at 96 hours, but was not different at other time periods ($p < 0.01$; Fig. 5D). In FW-challenged tilapia, gill *lepa* mRNA was higher than sham fish after 4 days, however this elevation was not significant (Fig. 5D). Several studies have shown extensive remodulation of mitochondria-rich cell (MRC) populations, along with cellular apoptosis (Caspase 3/7 activity), occur in the teleost gill after 72 hours of transfer to 2/3 SW (25 ppt; Kammerer and Kultz, 2009; Kammerer *et al.*, 2009). If local leptin signaling mediates either epithelial hyperplasia or vascularization, a decrease in *lepa* mRNA expression in the gill may be consistent with cellular remodulation during seawater adaptation. The response of gill leptin receptor (*lepr*) during salinity transfer is more difficult to interpret (Fig. 6A). Consistent with regulation during remodulation, *lepr* mRNA expression at 96 hours was higher in FW-challenged, and lower in SW-challenged fish, relative to initial (T_0) levels ($p < 0.05$; Fig. 6A). However, gill *lepr* mRNA was also higher in SW-challenged fish at 4 and 24 hours, relative to sham fish ($p < 0.001$), but not to T_0 fish (Fig. 6A). This may be explained by a stress response in the sham group, as *lepr* mRNA expression was significantly reduced in these fish, relative to T_0 ($p < 0.05$; Fig. 6A). Catecholamine administration has been shown to inhibit leptin secretion in cultured human adipocytes (Scriba *et al*., 2000). However, the peripheral regulation of teleost leptin or its receptor by the sympathetic stress response is currently unknown. Taken together, peripheral

leptin signaling may enhance cellular growth and differentiation in the teleost gill, however further examination is needed to address specific effects.

Both direct and indirect interactions with ion transporters suggested a role for leptin in osmoregulation as leptin is shown to be natriuretic, acting to increase urine sodium levels by decreasing Na^+, K^+-ATPase activity in the rat kidney (renal medulla; Beltowski *et al.*, 2004). In tilapia, treatment of pituitary cultures with human leptin induced rapid secretion of prolactin (Tipsmark *et al*., 2008), a freshwater adapting hormone reducing gill Na^+, K^+-ATPase activity and promoting development of FW-type MRC cells in the gill (Evans *et al.*, 2005; McCormick, 2001). In contrast, our data indicate a prominent response of hepatic *lepa* mRNA during seawater adaptation (Fig. 6B-D). Liver *lepa* mRNA expression increased 25-fold in SW-challenged fish after 4 hours and remained elevated for 24 hours (Fig. 6B). Hepatic *lepr* mRNA expression showed parallel changes at 4 hours, and declining thereafter (Fig. 6C). Hepatic *lepa* mRNA expression correlated significantly to plasma osmolality in SW-challenged fish ($p < 0.001$), but not in FW-challenged or sham groups (Fig. 6D). Thus, our evidence suggests leptin production, and possibly sensitivity, are enhanced during periods of acute hyperosmotic stress, however its function during seawater adaptation is unknown. Several recent studies in fish show either circulating leptin, hepatic *lepa* mRNA expression, or both increase during periods of fasting or stress (hypoxia), during which significant mobilization of energy reserves occur (Aguilar *et al.*, 2010; Bernier *et al.*, 2012; Bystriansky *et al.*, 2007; Gambardella *et al.*, 2012; Liu *et al.*, 2012; Trombley *et al.*, 2012). As acute seawater adaptation comprises up to 20% of total metabolic expenditure in tilapia

(Morgan *et al.*, 1997), increases in hepatic *lepa* mRNA expression may be associated with the mobilization of energy resources during this time. Future studies are needed to evaluate the potential role of leptin in mediating ion transporter abundance, expenditure of metabolic energy resources, or in the regulation of hormones mediating hydromineral balance.

In this study, we describe the molecular sequence of *lepa* and *lepr* in Mozambique tilapia, and report for the first time in vertebrates that leptin gene expression in the gill and liver is sensitivity to salinity. Currently, the function of leptin during periods of osmotic stress is unclear, however its enhanced production during hyperosmotic perturbations raises the possibility that the hormone may modulate energy metabolism and gill ion transport activity toward promoting physiological homeostasis in SW environments. Future studies should address these potential interactions, as well as the possible divergence between *lepa* and its gene paralogs (*e.g.*, *lepb*).

Acknowledgements

We wish to thank Brad Ring and John Davis (NCSU), and Dr. Andy McGinty (Pamlico Aquaculture Laboratory, Aurora, NC) for their assistance in animal husbandry. We also gratefully acknowledge the help of Dr. Eugene Won and Dr. William Johnstone III (NCSU) for their help and consultation in this work.

REFERENCES

Aguilar, A.J., Conde-Sieira, M., Polakof, S., Míguez, J.M., Soengas, J.L., 2010. Central leptin treatment modulates brain glucosensing function and peripheral energy metabolism of rainbow trout. *Peptides* 31, 1044-1054.

Ahima, R.S., Flier, J.S., 2000. Leptin. *Annu Rev Physiol* 62, 413-437.

Ahima, R.S., Osei, S.Y., 2004. Leptin signaling. *Physiol Behavior* 81, 223-241.

Ashwell, C.M., Czerwinski, S.M., Brocht, D.M., McMurtry, J.P., 1999. Hormonal regulation of leptin expression in broiler chickens. *Am J Physiology – Reg Int Comp Physiol* 276, R226-R232.

Attoub, S., Noe, V., Pirola, L., Bruyneel, E., Chastre, E., Mareel, M., Wymann, M.P., Gespach, C., 2000. Leptin promotes invasiveness of kidney and colonic epithelial cells via phosphoinositide 3-kinase-, rho-, and rac-dependent signaling pathways. *Faseb J* 14, 2329-2338.

Auperin, B., Rentier-Delrue, F., Martial, J.A., Prunet, P., 1994. Evidence that two tilapia (*Oreochromis niloticus*) prolactins have different osmoregulatory functions during adaptation to a hyperosmotic environment. *J Mol Endocrinol* 12, 13-24.

Bashamohideen, M., Parvatheswararao, V., 1972. Adaptations to osmotic stress in the fresh-water euryhaline teleost *Tilapia mossambica*. IV. Changes in blood glucose, liver glycogen and muscle glycogen levels. *Marine Biol* 16, 68-74.

Beltowski, J., Marciniak, A., Wojcicka, G., 2004. Leptin decreases renal medullary $Na^{(+)}$, $K^{(+)}$-ATPase activity through phosphatidylinositol 3-kinase dependent mechanism. *J Physiol Pharmacol* 55, 391-407.

Bernier, N.J., Gorissen, M., Flik, G., 2012. Differential effects of chronic hypoxia and feed restriction on the expression of leptin and its receptor, food intake regulation and the endocrine stress response in common carp. *J Exp Biol* 215, 2273-2282.

Borski, R.J., Hyde, G.N., Fruchtman, S., Tsai, W.S., 2001. Cortisol suppresses prolactin release through a non-genomic mechanism involving interactions with the plasma membrane. *Comp Biochem Physiol B Biochem Mol Biol* 129, 533-541.

Borski, R.J., Won, E.T., Baltzegar, D.A., 2011. Leptin stimulates hepatic growth hormone receptor expression: possible role in enhancing GH-mediated anabolic processes in fish. *Frontiers Endocrinol*; The inaugural meeting of the North American Society for Comparative Endocrinology, Ann Arbor, USA (Event Abstract).

Bouloumie, A., Drexler, H.C., Lafontan, M., Busse, R., 1998. Leptin, the product of *ob* gene, promotes angiogenesis. *Circ Res* 83, 1059-1066.

Bystriansky, J.S., Frick, N.T., Ballantyne, J.S., 2007. Intermediary metabolism of Arctic char *Salvelinus alpinus* during short-term salinity exposure. *J Exp Biol* 210, 1971-1985.

Cao, Y.B., Xue, J.L., Wu, L.Y., Jiang, W., Hu, P.N., Zhu, J., 2011. The detection of 3 leptin receptor isoforms in crucian carp gill and the influence of fasting and hypoxia on their expression. *Dom Animal Endocrinol* 41, 74-80.

Copeland, D.L., Duff, R.J., Liu, Q., Prokop, J., Londraville, R.L., 2011. Leptin in teleost fishes: an argument for comparative study. *Front Physiol* 2, 26.

Dean, D.B., Whitlow, Z.W., Borski, R.J., 2003. Glucocorticoid receptor upregulation during seawater adaptation in a euryhaline teleost, the tilapia (*Oreochromis mossambicus*). *Gen Comp Endocrinol* 132, 112-118.

Evans, D.H., 1999. Ionic transport in the fish gill epithelium. *J Exp Zool* 283, 641.

Evans, D.H., Piermarini, P.M., Choe, K.P., 2005. The multifunctional fish gill: dominant site of gas exchange, osmoregulation, acid-base regulation, and excretion of nitrogenous waste. *Physiol Rev* 85, 97-177.

Frøiland, E., Jobling, M., Björnsson, B.T., Kling, P., Ravuri, C.S., Jorgensen, E.H., 2012. Seasonal appetite regulation in the anadromous Arctic charr: evidence for a role of adiposity in the regulation of appetite but not for leptin in signalling adiposity. *Gen Comp Endocrinol* 178, 330-337.

Fuentes, E.N., Kling, P., Einarsdottir, I.E., Alvarez, M., Valdes, J.A., Molina, A., Bjornsson, B.T., 2012. Plasma leptin and growth hormone levels in the fine flounder (*Paralichthys adspersus*) increase gradually during fasting and decline rapidly after refeeding. *Gen Comp Endocrinol* 177, 120-127.

Gambardella, C., Gallus, L., Amaroli, A., Terova, G., Masini, M.A., Ferrando, S., 2012. Fasting and re-feeding impact on leptin and aquaglyceroporin 9 in the liver of European sea bass (*Dicentrarchus labrax*). *Aquaculture* 354-355, 1-6.

Gong, Y., Luo, Z., Zhu, Q.-L., Zheng, J.-L., Tan, X.-Y., Chen, Q.-L., Lin, Y.-C., Lu, R.-H., 2012. Characterization and tissue distribution of leptin, leptin receptor and leptin receptor overlapping transcript genes in yellow catfish *Pelteobagrus fulvidraco*. *Gen Comp Endocrinol* 182, 1-6.

Gonzalez, L.C., Pinilla, L., Tena-Sempere, M., Aguilar, E., 1999. Leptin 116-130 stimulates prolactin and luteinizing hormone secretion in fasted adult male rats. *Neuroendocrinology* 70, 213-220.

Gorissen, M., Bernier, N.J., Manuel, R., de Gelder, S., Metz, J.R., Huising, M.O., Flik, G., 2012. Recombinant human leptin attenuates stress axis activity in common carp (*Cyprinus carpio* L.). *Gen Comp Endocrinol* 178, 75-81.

Gorissen, M., Bernier, N.J., Nabuurs, S.B., Flik, G., Huising, M.O., 2009. Two divergent leptin paralogues in zebrafish (*Danio rerio*) that originate early in teleostean evolution. *J Endocrinol* 201, 329-339.

Heijden, A., Verbost, P., Eygensteyn, J., Li, J., Bonga, S., Flik, G., 1997. Mitochondria-rich cells in gills of tilapia (*Oreochromis mossambicus*) adapted to fresh water or seawater: quantification by confocal laser scanning microscopy. *J Exp Biol* 200, 55-64.

Huang, W., Dedousis, N., Bandi, A., Lopaschuk, G.D., O'Doherty, R.M., 2006. Liver triglyceride secretion and lipid oxidative metabolism are rapidly altered by leptin *in vivo*. *Endocrinology* 147, 1480-1487.

Huelsenbeck, J.P., Ronquist, F., 2001. MRBAYES: Bayesian inference of phylogenetic trees. *Bioinformatics* 17, 754-755.

Huising, M.O., Geven, E.J.W., Kruiswijk, C.P., Nabuurs, S.B., Stolte, E.H., Spanings, F.A.T., Verburg-van Kemenade, B.M.L., Flik, G., 2006. Increased leptin expression in common carp (*Cyprinus carpio*) after food intake but not after fasting or feeding to satiation. *Endocrinology* 147, 5786-5797.

Kammerer, B.D., Kultz, D., 2009. Prolonged apoptosis in mitochondria-rich cells of tilapia (*Oreochromis mossambicus*) exposed to elevated salinity. *J Comp Physiol B* 179, 535-542.

Kammerer, B.D., Sardella, B.A., Kultz, D., 2009. Salinity stress results in rapid cell cycle changes of tilapia (*Oreochromis mossambicus*) gill epithelial cells. *J Exp Zool A Ecol Genet Physiol* 311, 80-90.

Kling, P., Jonsson, E., Nilsen, T.O., Einarsdottir, I.E., Ronnestad, I., Stefansson, S.O., Björnsson, B.T., 2012. The role of growth hormone in growth, lipid homeostasis, energy utilization and partitioning in rainbow trout: interactions with leptin, ghrelin and insulin-like growth factor I. *Gen Comp Endocrinol* 175, 153-162.

Kling, P., Rønnestad, I., Stefansson, S.O., Murashita, K., Kurokawa, T., Björnsson, B.T., 2009. A homologous salmonid leptin radioimmunoassay indicates elevated plasma leptin levels during fasting of rainbow trout. *Gen Comp Endocrinol* 162, 307-312.

Kurokawa, T., Murashita, K., 2009. Genomic characterization of multiple leptin genes and a leptin receptor gene in the Japanese medaka, *Oryzias latipes*. *Gen Comp Endocrinol* 161, 229-237.

Kurokawa, T., Murashita, K., Suzuki, T., Uji, S., 2008. Genomic characterization and tissue distribution of leptin receptor and leptin receptor overlapping transcript genes in the pufferfish, *Takifugu rubripes*. *Gen Comp Endocrinol* 158, 108-114.

Kurokawa, T., Uji, S., Suzuki, T., 2005. Identification of cDNA coding for a homologue to mammalian leptin from pufferfish, *Takifugu rubripes*. *Peptides* 26, 745-750.

Li, G.-G., Liang, X.-F., Xie, Q., Li, G., Yu, Y., Lai, K., 2010. Gene structure, recombinant expression and functional characterization of grass carp leptin. *Gen Comp Endocrinol* 166, 117-127.

Liu, Q., Dalman, M., Chen, Y., Akhter, M., Brahmandam, S., Patel, Y., Lowe, J., Thakkar, M., Gregory, A.-V., Phelps, D., Riley, C., Londraville, R.L., 2012. Knockdown of leptin A expression dramatically alters zebrafish development. *Gen Comp Endocrinol* 178, 562-572.

Mancour, L.V., Daghestani, H.N., Dutta, S., Westfield, G.H., Schilling, J., Oleskie, A.N., Herbstman, J.F., Chou, S.Z., Skiniotis, G., 2012. Ligand-induced architecture of the leptin receptor signaling complex. *Mol Cell* 48, 655-661.

Martino, E.J., Able, K.W., 2003. Fish assemblages across the marine to low salinity transition zone of a temperate estuary. *Estuar Coast Shelf Sci* 56, 969-987.

McCormick, S.D., 2001. Endocrine control of osmoregulation in teleost fish. *Am Zool* 41, 781-794.

Miller, M.A., Pfeiffer, W., Schwartz, T., 2010. Creating the CIPRES Science Gateway for inference of large phylogenetic trees, Gateway Computing Environments Workshop (GCE), New Orleans, LA, pp. 1-8.

Morgan, J.D., Sakamoto, T., Grau, E.G., Iwama, G.K., 1997. Physiological and respiratory responses of the Mozambique tilapia (*Oreochromis mossambicus*) to salinity acclimation. *Comp Biochem Physiol A: Physiol* 117, 391-398.

Murashita, K., Uji, S., Yamamoto, T., Rønnestad, I., Kurokawa, T., 2008. Production of recombinant leptin and its effects on food intake in rainbow trout (*Oncorhynchus mykiss*). *Comp Biochem Physiol B: Biochem Mol Biol* 150, 377-384.

Page, R.D.M., 1996. Tree View: An application to display phylogenetic trees on personal computers. *CABIOS* 12, 357-358.

Pelis, R.M., McCormick, S.D., 2001. Effects of growth hormone and cortisol on $Na^{(+)}$-$K^{(+)}$-$2Cl^{(-)}$ cotransporter localization and abundance in the gills of Atlantic salmon. *Gen Comp Endocrinol* 124, 134-143.

Ron, B., Shimoda, S.K., Iwama, G.K., Grau, E.G., 1995. Relationships among ration, salinity, 17α-methyltestosterone and growth in the euryhaline tilapia, *Oreochromis mossambicus*. *Aquaculture* 135, 185-193.

Rønnestad, I., Nilsen, T.O., Murashita, K., Angotzi, A.R., Gamst Moen, A.-G., Stefansson, S.O., Kling, P., Thrandur Björnsson, B., Kurokawa, T., 2010. Leptin and leptin receptor genes in Atlantic salmon: cloning, phylogeny, tissue distribution and expression correlated to long-term feeding status. *Gen Comp Endocrinol* 168, 55-70.

Sakamoto, T., McCormick, S.D., 2006. Prolactin and growth hormone in fish osmoregulation. *Gen Comp Endocrinol* 147, 24-30.

Saleri, R., Giustina, A., Tamanini, C., Valle, D., Burattin, A., Wehrenberg, W.B., Baratta, M., 2004. Leptin stimulates growth hormone secretion via a direct pituitary effect combined with a decreased somatostatin tone in a median eminence-pituitary perifusion study. *Neuroendocrinology* 79, 221-228.

Scriba, D., Aprath-Husmann, I., Blum, W.F., Hauner, H., 2000. Catecholamines suppress leptin release from *in vitro* differentiated subcutaneous human adipocytes in primary culture via β1- and β2-adrenergic receptors. *Eur J Endocrinol* 143, 439-445.

Szucs, N., Varga, I., Jakab, C., Patocs, A., Glaz, E., Toth, M., Kiss, R., Racz, K., 2001. Leptin inhibits cortisol and corticosterone secretion in pathologic human adrenocortical cells. *Pituitary* 4, 71-77.

Tatusova, T.A., Madden, T.L., 1999. BLAST 2 Sequences, a new tool for comparing protein and nucleotide sequences. *FEMS Microbiol Lett* 174, 247-250.

Taylor, J.S., Braasch, I., Frickey, T., Meyer, A., Van de Peer, Y., 2003. Genome duplication, a trait shared by 22,000 species of ray-finned fish. *Genome Res* 13, 382-390.

Thompson, J.D., Gibson, T.J., Plewniak, F., Jeanmougin, F., Higgins, D.G., 1997. The CLUSTAL_X windows interface: flexible strategies for multiple sequence alignment aided by quality analysis tools. *Nucleic Acids Res* 25, 4876-4882.

Tipsmark, C.K., Breves, J.P., Seale, A.P., Lerner, D.T., Hirano, T., Grau, E.G., 2011. Switching of Na^+, K^+-ATPase isoforms by salinity and prolactin in the gill of a cichlid fish. *J Endocrinol* 209, 237-244.

Tipsmark, C.K., Strom, C.N., Bailey, S.T., Borski, R.J., 2008. Leptin stimulates pituitary prolactin release through an extracellular signal-regulated kinase-dependent pathway. *J Endocrinol* 196, 275-281.

Tipsmark, C.K.l.k., Luckenbach, J.A., Madsen, S.S.n., Borski, R.J., 2007. IGF-I and branchial IGF receptor expression and localization during salinity acclimation in striped bass. *Am J Physiol – Reg Int Comp Physiol* 292, R535-R543.

Torday, J.S., Sun, H., Wang, L., Torres, E., Sunday, M.E., Rubin, L.P., 2002. Leptin mediates the parathyroid hormone-related protein paracrine stimulation of fetal lung maturation. *Am J Physiol Lung Cell Mol Physiol* 282, L405-410.

Trombley, S., Maugars, G., Kling, P., Bjornsson, B.T., Schmitz, M., 2012. Effects of long-term restricted feeding on plasma leptin, hepatic leptin expression and leptin receptor expression in juvenile Atlantic salmon (*Salmo salar* L.). *Gen Comp Endocrinol* 175, 92-99.

Tseng, Y.-C., Hwang, P.-P., 2008. Some insights into energy metabolism for osmoregulation in fish. *Comp Biochem Physiol C: Toxicol Pharmacol* 148, 419-429.

Wabitsch, M., Jensen, P.B., Blum, W.F., Christoffersen, C.T., Englaro, P., Heinze, E., Rascher, W., Teller, W., Tornqvist, H., Hauner, H., 1996. Insulin and cortisol promote leptin production in cultured human fat cells. *Diabetes* 45, 1435-1438.

Wang, M.-Y., Lee, Y., Unger, R.H., 1999. Novel form of lipolysis induced by leptin. *J Biol Chem* 274, 17541-17544.

Won, E.T., Baltzegar, D.A., Picha, M.E., Borski, R.J., 2012. Cloning and characterization of leptin in a Perciform fish, the striped bass (*Morone saxatilis*): control of feeding and regulation by nutritional state. *Gen Comp Endocrinol* 178, 98-107.

Zabeau, L., Lavens, D., Peelman, F., Eyckerman, S., Vandekerckhove, J.l., Tavernier, J., 2003. The ins and outs of leptin receptor activation. *FEBS Letters* 546, 45-50.

Zhang, H., Chen, H., Zhang, Y., Li, S., Lu, D., Zhang, H., Meng, Z., Liu, X., Lin, H., 2012. Molecular cloning, characterization and expression profiles of multiple leptin genes and a leptin receptor gene in orange-spotted grouper (*Epinephelus coioides*). *Gen Comp Endocrinol* (2012) *doi*: 10.1016/j.ygcen.2012.09.008

Table 1. Primer sequences used in cloning and mRNA expression of *lepa* and *lepr* in the Mozambique tilapia (*O. mossambicus*). Abbreviations: *RACE*, Rapid Amplification of cDNA Ends; *qPCR*, quantitative Polymerase Chain Reaction; *gDNA*, genomic DNA; *underlined sequence*, RNA polymerase promoter region.

Primer	Primer Sequence (5' to 3')	Description
Leptin A (*lepa*)		
lep-F	GRA GAT GAA RTC DAA DGT RA	gradient PCR (43-60°C)
lep-R	CAG HGA RGA GAT KTC RRY CTT GAY CT	initial gDNA fragment
lep-5R1	GAC CCC TTT AAA GGC GTC CGG GAT CAG GCT AT	68-72°C; Primary 5' RACE
lep-5R2	CCA GCT GTT CAG CCA TCC ACT TCA CCT TCG AC	68°C; Nested 5' RACE
lep-3R1	CAC CTG CTG ATG ATT TGG ATG GAA CTT CCT CC	68-72°C; Primary 3' RACE
lep-3R2	TGA ATG GTT ACA ATA GCC TGA TCC CGG ACG CC	68°C; Nested 3' RACE
lepCDS-F	ATG GAC TAC GGT CTG GTG	60°C; coding sequence
lepCDS-R	TCA GCA AGT CTG CAG CTG	
lepTD-F	AGC TTT AAG CAT GGG CAC AGC AGC TCC TTT GC	64°C; tissue expression
lepTD-R	TGA GAG CCT CGA TGC CCA CGG TTT GAA TGA AT	profile
lep-NBF1	TGG ACT ACG GTC TGG TGC TAC TGT	57°C; Northern blot probe
lep-NBR1	CTT GCA GTG GCC CTG GTA CTT	(1° PCR amplicon)
lep-NBF2	GAC TAA TAC GAC TCA CTA TAG GGA TGG ACT ACG GTC TGG TGC	70°C; Northern blot probe
lep-NBR2	CTG ATT TAG GTG ACA CTA TAG AAT TGC CCC TGC CGC CAC AGA	(2° PCR amplicon)
q*lepa*-F	GGG TCT CCC AGA TCA AGT ACG A	60°C; qPCR
q*lepa*-R	TGC CGC CAC AGA TGA ATG	
Leptin receptor (*lepr*)		
lepr-F1	GGC CCT GAT TTC TGG AGA AT	47°C; initial
lepr-R1	TTG TAG GCT TCC ACA GTC ACA	gDNA fragment 1
lepr-F2	CCT GTG TTT GCT GAG GGA G	47°C; initial
lepr-R2	CCC ATG AAC ACT TCC TTG GAT TGG	gDNA fragment 2
lepr-5R1	AAC ACG TGG AAT GAA CGC ACA CAG TGG CCT TT	68-72°C; Primary 5' RACE
lepr-5R2	CCG CTT GAG GAC CGA CGC TGG ACT ACA AAT CC	68°C; Nested 5' RACE
lepr-5R3	GGC AGG AAC TCT GAG CAG AAC TGG TGG AGC CA	68°C; Nested 5' RACE 2
lepr-3R1	GCG CTC CTG CTC GTA CAA CTC TGT GGA GGA GC	68-72°C; Primary 3' RACE
lepr-3R2	TCA AGA AGA AGA GCA TGA GGT GAG ACG GGA GA	68°C; Nested 3' RACE
*lepr*TD-F	TTG TAG TCC AGC GTC GGT CC	57°C; tissue expression
*lepr*TD-R	TTG GGA GAG AAC CAG GGT GA	profile
lepr-NB5F1	GGA AGA GCC TCC ACT GTG GAG TGA	58°C; 5' Northern blot probe
lepr-NB5R1	CCA TGC AGG CAG GAC CCA	(1° PCR amplicon)
lepr-NB5F2	GAC TAA TAC GAC TCA CTA TAG GGA GCC TCC ACT GTG GAG TGA	70°C; 5' Northern blot probe
lepr-NB5R2	CTG ATT TAG GTG ACA CTA TAG AAT CCC GCT CTC TCG CTC TCC	(2° PCR amplicon)
lepr-NB3F1	CAT CAT CCT GTT TGT CAC CCT GGT	58°C; 3' Northern blot probe
lepr-NB3R1	CCA TCT CCA AAC CAC GAC AGC T	(1° PCR amplicon)

Table 1. Continued.

Primer	Primer Sequence (5' to 3')	Description
Leptin receptor (*lepr*)		
lepr-NB3F2	GAC TAA TAC GAC TCA CTA TAG GGT GTC ACC CTG GTT CTC TCC	70°C; 3' Northern blot probe (2° PCR amplicon)
lepr-NB3R2	CTG ATT TAG GTG ACA CTA TAG AAT CCA GCT CCC AGA GGC CAC	
q*lepr*-F	AAA TTC ACC GGA AGC AAA CCT	60°C; qPCR
q*lepr*-R	TGA AAT CGC CGC ACT GGT	
β-actin 1 (*bactin1*)		
bactinTD-F	TGA AAT CGC CGC ACT GGT	57°C; tissue expression profile
bactinTD-R	CCT GTT GGC TTT GGG GTT C	
qbactin-F	GAA ATC GCC GCA CTG GTT	60°C; qPCR
qbactin-R	CGA ATC CGG CCT TGC A	

Table 2. Genbank protein accession numbers for sequences used in the phylogenetic analysis of tilapia *lepa* and *lepr*.

Organism	Protein Name	Protein Accession No. (NCBI)
Carp (*Cyprinus carpio*)	Leptin-I	*CAH33828*
	Leptin-II	*CAH33827*
Catfish (*Ictalurus punctatus*)	Leptin (partial sequence)	*AAZ66785*
Chicken (*Gallus gallus*)	Leptin	*O42164*
	Leptin receptor	*NP_989654*
Cow (*Bos taurus*)	Leptin receptor	*DAA31276*
	Interleukin 6 receptor	*DAA31782*
Frog (*Xenopus laevis*)	Leptin	*NP_001089183*
	Granulocyte Colony Stimulating Factor receptor	*NP_001086935*
Frog (*Xenopus tropicalis*)	Leptin receptor	*NP_001037866*
Fugu (*Takifugu rupribes*)	Leptin	*NP_001027897*
	Leptin receptor	*NP_001124341*
	Interleukin 6	*NP_001027894*
Human (*Homo sapiens*)	Leptin	*NP_000221*
	Leptin receptor (isoform 1)	*NP_002294*
	Granulocyte Colony Stimulating Factor receptor	*NP_000751*
Medaka (*Oryzias latipes*)	Leptin A	*NP_001098190*
	Leptin B	*NP_001153914*
	Leptin receptor	*NP_001153915*
Mouse (*Mus musculus*)	Leptin	*NP_032519*
	Interleukin 6 receptor	*NP_034689*
Mozambique tilapia (*O. mossambicus*)	Leptin A (translated from *KC354702*)	Unaccessioned
	Leptin receptor (translated from *KC354703*)	Unaccessioned
Nile tilapia (*Oreochromis niloticus*)	Leptin A (predicted sequence, Leptin-like)	*XP_003440618*
	Leptin B (hypothetical protein, LOC100704338)	*XP_003445036.1*
Olive flounder (*Paralichthys olivaceus*)	Granulocyte Colony Stimulating Factor	*BAE16320*
Orange Spottted grouper (*Epinephelus coioides*)	Leptin A	*AFU55260*
	Leptin B	*AFU55261*
Rainbow trout (*Oncorhynchus mykiss*)	Interleukin 6	*NP_001118129*
	Granulocyte Colony Stimulating Factor receptor	*CAE83614*
Salmon (*Salmo salar*)	Leptin A1	*ACZ02412*
	Leptin A2	*ADI77098*
	Leptin receptor	*NP_001158237*
Spotted Puffer (*Tetraodon nigroviridis*)	Leptin	*BAD94451*
Striped bass (*Morone saxatilis*)	Leptin	*AFD34357*
Zebrafish (*Danio rerio*)	Leptin A	*NP_001122048*
	Leptin B	*NP_001025357*
	Leptin receptor	*NP_001106847*
	Granulocyte Colony Stimulating Factor	*CAQ64749*
	Interleukin 6 receptor	*NP_001107790*
	Granulocyte Colony Stimulating Factor receptor	*NP_001106848*

Figure 1. *ClustalX* multiple-sequence alignment of leptin proteins. Line drawing and highlighted regions denote key structural domains reported for each molecule: precursor signal peptide (*black shaded box*), four alpha helices (*A through D*; *grey shaded boxes*), and a common disulfide bond (*black cysteines*). Putative regions for tilapia and grouper leptins are based upon regions reported for striped bass leptin (Won *et al*., 2012). The accessioned protein sequences used are as follows: Mozambique tilapia (*Oreochromis mossambicus*) leptin a (predicted from KC354702), Nile tilapia (*Oreochromis niloticus*) leptin a (XP_003440618), Orange-spotted grouper (*Epinephelus coioides*) leptin a (AFU55260), Striped bass (*Morone saxatilis*) leptin (AFD34355), Medaka (*Oryzias latipes*) leptin a (NP_001098190), Zebrafish (*Danio rerio*) leptin a (NP_001122048), and Human (*Homo sapiens*) leptin (NP_000221). Symbols and abbreviations: *Dot* – identical amino acid residue, *Dash* – alignment gap.

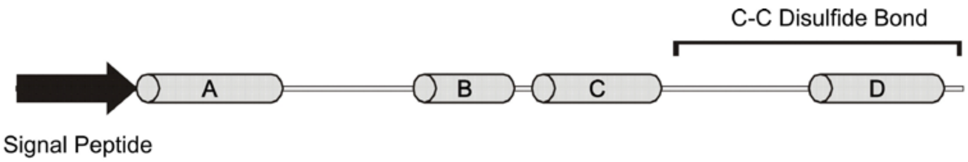


```
                          1          Signal Peptide              Helix A      50
Mozambique tilapia        -MDYGLVLLFSLFQALSMGTAAPLPVEVVT-MKSKVKWMAEQLVVRLDKD
Nile Tilapia              -.........................................-...................
Orange S. Grouper         -...T.A.....LHVF.V.........K-................N..
Striped Bass              -...T.AI...ML.L..VSM........K-................NR.
Medaka                    -..SA.V.FAF..HC.NVA...VNP.LQE-...N.IDI.KEPSL..ENI
Zebrafish                 -.RFPALRSTCILSM..LIHCI.VHQHDRKNV.LQA.TIIVRIREHI.GQ
Human                     MHWGT.CGFLW.WPY.FYVQ.V.IQKVQDD-T.TLI.TIVTRINDISHTQ

                          51                          Helix B                100
Mozambique tilapia        VQVP-------VNWTLNPPADDLDGTSSIVTVLNGYNSLIPDT-FKGVSQ
Nile Tilapia              .............................E.............-......
Orange S. Grouper         F..-------PGL..S....I...P......D......S..-.N....
Striped Bass              FE..-------AGL..S.........L....I.E......S.S-LI....
Medaka                    I.TS-------IGPKFS..S.E.N.L...MA..EECTNQ.S.N-.DEAKK
Zebrafish                 NLL.TLIIGDPGHYPEI.ADKPIQ.LG..METINTFHKVLQKLPN.H.D.
Human                     SVSSKQKV---TGLDFI.GLHPILTL.KMDQT.AV.QQILTSMPSRN.I.

                          101     Helix C                                  150
Mozambique tilapia        IKYDISSLTGYIHLWRQGHCSEQRPKPEVPGPLQELQSHKEFIQTVGIEA
Nile Tilapia              ..................................................
Orange S. Grouper         V.F........GQ.....T.....S..........R....H..S...
Striped Bass              V.V......FLSQ.........LS...V.....RR.K..H..SM..
Medaka                    ..V.....MDSMSE.SDK..G..------.STQA.N.TSRR.SI.ESMQ.
Zebrafish                 .RR.L.T.L..LEG----MDCTLKESTNGKALDAF.EDSASYPF.LEYMT
Human                     .SN.LEN.RDLL.VLAFSKSCHLPWASGLETLDSLGGVLEASGYSTEVV.

                          151   Helix D         171        Identity
Mozambique tilapia        LMRVKEFLNLLLKNLDQLETC              --
Nile Tilapia              .....................              99 %
Orange S. Grouper         ...............H.....              82 %
Striped Bass              ..............NH.....              74 %
Medaka                    VT.L.H..L..QN.S....I.              40 %
Zebrafish                 .N.L.Q.MQK.ID.....KI.              26 %
Human                     .S.LQGS.QDM.WQ..LSPG.              14 %
```

Figure 2. *ClustalX* multiple-sequence alignment of leptin receptor (*lepr*) proteins. The line drawing and highlighted regions denote identifiable domains reported for each molecule: precursor signal peptide (*black shaded box*), Fibronectin type III domain (FN3; *light gray shaded box*), Immunoglobulin-like C2-type domain (Ig; *dark gray shaded box*), WSxWS cell signaling motifs within the FN3 domain (*black box*), and cell signaling domains located within the intracellular region (Jak2/Stat; *white boxes*). The tilapia domain regions were identified from conserved regions in the Fugu and Medaka *lepr* proteins. The accessioned protein sequences used are as follows: Mozambique tilapia (*Oreochromis mossambicus*) leptin receptor (predicted from KC354703), Fugu (*Takifugu rubripes*) leptin receptor (NP_001124341), Atlantic salmon (*Salmo salar*) leptin receptor (NP_001158237), Medaka (*Oryzias latipes*) leptin receptor (NP_001153915), Zebrafish (*Danio rerio*) leptin receptor (NP_001106847), and Human (*Homo sapiens*) leptin receptor (NP_002294). Symbols and abbreviations: *Dot* – identical amino acid residue, *Dash* – alignment gap.


Extracellular
Intracellular
FN3
Ig
FN3
FN3
Signal Peptide
leptin binding domain
Jak2 boxes
Stat box
Mozambique Tilapia
Fugu
Salmon
Medaka
Zebrafish
Human
Fibronectin (FN3) domain
WSxWS motif
Ig-like C2 type domain
leptin binding domain

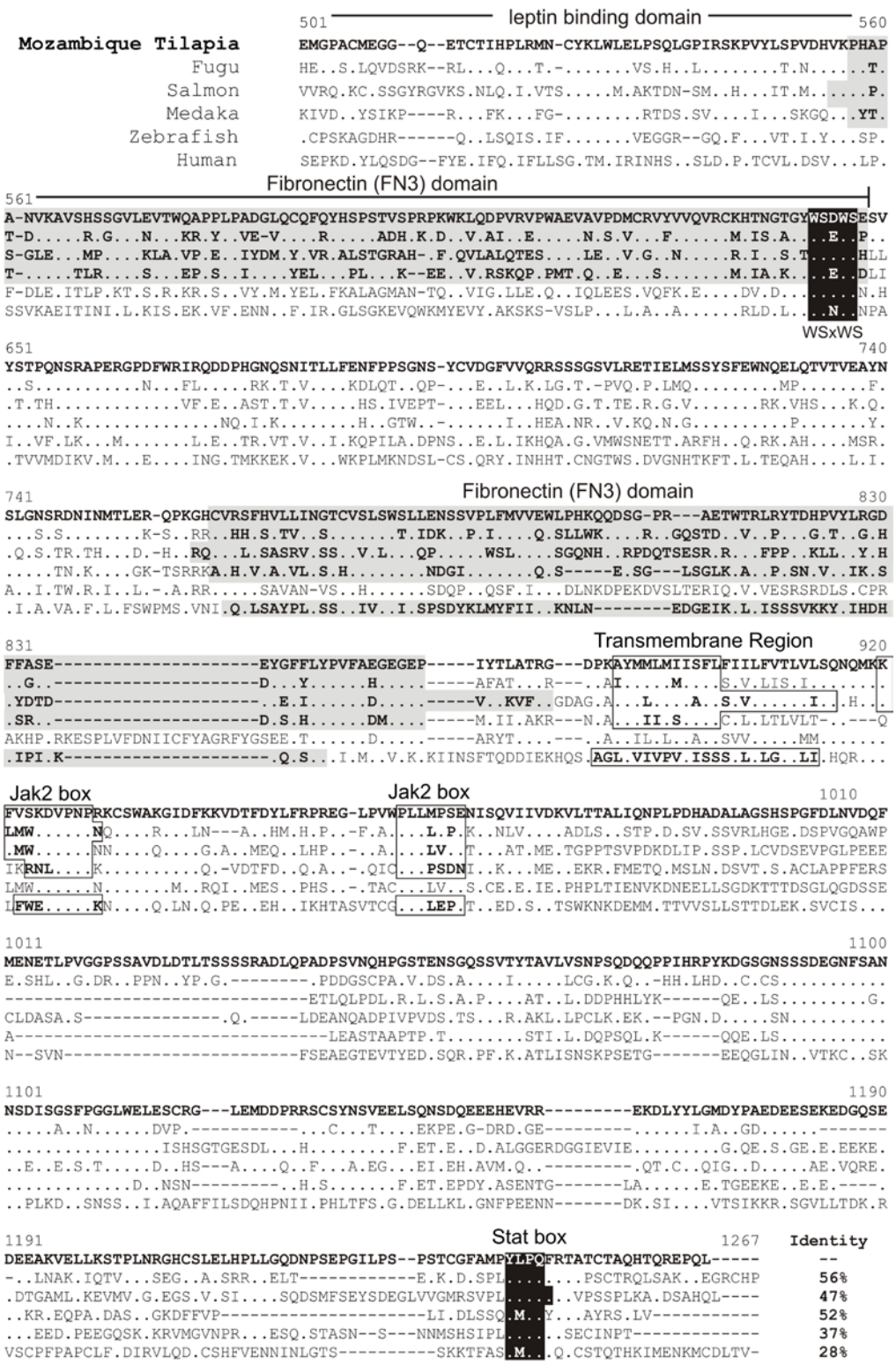
leptin binding domain
Mozambique Tilapia
Fugu
Salmon
Medaka
Zebrafish
Human
Fibronectin (FN3) domain
WSxWS
Fibronectin (FN3) domain
Transmembrane Region
Jak2 box
Jak2 box
Stat box
Identity

Figure 3. Unrooted consensus tree of vertebrate leptin (**A**) and leptin receptor (**B**) protein sequences. Numerical values represent clade-credibility support values (>50%) for each node. The peptides interleukin-6 (*il6*), granulocyte colony stimulating factor (*gcsf*), and their putative receptors (*il6r, gcsfr*) were used as outgroups in the analyses. Symbols: *asterisk* – node support is < 50%. Branch length scale = 0.1 expected amino acid changes per site. The protein accession (Genbank) numbers for all protein sequences are provided in Table 2.

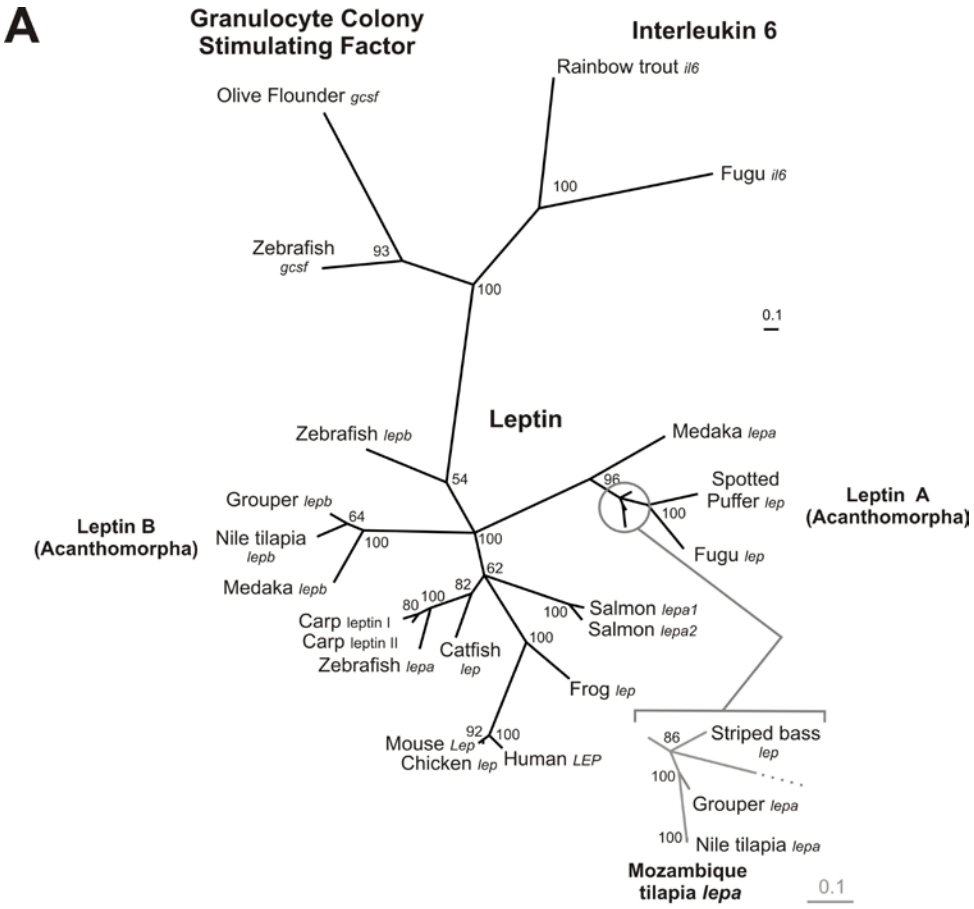
A
Granulocyte Colony Stimulating Factor
Interleukin 6
Rainbow trout il6
Olive Flounder gcsf
Fugu il6
Zebrafish gcsf
0.1
Leptin
Zebrafish lepb
Medaka lepa
Spotted Puffer lep
Leptin A (Acanthomorpha)
Grouper lepb
Leptin B (Acanthomorpha)
Nile tilapia lepb
Fugu lep
Medaka lepb
Salmon lepa1
Salmon lepa2
Carp leptin I
Carp leptin II
Zebrafish lepa
Catfish lep
Frog lep
Striped bass lep
Mouse Lep
Chicken lep
Human LEP
Grouper lepa
Nile tilapia lepa
Mozambique tilapia lepa
0.1
B
Human GCSFR
Frog gcsfr
Granulocyte Colony Receptor
Mouse Il6r
Cow il6r
Rainbow Trout gcsfr
Interleukin 6 Receptor
Zebrafish gcsfr
Zebrafish il6r
Leptin Receptor
0.1
Zebrafish lepr
Salmon lepr
Mouse Lepr
Cow lepr
Human LEPR
Medaka lepr
Mozambique tilapia lepr
Chicken lepr
Frog lepr
Fugu lepr

Figure 4. Tissue expression profile (**A**) and Northern Blot hybridizations of tilapia (**B**) *lepa* and (**C**) *lepr* mRNA. The tissue expression profile was performed by endpoint polymerase chain reaction (PCR) to determine presence or absence of mRNA (± assay). For the Northerns, hybridizations were performed using 0.5-12 µg of enriched mRNA from liver and fat tissue (*lepa*) or gill and muscle tissue (*lepr*). Both 5' and a 3' riboprobes were used in Northern detection of tilapia *lepr* mRNA. The housekeeping genes β-actin (*bactin*) and elongation factor 1-α (*ef1a*) were used as positive controls for the tissue expression profile and Northerns, respectively. The ladder demarcates the migration of a 0.5 to 6.0 kb RNA standard during gel electrophoresis. Symbols: *arrow* – a faint 1.25 kb band is detected for *lepa* in liver tissue.

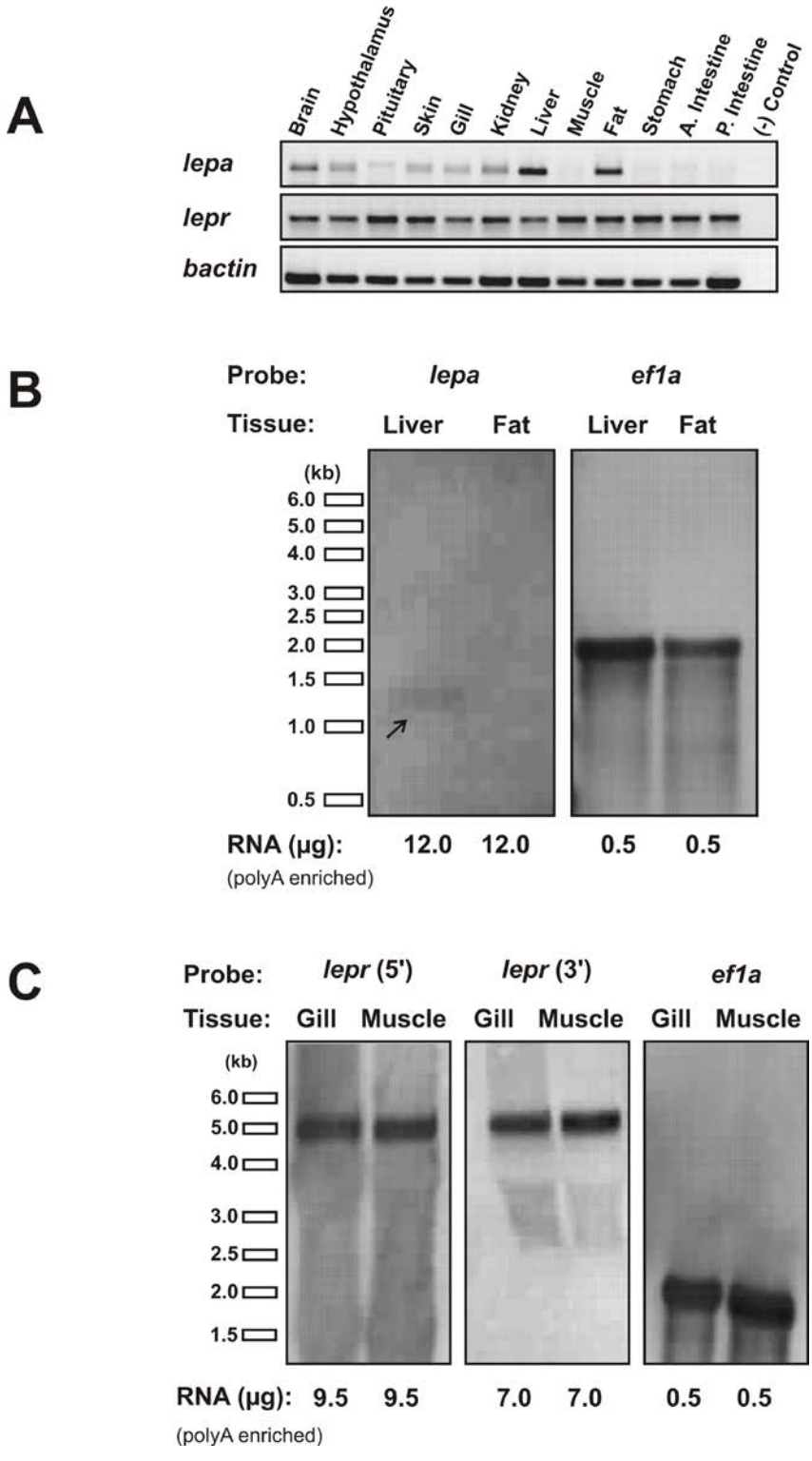
A
Brain
Hypothalamus
Pituitary
Skin
Gill
Kidney
Liver
Muscle
Fat
Stomach
A. Intestine
P. Intestine
(-) Control
lepa
lepr
bactin
B
Probe:
lepa
ef1a
Tissue:
Liver
Fat
Liver
Fat
(kb)
6.0
5.0
4.0
3.0
2.5
2.0
1.5
1.0
0.5
RNA (µg):
12.0
12.0
0.5
0.5
(polyA enriched)
C
Probe:
lepr (5')
lepr (3')
ef1a
Tissue:
Gill
Muscle
Gill
Muscle
Gill
Muscle
(kb)
6.0
5.0
4.0
3.0
2.5
2.0
1.5
RNA (µg):
9.5
9.5
7.0
7.0
0.5
0.5
(polyA enriched)

Figure 5. Effect of salinity transfer on (**A**) plasma osmolality, (**B**) freshwater and (**C**) seawater isoforms of gill Na^+, K^+-ATPase (α subunit) mRNA, and (**D**) gill *lepa* mRNA expression. All mRNA expression data were normalized to β-actin mRNA and expressed as fold change relative to initial fish (log_{10} scaling). Symbols and abbreviations: FW to SW (*open circle*) – freshwater acclimated fish transferred to 2/3 seawater (23 ppt); FW to FW (*closed circle*) – sham transfer of freshwater fish; SW to FW (*open square*) – seawater acclimated fish transferred to freshwater; SW to SW (*closed square*) – sham transfer of seawater fish; *asterisks* – significant differences to sham at same time (*** $p < 0.001$, ** $p < 0.01$, * $p < 0.05$), *letters* – groups with different letters are significantly different across time ($p < 0.05$). Plotted values reflect the group mean ± SEM (n = 8-12).

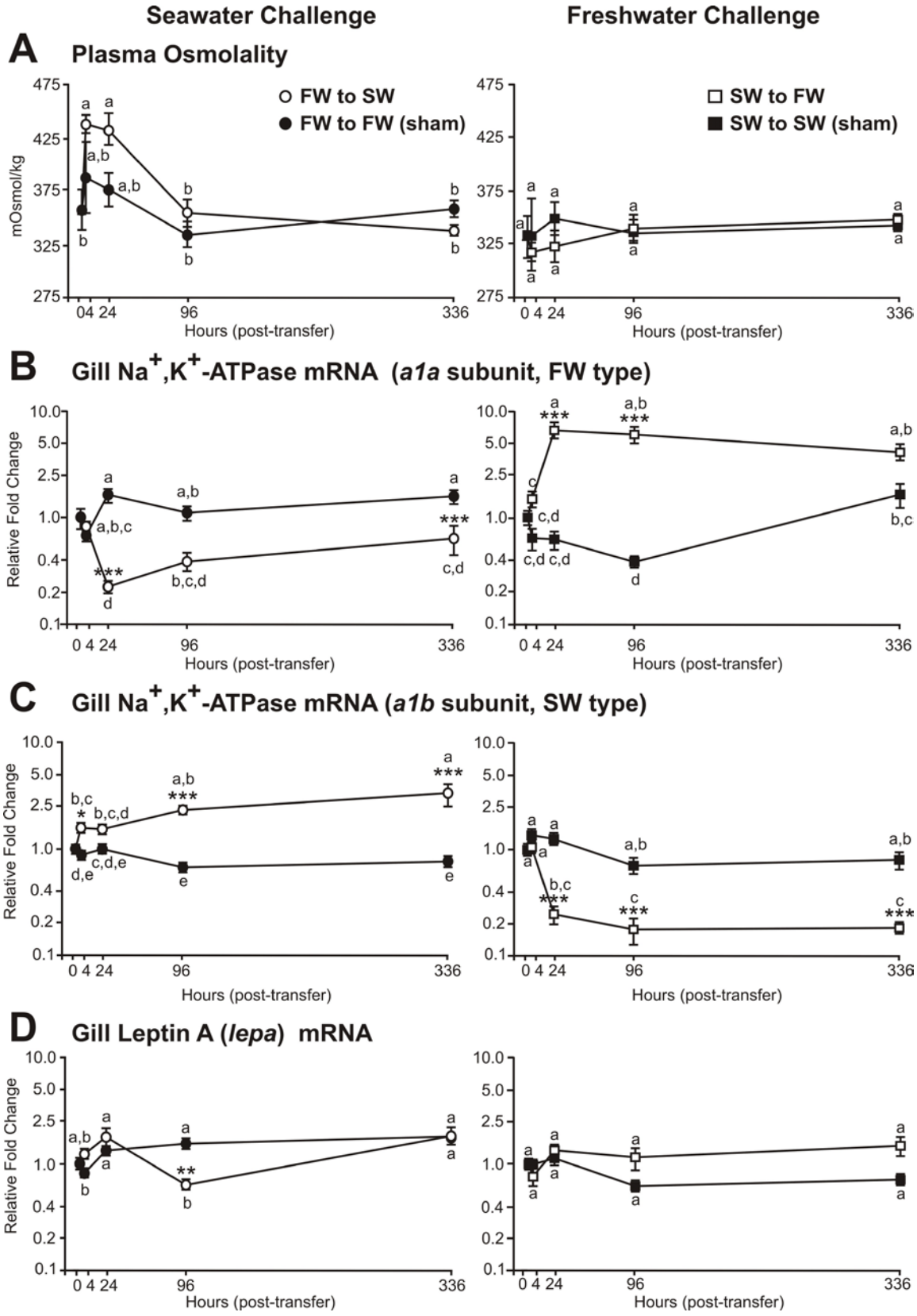
Seawater Challenge
Freshwater Challenge
A
Plasma Osmolality
mOsmol/kg
FW to SW
FW to FW (sham)
SW to FW
SW to SW (sham)
Hours (post-transfer)
B
Gill Na+,K+-ATPase mRNA (a1a subunit, FW type)
Relative Fold Change
C
Gill Na+,K+-ATPase mRNA (a1b subunit, SW type)
D
Gill Leptin A (lepa) mRNA

Figure 6. Effect of salinity transfer on (**A**) gill *lepr* mRNA expression, and liver mRNA expression of (**B**) *lepa* and (**C**) *lepr*. (**D**) Correlation of hepatic *lepa* mRNA and plasma osmolality. The mRNA expression data presented in (A-C) are normalized to β-actin mRNA and expressed as fold change relative to initial fish ($\log_{10}$ scaling) Symbols and abbreviations: FW to SW (*open circle*) – freshwater acclimated fish transferred to 2/3 seawater (23 ppt); FW to FW (*closed circle*) – sham transfer of freshwater fish; SW to FW (*open square*) – seawater acclimated fish transferred to freshwater; SW to SW (*closed square*) – sham transfer of seawater fish; *asterisks* – significant differences to sham at same time (*** $p < 0.001$, ** $p < 0.01$, * $p < 0.05$), *letters* – groups with different letters are significantly different across time ($p < 0.05$). Except for linear correlations (D), all plotted values reflect the group mean ± SEM (n = 8-12).

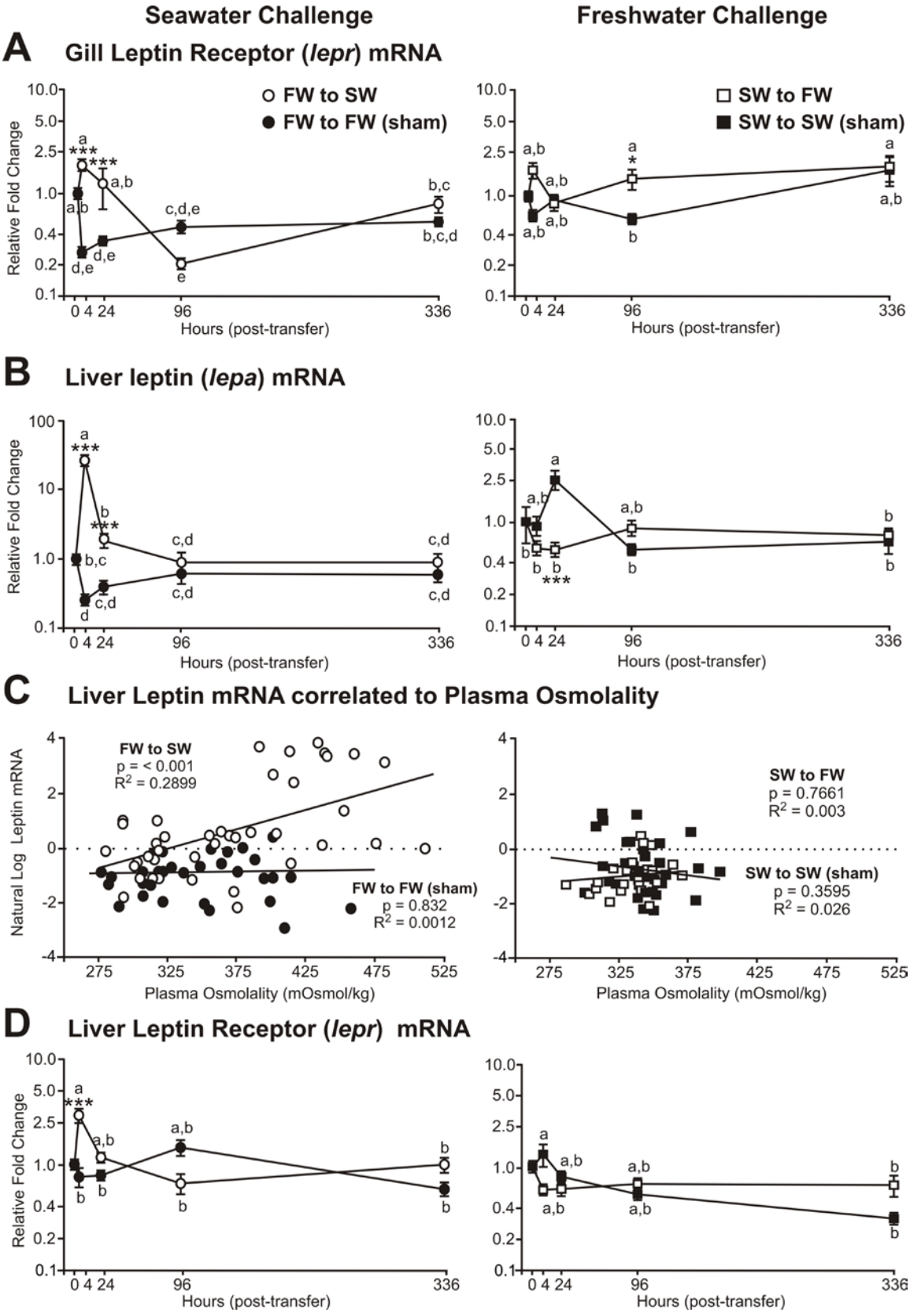
Seawater Challenge
Freshwater Challenge
A
Gill Leptin Receptor (lepr) mRNA
FW to SW
FW to FW (sham)
SW to FW
SW to SW (sham)
Relative Fold Change
Hours (post-transfer)
B
Liver leptin (lepa) mRNA
C
Liver Leptin mRNA correlated to Plasma Osmolality
Natural Log Leptin mRNA
Plasma Osmolality (mOsmol/kg)
FW to SW
p = < 0.001
R2 = 0.2899
FW to FW (sham)
p = 0.832
R2 = 0.0012
SW to FW
p = 0.7661
R2 = 0.003
SW to SW (sham)
p = 0.3595
R2 = 0.026
D
Liver Leptin Receptor (lepr) mRNA

CHAPTER IV

Coordinated Energy Mobilization During Acute Seawater Adaptation: A Novel Action for Leptin in Teleost Fishes[2]

[2] This chapter is being prepared for submission as the following: David A. Baltzegar, Benjamin J. Reading, Jonathon D. Douros, and Russell J. Borski (2013). A novel action for leptin in energy mobilization during acute seawater adaptation in teleost fishes. *Endocrinology* (manuscript in preparation)

Abstract

Osmoregulation is critical feature of life, yet little is known about how energy reserves are mobilized to deal with this metabolically expensive process, particularly in teleost fishes. In this study, we examined the effects of acute salinity transfer (72 hours) and *in vivo* actions of leptin and cortisol on blood metabolites and hepatic energy reserves in the euryhaline Mozambique tilapia (*O. mossambicus*). Transfer to 2/3 seawater (SW, 25 ppt) significantly increased plasma levels of glucose, amino acids, and lactate relative to sham fish, without significant changes in liver glycogen content or glycogen phosphorylase (*gyp*) mRNA. Plasma glucose levels positively correlated to amino acids ($R^2 = 0.614$), but not to lactate. Liver triglycerides, as well as the mRNA expression of lipases (*hsl*, *lpl*), leptin (*lepa*), and leptin receptor (*lepr*), increased significantly during SW transfer, but no significant changes in plasma free fatty acids or triglycerides were observed. In sham fish, a significant reduction in plasma triglycerides occurred, presumably due to fasting. Both exogenous leptin and cortisol administration significantly increased plasma glucose levels, however only leptin decreased liver glycogen content. Leptin administration decreased hormone-sensitive lipase and lipoprotein lipase mRNA expression, whereas cortisol significantly increased expression of these lipases. Our results suggest two sequential mechanisms of glucose mobilization to the blood following acute SW transfer: (1) hepatic glycogenolysis induced by non-genomic actions of leptin, followed by (2) cortisol-mediated gluconeogenesis of amino acids in the liver. The conversion of ketogenic amino acids during the gluconeogenesis phase may account for the observed increase in liver triglycerides. This is the first study to identify a potential hyperglycemic function for leptin during osmotic stress in basal vertebrates.

Introduction

Adaptive osmoregulation in teleost fishes is an important model to understand how tissues manipulate ion fluxes to achieve homeostasis or generate potential energy (Evans, 1999). In the wild, the ability of some fish species to survive across a broader salinity range may confer significant ecological advantages over competitors (Martino and Able, 2003). This process is metabolically expensive, resulting in rapid increases in local ATP usage and respiratory rates, particularly when freshwater adapted fish are exposed to seawater (Bashamohideen and Parvatheswararao, 1972; Morgan *et al*., 1997; Tseng and Hwang, 2008). Adaptation to full-strength seawater (35 ppt) is estimated to comprise 20-68% of total metabolic energy expenditure, depending upon the species, age, and relative size of the animal (Bœuf and Payan, 2001; Morgan *et al*., 1997; Tseng and Hwang, 2008). Increases in metabolic demand are attributed to greater levels of active transport, as multi-fold increases in Na^+, K^+-ATPase activity are reported in the gill, brain, and kidney (Bashamohideen and Parvatheswararao, 1972; Morgan *et al*., 1997; Tseng and Hwang, 2008). For the last 40 years, research has largely focused on metabolic requirements of the gill with relatively few studies addressing systemic changes in energy mobilization during acute periods of osmoregulatory stress (Bashamohideen and Parvatheswararao, 1972; Bœuf and Payan, 2001; Bystriansky *et al*., 2007; Evans *et al*., 2005; Mommsen *et al*., 1999; Morgan *et al*., 1997; Polakof *et al*., 2006; Sangiao-Alvarellos *et al*., 2005; Tseng and Hwang, 2008)

Glucose has been consistently identified as the dominant blood metabolite utilized during osmotic stress (Mommsen, 1984; Tseng and Hwang, 2008). In teleost fishes, the gill is the

dominant site of monovalent ion exchange with the environment, and is considered *glucose-obligate* (Bashamohideen and Parvatheswararao, 1972; Crockett *et al*., 1999; Leblanc and Ballantyne, 1993; Mommsen, 1984). Elevated blood glucose is commonly reported during seawater adaptation and studies point to many potential sources of glucose for the gill (Aragão *et al*., 2010; Bashamohideen and Parvatheswararao, 1972; Fiess *et al*., 2007; Polakof *et al*., 2006). Tseng and colleagues (2007) identified glycogen-rich cells in the gill lamellae, which are capable of glucose transport to ion-secreting cells. These or other cells may also be competent for gluconeogenic conversion of lactate and amino acids (Bystriansky *et al*., 2007; Tseng *et al*., 2008). Yet, the gill itself may only consume a small percentage (3-8%) of the energy expended during seawater adaptation. Therefore the metabolic demands of other tissues, such as the kidney and brain, must also be considered (Bystriansky *et al*., 2007; Morgan and Iwama, 1999; Sangiao-Alvarellos *et al*., 2005). The brain is a large consumer of glucose in mammals (Abi-Saab *et al*., 2002). In fishes, studies of brain metabolism during osmotic stress are few but increases in both ATPase activity and glucose utilization have been reported (Sangiao-Alvarellos *et al*., 2005; Tseng and Hwang, 2008).

Although lipid energy sources are commonly utilized in fish during periods of starvation, data reported for lipid mobilization during salinity transfer are equivocal (Tseng and Hwang, 2008). Plasma free-fatty acids, triglycerides, and liver fatty acid oxidation (*i.e*., 3' hydroxyacyl-CoA dehydrogenase activity, HOAD) were unchanged during the first 96 hours of salinity transfer in gilthead sea bream (*Sparus aurata*) and Arctic char (*Salvelinus alpinus*) (Bystriansky *et al*., 2007; Sangiao-Alvarellos *et al*., 2005). Increases in plasma triglycerides

and liver HOAD activity were reported for fish acclimated to SW for longer periods, suggesting temporal differences in metabolic needs (Sangiao-Alvarellos *et al*., 2005; Tseng and Hwang, 2008). The lack of evidence for lipid mobilization during the early phase is surprising, considering that important SW-adapting hormones such as cortisol and growth hormone have well-demonstrated lipolytic effects (Djurhuus *et al*., 2004; Mommsen *et al*., 1999). These observations suggest our current understanding of both carbohydrate and lipid metabolism during salinity adaptation is incomplete.

Despite the recent identification of leptin for many fish species, its functional role in regulating feeding behavior and energy expenditure remain unclear (Copeland *et al*., 2011). In teleost fishes, including tilapia, leptin is produced primarily in the liver, an important storage site for carbohydrates and lipids (Kurokawa and Murashita, 2009; Kurokawa *et al*., 2005; Chapter 3). In contrast to the established paradigm, leptin levels commonly increase in fishes during periods of fasting, where in mammals levels typically decline (Froiland *et al*. 2012; Fuentes *et al*., 2012; Gambardella *et al*., 2012; Kling *et al*., 2009; Trombley *et al*. 2012). Yet, fish studies using heterologous or native leptin administration *in vivo* consistently report a decline in appetite (de Pedro *et al*., 2006; Murashita *et al*., 2008; Won *et al*., 2012). In mammals, leptin exerts significant lipolytic actions on both liver and adipose tissue, and may also exert marginal hypoglycemic effects peripherally (Benomar *et al*., 2006; Bryson *et al*., 1999; Huang *et al*., 2006; Wang *et al*. 1999). Recently, we identified a significant increase in leptin A (*lepa*) mRNA expression in the liver of tilapia within 4 hours of seawater

transfer (Chapter 3). As seawater adaptation may require significant mobilization of energy stores, it is unknown whether leptin may be involved in this process.

In this study, we examined the effect of salinity transfer on blood metabolites, hepatic energy reserves, hepatic leptin A *(lepa) and* leptin receptor *(lepr)* gene expression in Mozambique tilapia (*Oreochromis mossambicus*). We then assessed the metabolic roles of two hormones, leptin and cortisol, during seawater adaptation by examination of their effects on carbohydrate and lipid metabolism *in vivo*. From these observations, we show glucose is mobilized to the blood over time initially through leptin actions in promoting glycogenolysis within the first 12 hours of salinity transfer. This is likely followed by cortisol-induced gluconeogenesis of amino acids. Significant changes in liver and plasma triglycerides were also observed, which may point to lipogenic conversion of ketogenic amino acids (through the production of acetyl CoA) during gluconeogenesis. These results represent the first coordinated model of energy mobilization during acute hyperosmotic stress, and identify leptin as novel metabolic regulator of salinity adaptation in teleost fishes.

Methods and Materials

Seawater challenge

Adult male tilapia (N= 72; 44 g mean body weight) were acclimated for 3 weeks in freshwater (FW; salinity 0.5 ppt, hardness 74-84 mg/L, alkalinity 126-178 mg/L, pH 8.0) or 2/3 seawater (2/3 SW; Crystal Sea ® salt mix, Marine Enterprises, Baltimore, MD, 23 ppt

salinity, pH 8.0). Fish were held at constant temperature (24-26 °C) and photoperiod (12:12 h light-dark) and fed daily (2 % body weight; 40% protein / 10% fat, Ziegler Brothers, Gardner, PA). Fish from all groups were fasted 24 hours prior to sampling, and during the experiment. FW acclimated fish were transferred to 2/3 SW (hyperosmoregulatory challenge) or sham transferred to FW (sham transfer). Fish from both treatment groups were sampled at 0, 4, 12, 24, and 72 hours afterward.

Recombinant leptins

Recombinant human leptin was purchased courtesy of Dr. A.F. Parlow (National Hormone & Peptide Program, Harbor – UCLA Medical Center, Torrance, CA). Recombinant tilapia *lepa* was developed in our laboratory (courtesy of J. D. Douros) using a Champion™ pET151 Directional TOPO expression kit and provided protocols (Life Technologies, Carlsbad, CA). Briefly, the mature peptide sequence of Mozambique tilapia *lepa* (*Genbank Acc. No*. KC354702) was cloned into an IPTG-inducible expression vector and screened for viable colonies. From induced culture media, the protein was extracted from pelleted cells by lysozyme digestion and by cell sonification. The recombinant protein was purified by two-rounds of double nickel-affinity chromatography followed by size-selective centrifugation (10 and 35 kDa). The eluted protein was dialyzed in $NaCO_3$ for 4 hours before overnight lyophilization.

In vivo injection

Adult male fish (N = 112; 94 g mean weight) were acclimated for 3 weeks in recirculating tank systems (salinity, 11-13 ppt; hardness, 209 –263 mg/L; alkalinity, 127-152 mg/L; pH, 7.5-8.0) and fed daily (3% body weight). The feed, temperature, and photoperiod regimes were the same as for the salinity challenge. Fish were fasted for 24 hours prior to the study, and then for the duration of the experiment. Before injection, fish were anesthetized in buffered MS-222 (Aquatic Eco-Systems, Apopka, FL) and individually weighed. The animals then received one of the following intraperitoneal injections before being returned to housing tanks: human recombinant leptin, 0.5 or 5.0 µg/g BW; tilapia recombinant leptin A, 0.5 or 5.0 µg/g BW; or cortisol (17-Hydroxycorticosterone, Sigma-Aldrich, St. Louis, MO), 10.0 µg/g BW. Control fish received either PBS (leptin vehicle; 329 mOsmol, pH 8.0) or soybean oil (cortisol vehicle). The dosage volumes were 3 µL/g BW for the leptin injections, and 1 µL/g BW for the cortisol injections. Fish injected with cortisol and leptin were held in different tank systems that did not share a common recirculating water supply. Fish were sampled at 6 hours and 24 hours post-injection.

Sampling

Fish were anesthetized in buffered MS-222 before blood and tissue collection. Following decapitation, 100 mg of gill and liver tissue were collected for RNA isolation and stored in RNAlater (Life Technologies, Grand Island, NY) overnight at 4°C and then frozen at –80°C until use. Adjacent sections of liver tissue (50 –100 mg) were collected for glycogen and

triglyceride assays and frozen in liquid N_2. Liver tissue, collected for alanine transaminase activity, was immersed in 1 mL of ice cold SEI Buffer (150 mM Sucrose, 50 mM Imidazole, 10 mM EDTA, pH 7.5) for 30 minutes and then frozen in liquid N_2. Blood (0.25-1.0 mL) was collected from the caudal vein using heparinized syringes (10 mg/mL in 0.9% NaCl) and kept on ice during sampling. Plasma was collected by centrifugation of blood for 15 minutes at 3,000 x *g* and stored at –20° C until use. All procedures were performed in accordance protocols approved by the North Carolina State University *Institutional Animal Care* and *Use Committee*.

Metabolic assays

Plasma osmolality (mOsmol) was measured in duplicate using a VAPRO vapor pressure osmometer (WesCor, Logan, UT). All metabolic assays were performed using colorimetric reagents and protocols provided by Abcam (Cambridge, MA) using a *ELx800* microplate reader (BioTek Instruments, Winooski, VT) containing 450nm and 570 nm optical filters. Sample loading volumes were tested empirically to fall within standard curve ranges (R^2 = 0.98-0.99). All assays were performed using a background control. *Glycogen*: tissue was thawed on ice and weighed before homogenization in 1.25 mL of water. The homogenate was boiled for 5 minutes and then centrifuged (4°C/ 13,000 x *g* for 5 minutes). Diluted supernatant (1:25 in water; 4 µL) was used for detection. *Triglycerides*: tissue samples were weighed and homogenized in 1 mL of 5% Triton X-100. Homogenate was then heated (85°C) and cooled twice before centrifugation. One to eight microliters of the supernatant was used for assay detection. For plasma measurements, 5 µL of neat plasma were used in

the assay. All samples were subtracted against a control for free glycerol. *Alanine transaminase activity*: liver tissue was thawed on ice and removed of residual SEI buffer before weighing. Tissues were sonicated (15 seconds) in 250 µL of ice-cold assay buffer (kit-provided). The homogenate was centrifuged at 4 °C for 10 minutes. Two microliters of sample homogenate or positive control were then compared to a non-kinetic pyruvate standard (1-12 nmol) after color development stabilized. Readings were taken kinetically at 1-minute intervals for 60 minutes, with linear range observed from 11 to 19 minutes. *Glucose*: Two microliters of neat plasma was measured in duplicate. *L-Amino acids*: Five microliters of plasma were used. Reagents react with all L-enantiomer amino acids except glycine. *Free fatty acids*: long chain fatty acids were detected by enzymatic production of acyl-CoA. Thirty microliters of plasma were used and compared against a palmitic acid standard (1-10 nmol). *Lactate*: four microliters of plasma were used in the assay. Optical Density readings (450 nm) were subtracted against an additional control for free NADH.

mRNA expression

Total RNA was isolated from sample tissues using TRI reagent (Molecular Research Center, Cincinnati, OH), coupled with on-column affinity purification and DNAse treatment (*Direct-zol* minipreps, Zymo Research, Irvine, CA). RNA quality was assessed by 18S and 28S ribosomal band integrity in gel electrophoresis, and by $OD_{260:280}$ ratios (range 1.9-2.0) using a Nanodrop 1000 spectrophotometer (Thermo Scientific, Wilmington, DE). Total RNA (1.25 µg) was reversed transcribed using random priming hexamers (High Capacity cDNA Synthesis kit, Life Technologies). The mRNA expression of target genes was measured using

SYBR Green Quantitative Real-Time PCR (qPCR). All primers used in this study are listed in Table C1 (Appendix C). These were designed using ABI Primer Express (*v3.0*). Primers for *O. mossambicus* gill Na^+, K^+-ATPase alpha subunits (*atpa1a, atpa1b*) were described previously (Tipsmark *et al*., 2011). Assays were performed using 12-25 ng of cDNA template and 75 nM primer concentrations with Brilliant II SYBR Green master mix (Agilent, Santa Clara, CA). Triplicate runs for all samples, standards, and negative controls were performed on an ABI 7900HT sequence detection system. The cycling parameters were as follows: 1 cycle—95°C for 10 minutes; 40 cycles—95°C for 30 s, 60°C for 60 s, and 72°C for a 60 s extension. Pooled cDNA samples were used to account for assays using multiple plates (across-plate normalization), with negative controls run on each plate. Cycle threshold (Ct) values for experimental samples were analyzed by absolute quantification, using standard curves derived from 2-fold serially diluted cDNA pools for each tissue (R^2 = 0.98-0.99). Sample data were then normalized to mRNA expression of the housekeeping gene beta-actin (*bactin1*). For the salinity challenge, normalized values are expressed as relative fold changes to the mean of the time 0 group (initial acclimated fish; used here as the calibrator value). For the injection studies, normalized values were expressed as relative fold change to the mean of the six-hour sham vehicle groups. Specific amplification of gene targets was verified by melting curve profiles and gel electrophoresis.

Statistical procedures

All statistical analyses were performed using JMP (*v*9, SAS Institute, Cary, NC). For the salinity challenge, a two-way factorial ANOVA was employed to test the effects of

treatment, time, and their interaction. If whole-model effects were significant, groups were compared by Tukey's HSD test for multiple comparisons. Linear correlations of plasma glucose were performed separately for each treatment group after bivariate analysis in JMP. For statistical purposes, the 0 time point (for each challenge) was treated as both a FW and SW exposure group. One-way ANOVA analysis was employed to examine treatment effects at time points for the injection studies. Significant effects against the controls were tested post hoc using Dunnett's test. The nominal level of significance accepted for all tests was $p < 0.05$.

Results

Freshwater (FW) acclimated tilapia were hyperosmotically challenged to 2/3 seawater (SW). Plasma osmolality was significantly elevated after 4 hours in SW-challenged fish, rising to maximum level at 24 hours (Fig. 1A, $p < 0.001$). Plasma osmolality in SW fish subsequently declined by 72 hours, remaining significantly elevated compared to sham fish ($p < 0.01$). In tilapia, two isoforms of the alpha subunit for gill Na^+, K^+-ATPase have been described, a SW-isoform (*atpa1b*) and a FW-isoform (*atpa1a*) (25). During salinity transfer, gill mRNA expression of *atpa1b* increased for SW fish after 12 hours, and remained significantly elevated for the duration of the study ($p < 0.001$; Fig. 1B). In contrast, gill mRNA levels of *atpa1a* decreased significantly by 12 hours ($p < 0.001$), but afterwards were not different from the sham group (Fig. 1C).

Blood metabolites were examined from plasma of sham and SW-challenged tilapia (Fig. 1D – I). Plasma glucose levels were significantly higher in SW fish at all times post-transfer ($p < 0.05$; Fig. 1D). Mean glucose values of SW-challenged fish reached 8 mM ($p < 0.001$) by 12 hours, then declined by 72 hours (3mM; $p < 0.05$). Mean plasma amino acid levels were also significantly higher in SW fish at all times post-transfer ($p < 0.05$; Fig. 1E), reaching maximum levels at 12 hours (2mM), and then gradually declining. Mean plasma lactate levels were significantly higher for SW fish only at 24 and 72 hours ($p < 0.01$; Fig. 1F). Non-esterified (free) fatty acid levels in SW fish were not significantly different from initial (T_0) values at any time point, however mean levels were significantly higher in the sham group at 4 hours ($p < 0.05$; Fig. 1G). Total plasma triglycerides in SW fish did not change from T_0 levels at any time point (Fig. 1H). In the FW sham group, plasma triglyceride levels steadily decreased from 4 to 72 hours post-transfer, and were significantly lower than SW fish at 72 hours ($p < 0.05$; Fig. 1H). Plasma amino acid and lactate levels were both compared to plasma glucose using bivariate analysis (Fig. 1I-J). In both comparisons, the FW sham group showed no significant correlation to plasma glucose ($R^2 = 0.072$ and 0.0009; respectively). For FW fish transferred to SW, a significant positive correlation of glucose and total amino acids was observed (slope > 0; $R^2 = 0.614$; $p < 0.001$; Fig. 1I). No significant correlation was observed between plasma glucose and lactate levels in SW fish ($R^2 = 0.0309$; Fig. 1J). Hepatic glycogen levels showed a decline at 12 and 24 h of SW transfer, but levels did not significantly different compared with sham-transferred fish (Fig. 2A). Glycogen phosphorylase (*gyp*) mRNA expression was significantly lower in SW fish at 4 hours ($p < 0.01$; Fig. 2B), but was not different from sham fish at later times (Fig. 2B). Hepatic

triglyceride levels rose sharply in SW fish at 24 hours ($p < 0.001$), and then gradually declined by 72 hours (Fig. 2C). Hormone-sensitive lipase (*hsl*) mRNA in the liver was significantly elevated for SW fish at 4, 12, and 24 hours post-transfer, but was not significantly different at 72 hours ($p < 0.05$ to 0.001; Fig. 2D). Hepatic lipoprotein lipase (*lpl*) mRNA was also significantly higher in SW fish at 4 and 12 hours post-transfer ($p < 0.001$), but then levels declined and were significantly lower than sham fish at 72 hours ($p < 0.01$; Fig. 2E).

Hepatic leptin A (*lepa*) mRNA increased 25-fold in SW-transferred fish after 4 hours ($p < 0.001$), and then levels declined afterwards, and were not different from sham fish at 12, 24, and 72 hours (Fig. 2F). Hepatic leptin receptor mRNA was also significantly elevated in SW fish at 12 hours ($p < 0.01$), but not at 24, or 72 hours (Fig. 2G).

Changes in plasma glucose, liver glycogen, and liver *gyp* mRNA were examined in response to *in vivo* injections of leptin and cortisol on carbohydrate metabolism (Fig. 3A-C). Tilapia and human leptin increased plasma glucose levels in a dose dependent manner at 6 hours post-injection ($p < 0.001$; Fig. 3A). At 24 hours, only fish injected with human leptin (low dose) had significantly higher glucose compared to control fish ($p < 0.05$; Fig. 3A). Cortisol-injected fish had significantly higher glucose levels at both 6 and 24 hours ($p < 0.05$; Fig. 3A). Treatment with human and tilapia leptin significantly decreased liver glycogen content after 6 hours ($p < 0.05$; Fig. 3B), but glycogen levels were not different at 24 hours relative to control fish. No significant differences in liver glycogen were observed between cortisol-

injected and control fish (Fig. 3B). Liver glycogen phosphorylase (*gyp*) mRNA expression levels were not significantly different in leptin-injected fish (6 or 24 hours), but cortisol-injected fish had significantly higher *gyp* mRNA expression at 6 hours ($p < 0.05$), but not at 24 hours, relative to sham-injected fish (Fig. 3C).

Plasma amino acid levels and liver alanine transaminase (ALT) activity were examined from injected fish (Fig. 3D-E). Plasma amino acids were unchanged 6 hours after leptin or cortisol injection, but were significantly higher at 24 hours after injection with human leptin ($p < 0.01$ to 0.05; Fig. 3D). Amino acids were not significantly different in cortisol-injected fish at 24 hours (Fig. 3D). No significant changes in liver ALT activity were observed in leptin or cortisol injected fish (Fig. 3E).

Hepatic triglyceride levels and lipase (*hsl*, *lpl*) mRNA expression were measured to examine leptin and cortisol effects upon lipid metabolism (Fig. 4). Mean liver triglycerides were significantly higher ($p < 0.05$) in fish injected with human leptin (5.0 µg/g BW) after 6 hours, relative to control (Fig. 4A). For cortisol, no significant difference in liver triglycerides was observed at 6 or 24 hours (Fig. 4A). Liver *hsl* mRNA declined 2-fold at 6 hours following low dose tilapia leptin injection ($p < 0.05$; Fig. 4B). By contrast, cortisol-injected fish had significantly higher *hsl* mRNA levels at 6 hours, relative to sham fish ($p < 0.01$; Fig 4B). At 24 hours, no significant changes in *hsl* mRNA were observed with either hormone (Fig. 4B). Liver *lpl* mRNA expression levels were significantly lower at 6 hours for fish injected with tilapia leptin (both doses; $p < 0.01$ to 0.05; Fig. 4C). Cortisol-injected fish had significantly higher *lpl* mRNA expression at 6 hours, relative to sham fish ($p < 0.05$; Fig. 4D). No

significant differences in *lpl* mRNA expression were observed for either hormone at 24 hours (Fig. 4C).

Discussion

A comprehensive understanding of energy mobilization during osmotic stress remains elusive despite many contributions to osmoregulatory research (Tseng and Hwang, 2008). Historically, research has focused on local metabolism and energy usage of the gill, however recent studies identify osmoregulation as a *global* stressor, requiring significant energy mobilization for use by many tissues (Jürss *et al*., 1995; Mommsen, 1984; Morgan and Iwama, 1999). In this study, seawater (SW) transferred fish had significantly higher levels of plasma glucose, with the highest increase occurring 12 hours prior to the peak elevation of plasma osmolality or gill Na^+, K^+-ATPase mRNA (Figs. 1A, 1B, 1D). Concomitant changes in plasma free-fatty acids or triglyceride levels did not occur (Figs. 1G, 1H). Together, these observations support previous findings of preferential utilization of glucose during osmoregulatory stress (Fiess et al., 2007; Tseng and Hwang, 2008).

Significant decreases in hepatic glycogen during hyperosmotic adaptation have been reported, both for Mozambique tilapia and Gilthead sea bream (*Sparus aurata*) (Chang *et al*., 2007; Polakof *et al*., 2006). Tilapia liver glycogen levels were reduced within 12 hours of SW transfer, and then remained constant for 7 days at significantly lower levels relative to sham fish (Chang *et al*., 2007). In our study, liver glycogen was reduced within the first 24 hours of SW transfer, but levels were not significantly different from sham fish (Fig. 2A).

The lack of a significant decline in liver glycogen during SW transfer could be masked by fasting effects, as suggested by the steady decline observed for sham-transferred fish (Fig. 2A). Overall, glycogenolysis is likely a critical component for mobilizing carbohydrate resources during salinity adaptation. Although the hormonal mechanisms controlling this process are unknown, our results suggest that leptin may be a strong candidate. We found in SW-challenged fish that hepatic *lepa* mRNA increased 25-fold after 4 hours, and *lepr* mRNA after 12 hours (Figs. 2F, 2G), in parallel with initial changes in plasma glucose. Administration of human leptin induced a dose dependent increase in plasma glucose at 6, but not 24 hours, *in vivo* (Fig. 3A). Both tilapia and human leptin significantly reduced liver glycogen content at the high dose (5.0 µg) by 6 hours (Fig. 3B). Thus it would appear, in contrast to what is observed in mammals, that leptin may serve as a hyperglycemic factor critical to meeting energy requirements of seawater challenge.

Recent studies are supportive of a link between leptin and carbohydrate mobilization in poikilotherms, yet how leptin is regulated by changes in energy state, or the mechanism of action inducing glycogenolysis is unclear (Aguilar *et al*., 2010; Fröiland *et al*., 2012; Gambardella *et al*., 2012; Paolucci *et al*., 2006). In rainbow trout (*Oncorhynchus mykiss*), intra-cerebroventricular injection of human leptin resulted in a peripheral decrease of liver glycogen, consistent with both a glucosensing function for leptin and glycogenolysis mediated through a sympathetic (catecholamine) response (Aguilar *et al*., 2010). Our data point to a possible paracrine effect for leptin, as increases in *lepa* and *lepr* mRNA were observed in the liver, the source of circulating leptin in fishes (Kurokawa and Murashita,

2009; Kurokawa *et al*., 2005). Leptin administration reduced hepatic glycogen without appreciable changes in glycogen phosphorylase (*gyp*) mRNA expression in the present study (Fig. 3C). As this enzyme is rate limiting in glycogen catabolism, we hypothesize leptin may exert a non-genomic effect through activation of cellular kinases (Chang *et al*., 2007; Mancour *et al*., 2012). This is consistent with observations in the lizard (*Podarcis sicula*), where increases in liver tyrosine-phosphorylated proteins were observed after leptin injection (Paolucci *et al*., 2006). Recently, an increase in hepatic *lepa* mRNA expression was also reported in zebrafish under induced hypoxic conditions (Chu *et al*., 2010). As hypoxia is a global stressor, it is possible that leptin may also promote glucose mobilization under these conditions as well (Bernier *et al*., 2012; Gorissen *et al*., 2009; Oltmanns *et al*., 2004). We found that homologous and heterologous leptin were ineffective in altering either gill Na^+, K^+, -ATPase mRNA or plasma osmolality suggesting the hormone's effect may be limited to regulation of energy expenditure, rather than hydromineral balance, although future studies are required to more thoroughly assess this component (Fig. C3; Appendix C). Overall, results here suggest both leptin production and sensitivity are enhanced during SW acclimation, and the hormone may function as a hyperglycemic factor during acute periods of energy expenditure in teleosts and perhaps other poikliotherms. Whether leptin is directly responsive to alterations in ambient osmotic pressure or other factors sensitive to salinity remains to be determined.

In mammals leptin is *adipostatic*, circulating in proportion to total fat stores, and promotes satiety by down-regulation of orexigenic factors in the hypothalamus (Copeland *et al*., 2011).

High levels of circulating leptin are lipolytic, reducing total triglycerides by increasing oxidative metabolism and reducing VLDL secretion in the liver (Huang *et al*., 2006). Potential lipolytic effects for leptin in fish remain unclear (Frøiland *et al*., 2012, Copeland *et al*., 2011), although knockdown of leptin reduces yolk absorption in developing zebrafish (Liu *et al*., 2012). In this study, liver triglycerides were unchanged and hepatic lipase mRNA was reduced in leptin-injected fish (Fig. 4A-C), suggesting the hormone has little effect on lipolysis. Further, were leptin lipolytic one would expect a reduction in hepatic or plasma triglycerides during SW challenge when *lepa* expression is elevated. However, hepatic triglycerides increased and plasma triglycerides and free fatty acids were unchanged in SW transferred fish (Figs. 1G, 1H, 2C). Hence, it would appear that leptin preferentially mobilizes carbohydrate energy reserves rather than lipids in tilapia and possibly other poikilotherms. Taken together, studies suggest leptin functions as a metabolic regulator in all vertebrates, but its unique effects on discrete energy reserves have diverged from the classic mouse paradigm. Multiple factors may have contributed to this variation: partial or complete neofunctionalization of leptin paralogs (*lepa* and *lepb*), differences between homothermic and poikilothermic metabolism, or the degree of regulation by other hormones (e.g., insulin and glucagon) (Kurokawa and Murashita, 2009; Moon, 2001; Paolucci *et al*., 2006; Wright *et al*., 2000; Zhang *et al*., 2012).

Until recently, gluconeogenesis was not closely examined during SW adaptation despite reports of elevated levels of amino acids and nitrogen excretion rates (Aragão *et al*., 2010; Bystriansky *et al*., 2007; Evans *et al*., 2005; Polakof *et al*., 2006). This lack of attention could

be attributed to two factors: (*1*) free amino acids were thought to act primarily as solutes to counter osmotic forces, and (*2*) reported decreases in glycogen point to glycogenolysis as the source of glucose (Chang *et al*., 2007; Tseng and Hwang, 2008). In the teleost oocyte, free amino acids act as osmotic effectors but are also utilized as diffusible nutrients to support early embyrogenesis (Matsubara *et al*., 1999; Reading and Sullivan, 2011; Reading *et al*., 2008). Therefore, circulating free amino acids in the blood may serve a similar dual role, acting as both a counter osmolyte and a gluconeogenic substrate. In the present studies both plasma amino acid and lactate levels are elevated in the blood of SW fish (Figs. 1E, 1F), but only amino acids correlated significantly to plasma glucose (Figs. 1I, 1J). Moreover, previous work in tilapia demonstrates that declines in glycogen stabilize after 12 h of SW acclimation (Chang *et al*., 2007), despite a continued elevation in glucose beyond this period, as observed in the present study (Fig. 1D). These observations support gluconeogenic conversion of amino acids may augment blood glucose levels during sustained (>12 h) periods of salinity acclimation.

Although cortisol-mediated gluconeogenesis is well described in mammals and in some fish species (Djurhuus *et al*., 2004; Mommsen *et al*., 1999; Vijayan *et al*., 1996), we observed a stronger lipolytic than gluconeogenic effect for cortisol. Significantly higher levels of plasma glucose were observed in cortisol-injected fish at 6 and 24 hours (Fig. 3A), however plasma amino acids and liver alanine transaminase activity were not different from control fish (Figs. 3D, 3E). Whether this lack of effect is due to a single acute dosage is uncertain. Rising serum levels of cortisol, as well as increased sensitivity, are well demonstrated in teleost fishes

during salinity adaptation (Marshal *et al*., 1999; Jacob and Taylor, 1983). In sea bream (*Sparus aurata*), significant increases in amino acids and transaminase activity were reported for long-term acclimated (14 day) fish (Polakof *et al*., 2006). These observations may indicate sustained levels of cortisol are required to initiate gluconeogenesis. Interestingly, we observed a significant increase in plasma amino acids in fish injected with human leptin after 24 hours (Fig. 3D), suggesting leptin may exhibit a slight proteolytic effect. Consistent with lipolytic actions (Djurhuss *et al*., 2004; Mommsen *et al*., 1999), cortisol enhanced mRNA expression of hepatic lipases (*lpl*, *hsl*) (Fig. 4B-C). Cortisol also significantly induced hepatic leptin receptor mRNA expression, but not leptin mRNA itself, suggesting leptin sensitivity may increase in response to conditions of elevated glucocorticoids (Figs. C1A and C1B; Appendix C).

Although seemingly paradoxical, the effects observed upon lipid metabolism during the SW challenge may be related to glucose mobilization for obligatory tissues. Liver triglyceride levels doubled in SW fish from 12 to 24 hours, and remained elevated thereafter (Fig. 2C). During this time, lipoprotein lipase (*lpl*) and hormone-sensitive lipase (*hsl*) mRNA also increased sharply by 12 h and over 24 h, respectively (Fig. 2E, 2F). This suggests hepatic triglyceride accumulation and mobilization may occur, either for oxidative catabolism or export to peripheral tissues, despite little change to blood lipid levels. Plasma triglycerides did not change in SW transferred fish, but a significant decrease was observed in sham animals over the 72 h experiment, where all fish were fasted (Fig. 1H). Therefore, the liver may export excess triglycerides in the form of large lipid transfer proteins (LTTP's) to the

blood for use by tissues capable of lipid catabolism (e.g., somatic muscle) (Smolenaars *et al*., 2007), thus ameliorating a decline from fasting. The increase of lipids in the liver may also provide a source to balance the energy deficits of gluconeogenesis (Van Der Boon *et al*., 1991; Vijayan *et al*., 1996). No change in levels of plasma free fatty acids were observed in SW fish, suggesting the increase in hepatic triglycerides did not result from the mobilization of lipids in adipose tissue (Fig. 1G). We attempted to evaluate plasma levels of beta-hydroxybutyrate (ketone) and free glycerol, but levels were below assay detection (data not shown). Instead, lipogenesis in the liver may result from the accumulation of acetyl-CoA derivatives by catabolism of ketogenic amino acids, such as leucine and isoleucine (Fig. 5) (Jürss *et al*., 1995). Elevated levels of these amino acids during salinity adaptation have been previously reported (Bystriansky *et al*., 2007). Based on these observations, we propose a model of energy mobilization in the teleost liver during SW adaptation (Fig. 5). Free amino acids, released into the blood from muscle proteolysis, can be utilized by the liver directly (e.g., TCA cycle) or converted to glucose (glucogenic amino acids) or fatty acids (ketogenic amino acids), the latter stored as triglycerides (Fig. 5). Hepatic export of lipids (e.g., as LLTP's) to oxidatively-competent tissues spares glucose for use by obligate tissues, and is consistent with glucose-fatty acid (Randle) cycle dynamics (Frayn, 2003).

Osmoregulation is both a critical and bioenergetically expensive component of survival for all vertebrates, yet relatively few studies have examined energy mobilization from a systemic perspective in basal groups. In fishes, the liver is not always the largest carbohydrate or lipid reserve, however it is generally first-utilized under catabolic conditions (Tseng and Hwang,

2008). We propose a model unifying historical and present observations during salinity transfer to better understand energy mobilization during acute stress, as well as the functional interplay between discrete sources of energy (Fig. 5). Our results suggest two sequential mechanisms of glucose mobilization to the blood following acute SW transfer: (1) hepatic glycogenolysis induced by non-genomic actions of leptin, followed by (2) potential gluconeogenesis of amino acids in the liver. This is the first study to demonstrate that leptin expression is sensitive to osmotic stress and may function as a novel hyperglycemic factor of salinity adaptation in teleost fishes. The interactions of leptin with canonical regulators of glucose metabolism, or with other osmoregulatory hormones, remain to be described (Borski *et al*., 2011; Tipsmark *et al*., 2008).

Acknowledgements

We wish to thank Andy McGinty (Pamlico Aquaculture Facility, Aurora, NC), Brad Ring, and John Davis (NCSU, Raleigh, NC) for the husbandry and care of the research animals used in this study.

REFERENCES

Abi-Saab, W.M., Maggs, D.G., Jones, T., Jacob, R., Srihari, V., Thompson, J., Kerr, D., Leone, P., Krystal, J.H., Spencer, D.D., During, M.J., Sherwin, R.S., 2002. Striking differences in glucose and lactate levels between brain extracellular fluid and plasma in conscious human subjects: effects of hyperglycemia and hypoglycemia. *J Cereb Blood Flow Metab* 22, 271-279.

Aguilar, A.J., Conde-Sieira, M., Polakof, S., Míguez, J.M., Soengas, J.L., 2010. Central leptin treatment modulates brain glucosensing function and peripheral energy metabolism of rainbow trout. *Peptides* 31, 1044-1054.

Aragão, C., Costas, B., Vargas-Chacoff, L., Ruiz-Jarabo, I., Dinis, M., Mancera, J., Conceição, L., 2010. Changes in plasma amino acid levels in a euryhaline fish exposed to different environmental salinities. *Amino Acids* 38, 311-317.

Bashamohideen, M., Parvatheswararao, V., 1972. Adaptations to osmotic stress in the fresh-water euryhaline teleost *Tilapia mossambica*. IV. Changes in blood glucose, liver glycogen and muscle glycogen levels. *Mar Biol* 16, 68-74.

Benomar, Y., Naour, N., Aubourg, A., Bailleux, V., Gertler, A., Djiane, J., Guerre-Millo, M., Taouis, M., 2006. Insulin and leptin induce *Glut4* plasma membrane translocation and glucose uptake in a human neuronal cell line by a phosphatidylinositol 3-kinase-dependent mechanism. *Endocrinology* 147, 2550-2556.

Bernier, N.J., Gorissen M., Flik, G., 2012. Differential effects of chronic hypoxia and feed restriction on the expression of leptin and its receptor, food intake regulation and the endocrine stress response in common carp. *J Exp Biol* 215, 2273-2282.

Bœuf, G., Payan, P., 2001. How should salinity influence fish growth? *Comp Biochem Physiol C*: 130, 411-423.

Borski, R.J., Won, E.T., Baltzegar, D.A., 2011. Leptin stimulates hepatic growth hormone receptor expression: possible role in enhancing GH-mediated anabolic processes in fish. *Frontiers Endocrinol*; The inaugural meeting of the North American Society for Comparative Endocrinology, Ann Arbor, USA (Event Abstract).

Bryson, J.M., Phuyal, J.L., Swan, V., Caterson, I.D., 1999. Leptin has acute effects on glucose and lipid metabolism in both lean and gold thioglucose-obese mice. *Am J Physiol Endocrinol Metab* 277, E417-E422.

Bystriansky, J.S., Frick, N.T., Ballantyne, J.S., 2007. Intermediary metabolism of Arctic char *Salvelinus alpinus* during short-term salinity exposure. *J Exp Biol* 210, 1971-1985.

Chang, J.C.-H., Wu, S.-M., Tseng, Y.-C., Lee, Y.-C., Baba, O., Hwang, P-P., 2007. Regulation of glycogen metabolism in gills and liver of the euryhaline tilapia (*Oreochromis mossambicus*) during acclimation to seawater. *J Exp Biol* 210, 3494-3504.

Chu, D.L., Li, V.W., Yu, R.M., 2010. Leptin: clue to poor appetite in oxygen-starved fish. *Mol Cell Endocrinol* 319, 143-146.

Copeland, D.L., Duff, R.J., Liu, Q., Prokop, J., Londraville, R.L., 2011. Leptin in teleost fishes: an argument for comparative study. *Front Physiol* 2, 26.

Crockett, E.L., Londraville, R.L., Wilkes, E.E., Popesco, M.C., 1999. Enzymatic capacities for β-oxidation of fatty fuels are low in the gill of teleost fishes despite presence of fatty acid-binding protein. *J Exp Zool* 284, 276-285.

de Pedro, N., Martínez-Alvarez, R., Delgado, M.J., 2006. Acute and chronic leptin reduces food intake and body weight in goldfish (*Carassius auratus*). *J Endocrinol* 188, 513-520.

Djurhuus, C.B., Gravholt, C.H., Nielsen, S., Pedersen, S.B., Moller, N., Schmitz, O., 2004. Additive effects of cortisol and growth hormone on regional and systemic lipolysis in humans. *Am J Physiol Endocrinol Metab* 286, E488-494.

Evans, D.H., 1999. Ionic transport in the fish gill epithelium. *J Exp Zool* 283, 641-652.

Evans, D.H., Piermarini, P.M., Choe, K.P., 2005. The multifunctional fish gill: dominant site of gas exchange, osmoregulation, acid-base regulation, and excretion of nitrogenous waste. *Physiol Rev* 85, 97-177.

Fiess, J.C., Kunkel-Patterson, A., Mathias, L., Riley, L.G., Yancey, P.H., Hirano, T., Grau, E.G., 2007. Effects of environmental salinity and temperature on osmoregulatory ability, organic osmolytes, and plasma hormone profiles in the Mozambique tilapia (*Oreochromis mossambicus*). *Comp Biochem Physiol A* 146, 252-264.

Frayn, K.N., 2003. The glucose-fatty acid cycle: a physiological perspective. *Biochem Soc Trans* 31, 1115-1119.

Frøiland, E., Jobling, M., Björnsson, B.T., Kling, P., Ravuri, C.S., Jørgensen, E.H., 2012. Seasonal appetite regulation in the anadromous Arctic charr: evidence for a role of adiposity in the regulation of appetite but not for leptin in signaling adiposity. *Gen Comp Endocrinol* 178, 330-337.

Fuentes, E.N., Kling, P., Einarsdöttir, I.E., Alvarez, M., Valdés, J.A., Molina, A., Björnsson, B.T., 2012. Plasma leptin and growth hormone levels in the fine flounder (*Paralichthys adspersus*) increase gradually during fasting and decline rapidly after refeeding. *Gen Comp Endocrinol* 177, 120-127.

Gambardella, C., Gallus, L., Amaroli, A., Terova, G., Masini, M.A., Ferrando, S., 2012. Fasting and re-feeding impact on leptin and aquaglyceroporin 9 in the liver of European sea bass (*Dicentrarchus labrax*). *Aquaculture* 354-355, 1-6.

Gorissen, M., Bernier, N.J., Manuel, R., de Gelder, S., Metz, J.R., Huising, M.O., Flik, G., 2012. Recombinant human leptin attenuates stress axis activity in common carp (*Cyprinus carpio* L.). *Gen Comp Endocrinol* 178, 75-81.

Huang, W., Dedousis, N., Bandi, A., Lopaschuk, G.D., O'Doherty, R.M., 2006. Liver triglyceride secretion and lipid oxidative metabolism are rapidly altered by leptin *in vivo*. *Endocrinology* 147, 1480-1487.

Jacob, W.F., Taylor, M.H., 1983. The time course of seawater acclimation in *Fundulus heteroclitus* L. *J Exp Zool* 228, 33-39.

Jürss, K., Bastrop, R., Mommsen, T.P., 1995. Chapter 7: Amino acid metabolism in fish. *In*: Biochemistry and Molecular Biology of Fishes, Elsevier 4, 159-189.

Kling, P., Rønnestad, I., Stefansson, S.O., Murashita, K., Kurokawa, T., Björnsson, B.T., 2009. A homologous salmonid leptin radioimmunoassay indicates elevated plasma leptin levels during fasting of rainbow trout. *Gen Comp Endcrinol* 162, 307-312.

Kurokawa, T., Uji, S., Suzuki, T., 2005. Identification of cDNA coding for a homologue to mammalian leptin from pufferfish, *Takifugu rubripes*. *Peptides* 26, 745-750.

Kurokawa, T., Murashita, K., 2009. Genomic characterization of multiple leptin genes and a leptin receptor gene in the Japanese medaka, *Oryzias latipes*. *Gen Comp Endocrinol* 161, 229-237.

Leblanc, P.J., Ballantyne, J.S., 1993. β-Hydroxybutyrate dehydrogenase in teleost fish. *J Exp Zool* 267, 356-358.

Liu, Q., Dalman, M., Chen, Y., Akhter, M., Brahmandam, S., Patel, Y., Lowe, J., Thakkar, M., Gregory, A.-V., Phelps, D., Riley, C., Londraville, R.L., 2012. Knockdown of leptin A expression dramatically alters zebrafish development. *Gen Comp Endocrinol* 178, 562-572.

Mancour, L. V., Daghestani, H.N., Dutta, S., Westfield, G.H., Schilling, J., Oleskie, A.N., Herbstman, J.F., Chou, S.Z., Skiniotis, G., 2012. Ligand-induced architecture of the leptin receptor signaling complex. *Mol Cell* 48, 655-661.

Martino, E.J., Able, K.W., 2003. Fish assemblages across the marine to low salinity transition zone of a temperate estuary. *Estuarine Coast Shelf Sci* 56, 969-987.

Marshall, W.S., Emberley, T.R., Singer, T.D., Bryson, S.E., McCormick, S.D., 1999. Time course of salinity adaptation in a strongly euryhaline estuarine teleost, *Fundulus heteroclitus*: a multivariable approach. *J Exp Biol* 202, 1535-1544.

Matsubara, T., Ohkubo, N., Andoh, T., Sullivan, C.V., Hara, A., 1999. Two forms of vitellogenin, yielding two distinct lipovitellins, play different roles during oocyte maturation and early development of Barfin flounder, *Verasper moseri*, a marine teleost that spawns pelagic eggs. *Dev Biol* 213, 18–32.

Mommsen, T.P., 1984. Metabolism of the fish gill. *In*: Hoar WS, Randall DJ (*eds*). Fish Physiology. Academic Press, Orlando, FL, 203-238.

Mommsen, T.P., Vijayan, M.M., Moon, T.W., 1999. Cortisol in teleosts: dynamics, mechanisms of action, and metabolic regulation. *Rev Fish Biol Fish* 9, 211-268.

Moon, T.W., 2001. Glucose intolerance in teleost fish: fact or fiction? *Comp Biochem Physiol B* 129, 243-249.

Morgan, J.D., Sakamoto, T., Grau, E.G., Iwama, G.K., 1997. Physiological and respiratory responses of the Mozambique tilapia (*Oreochromis mossambicus*) to salinity acclimation. *Comp Biochem Physiol A* 117, 391-398.

Morgan, J.D., Iwama, G.K., 1999. Energy cost of NaCl transport in isolated gills of cutthroat trout. *Am J Physiol: Reg, Int Comp Physiol* 277, R631-R639.

Murashita, K., Uji, S., Yamamoto, T., Rønnestad, I., Kurokawa, T., 2008. Production of recombinant leptin and its effects on food intake in rainbow trout (*Oncorhynchus mykiss*). *Comp Biochem Physiol B: Biochem Mol Biol* 150, 377-384.

Oltmanns, K.M., Gehring, H., Rudolf, S., Schultes, B., Rook, S., Schweiger, U., Born, J., Fehm, H.L., Peters, A., 2004. Hypoxia causes glucose intolerance in humans. *Am J Resp Critical Care Med* 169, 1231-1237.

Paolucci, M., Buono, S., Sciarrillo, R., Putti, R., 2006. Effects of leptin administration on the endocrine pancreas and liver in the lizard *Podarcis sicula*. *J Exp Zool A* 305, 383-395.

Polakof, S., Arjona, F.J., Sangiao-Alvarellos, S., del Río, M.M.P., Mancera, J.M., Soengas, J.L., 2006. Food deprivation alters osmoregulatory and metabolic responses to salinity acclimation in gilthead sea bream *Sparus aurata*. *J Comp Physiol B* 176: 441-452.

Reading, B.J., Hiramatsu, N., Sawaguchi, S., Matsubara, T., Hara, A., Lively, M.O., Sullivan, C.V., 2008. Conserved and variant molecular and functional features of multiple egg yolk precursor proteins (vitellogenins) in White Perch (*Morone americana*) and other teleosts. *Mar Biotechnol* 11, 169-187.

Reading, B.J., Sullivan, C.V., 2011. Chapter 257: Vitellogenesis in fishes. *In*: Farrell, A.P., Stevens, E.D., Cech, J.J., Richards, J.G. (*eds*). Encyclopedia of fish physiology: from genome to environment. Academic Press, Elsevier, p. 635-646.

Sangiao-Alvarellos, S., Arjona, F.J., del Río, M.P.M., Míguez, J.M., Mancera, J.M., Soengas, J.L., 2005. Time course of osmoregulatory and metabolic changes during osmotic acclimation in *Sparus aurata*. *J Exp Biol* 208, 4291-4304.

Smolenaars, M.M., Madsen, O., Rodenburg, K.W., Van der Horst, D.J., 2007. Molecular diversity and evolution of the large lipid transfer protein superfamily. *J Lipid Res* 48, 489-502.

Tipsmark, C.K., Strom, C.N., Bailey, S.T., Borski, R.J., 2008. Leptin stimulates pituitary prolactin release through an extracellular signal-regulated kinase-dependent pathway. *J Endocrinol* 196, 275-281.

Tipsmark, C.K., Breves, J.P., Seale, A.P., Lerner, D.T., Hirano, T., Grau, E.G., 2011. Switching of Na^+, K^+-ATPase isoforms by salinity and prolactin in the gill of a cichlid fish. *J Endocrinol* 209, 237-244.

Trombley, S., Maugars, G., Kling, P., Björnsson, B.T., Schmitz, M., 2012. Effects of long-term restricted feeding on plasma leptin, hepatic leptin expression and leptin receptor expression in juvenile Atlantic salmon (*Salmo salar* L). *Gen Comp Endocrinol* 175, 92-99.

Tseng, Y.-C., Huang, C.-J., Chang, J.C.-H., Teng, W.-Y., Baba, O., Fann, M.-J., Hwang, P.-P., 2007. Glycogen phosphorylase in glycogen-rich cells is involved in the energy supply for ion regulation in fish gill epithelia. *Am J Physiol: Reg, Int Comp Physiol* 293, R482-R491.

Tseng, Y.-C., Hwang, P.-P., 2008. Some insights into energy metabolism for osmoregulation in fish. *Comp Biochem Physiol C* 148, 419-429.

Tseng, Y.-C., Lee, J.-R., Chang, J.C.-H., Kuo, C.-H., Lee, S.-J., Hwang, P.-P., 2008. Regulation of lactate dehydrogenase in tilapia (*Oreochromis mossambicus*) gills during acclimation to salinity challenge. *Zool Studies* 47, 473-480.

Van Der Boon, J., Van Den Thillart, G.E.E.J.M., Addink, A.D.F., 1991. The effects of cortisol administration on intermediary metabolism in teleost fish. *Comp Biochem Physiol A* 100, 47-53.

Vijayan, M., Mommsen, T., Glémet, H.C., Moon, T., 1996. Metabolic effects of cortisol treatment in a marine teleost, the sea raven. *J Exp Biol* 199, 1509-1514.

Wang, M.Y., Lee, Y., Unger, R.H., 1999. Novel form of lipolysis induced by leptin. *J Biol Chem* 274, 17541-17544.

Won, E.T., Baltzegar, D.A., Picha, M.E., Borski, R.J., 2012. Cloning and characterization of leptin in a perciform fish, the striped bass (*Morone saxatilis*): control of feeding and regulation by nutritional state. *Gen Comp Endocrinol*. 178, 98-107.

Wright, J.R., Bonen, A., Conlon, J.M., Pohajdak, B., 2000. Glucose homeostasis in the teleost fish tilapia: insights from Brockmann Body xenotransplantation studies. *Am Zool* 40: 234-245.

Zhang, H., Chen, H., Zhang, Y., Li, S., Lu, D., Zhang, H., Meng, Z., Liu, X., Lin, H., 2012. Molecular cloning, characterization and expression profiles of multiple leptin genes and a leptin receptor gene in orange-spotted grouper (*Epinephelus coioides*). *Gen Comp Endocrinol* (2012) *doi*: 10.1016/j.ygcen.2012.09.008.

Figure 1. Effect of salinity transfer on plasma osmolality, gill ATPase (*atpa1a* and *atpalb*) mRNA expression, and plasma metabolites. Freshwater-acclimated tilapia were transferred to freshwater (FW to FW; sham) or to 2/3 seawater (FW to SW). (**A**) Osmolality (mOsmol/kg). (**B**) Gill *atpa1b* (seawater type) mRNA. (**C**) Gill *atpa1a* (freshwater type) mRNA. (**D**) Glucose (mM). (**E**) Amino acids (mM). (**F**) Lactate (mM). (**G**) Free-fatty acids (µM). (**H**) Triglycerides (µM). (**I**) Correlation of plasma glucose to amino acids. (J) Correlation of plasma glucose to lactate. *Symbols*: asterisks denote significant effects against sham at a given time *** $p < 0.001$, ** $p < 0.01$, * $p < 0.05$; groups with different letters are significantly different across time, $p < 0.05$. The mRNA data is expressed as fold change relative to initial (T_0) fish. Except for correlations, values represent group mean ± SEM (n = 5-8).

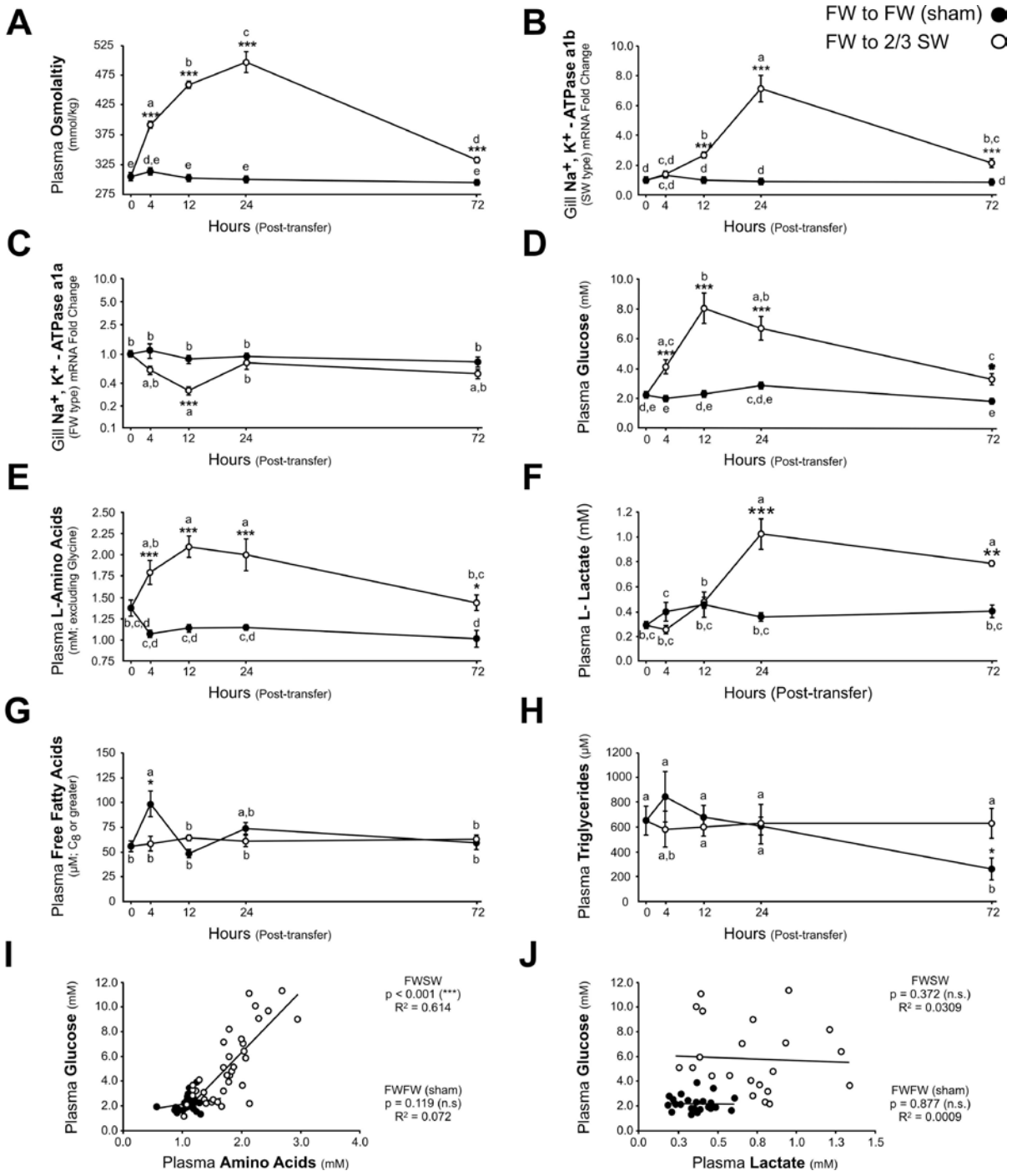
A
Plasma Osmolaltiy (mmol/kg)
Hours (Post-transfer)
B
FW to FW (sham)
FW to 2/3 SW
Gill Na+, K+ - ATPase a1b (SW type) mRNA Fold Change
Hours (Post-transfer)
C
Gill Na+, K+ - ATPase a1a (FW type) mRNA Fold Change
Hours (Post-transfer)
D
Plasma Glucose (mM)
Hours (Post-transfer)
E
Plasma L-Amino Acids (mM; excluding Glycine)
Hours (Post-transfer)
F
Plasma L- Lactate (mM)
Hours (Post-transfer)
G
Plasma Free Fatty Acids (μM; C8 or greater)
Hours (Post-transfer)
H
Plasma Triglycerides (μM)
Hours (Post-transfer)
I
Plasma Glucose (mM)
Plasma Amino Acids (mM)
FWSW
p < 0.001 (***)
R² = 0.614
FWFW (sham)
p = 0.119 (n.s)
R² = 0.072
J
Plasma Glucose (mM)
Plasma Lactate (mM)
FWSW
p = 0.372 (n.s.)
R² = 0.0309
FWFW (sham)
p = 0.877 (n.s.)
R² = 0.0009

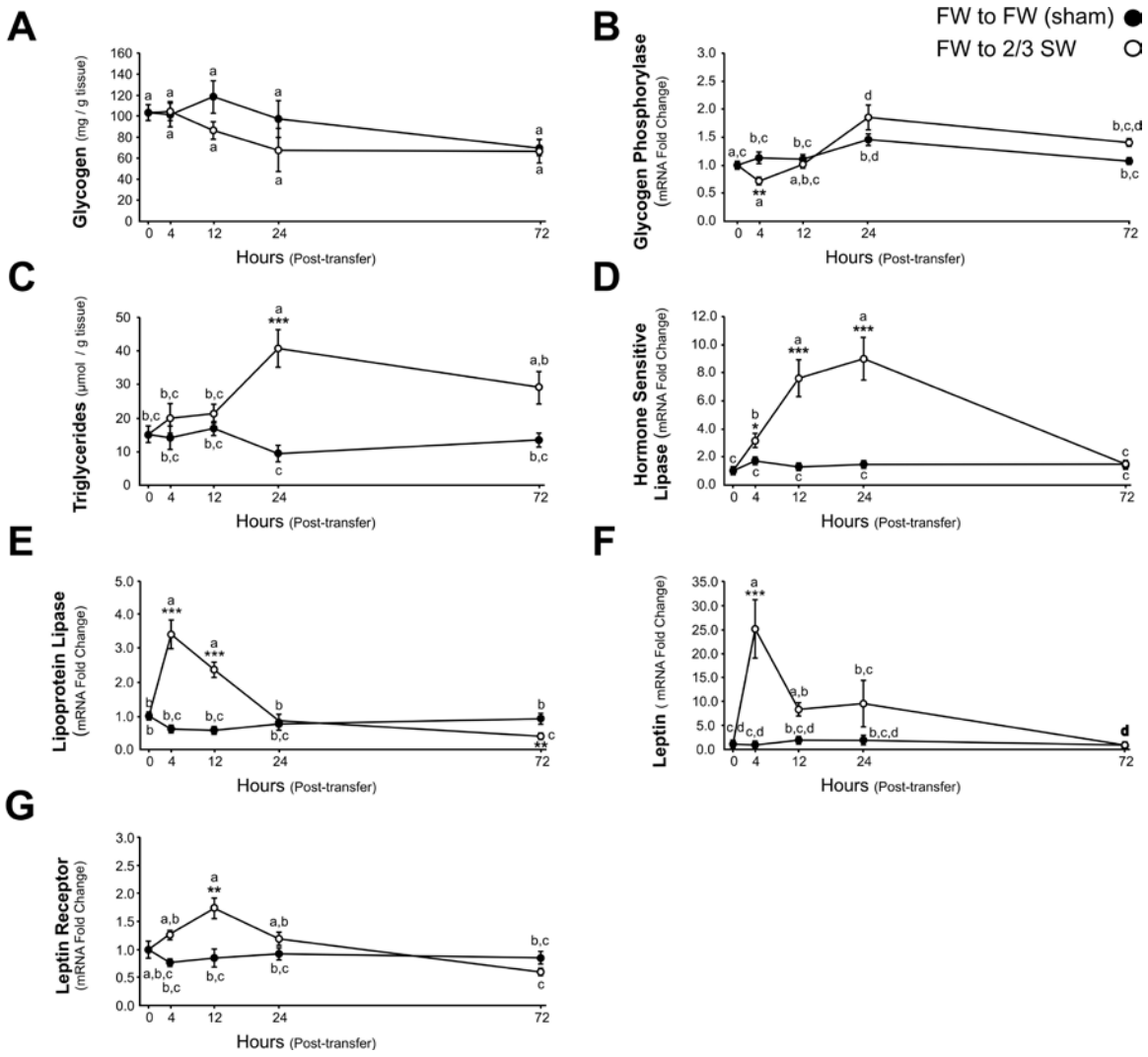

Figure 2. Effect of salinity transfer on liver glycogen, triglycerides, and mRNA expression of metabolic genes. Freshwater-acclimated tilapia were transferred to freshwater (FW to FW; sham) or to 2/3 seawater (FW to SW). **(A)** Glycogen (mg/gram tissue) (**B**) Glycogen phosphorylase (*pyg*) mRNA expression. (**C**) Triglycerides (µg/ gram tissue). (**D**) Hormone-sensitive lipase (*hsl*) mRNA expression. (**E**) Lipoprotein lipase (*lpl*) mRNA expression. (**F**) Leptin (*lepa*) mRNA expression. (**G**) Leptin receptor (*lepr*) mRNA expression. *Symbols*: asterisks denote significant effects against sham at a given time *** $p < 0.001$, ** $p < 0.01$, * $p < 0.05$; groups with different letters are significantly different across time, $p < 0.05$. The mRNA data is expressed as fold change relative to initial (T_0) fish. Values represent group mean ± SEM (n = 5-8).

Figure 3. *In vivo* effects of leptin or cortisol on carbohydrate and protein metabolism. *Leptin* – intraperitoneal (IP) injection of tilapia or human leptin (0.5 and 5.0 µg/ g BW) or sham (PBS; phosphate buffered saline). *Cortisol* –IP injection of 10 µg/ g BW or sham (soybean oil). **(A)** Plasma glucose (mM). (**B**) Liver glycogen (mg/ g tissue). (**C**) Liver glycogen phosphorylase (*pyg*) mRNA. (**D**) Plasma amino acids (mM). (**E**) Liver alanine transaminase activity (µmol pyruvate/ gram-hour). *Symbols*: asterisks denote significant effects against sham at a given time *** $p < 0.001$, ** $p < 0.01$, * $p < 0.05$. All mRNA data are expressed as fold change relative to the 6-hour sham groups. Values represent the group mean ± SEM (n = 5-8).

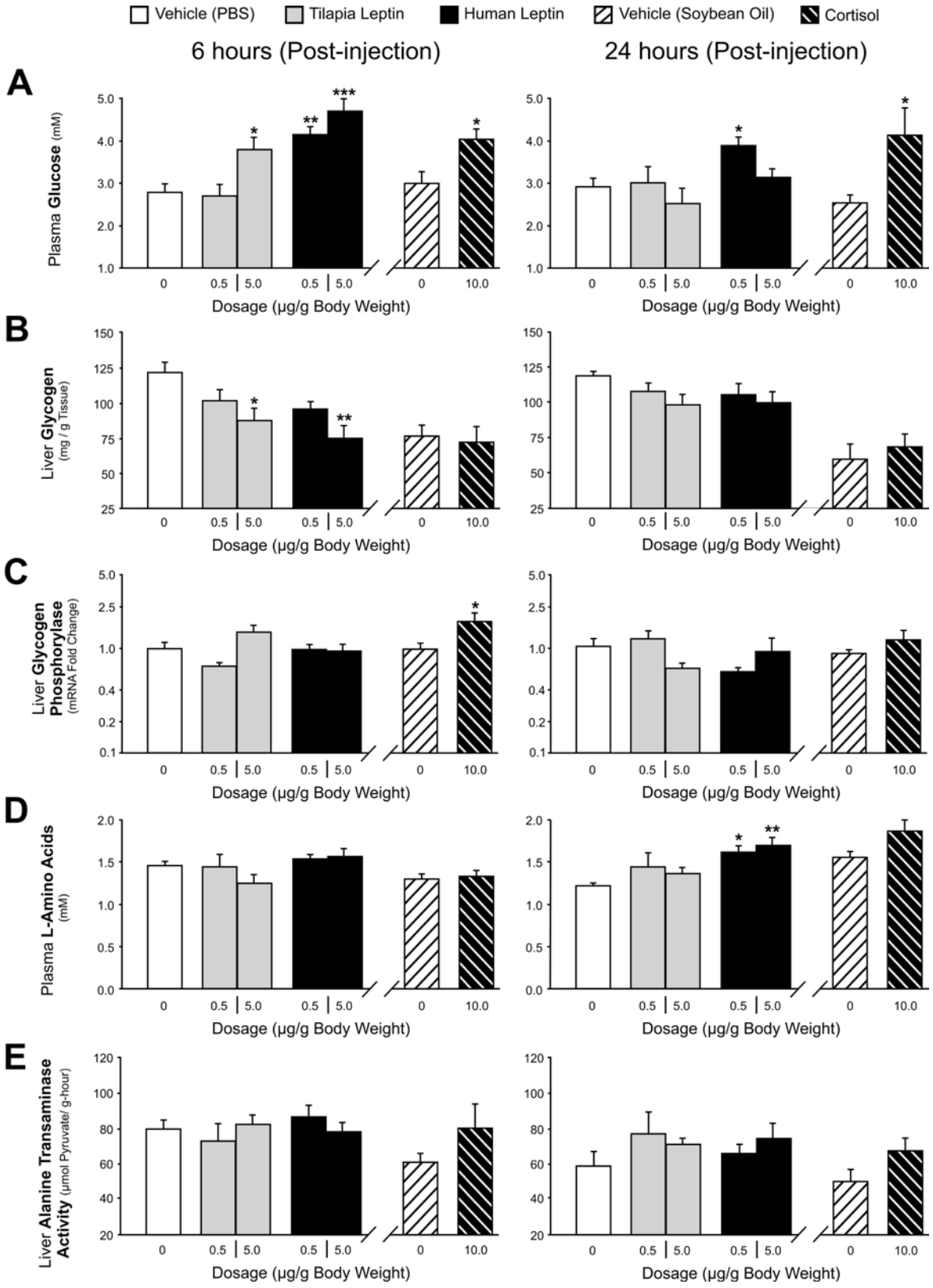
Vehicle (PBS)
Tilapia Leptin
Human Leptin
Vehicle (Soybean Oil)
Cortisol
6 hours (Post-injection)
24 hours (Post-injection)
A
Plasma Glucose (mM)
B
Liver Glycogen (mg / g Tissue)
C
Liver Glycogen Phosphorylase (mRNA Fold Change)
D
Plasma L-Amino Acids (mM)
E
Liver Alanine Transaminase Activity (µmol Pyruvate/ g-hour)
Dosage (µg/g Body Weight)
0
0.5
5.0
10.0

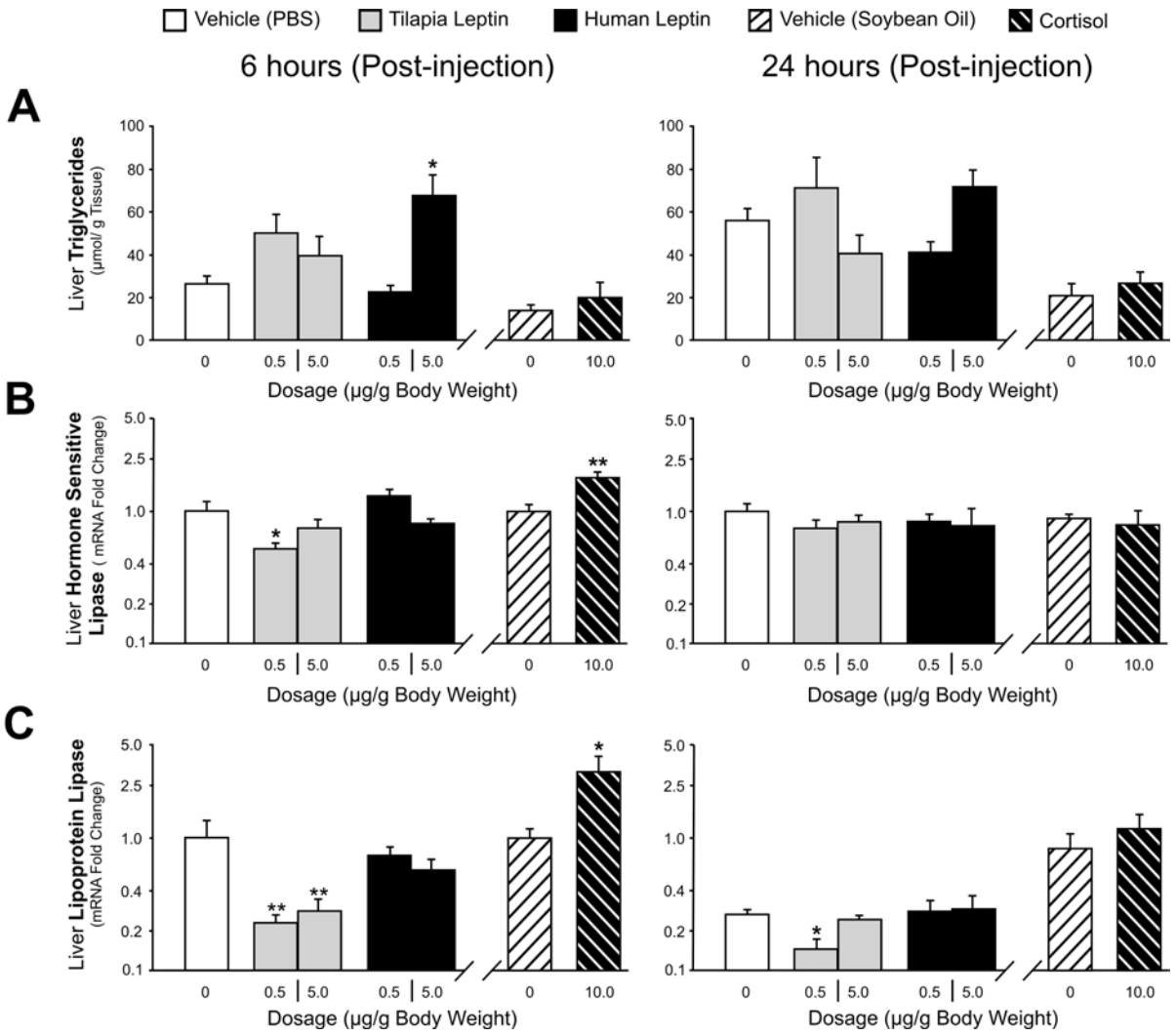

Figure 4. *In vivo* effects of leptin or cortisol on lipid metabolism. *Leptin* –intraperitoneal (IP) injection of tilapia or human leptin (0.5 and 5.0 µg/ g BW) or sham (PBS; phosphate buffered saline). *Cortisol* –IP injection of 10 µg/ g BW or sham (soybean oil). **(A)** Liver triglycerides (µmol/ gram tissue). (**B**) Liver hormone-sensitive lipase (*hsl*) mRNA (**C**) Liver lipoprotein lipase (*lpl*) mRNA. *Symbols*: asterisks denote significant effects against sham at a given time *** $p < 0.001$, ** $p < 0.01$, * $p < 0.05$. All mRNA data are expressed as fold change relative to the 6-hour sham groups. Values represent the group mean ± SEM (n = 5-8).

Figure 5. Proposed bioenergetic model of carbohydrate and lipid mobilization during hyperosmotic stress. Osmosensitive tissues are glucose obligate, but may utilize local sources through glycogen catabolism (glycogenolysis) or through gluconeogenesis of lactate. During acute stress additional glucose is required, and first is mobilized to the blood by hepatic glycogenolysis in the liver. Secondly, levels of blood amino acids (glucogenic and ketogenic) rise as a result of muscle proteolysis, and undergo transamination and deamination reactions in the liver. Glucogenic amino acids can be utilized directly by the liver (Krebs cycle), or converted to glucose via gluconeogenesis. Ketogenic amino acids can also be directly utilized, or sequestered as triglycerides following fatty acid synthesis and lipogenesis. Accumulated triglycerides can be desterified and used locally (oxidation), or exported as lipoproteins to tissues capable of local lipid catabolism. *Symbols and abbreviations*: FA, fatty acid; VLDL, very low-density lipoproteins; ATP – adenosine triphosphate; ?, potential metabolic actions.

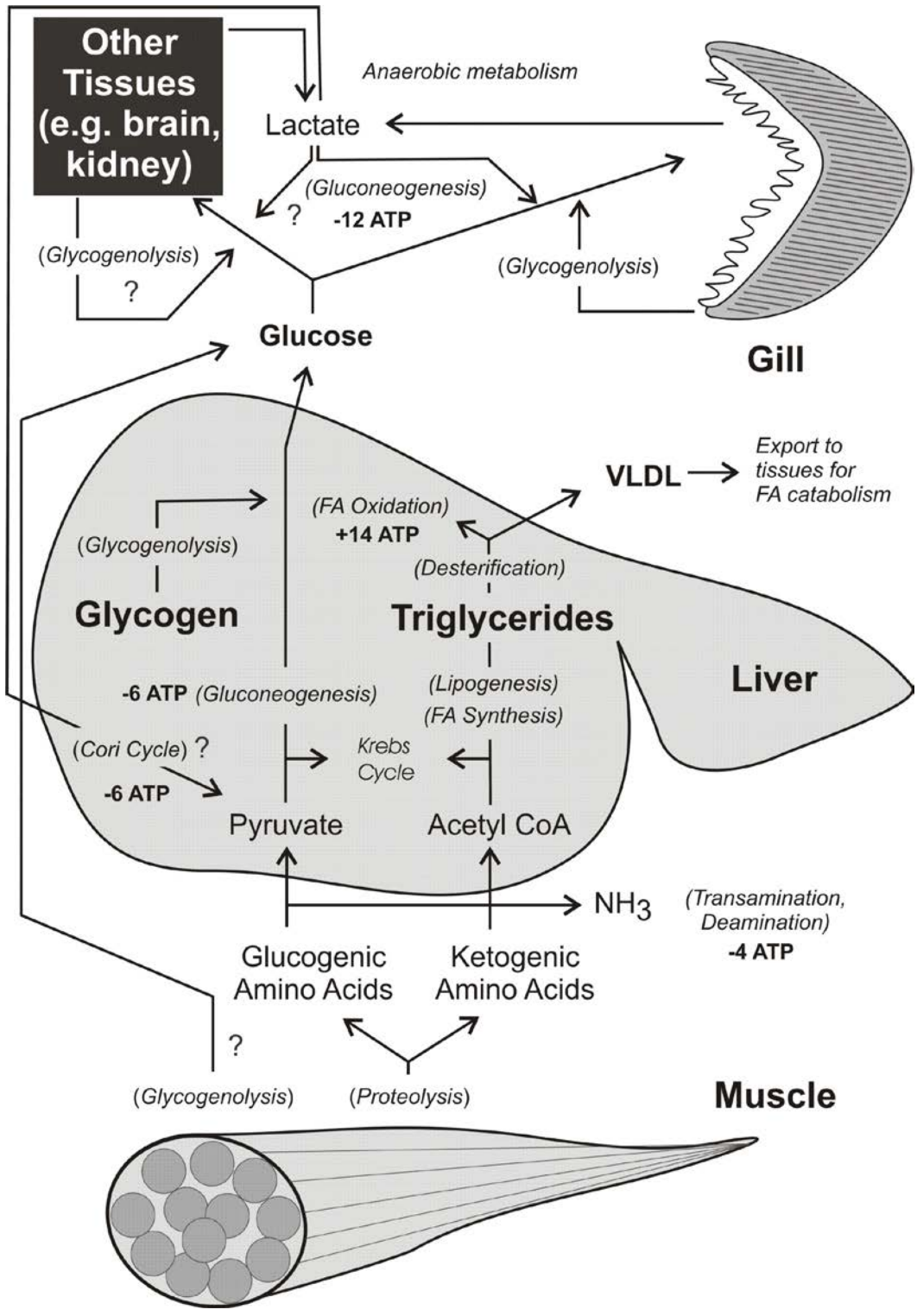
Other Tissues (e.g. brain, kidney)
Anaerobic metabolism
Lactate
(Gluconeogenesis)
?
-12 ATP
(Glycogenolysis)
?
(Glycogenolysis)
Glucose
Gill
VLDL
Export to tissues for FA catabolism
(FA Oxidation)
+14 ATP
(Glycogenolysis)
(Desterification)
Glycogen
Triglycerides
Liver
-6 ATP (Gluconeogenesis)
(Lipogenesis)
(FA Synthesis)
(Cori Cycle) ?
-6 ATP
Krebs Cycle
Pyruvate
Acetyl CoA
NH3
(Transamination, Deamination)
-4 ATP
Glucogenic Amino Acids
Ketogenic Amino Acids
?
(Glycogenolysis)
(Proteolysis)
Muscle

APPENDICES

Appendix A

Chapter One Supplemental Information

Table A1. Reference sequences used in phylogenetic analysis.

Taxa	Protein	NCBI Accession No.
Danio rerio	claudin a	NP_571837
	claudin b	NP_571838
	claudin c	AAH65424
	claudin d	AAH78260
	claudin e	AAL01832
	claudin h	AAH53223
	claudin-4-like (LOC100147871)	XP_001919418
	claudin-3-like (LOC792492)	XP_001332015
	uncharacterized protein (LOC550468)	NP_001017771
	uncharacterized protein (LOC678612)	NP_001035450
Homo sapiens	claudin 3	AAC78277
	claudin 4	EAW69639
	claudin 8	AAH58004
	claudin 10	AAH10920
	claudin domain containing 1	AAH95441
Oreochromis mossambicus	claudin 3c	JQ412916
	claudin 28a	ABY60421
	claudin 30	ABY60422
Oreochromis niloticus	claudin-3-like (LOC100693661)	XP_003459498
	claudin-4-like (LOC100696760)	XP_003457569
	claudin-4-like (LOC100692852)	XP_003459495
	claudin-4-like (LOC100701009)	XP_003447026
	claudin-4-like (LOC100700473)	XP_003447024
	claudin-4-like (LOC100700739)	XP_003447025
	claudin-like protein (LOC100692042)	XP_003459492
	claudin-like protein (LOC100701826)	XP_003447029
Salmo salar	claudin 3a	DAA06146
	claudin 3b (partial sequence)	DAA06147
	claudin 3c	DAA06148
	claudin 27a	DAA06164
	claudin 28a	DAA06165
	claudin 28b	DAA06166
	claudin 30	DAA06169
Takifugu rubripes	claudin 3a	AAT64047
	claudin 3b	AAT64048
	claudin 3c	AAT64057
	claudin 3d	AAT64058
	claudin 27a	AAT64051
	claudin 27c	AAT64060
	claudin 28a	AAT64053
	claudin 28b	AAT64065
	claudin 29a	AAT64062
	claudin 29b	AAT64061
	claudin 30a	AAT64050
	claudin 30b	AAT64054
	claudin 30c	AAT64059
	claudin 30d	AAT64066

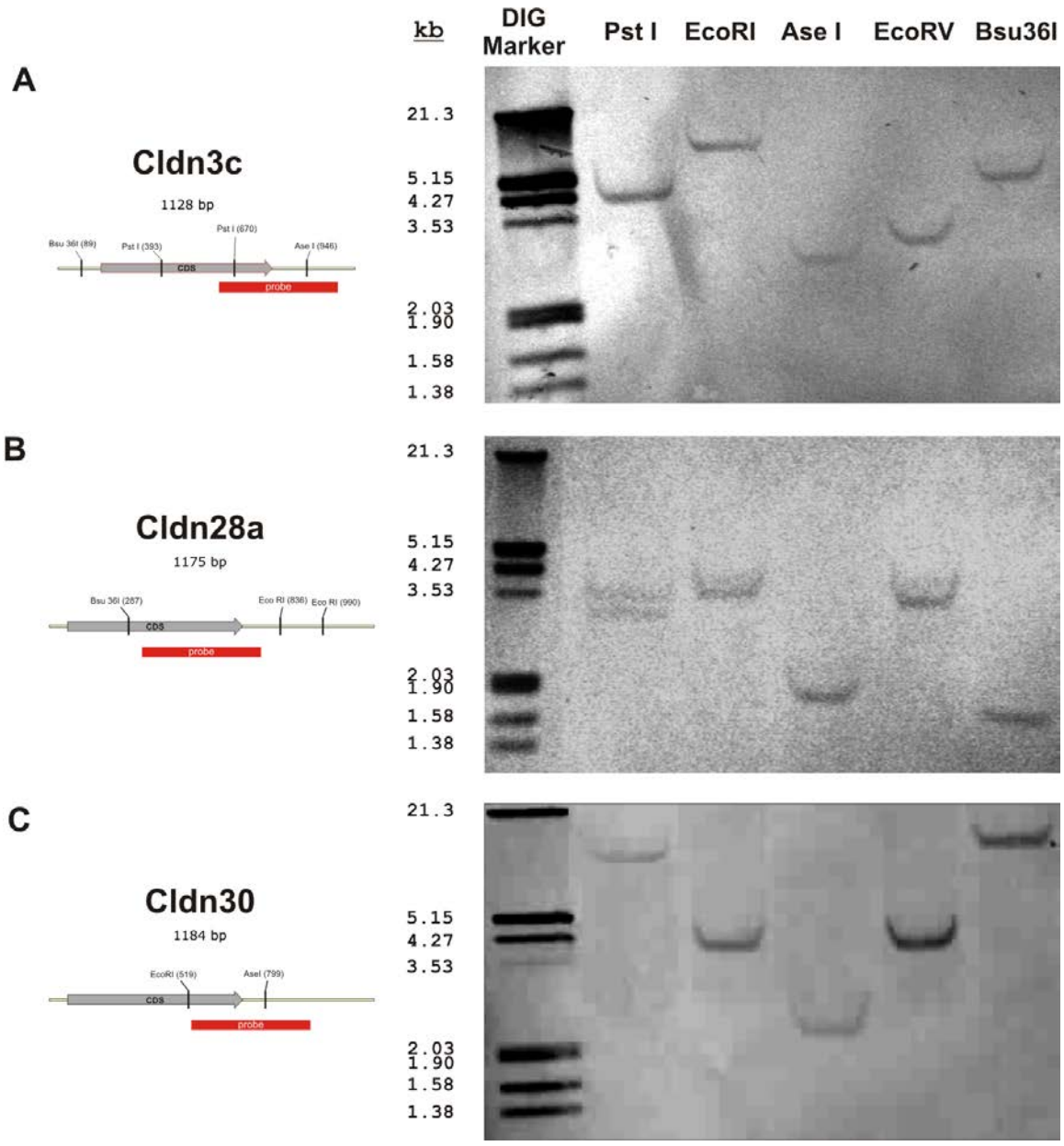

Figure A1. RNA: DNA blot hybridizations. Tilapia genomic DNA was digested with restriction enzymes that cut 5' or 3' from the probe-binding region. A schematic for each gene, containing known restriction sites and the probe binding region, is provided.

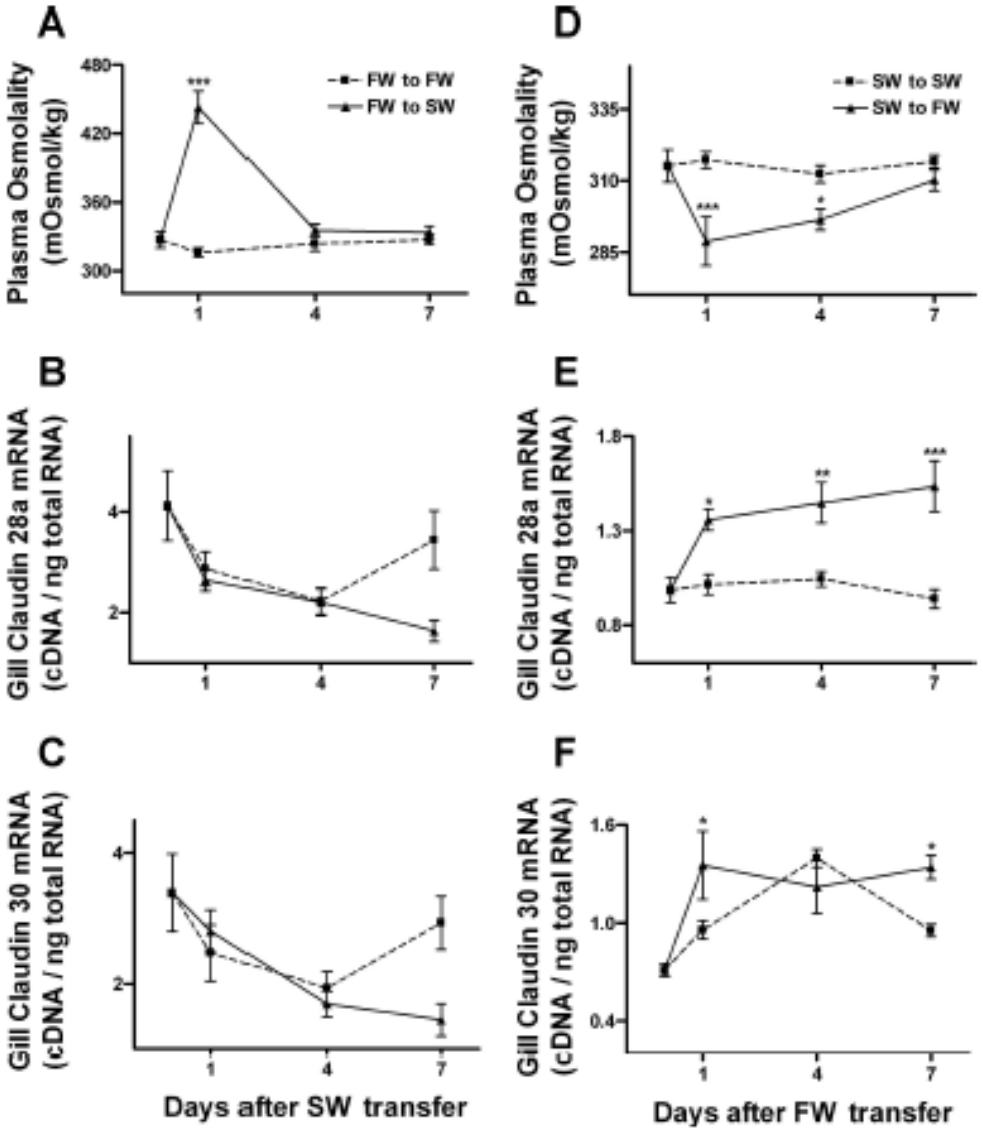

Figure A2. Effects of salinity transfer on plasma osmolality and gill claudin 28a and claudin 30 mRNA levels. Values represent means ± SE (n = 7-10). * $P < 0.05$, ** $P < 0.01$, *** $P < 0.001$, significant effects compared to sham fish (FW to FW or SW to SW). This figure was reproduced from Tipsmark, C.K., **Baltzegar, D.A**., Ozden, O., Grubb, B.J., Borski, R.J., 2008a. Salinity regulates claudin mRNA and protein expression in the teleost gill. *Am J Physiol Regul Integr Comp Physiol* 294, R1004-1014. The molecular cloning of these claudins, and the salinity transfer data depicted here represent contributed work by this author.

Appendix B

Chapter Two Supplemental Information

Table B1. List of identified claudin genes in the zebrafish (*D. rerio*), with proposed revisions to current nomenclature. Asterisks denote redundant NCBI database entries, annotation errors, or the presence of identical genomic positions in the *Zv9* assembly (unresolved assembly errors).

Proposed Name	Current Name *(NCBI Gene ID No.)*	Nucleotide Acc. No. (NCBI)	Protein Acc. No. (NCBI)	*Ensembl* Zebrafish Genome Reference Assembly Chromosome_CDS (start ... end)_strand
claudin 1	claudin 1 (*81590*)	NM_131770	NP_571845	Chr:2_88773... 91785_reverse
claudin 2	claudin 2 (*562525*)	NM_001004559	NP_001004559	Chr:21_36971084...36971896_forward
claudin 3a	LOC792492 (*792492*)	XM_001331979	XP_001332015	Chr:15_2945415...2946062_forward (unannotated)
*	LOC100334283 (*100334283*)	XM_002665891	XP_002665937	Chr:15_2676329...2676976_forward
claudin 3c	claudin h (*81587*)	NM_131767	NP_571842	Chr:21_25120506...25121150_reverse
claudin 3d	claudin c (81582)	NM_131764	NP_571839	Chr:21_25135206...25135862_reverse
claudin 5a	claudin 5a (*406559*)	NM_213274	NP_998439	Chr:8_4906610...4907257_forward
claudin 5b	claudin 5b (*450023*)	NM_001006044	NP_001006044	Chr:10_45496710...45497363_forward
claudin 5c	LOC100151512 (*100151512*)	XM_001923783	XP_001923818	Chr:15_2934835... 2935488_forward (unannotated)
*	LOC100333734 (100333734)	XM_002664536	XP_002664582	Chr:15_2665209... 2665862_forward
claudin 5-like	claudin g (*81586*)	NM_180965	NP_851296	Chr:1_33278018...33278647_reverse
claudin 7a	claudin 7b (*60635*)	NM_131637	NP_571712	Chr:10_22346127... 22350359_reverse
claudin 7b	claudin 7a (436612)	NM_001002340	NP_001002340	Chr:7_23783553...23793227_forward
claudin 8a	LOC100006193 (*100006193*)	XM_001344989	XP_001345025	Chr:15_41097151...41097810_forward
*	LOC555298 (555298)	XM_677769	XP_682861	Region spans 5' gene (TIAM1) to LOC100006193
claudin 8b	claudin 8 (*445278*)	NM_001003733	NP_001003733	Chr:15_41111106...41111921_forward
claudin 8c	claudin 17 (*100001934*)	NM_001110530	NP_001104000	Chr:15_41121331...41122338_forward
claudin 8d	zgc:110333 (*550497*)	NM_001017799	NP_001017799	Chr:15_41102314...41103219_forward
claudin 8-like	claudin j (*81589*)	NM_131769	NP_571844	Chr:15_2623500...2624132_reverse
claudin 10a	claudin 10 (*368619*)	NM_001007037	NP_001007038	Chr:6_7216109...7222801_reverse
claudin 10b	LOC100004456 (*100004456*)	NM_001113655	NP_001107127	Chr:9_282144...284420_reverse
*	zgc:110625 (*553640*)	NM_001020613	NP_001018449	same as LOC100004456
claudin 10c	claudin 10-like 2 (*337652*)	XM_001919365	XP_001919400	Chr:9_274026...276495_reverse

Table B1 Continued.

Proposed Name	Current Name *(NCBI Gene ID No.)*	Nucleotide Acc. No. (NCBI)	Protein Acc. No. (NCBI)	*Ensembl* Zebrafish Genome Reference Assembly Chromosome_CDS (start ... end)_strand
*	LOC553586 (*553586*)	same	same	
claudin 10d	dZ228E24.5 (*563994*)	XM_687354	XP_692446	Chr:6_7157218...7162031_forward
claudin 10e	LOC556021 (*556021*)	XM_678711	XP_683803	Chr:6_7208805... 7205817_reverse
*	si:busm1-52i16.2 (*368618*)	AL591370	CAD24438	genomic clone overlapping LOC556021 region
claudin 11a	claudin 11a (*436897*)	NM_001002624	NP_001002624	Chr:2_26146071...26149150_reverse
claudin 11b	claudin 11b (*81592*)	NM_131772	NP_571847	Chr:24_27229281...27235986_forward
claudin 12	claudin 12 (*81593*)	NM_131773	NP_571848	Chr:16_46073006...46075387_reverse
claudin 12-like	zgc:63990 (*406640*)	NM_214763	NP_999928	Chr:8_19089738...19102175_reverse
claudin 15a	claudin 15a (*573644*)	NM_200404	NP_956698	Chr:7_21974597...21969086_reverse
claudin 15b	claudin 15b (*678556*)	NM_001040314	NP_001035404	Chr:5_63492751...63537844_forward
claudin 15-like a	claudin 15-like a (*81591*)	NM_131771	NP_571846	Chr:2_5151108...5159731_reverse (cldn10l1a)
claudin 15-like b	claudin 15-like b (*436719*)	NM_001002446	NP_001002446	Chr:15_44769870...44792143_forward (cldn10l1b)
claudin 16	LOC793915 (*793915*)	XM_001333735	XP_001333771	Chr:22_23628657...23631907_reverse (ENSDARG00000042640)
*				Chr:22_23427106...23430356_reverse (ENSDARG00000074549)
claudin 18	LOC557209 (557209)	XM_002660816	XP_002660862	Chr:2_22977995...22980961_forward
claudin 19	claudin 19 (*550431*)	NM_001017736	NP_001017736	Chr:11_40248134...40278139_reverse
claudin 20a		CU695076		Chr:17_49392009...49392740_forward (ENSDARG00000077430)
claudin 20b	LOC100330246 (*100330246*)	XM_002667609	XP_002667655	Chr:20_4405095...4405964_forward (ENSDARG00000067725)
claudin 23a1	LOC567620 (*567620*)	XM_690921	XP_696013	Chr:10_15081272...15082042_reverse
claudin 23a2	si:ch211-95j8.2 (*553515*)	XM_001337411	XP_001337447	Chr:10_15076483...15077478_reverse (LOC553515)
claudin 23b	LOC794676 (*794676*)	XM_001332989	XP_001333025	Chr:17_26826324...26826998_forward
claudin 25-like	LOC793143 (*793143*)	NM_001122706	NP_001116178	Chr:5_13915604...13916266_reverse (NP_001116178)
claudin 28a	claudin e (*81584*)	NM_131765	NP_571840	Chr:15_2631418...2632047_reverse
claudin 28c	LOC796314 (*796314*)	XM_001334911	XP_001334947	Chr:21_25169180...25169749_forward (unannotated)
claudin 28d	claudin f (*81585*)	NM_131766	NP_571841	Chr:15_2643148...2643849_reverse

Table B1 Continued.

Proposed Name	Current Name *(NCBI Gene ID No.)*	Nucleotide Acc. No. (NCBI)	Protein Acc. No. (NCBI)	*Ensembl* Zebrafish Genome Reference Assembly Chromosome_CDS (start ... end)_strand
claudin 29a	claudin d (*81583*)	NM_180964	NP_851295	Chr:21_25157512...25158138_forward
claudin 29b	zgc:112437 (*550468*)	NM_001017771	NP_001017771	Chr:21_25154010...25154642_reverse
claudin 30a	claudin a (*81580*)	NM_131762	NP_571837	Chr:15_2648108...2648728_reverse
claudin 30c	claudin b (*81581*)	NM_131763	NP_571838	Chr:21_25145838...25146485_forward
claudin 30d	zgc:136892 (*678612*)	NM_001040360	NP_001035450	Chr:21_25174123...25175007_forward
claudin 31a	claudin k (*445070*)	NM_001003464	NP_001003464	Chr:3_47641103...47641753_forward
claudin 31b	LOC100334365 (*100334365*)	XM_002660588	XP_002660634	Chr:1_56986281...56990032_reverse
claudin 32	claudin i (*569084*)	NM_131768	NP_571843	Chr:3_31074067...31076546_forward
claudin 33a	LOC100002327 (*100002327*)	XM_001342099	XP_001342135	Chr:11_45262728...45263393_forward
claudin 33b	zgc:153311 (*751666*)	NM_001045383	NP_001038848	Chr:6_30174871...30175536_reverse
claudin 34	LOC568833 (*568833*)	XM_692189	XP_697281	Chr:6_30154558...30155283_forward
claudin 35	LOC570842 (*570842*)	XM_694364	XP_699456	Chr:19_49510163...49510849_reverse
claudin 37	LOC100147871 (*100147871*)	XM_001919383	XP_001919418	Chr:21_25152034...25152669_forward

Table B2. List of all taxa sequences used in the phylogenetic analysis of zebrafish claudins. Zebrafish NCBI records updated or reclassified during the period of our analysis, as part of ongoing NCBI database and genomic assembly revisions, were noted as necessary to reflect current status (double asterisks). These updated records are current as of October 30, 2011.

Organism	Official Gene Name	Gene ID No. (NCBI *Gene*)	NCBI Nucleotide Accession No.	NCBI Protein Accession No.
Danio rerio	claudin 1	81590	NM_131770	NP_571845
	claudin 2	562525	NM_001004559	NP_001004559
	LOC792492	792492	XM_001331979	XP_001332015
	claudin h	81587	NM_131767	NP_571842
	claudin c	81582	NM_131764	NP_571839
	claudin 5a	406559	NM_213274	NP_998439
	claudin 5b	450023	NM_001006044	NP_001006044
	LOC100151512	100151512	XM_001923783	XP_001923818
	claudin g	81586	NM_180965	NP_851296
	claudin 7 (reclassified *cldn7b*)	60635	NM_131637	NP_571712
	zgc:92192 (reclassified *cldn7a*)	436612	NM_001002340	NP_001002340
	LOC100006193	100006193	XM_001344989	XP_001345025
	*** replaced with LOC100536513, 100536513, XM_003200083, XP_003200131, 100% protein identity*			
	claudin 8	445278	NM_001003733	NP_001003733
	claudin 17	100001934	NM_001110530	NP_001104000
	zgc:110333	550497	NM_001017799	NP_001017799
	claudin j	81589	NM_131769	NP_571844
	claudin 10	368619	NM_001007037	NP_001007038
	LOC100004456	100004456	NM_001113655	NP_001107127
	*** reclassified as zgc:110625, 100004456, NM_001020613, NP_001018449, 99% protein identity*			
	claudin 10-like2	553386	XM_001919365	XP_001919400
	*** also listed as uncharacterized loci LOC553386, XM_001919365, XP_001919400, exact sequence match*			
	dZ228E24.5	563994	XM_687354	XP_692446

Table B2 Continued.

Organism	Official Gene Name	Gene ID No. (NCBI *Gene*)	NCBI Nucleotide Accession No.	NCBI Protein Accession No.
Danio rerio	LOC556021	556021	XM_678711	XP_683803
	*** also listed as si:busm1-52i16.2, AL591370,CAD24438 genomic clone overlapping LOC556021*			
	zgc:92247 (*reclassified cldn11a*)	436897	NM_001002624	NP_001002624
	claudin 11 (*reclassified cldn11b*)	81592	NM_131772	NP_571847
	claudin 12	81593	NM_131773	NP_571848
	zgc:63990	406640	NM_214763	NP_999928
	claudin 15 (*reclassified cldn15a*)	573644	NM_200404	NP_956698
	zgc:136755 (*reclassified cldn15b*)	678556	NM_001040314	NP_001035404
	claudin 10-like 1a (*cldn15-like a*)	81591	NM_131771	NP_571846
	claudin 10-like 1b (*cldn15-like b*)	436719	NM_001002446	NP_001002446
	LOC793915	793915	XM_001333735	XP_001333771
	*** record is currently discontinued, but loci still present in current genomic assembly (Zv9).*			
	LOC557209	557209	BC154668	AAI54669
	*** new sequence records available, XM_002660816, XP_002660862, 100% protein identity to previous record.*			
	claudin 19	550431	NM_001017736	NP_001017736
	claudin 20 (*unidentified*)	none	CU695076	
	*** sequence annotated in Ensembl as ENSDARG00000077430, ENSDARP00000104086 (protein) in Zv9.*			
	LOC100151228	100151228	XM_001921259	XP_001921294
	*** record replaced with LOC100330246, 100330246, XM_002667609, XP_002667655. 100% protein identity*			
	LOC567620	567620	XM_690921	XP_696013
	LOC553515	553515	XM_001337411	XP_001337447
	*** reclassified as si:ch211-95j8.2, 553515, XM_001337411, XP_001337447, exact sequence match.*			
	LOC794676	794676	XM_001332989	XP_001333025
	DKEY-98F17.3	793143	NM_001122706	NP_001116178
	*** reclassified as LOC793143, exact sequence match.*			
	claudin e	81584	NM_131765	NP_571840

Table B2 Continued.

Organism	Official Gene Name	Gene ID No. (NCBI *Gene*)	NCBI Nucleotide Accession No.	NCBI Protein Accession No.
Danio rerio	LOC796314	796314	XM_001334911	XP_001334947
	*** new sequence records available, XM_003200840, XP_003200888, 99% protein identity to previous record.*			
	claudin f	81585	NM_131766	NP_571841
	claudin d	81583	NM_180964	NP_851295
	zgc:112437	550468	NM_001017771	NP_001017771
	claudin a	81580	NM_131762	NP_571837
	claudin b	81581	NM_131763	NP_571838
	zgc:136892	678612	NM_001040360	NP_001035450
	claudin k	445070	NM_001003464	NP_001003464
	LOC100004771	100004771	XM_001343954	XP_001343990
	*** record replaced with LOC100334365, 100334365, XM_002660588, XP_002660634. 99% protein identity*			
	claudin i	569084	NM_131768	NP_571843
	LOC100002327	100002327	XM_001342099	XP_001342135
	zgc:153311	751666	NM_001045383	NP_001038848
	LOC568833	568833	XM_692189	XP_697281
	LOC570842	570842	XM_694364	XP_699456
	LOC100147871	100147871	XM_001919383	XP_001919418
	CH211-217K17.5	554386	NM_001161597	NP_001155069
	*** record replaced with LOC445294, 445294, NM_001003751, 001003751. 100% identity to previous record*			
	* *identified as claudin domain containing 1 (cldnD1) in our analysis, used as an outgroup sequence.*			
	peripheral myelin protein 22a	334817	NM_201311	NP_958468
	peripheral myelin protein 22b	678607	NM_001040355	NP_001035445
H. sapiens	claudin 1	9076	NM_021101	NP_066924
	claudin 2	9075	NM_020384	NP_065117
	claudin 3	1365	NM_001306	NP_001297

Table B2 Continued.

Organism	Official Gene Name	Gene ID No. (NCBI *Gene*)	NCBI Nucleotide Accession No.	NCBI Protein Accession No.
H. sapiens	claudin 4	1364	NM_001305	NP_001296
	claudin 5	7122	NM_001130861	NP_001124333
	claudin 6	9074	NM_021195	NP_067018
	claudin 7	1366	NM_001307	NP_001298
	claudin 8	9073	NM_199328	NP_955360
	claudin 9	9080	NM_020982	NP_066192
	claudin 10 *(transcript variant b)*	9071	NM_006984	NP_008915
	claudin 10 *(transcript variant a)*	9071	NM_182848	NP_878268
	claudin 11	5010	NM_005602	NP_005593
	claudin 12	9069	NM_012129	NP_036261
	claudin 14	23562	NM_144492	NP_001139549
	claudin 15	24146	NM_014343	NP_055158
	claudin 16	10686	NM_006580.2	NP_006571
	claudin 17	26285	NM_012131	NP_036263
	claudin 18	51208	NM_016369	NP_001002026
	claudin 19	149461	NM_148960	NP_683763
	claudin 20	49861	NM_001001346	NP_001001346
	claudin 22	53842	NM_001111319	NP_001104789
	claudin 23	137075	NM_194284	NP_919260
	claudin 24	100132463	XM_001714660	XP_001714712
	claudin 25	644672	NM_001101389	NP_001094859
	claudin domain containing 1	56650	NM_001040181	NP_001035271
	claudin domain containing 2	125875	NM_152353	NP_689566
	transmembrane protein 204	79652	NM_024600	NP_078876
	peripheral myelin protein 22	5376	NM_000304	NP_000295

Table B2 Continued.

Organism	Official Gene Name	Gene ID No. (NCBI *Gene*)	NCBI Nucleotide Accession No.	NCBI Protein Accession No.
M. musculus	claudin 1	12737	NM_016674	NP_057883
	claudin 2	12738	NM_016675	NP_057884
	claudin 3	12739	NM_009902	NP_034032
	claudin 4	12740	NM_009903	NP_034033
	claudin 5	12741	NM_013805	NP_038833
	claudin 6	54419	NM_018777	NP_061247
	claudin 7	53624	NM_016887	NP_058583
	claudin 8	54420	NM_018778	NP_061248
	claudin 9	56863	NM_020293	NP_064689
	claudin 10A *(transcript variant b)*	58187	*NM_021386*	NP_067361
	claudin 10A *(transcript variant a)*	58187	NM_023878	NP_076367
	claudin 11	18417	NM_008770	NP_032796
	claudin 12	64945	NM_022890	NP_075028
	claudin 13	57255	NM_020504	NP_065250
	claudin 14	56173	NM_001165925	NP_001159397
	claudin 15	60363	NM_021719	NP_068365
	claudin 16	114141	NM_053241	NP_444471
	claudin 17	239931	NM_181490	NP_852467
	claudin 18	56492	NM_019815	NP_062789
	claudin 19	242653	NM_001038590	NP_001033679
	claudin 20	621628	NM_001101560	NP_001095030
	claudin 22	75677	NM_029383	NP_083659
	claudin 23	71908	NM_027998	NP_082274
	claudin 25	100042785	XM_001478811	XP_001478861
	claudin domain containing 1	224250	NM_171826	NP_741968
	claudin domain containing 2	74276	NM_028849	NP_083125

Table B2 Continued.

Organism	Official Gene Name	Gene ID No. (NCBI *Gene*)	NCBI Nucleotide Accession No.	NCBI Protein Accession No.
M. musculus	LOC100039801	100039801	NM_001111318	NP_001104788
	LOC100045502	100045502	XM_001474412	XP_001474462
	peripheral myelin protein 22	18858	NM_008885	NP_032911
	claudin 22	75677	NM_029383	NP_083659
	claudin 23	71908	NM_027998	NP_082274
	claudin 25	100042785	XM_001478811	XP_001478861
	claudin domain containing 1	224250	NM_171826	NP_741968
	claudin domain containing 2	74276	NM_028849	NP_083125
	LOC100039801	100039801	NM_001111318	NP_001104788
	LOC100045502	100045502	XM_001474412	XP_001474462
	peripheral myelin protein 22	18858	NM_008885	NP_032911
T. rubripes	claudin 1	none	AY554352	AAT64078
	claudin 2	none	AY554353	AAT64079
	claudin 3a	none	AY554377	AAT64047
	claudin 3b	none	AY554378	AAT64048
	claudin 3c	none	AY554367	AAT64057
	claudin 3d	none	AY554368	AAT64058
	claudin 5a	none	AY554341	AAT64067
	claudin 5b	none	AY554361	AAT64087
	claudin 5c	none	AY554379	AAT64049
	claudin 6	none	AY554385	AAT64055
	claudin 7a	none	AY554343	AAT64069
	claudin 7b	none	AY554347	AAT64073
	claudin 8a	none	AY554387	AAT64043
	claudin 8b	none	AY554388	AAT64044

Table B2 Continued.

Organism	Official Gene Name	Gene ID No. (NCBI *Gene*)	NCBI Nucleotide Accession No.	NCBI Protein Accession No.
T. rubripes	claudin 8c	none	AY554389	AAT64045
	claudin 8d	none	AY554390	AAT64046
	claudin 10a	none	AY554359	AAT64085
	claudin 10b	none	AY554396	AAT64094
	claudin 10c	none	AY554395	AAT64093
	claudin 10d	none	AY554391	AAT64041
	claudin 10e	none	AY554392	AAT64042
	claudin 11a	none	AY554358	AAT64084
	claudin 11b	none	AY554355	AAT64081
	claudin 12	none	AY554346	AAT64072
	claudin 13	none	AY554386	AAT64056
	claudin 14a	none	AY554349	AAT64075
	claudin 14b	none	AY554393	AAT64039
	claudin 15a	none	AY554365	AAT64091
	claudin 15b	none	AY554357	AAT64083
	claudin 18	none	AY554344	AAT64070
	claudin 19	none	AY554362	AAT64088
	claudin 20a	none	AY554350	AAT64076
	claudin 20b	none	AY554354	AAT64080
	claudin 23a	none	AY554348	AAT64074
	claudin 23b	none	AY554345	AAT64071
	claudin 25	none	AY554364	AAT64090
	claudin 26	none	AY554363	AAT64089
	claudin 27a	none	AY554381	AAT64051
	claudin 27b	none	AY554382	AAT64052
	claudin 27c	none	AY554370	AAT64060

Table B2 Continued.

Organism	Official Gene Name	Gene ID No. (NCBI *Gene*)	NCBI Nucleotide Accession No.	NCBI Protein Accession No.
T. rubripes	claudin 27d	none	AY554374	AAT64064
	claudin 28a	none	AY554383	AAT64053
	claudin 28b	none	AY554375	AAT64065
	claudin 28c	none	AY554373	AAT64063
	claudin 29a	none	AY554372	AAT64062
	claudin 29b	none	AY554371	AAT64061
	claudin 30a	none	AY554380	AAT64050
	claudin 30b	none	AY554384	AAT64054
	claudin 30c	none	AY554369	AAT64059
	claudin 30d	none	AY554376	AAT64066
	claudin 31	none	AY554351	AAT64077
	claudin 32a	none	AY554360	AAT64086
	claudin 32b	none	AY554356	AAT64082
	claudin 33a	none	AY554366	AAT64092
	claudin 33b	none	AY554394	AAT64040
	claudin 33c	none	AY554342	AAT64068
	claudin domain containing 1	none	none	none
	*** identified in Ensembl Fugu genome: CLDND1(1of 2), ENSTRUT00000022534, ENSTRUP00000022441*			
	transmembrane protein 204	none	none	none
	*** identified in Ensembl Fugu genome: TMEM204, ENSTRUT00000038356, ENSTRUP00000038219*			
	peripheral myelin protein 22 1	none	none	none
	*** identified in Ensembl Fugu genome: PMP22 (1of2), ENSTRUT00000002335, ENSTRUP00000002325*			
	peripheral myelin protein 22 2	none	none	none
	*** identified in Ensembl Fugu genome: PMP22 (2of2), ENSTRUT00000024511, ENSTRUP00000024412*			

Table B2 Continued.

Organism	Official Gene Name	Gene ID No. (NCBI *Gene*)	NCBI Nucleotide Accession No.	NCBI Protein Accession No.
X. tropicalis	claudin 1	548421	NM_001015704	NP_001015704
	XM_002940407	100489170	XM_002940407	XP_002940453
	claudin 3	448229	NM_001005709	NP_001005709
	claudin 4	549417	NM_001016663	NP_001016663
	claudin 5	448343	NM_001006706	NP_001006707
	claudin 6, gene 1	394468	NM_203542	NP_988873
	LOC100493413	100493413	XM_002941691	XP_002941737
	claudin 8, gene 2	100145356	NM_001126825	NP_001120297
	claudin 7	394674	NM_203746	NP_989077
	LOC100485738	100485738	XM_002938439	XP_002938485
	LOC100496232	100496232	XM_002939526	XP_002939572
	LOC100492817	100492817	XM_002931548	XP_002931594
	claudin 12	549605	NM_001016851	NP_001016851
	LOC100491910	100491910	XM_002941528	XP_002941574
	claudin 15	100124975	NM_001102909	NP_001096379
	LOC100496309	100496309	XM_002934041	XP_002934087
	LOC100485900	100485900	XM_002938440	XP_002938486
	LOC100492900	100492900	XM_002938116	XP_002938162
	LOC100490546	100490546	XM_002937034	XP_002937080
	novel gene	none	none	none
	** *identified in Ensembl X. tropicalis genome: novel gene, ENSXETT00000005008, ENSXETP00000005008*			
	claudin domain containing 1	549013	NM_001016259	NP_001016259
	peripheral myelin protein 22	594946	NM_001030381	NP_001025552
	LOC100135192	100135192	NM_001113895	NP_001107367

Table B3. Proposed interim reclassification schema for major vertebrate claudin groups. Gene nomenclature is revised in a manner reflective of homology (among group members) while minimizing further ambiguity associated with reclassification. Zebrafish claudins (identified in Table B1) are not depicted unless they form a new claudin group. *Symbols*: →, reclassified to; (new group), formation of a novel group of claudins.

Claudin Group	Lineage	Proposed Interim Reclassification
1	all vertebrates	*no change*
2	all vertebrates	*no change*
3	all vertebrates	homology unresolved, *no proposed changes*
4	all vertebrates	mouse: *Cldn4 → Cldn4α*; *Cldn13 → Cldn4β*
4-like	unknown	(**new group**) *X. tropicalis*: *LOC100493413 → cldn4l1, cldn6.1 → cldn4l2*
5	all vertebrates	*no change*
5-like	unknown	(**new group**) zebrafish: *cldng → cldn5l*
6	mammals?	human, mouse: claudin 6 → claudin 6α; claudin 9 → claudin 6β
7	all vertebrates	homology unresolved, *no proposed changes*
8	all vertebrates	human, mouse: claudin 8 → claudin 8α; claudin 17 → claudin 8β
8-like	teleost	(**new group**) pufferfish *cldn6 → cldn8l*
9	----------	*group closed (see group 6)*
10	all vertebrates	*no change*
11	all vertebrates	*no change*
12	all vertebrates	*no change*
12-like	unknown	(**new group**) zebrafish: *zgc:63990 → cldn12l*
13	----------	*group closed (see groups 4, 36)*
14	all vertebrates	pufferfish: *cldn14a → cldn14*, *cldn14b → cldn34*
15	all vertebrates	*no change*
15-like	teleost	pufferfish: *cldn25 → cldn15la*, *cldn26 → cldn15lb*
16	all vertebrates	*no change*
17	----------	*group closed (see group 8)*
18	all vertebrates	homology unresolved, *no proposed changes*
19	all vertebrates	*no change*
20	all vertebrates	*no change*

Table B3 Continued.

Claudin Group	Lineage	Proposed Interim Reclassification
21	----------	*group closed, no current members*
22	mammal ?	human, mouse: claudin 22 → claudin 22α; claudin 24 → claudin 22β
23	all vertebrates	*no change*
24	----------	*group closed (see group 22)*
25-like	teleost ?	(**new group**) pufferfish*: cldn33c → cldn25l*
26	----------	*group closed (see group 15-like)*
27	----------	*group closed (see groups 28, 37)*
28	teleost	pufferfish: *cldn27b → cldn28d, cldn27d → cldn28e*
29	teleost	*no change*
30	teleost	*no change*
31	teleost	*no change*
32	teleost	pufferfish: *cldn32a → cldn32, cldn32b → cldn35*
33	teleost	pufferfish: *cldn33c → cldn25l, no other changes*
34	teleost	(**new group**) pufferfish: *cldn14b → cldn34*
35	teleost	(**new group**) pufferfish: *cldn32b → cldn35*
36	teleost	(**new group**) pufferfish: *cldn13 → cldn36*
37	teleost	(**new group**) pufferfish: *cldn27a → cldn37a, cldn27c → cldn37b*

Table B4. List of PCR primer pairs used in the tissue expression profile of zebrafish claudins.

Gene Name (*current name*)	**Orientation**	**Primer Sequence (5' to 3')**	**T_A (° C)**	**Amplicon Size (bp)**
bactin1	sense	GGT ATG TGC AAA GCC GGT TT	54	409
	antisense	TAC CAG TAG TAC GAC CAG AAG CGT		
claudin 1 (*same*)	sense	GGC TGC AGA TGC TGG GTT AC	59	435
	antisense	CGA AGA ACT TCT GCC GGA TCT		
claudin 2 (*same*)	sense	ATG GCG ATT CTA GCA CTG GAG T	58	400
	antisense	TCA ACG ATA AAA GCC CAG CC		
claudin 3a (*LOC792492*)	sense	ATT GGA GCT CGT GGG GAT TAT	57	416
	antisense	TGA TAC TAT TAG CCG ACC AGG ACA		
claudin 3c (*claudin h*)	sense	CAT TGC CCT GGG TAT TAT TGG T	54	408
	antisense	TCC CGA ATG ATC TGG TTT GC		
claudin 3d (*claudin c*)	sense	GGC GTC TTT TGG TTT GGA GTT	57	418
	antisense	TGC AGA CCA GCA CAC AGG AA		
claudin 5a (*same*)	sense	TTT GGA GCT CCT GGG TCT GA	59	436
	antisense	CGG GTT ATA GAA GTC GGA GAT GAT		
claudin 5b (*same*)	sense	GCA TGT CTG GAG ATT GTT GGA CT	57	405
	antisense	CCA GCA CAG AGG AAT CAG AAC A		
claudin 5c (*LOC100151512*)	sense	GGT TTG GAG ATA TTG GGG ATG A	57	405
	antisense	TGT CCA GCA GAC GGC AAC TA		
claudin 5-like (*claudin g*)	sense	TGT CTA CTG GCT TGC AGC TCC	54	402
	antisense	GTG GCA CCA AAC CCA AGA TC		
claudin 7a (*claudin 7b*)	sense	GGA CTG CAA CTC CTA GGG TTT ACT	56	450
	antisense	AGG TGT GAA GGG GTT GTA GAA ATC		
claudin 7b (*claudin 7a*)	sense	TTC AGT TGC TTG GGT TCG GT	57	413
	antisense	ATT ATG GGC AAA CCA CGA GC		
claudin 8a (*LOC100006193*)	sense	GAG GGA CAA ACT GAA GAT CCT AGC	57	416
	antisense	CAA TGG TGT TTG TTG TCC AGC T		
claudin 8b (*claudin 8*)	sense	TGG GAA TGT GCG TGA CCA TA	58	417
	antisense	AGT CCC GAA TAA TGG CAT TCC		
claudin 8c (*claudin 17*)	sense	ATG GTT CAG GGT CCG TGT GA	57	411
	antisense	GAC AGG GAT GAC GAT GCA AAA		
claudin 8d (*zgc:110333*)	sense	GTC TTA CAC GGC TGG CTC GT	57	414

Table B4 Continued.

Gene Name (*current name*)	**Orientation**	**Primer Sequence (5' to 3')**	**T_A (° C)**	**Amplicon Size (bp)**
	antisense	CAC ATA AGA CCC CTG GCT GC		
claudin 8-like (*claudin j*)	sense	CTC TGC AGG TTT TGG GAA TCA	57	427
	antisense	AAG TCC CTT ATA ATG GAG TCG GC		
claudin 10a (*claudin 10*)	sense	TCC GGA TGG ATT CTG GTG TC	56	472
	antisense	TAC TCA GCA CAG ATC CTG CCC		
claudin 10b (*LOC100004456*)	sense	TGA GGA ACA TGG CGA GAG AGA	58	423
	antisense	TCC TGT GAG CGT AGA GCG AGT A		
claudin 10c (*claudin 10-like 2*)	sense	TGA TCC AGG TGT TGG GGT TC	58	490
	antisense	CCC ACA GAT ACG GTC TTC TTT CTT		
claudin 10d (*dZ228E24.5*)	sense	GCC AGT CGA ACA GTG ATC ATG TA	54	408
	antisense	TGT CAT TCC AGA AAG CCC TGA		
claudin 10e (*LOC556021*)	sense	GGG GTT TCT GTT GTC GGT GA	57	424
	antisense	AAG CCA GCA ATT GTA GGG TTG T		
claudin 11a (*same*)	sense	TGA TGA GTT TTC TCG GCT GGA	56	432
	antisense	AGC CAA AGG ACA TCA GAC CCT		
claudin 11b (*same*)	sense	GTC GGC TGG ATT GGG ATA ATA A	57	412
	antisense	CAA AAG ACA TCA GGC CGT CC		
claudin 12 (*same*)	sense	CAC TAA TGC GTT CGC CTT TGT	56	412
	antisense	TCC ACC TAG AAA CAG AAG CAT CC		
claudin 12-like (*zgc:63990*)	sense	AGC AGA GGA AGT GCG CGT GT	59	500
	antisense	GGT TCA GGC AGT AGA GAA TGG C		
claudin 15a (*same*)	sense	GAT CAT TGA AGC CGT GGC TC	57	410
	antisense	CAG CGT ACC ATG ACA CTG ATA TCA		
claudin 15b (*same*)	sense	GGG TTT TTT GGG TTG TGG GT	54	421
	antisense	TGG GTA AAG CGG GTC AAA GA		
claudin 15-like a (*same*)	sense	CTA CAG CAT TAG AGG TGA CGG GA	54	405
	antisense	AAG ATA CCC CCA CCA TAG TGC A		
claudin 15-like b (*same*)	sense	GTG GGC TGG TGT TTG GAG TC	57	420
	antisense	TGT GCC TCC ATA AAA CGG GT		
claudin 16 (*LOC793915*)	sense	GCT GGA TTA TGT GGC CTG CT	54	439
	antisense	ACA CAC CTC CGA ATA AAC AGA GC		

Table B4 Continued.

Gene Name (*current name*)	**Orientation**	**Primer Sequence (5' to 3')**	**T_A (° C)**	**Amplicon Size (bp)**
claudin 18 (*LOC557209*)	sense	GCT CTG CAG ACC ACA GGC TT	59	447
	antisense	GGG CAT CAT GAA ACT AGG CAC T		
claudin 19 (*same*)	sense	GCC AAC TCT GGG TTT CAG CTT	57	432
	antisense	AGA CAC CTG TGC GGC ATA CC		
claudin 20a (*unidentified*)	sense	GCA GAT CTT CGC CTT TGT GC	59	405
	antisense	TTT GTG TAC CAA GAA GCG GGA		
claudin 20b (*LOC100330246*)	sense	CCG TCT TCC ACT ATG CAG ATG TT	59	403
	antisense	CGG GCA CCA AAC ATA GGA TC		
claudin 23a1 (*LOC567620*)	sense	CAA CAA CAT CAG CGG GGA GT	58	428
	antisense	AGC CGA TAG ACA TCA CCA AAC C		
claudin 23a2 (*si:ch211-95j8.2*)	sense	AGC AGA AAC CAG TTT CAC CAG AC	57	445
	antisense	GAA CAG AAA ATA AGT AGG CCA CCC		
claudin 23b (*LOC794676*)	sense	TGC ACA CTC CAG CAT CCA TGC	59	416
	antisense	TAA TGC AGC CAG GCT GAG CAC ACC		
claudin 25-like (*LOC793143*)	sense	TGC TGT TCA CCA CCA AGT TTG T	56	418
	antisense	GCC ATA AAT GAA ACA GCC GC		
claudin 28a (*claudin e*)	sense	GAG AGA TCC TGG GCA TGT GC	58	486
	antisense	ATC CGA TGT ACA GCG AAG CC		
claudin 28c (*LOC796314*)	sense	GAC AGT TCG TGG CTG CAT TTC	54	400
	antisense	CAG CAG ACA GCA ACA AGG CA		
claudin 28d (*claudin f*)	sense	GGT TTT GTG GGC ATC TGC AT	57	417
	antisense	CGT CTG AAT GGT GGT CAC ACT AA		
claudin 29a (*claudin d*)	sense	GCA TCT GTT GGG CTT CAG CT	57	407
	antisense	CAC ACC GGG ATC AAA CAA AGA		
claudin 29b (*zgc:112437*)	sense	TGG GGA TGC AGA TTT TAG GAG T	58	445
	antisense	AGC AGC GGG TTG TAG AAA TCC		
claudin 30a (*claudin a*)	sense	GGG TAT AGC CCT GGC AGT GAT	56	437
	antisense	CGC TGT TGG TCA TAG GGT TGT		
claudin 30c (*claudin b*)	sense	ATC TTT GGG TGG ATC GGA GTC	57	432
	antisense	CCT CTT CTG TGC CTG GAC CA		
claudin 30d (*zgc:136892*)	sense	CTT TGG CTT TAA TGG GAT GGA C	56	410

Table B4 Continued.

Gene Name (*current name*)	**Orientation**	**Primer Sequence (5' to 3')**	**T_A (° C)**	**Amplicon Size (bp)**
	antisense	AAA CGC CTT TAC CAC CAT GC		
claudin 31a (*claudin k*)	sense	CAT GTG GAG GGT CAC AGC CT	57	414
	antisense	AAG TAG AGA GCG GGT CCA AGC		
claudin 31b (*LOC100334365*)	sense	GCA GGT GAT GGG TGT GGT TC	59	411
	antisense	ACG ACA TAT GCG TTC CAG CAC		
claudin 32 (*claudin i*)	sense	TGC AGA TTG TGT GTG TGG CTC	58	445
	antisense	TCA GGA ACC ATC GGG TTG TTA		
claudin 33a (*LOC100002327*)	sense	TCT GGA GCT GCT GGG AGT GT	57	404
	antisense	CAT AGG AGA CCG GCA CGA TC		
claudin 33b (*zgc:153311*)	sense	CAC GGT GGC TCT GGA ACT CT	57	464
	antisense	GCA CCA CAT GAG GCA CAC TCT		
claudin 34 (*LOC568833*)	sense	GCT TAC CTG GCG CAA TCT GT	57	407
	antisense	GTG GCA GTC AAC CAA TAC AAG CT		
claudin 35 (*LOC570842*)	sense	GGT AAA CAC GGG CAT GCA GT	57	419
	antisense	CTG TCC AGG AAA CTG GCA CC		
claudin 37b (*LOC100147871*)	sense	GGC ATC TCA AGG CAT CCA GA	57	419
	antisense	GCG CTG ACC AGC AAA TAG GTA		

Table B5. BLASTn search results of the zebrafish claudin PCR amplicons. Obtained from the tissue expression profile, these were searched against the non-redundant nucleotide database (NCBI) using the criterion {Organism = *Danio rerio* txid7955} on August 20, 2010. Sequences obtained by forward Sanger sequencing using the sense primers listed in Table B4.

PCR Amplicon Proposed Name (*Current*)	BLASTn Match (NCBI Acc. No.)	BLASTn Match (Description)	Max Bit Score	E value
b-actin1	NM_131031.1	Danio rerio bactin1 (bactin1), mRNA >gb|AF057040.1| Danio rerio beta-actin mRNA	623	1e-176
claudin 1	NM_131770.1	Danio rerio claudin 1 (cldn1), mRNA >gb|AF359436.1|AF359436 Danio rerio claudin 19 (cldn19) mRNA	610	1e-172
claudin 2	NM_001004559.2	Danio rerio claudin 2 (cldn2), mRNA	652	0.0
claudin 3a *(LOC792492)*	XM_001331979.3	PREDICTED: Danio rerio Claudin-3-like (LOC792492), mRNA	673	0.0
claudin 3c *(cldnh)*	BC165027.1	Danio rerio claudin h, mRNA (cDNA clone MGC:192202 IMAGE:100060511)	676	0.0
claudin 3d *(cldnc)*	NM_131764.1	Danio rerio claudin c (cldnc), mRNA >gb|AF359432.1|AF359432 Danio rerio claudin c (cldnc) mRNA	673	0.0
claudin 5a	NM_213274.1	Danio rerio claudin 5a (cldn5a), mRNA >gb|BC068370.1| Danio rerio zgc:85723	712	0.0
claudin 5b	NM_001006044.1	Danio rerio claudin 5b (cldn5b), mRNA	654	0.0
claudin 5c (*LOC100151512*)	XM_001923783.2	PREDICTED: Danio rerio claudin 5c-like (LOC100151512), mRNA	468	6e-130
claudin 5-like *(cldng)*	BC115079.1	Danio rerio claudin g, mRNA (cDNA clone MGC:136312 IMAGE:7923124), complete cds	403	2e-110
claudin 7a *(cldn7b)*	NM_131637.1	Danio rerio claudin 7b (cldn7b), mRNA >emb|AJ011788.1| Brachydanio rerio claudin-like gene	743	0.0
claudin 7b *(cldn7a)*	NM_001002340.1	Danio rerio claudin 7a (cldn7a), mRNA >gb|BC075926.1| Danio rerio zgc:92192, mRNA	675	0.0
claudin 8a *(LOC55298)*	XM_677769.4	PREDICTED: Danio rerio claudin 8-like (LOC555298), mRNA	662	0.0
claudin 8b *(cldn8)*	NM_001003733.1	Danio rerio claudin 8 (cldn8), mRNA >gb|BC077161.1| Danio rerio claudin 8, mRNA	669	0.0
claudin 8c *(cldn17)*	NM_001110530.1	Danio rerio claudin 17 (cldn17), mRNA >gb|BC153385.1| Danio rerio zgc:173444, mRNA	588	4e-166
claudin 8d (*zgc:110333*)	NM_001017799.2	Danio rerio zgc:110333 (zgc:110333), mRNA >gb|BC129277.1| Danio rerio zgc:110333, mRNA	647	0.0
claudin 8-like *(cldnj)*	NM_131769.1	Danio rerio claudin j (cldnj), mRNA >gb|AF359430.1|AF359430 Danio rerio claudin j (cldnj) mRNA	577	1e-162
claudin 10a *(cldn10)*	***** not detected in our PCR analysis (tissue expression or whole fish cDNA preparations)***			
claudin 10b *(LOC100004456)*	NM_001113655.1	Danio rerio hypothetical protein LOC100004456 (LOC100004456), mRNA	708	0.0
claudin 10c *(claudin 10-like 2)*	BC093313.1	Danio rerio claudin 10-like2, mRNA (cDNA clone IMAGE:7405545), partial cds	970	0.0
claudin 10d *(dZ228E24.5)*	XM_687354.3	PREDICTED: Danio rerio similar to claudin 10 (dZ228E24.5), mRNA	632	2e-179
claudin 10e *(LOC556021)*	XM_678711.1	PREDICTED: Danio rerio hypothetical LOC556021 (LOC556021), mRNA	713	0.0
claudin 11a	NM_001002624.1	Danio rerio claudin 11a (cldn11a), mRNA >gb|BC075960.1| Danio rerio zgc:92247, mRNA	702	0.0
claudin 11b	NM_131772.2	Danio rerio claudin 11b (cldn11b), mRNA >gb|BC139523.1| Danio rerio claudin 11, mRNA	604	4e-171

Table B5 Continued.

PCR Amplicon Proposed Name (*Current*)	BLASTn Match (NCBI Acc. No.)	BLASTn Match (Description)	Max Bit Score	E value
claudin 12	NM_131773.1	Danio rerio claudin 12 (cldn12), mRNA >gb|AF359433.1|AF359433 Danio rerio	697	0.0
claudin 12-like *(zgc:63390)*	NM_214763.1	Danio rerio zgc:63990 (zgc:63990), mRNA >gb|BC057424.1| Danio rerio zgc:63990, mRNA	721	0.0
claudin 15a *(cldn15a, cldn15)*	NM_200404.1	Danio rerio claudin 15 (cldn15), mRNA >gb|BC054577.1| Danio rerio claudin 15 like, mRNA	654	0.0
claudin 15b *(cldn15b,zgc:136755)*	NM_001040314.1	Danio rerio zgc:136755 (zgc:136755), mRNA >gb|BC115253.1| Danio rerio zgc:136755, mRNA	664	0.0
claudin 15-like a (*cldn10l1a*)	NM_131771.1	Danio rerio claudin 10-like 1a (cldn10l1a), mRNA >gb|AF359427.1|AF359427 Danio rerio	651	0.0
claudin 15-like b (*cldn10l1b*)	NM_001002446.1	Danio rerio claudin 10-like 1b (cldn10l1b), mRNA >gb|BC076025.1| Danio rerio zgc:92349, mRNA	678	0.0
claudin 16 *(LOC793915)*	CT009593.9	Zebrafish DNA sequence from clone CH73-6K16 in linkage group 22, complete sequence	732	7e-80
claudin 18 *(LOC557209)*	***** No significant similarity found.***			
claudin 19	NM_001017736.1	Danio rerio claudin 19 (cldn19), mRNA >gb|BC093218.1| Danio rerio zgc:112141, mRNA	693	0.0
claudin 20a	CU695076.26	Zebrafish DNA sequence from clone CH73-342I4, complete sequence	638	0.0
claudin 20b *(LOC100151228)*	XM_002667609.1	PREDICTED: Danio rerio claudin 20a-like (LOC100330246), mRNA	645	0.0
claudin 23a1 *(LOC567620)*	XM_690921.3	PREDICTED: Danio rerio claudin 23-like (LOC567620), mRNA	699	0.0
claudin 23a2 *(si:ch211-95j8.2)*	***** not detected in our PCR analysis (tissue expression or whole fish cDNA preparations)***			
claudin 23b *(LOC794676)*	***** No significant similarity found.***			
claudin 25-like *(LOC793143)*	NM_001122706.1	Danio rerio novel protein similar to human claudin 22 (CLDN22) (LOC793143), mRNA	673	0.0
claudin 28a *(cldne)*	NM_131765.1	Danio rerio claudin e (cldne), mRNA >gb|AF359425.1|AF359425 Danio rerio claudin e (cldne) mRNA	257	7e-35
claudin 28c *(LOC796314)*	XM_001334911.3	PREDICTED: Danio rerio claudin 28c-like (LOC796314), mRNA	584	6e-165
claudin 28d *(cldnf)*	NM_131766.1	Danio rerio claudin f (cldnf), mRNA >gb|AF359424.1|AF359424 Danio rerio claudin f (cldnf) mRNA	676	0.0
claudin 29a *(cldnd)*	NM_180964.2	Danio rerio claudin d (cldnd), mRNA >emb|AJ011789.1| Brachydanio rerio mRNA for claudin-like gene	612	3e-173
claudin 29b *(zgc:112437)*	NM_001017771.1	Danio rerio zgc:112437 (zgc:112437), mRNA >gb|BC093308.1| Danio rerio zgc:112437, mRNA	726	0.0
claudin 30a *(cldna)*	NM_131762.2	Danio rerio claudin a (cldna), mRNA	704	0.0
claudin 30c *(cldnb)*	NM_131763.2	Danio rerio claudin b (cldnb), mRNA	525	4e-147
claudin 30d *(zgc:136892)*	NM_001040360.1	Danio rerio zgc:136892 (zgc:136892), mRNA >gb|BC115315.1| Danio rerio zgc:136892, mRNA	652	0.0
claudin 31a *(cldnk)*	NM_001003464.1	Danio rerio claudin k (cldnk), mRNA >gb|BC078365.1| Danio rerio claudin k, mRNA	303	2e-80
claudin 31b *(LOC100334365)*	XM_002660588.1	PREDICTED: Danio rerio claudin 6-like (LOC100334365), mRNA	584	6e-165

Table B5 Continued.

PCR Amplicon Proposed Name (*Current*)	BLASTn Match (NCBI Acc. No.)	BLASTn Match (Description)	Max Bit Score	E value
claudin 32 *(claudin i)*	NM_131768.2	Danio rerio claudin i (cldni), mRNA	725	0.0
claudin 33a *(LOC100002327)*	XM_001342099.1	PREDICTED: Danio rerio claudin 17-like (LOC100002327), mRNA	664	0.0
claudin 33b *(zgc:153311)*	NM_001045383.1	Danio rerio zgc:153311 (zgc:153311), mRNA >gb|BC122231.1| Danio rerio zgc:153311, mRNA	769	0.0
claudin 34 *(LOC568833)*	XM_692189.4	PREDICTED: Danio rerio claudin 14b-like, transcript variant 2 (LOC568833), mRNA	649	0.0
claudin 35 *(LOC570842)*	XM_694364.2	PREDICTED: Danio rerio claudin 32b-like (LOC570842), mRNA	680	0.0
claudin 37 *(LOC10014781)*	XM_001919383.1	PREDICTED: Danio rerio claudin 27c-like (LOC100147871), mRNA	701	0.0
claudin 12	NM_131773.1	Danio rerio claudin 12 (cldn12), mRNA >gb|AF359433.1|AF359433 Danio rerio	697	0.0

A

(Hs_CLDN4:0.070577,Mm_Cldn4:0.107161,Mm_Cldn13:0.755335,(((((((Dr_47871:0.166547,Tr_Cldn27c:0.112597):0.074840,Tr_Cldn27a:0.256272):0.063218,(((Tr_Cldn28a:0.102574,DrCLDN_E:0.137587):0.043257,Tr_Cldn28b:0.092571):0.085712,((Dr_L796314:0.361235,Tr_Cldn28c:0.157392):0.220138,((DrCLDN_F:0.203226,Tr_Cldn27b:0.225374):0.244347,Tr_Cldn27d:0.585758):0.179937):0.114727):0.078399):0.050870,(((DrCLDN_A:0.166240,DrCLDN_B:0.150428):0.073659,(Tr_Cldn30b:0.168428,(Tr_Cldn30d:0.293826,Dr_Z136892:0.401115):0.162196):0.191236):0.065761,(Tr_Cldn30a:0.144700,Tr_Cldn30c:0.165165):0.057782):0.089843):0.041013,((Dr_112437:0.238912,Tr_Cldn29b:0.184723):0.086017,(DrCLDN_D:0.185649,Tr_Cldn29a:0.108899):0.077506):0.048812):0.067960,(((((Dr_0151512:0.164501,Tr_Cldn5c:0.208318):0.217344,(((DrCLDN_5a:0.111839,Tr_Cldn5a:0.088855):0.053559,(DrCLDN_5b:0.173145,Tr_Cldn5b:0.160306):0.045321):0.136107,((Hs_CLDN5v1:0.038072,Mm_Cldn5:0.056701):0.262753,Xt_CLDN5:0.153720):0.123564):0.117274):0.065892,(DrCLDN_G:0.270040,((DrCLDN_K:0.123468,Tr_Cldn31:0.099355):0.120621,Dr_LOC4771:0.506965):0.229679):0.079241):0.049399,((((Dr_792492:0.099959,Tr_Cldn3a:0.124673):0.069319,((DrCLDN_C:0.156730,Tr_Cldn3d:0.162447):0.082920,Tr_Cldn3b:0.259629):0.105339):0.060031,(DrCLDN_H:0.133975,Tr_Cldn3c:0.147540):0.089250):0.043869,((Hs_CLDN3:0.044175,Mm_Cldn3:0.051705):0.159208,Xt_CLDN3:0.124075):0.046332):0.047675,((Hs_CLDN6:0.051683,Mm_Cldn6:0.081357):0.160266,(Hs_CLDN9:0.013257,Mm_Cldn9:0.022343):0.128611):0.122783,((DrCLDN_I:0.136281,Tr_Cldn32a:0.169357):0.289051,((((Dr_LOC6193:0.323993,Tr_Cldn8a:0.347837):0.123883,((Dr_Z110333:0.222369,Tr_Cldn8d:0.127268):0.287616,((DrCLDN_8:0.224305,Tr_Cldn8b:0.123607):0.125548,(Tr_Cldn8c:0.276320,DrCLDN_17:0.411069):0.100516):0.127541):0.176216):0.148959,((Hs_CLDN17:0.090898,Mm_Cldn17:0.116484):0.279495,((Hs_CLDN8:0.102405,Mm_Cldn8:0.093052):0.139463,((Xt_CLDN8:0.034082,Xt_CLDN17:0.065586):0.030268,Xt_0145356:0.016220):0.225195):0.112093):0.082072):0.214845,((Dr_L570842:0.058004,Tr_Cldn32b:0.062709):0.385009,(((((((Dr_ZG92192:0.092727,Tr_Cldn7b:0.099906):0.107501,DrCLDN_7:0.155096):0.063907,Tr_Cldn7a:0.076490):0.146466,Xt_MG75689:0.153931):0.108407,(Hs_CLDN7:0.056543,Mm_Cldn7:0.034088):0.167329):0.066612,(((Hs_CLDN1:0.024587,Mm_Cldn1:0.081086):0.139677,Xt_CLDN1:0.232187,(DrCLDN_1:0.258084,Tr_Cldn1:0.174605):0.211365):0.104765,(((Tr_Cldn19:0.073348,DrCLDN_19:0.132003):0.051744,Xt_CLDN19:0.049997):0.130450,(Hs_CLDN19i:0.038234,Mm_Cldn19i:0.014737):0.130603):0.280054):0.076898):0.134048,((((DrCLDN_20:0.081127,Tr_Cldn20a:0.062387):0.100640,Dr_L151228:0.232868):0.073301,Tr_Cldn20b:0.358084):0.210327,(Hs_CLDN20:0.127963,Mm_Cldn20:0.165857):0.210126):0.323765,(((Hs_CLDN14v:0.059187,Mm_Cldn14v:0.016609):0.153814,Tr_Cldn14a:0.619969):0.094532,Xt_CLDN14:0.245977):0.146414,((DrCLDN_2:0.251415,Tr_Cldn2:0.295065):0.197379,((Hs_CLDN2:0.043190,Mm_Cldn2:0.053768):0.191786,Xt_CLDN2:0.311208):0.180398):0.164953,(((((((Dr_L556021:0.266337,Tr_Cldn10e:0.276740):0.336050,Dr_CLD10L2:0.314536):0.274028,(Tr_Cldn10c:0.255617,(Tr_Cldn10d:0.180326,Dr_dZ228E2:0.444608):0.129233):0.226310):0.163535,((Dr_LOC4456:0.186873,((Xt_CLDN10:0.134372,(((Hs_CLDN10_:0.041404,Mm_Cldn10A:0.010973):0.268251,Mm_Cld10Ab:0.013924):0.052642,Hs_CLD10ib:0.011611):0.188992):0.077073,(DrCLDN_10:0.129239,Tr_Cldn10a:0.106453):0.153614):0.071261):0.081382,Tr_Cldn10b:0.076706):0.158254):0.198627,((Tr_Cldn15a:0.097143,(Tr_Cldn15b:0.151910,DrCLDN_15:0.194884,Dr_ZGC1367:0.367535):0.057980):0.207982,((Hs_CLDN15:0.080698,Mm_Cldn15:0.166718):0.217149,Xt_CLD15_1:0.288697):0.118818):0.150274):0.100438,((DrCLD10L1a:0.232888,Tr_Cldn25:0.391599):0.140853,(DrCLD10L1b:0.181925,Tr_Cldn26:0.378768):0.208318):0.252338):0.196400,(((((Dr_ZG92247:0.142774,Tr_Cldn11a:0.252747):0.064066,DrCLDN_11:0.398427):0.083543,Tr_Cldn11b:0.385574):0.147584,((Hs_CLDN11:0.036860,Mm_Cldn11:0.029025):0.171463,Xt_CLDN11:0.191058):0.095678):0.484135,((Hs_CLDN16:0.021361,Mm_Cldn16:0.062838):0.098249,Xt_CLDN16:0.165120):0.780956,Dr_L793915:0.699843):0.139452):0.146467,(DR_L568833:0.426934,Tr_Cldn14b:0.319999):0.831391,((Dr_L557209:0.653951,Tr_Cldn18:0.451591):0.252845,((Hs_CLD18i2:0.065486,Xt_CLDN18:0.177757):0.050031,Mm_Cldn18:0.092281):0.293008):0.276252,((((Dr_DKEY98F:0.325879,Tr_Cldn33c:0.239189):0.371270,((Hs_CLDN22:0.085463,Hs_CLDN24:0.053133):0.074272,((Mm_L039801:0.004501,Mm_LO45502:0.004264):0.044473,Mm_Cldn22:0.074916):0.134028):0.116076):0.171973,(Hs_CLDN25:0.162210,Mm_Cldn25:0.094919):0.247773):0.202479,(((((Dr_LOC2327:0.330280,Dr_Z153311:0.442707):0.087350,Tr_Cldn33a:0.409394):0.109434,Tr_Cldn33b:0.257530):0.186108,Xt_CLDN22v:0.687799):0.203325):0.246783,((((Dr_L553515:0.308438,Tr_Cldn23a:0.256519):0.150167,Dr_L567620:0.296813):0.376248,(Hs_CLDN23:0.121911,Mm_Cldn23:0.121160):0.381310):0.172199,(Dr_L794676:0.137254,Tr_Cldn23b:0.130466):0.662206):0.414294,((DrCLDN_12:0.134702,Tr_Cldn12:0.238575):0.199811,((Hs_CLDN12:0.054757,Mm_Cldn12:0.039847):0.132177,Xt_CLDN12:0.226149):0.176377):0.790529,(((Dr_CH21121:0.199946,Tr_CldnD1:0.217946):0.174600,((Hs_CLDND1v:0.050261,Mm_Cldnd1:0.042021):0.196840,Xt_CLDND1:0.272912):0.169009):0.696390,(((Hs_TMEM204:0.132334,Xt_TMEM204:0.109248):0.138801,Tr_TMEM204:0.152096):0.950008,((((Dr_PMP22a:0.265872,Tr_Pmp22_1:0.194839):0.208213,(((Hs_PMP22:0.076658,Mm_Pmp22:0.076545):0.064667,Xt_MG69407:0.147789):0.197306,Dr_PMP22b:0.134196):0.081967):0.181745,Tr_Pmp22_2:0.235910):0.453029,(Hs_CLDND2:0.206321,Mm_Cldnd2:0.143256):0.589459):0.171188):0.248948):0.416026,Tr_Cldn13:0.923774,Dr_ZG63990:1.118455):0.078083):0.078256):0.108424):0.072570,(DrCLDN_J:0.153664,Tr_Cldn6:0.239939):0.351615):0.058851,(Xt_CLDN6.1:0.050778,Xt_CLDN6SK:0.033072):0.158487):0.059226):0.053463,Xt_CLDN4:0.120814):0.110102);

B

(Hs_CLDN4:0.072057,(((((Dr_47871:0.170017,Tr_Cldn27c:0.109947):0.088596,Tr_Cldn27a:0.251446):0.070913,(((Tr_Cldn28a:0.105017,DrCLDN_E:0.135820):0.035977,Tr_Cldn28b:0.104965):0.085521,((Dr_L796314:0.377811,Tr_Cldn28c:0.144294):0.253755,((DrCLDN_F:0.225776,Tr_Cldn27b:0.206351):0.253220,Tr_Cldn27d:0.621341):0.239891):0.107755):0.060800):0.042505,((Dr_112437:0.242453,Tr_Cldn29b:0.196077):0.073630,(DrCLDN_D:0.175427,Tr_Cldn29a:0.113305):0.088542):0.071096,(((DrCLDN_A:0.167903,DrCLDN_B:0.154512):0.083386,Tr_Cldn30c:0.161212):0.052946,(Tr_Cldn30a:0.154090,(Tr_Cldn30b:0.157765,(Tr_Cldn30d:0.298015,Dr_Z136892:0.406552):0.174308):0.212542):0.054398):0.085290):0.071400,((((Dr_0151512:0.161771,Tr_Cldn5c:0.219921):0.225242,(((DrCLDN_5a:0.110373,Tr_Cldn5a:0.084710):0.047097,(DrCLDN_5b:0.171190,Tr_Cldn5b:0.155659):0.059505):0.117542,((Hs_CLDN5v1:0.036317,Mm_Cldn5:0.061484):0.294056,Xt_CLDN5:0.139484):0.147198):0.137824):0.073145,((Hs_CLDN6:0.052786,Mm_Cldn6:0.078691):0.172525,(Hs_CLDN9:0.011298,Mm_Cldn9:0.025548):0.139280):0.126252,DrCLDN_G:0.313137,((DrCLDN_K:0.125407,Tr_Cldn31:0.100101):0.129186,Dr_LOC4771:0.565684):0.277337):0.055305,((((Dr_792492:0.120146,Tr_Cldn3a:0.106070):0.078712,(DrCLDN_H:0.128992,Tr_Cldn3c:0.147991):0.076875):0.060533,((DrCLDN_C:0.147890,Tr_Cldn3d:0.158173):0.077724,Tr_Cldn3b:0.259132):0.119774):0.048469,((Hs_CLDN3:0.045051,Mm_Cldn3:0.052002):0.167689,Xt_CLDN3:0.104127):0.043527):0.051952,(Xt_CLDN6.1:0.048620,Xt_CLDN6SK:0.034125):0.153395,(DrCLDN_I:0.129677,Tr_Cldn32a:0.166696):0.338538,(DrCLDN_J:0.158165,Tr_Cldn6:0.246395):0.316707,((((Dr_LOC6193:0.352554,Tr_Cldn8a:0.345132):0.136066,((Dr_Z110333:0.195675,Tr_Cldn8d:0.156441):0.296240,((DrCLDN_8:0.207219,Tr_Cldn8b:0.126074):0.136396,(Tr_Cldn8c:0.273914,DrCLDN_17:0.451388):0.135860):0.122607):0.172530):0.164032,(((Hs_CLDN17:0.080256,Mm_Cldn17:0.127073):0.342081,(Hs_CLDN8:0.081196,Mm_Cldn8:0.105296):0.121413):0.137335,(Xt_CLDN8:0.034401,Xt_0145356:0.030070,Xt_CLDN17:0.056438):0.203340):0.102855):0.199220,((Dr_L570842:0.055886,Tr_Cldn32b:0.065038):0.356118,(((((Dr_ZG92192:0.099782,Tr_Cldn7b:0.091666):0.108657,Tr_Cldn7a:0.096751):0.067668,DrCLDN_7:0.128508):0.142706,Xt_MG75689:0.151677):0.114689,((((Hs_CLDN1:0.020247,Mm_Cldn1:0.084561):0.163338,Xt_CLDN1:0.233962):0.077582,(DrCLDN_1:0.273155,Tr_Cldn1:0.165142):0.224565):0.089818,(((Tr_Cldn19:0.071054,DrCLDN_19:0.130860):0.053823,Xt_CLDN19:0.049120):0.122928,(Hs_CLDN19i:0.038013,Mm_Cldn19i:0.016302):0.149164):0.315372):0.088738):0.054279,(Hs_CLDN7:0.051383,Mm_Cldn7:0.037091):0.158298):0.132001,(((((((Dr_L556021:0.269511,Tr_Cldn10e:0.270033):0.416736,Dr_CLD10L2:0.345559):0.311133,(Tr_Cldn10c:0.268795,(Tr_Cldn10d:0.235603,Dr_dZ228E2:0.457464):0.110162):0.289404):0.133675,(((Dr_LOC4456:0.187559,Tr_Cldn10b:0.122303):0.066111,(Xt_CLDN10:0.143842,(((Hs_CLDN10_:0.045540,Mm_Cldn10A:0.006770):0.274691,Mm_Cld10Ab:0.011446):0.056950,Hs_CLD10ib:0.008362):0.181384):0.083413):0.063419,(DrCLDN_10:0.115587,Tr_Cldn10a:0.110661):0.142694):0.153555):0.207484,((Tr_Cldn15a:0.097908,((Tr_Cldn15b:0.156876,DrCLDN_15:0.191645):0.037005,Dr_ZGC1367:0.398776):0.055734):0.208399,((Hs_CLDN15:0.091474,Mm_Cldn15:0.164820):0.223785,Xt_CLD15_1:0.314677):0.138628):0.162210):0.114654,((DrCLD10L1a:0.205002,Tr_Cldn25:0.456157):0.171598,(DrCLD10L1b:0.165432,Tr_Cldn26:0.389967):0.233939):0.286950):0.236430,((((Dr_ZG92247:0.142070,Tr_Cldn11a:0.271188):0.072644,DrCLDN_11:0.403809,Tr_Cldn11b:0.450920):0.116398,((Hs_CLDN11:0.046328,Mm_Cldn11:0.020368):0.168134,Xt_CLDN11:0.209602):0.130214):0.594241,((Hs_CLDN16:0.029188,Mm_Cldn16:0.059762):0.136978,Xt_CLDN16:0.128336):1.034881,Dr_L793915:0.749107):0.147373):0.124481,((Dr_L557209:0.592657,(Tr_Cldn18:0.390636,(((((Dr_CH21121:0.222546,Tr_CldnD1:0.248368):0.213397,(Hs_CLDND1v:0.047910,Mm_Cldnd1:0.046028):0.191333):0.138693,Xt_CLDND1:0.276681):0.839541,(Hs_TMEM204:0.134865,(Xt_TMEM204:0.108253,Tr_TMEM204:0.180352):0.102354):1.230916):0.346933,(((Dr_PMP22a:0.256533,Tr_Pmp22_1:0.224218):0.203554,(((Hs_PMP22:0.066585,Mm_Pmp22:0.086242):0.079402,Xt_MG69407:0.127025):0.187536,Dr_PMP22b:0.136391):0.074347):0.204393,Tr_Pmp22_2:0.295422):0.557721,(Hs_CLDND2:0.205801,Mm_Cldnd2:0.157198):0.597077):0.682628):0.156084):0.277240,((Hs_CLD18i2:0.065407,Xt_CLDN18:0.175214):0.045336,Mm_Cldn18:0.093716):0.298601):0.441790):0.106404):0.085315,((((DrCLDN_20:0.088037,Tr_Cldn20a:0.052997):0.098608,(Dr_L151228:0.215400,Tr_Cldn20b:0.410055):0.064176):0.246353,(Hs_CLDN20:0.109470,Mm_Cldn20:0.184391):0.198234):0.389221,((((Hs_CLDN14v:0.056913,Mm_Cldn14v:0.019586):0.155037,Tr_Cldn14a:0.764731):0.104784,Xt_CLDN14:0.245670):0.169541,((DrCLDN_2:0.258628,Tr_Cldn2:0.308162):0.222903,((Hs_CLDN2:0.044603,Mm_Cldn2:0.050321):0.207329,Xt_CLDN2:0.298702):0.222555):0.127944):0.115364):0.180949,(DR_L568833:0.464898,Tr_Cldn14b:0.337761):1.048471,((((Dr_DKEY98F:0.335005,Tr_Cldn33c:0.253958):0.406238,((Hs_CLDN22:0.087642,Hs_CLDN24:0.060260):0.073682,((Mm_L039801:0.004432,Mm_LO45502:0.004560):0.050319,Mm_Cldn22:0.074783):0.147936):0.139313):0.146111,(Hs_CLDN25:0.168141,Mm_Cldn25:0.105102):0.347691):0.256339,((((Dr_LOC2327:0.369444,Tr_Cldn33a:0.470490):0.102569,Dr_Z153311:0.454573):0.135761,Tr_Cldn33b:0.282406):0.209266,Xt_CLDN22v:0.775199):0.213841):0.350316,(((((Dr_L553515:0.312288,Tr_Cldn23a:0.270976):0.139255,Dr_L567620:0.354022):0.391569,(Hs_CLDN23:0.142908,Mm_Cldn23:0.112786):0.496512):0.238279,(Dr_L794676:0.128097,Tr_Cldn23b:0.149257):0.781487):0.474580,((DrCLDN_12:0.143686,Tr_Cldn12:0.234216):0.160735,((Hs_CLDN12:0.052505,Mm_Cldn12:0.043529):0.119929,Xt_CLDN12:0.243962):0.243801):1.138492):0.283352,Tr_Cldn13:1.082875,Dr_ZG63990:1.436511):0.117953):0.148066):0.056942,Xt_CLDN4:0.118212):0.110980,(Mm_Cldn4:0.087801,Mm_Cldn13:0.948084):0.037650);

Figure B1. Phylogeny tree-files. Raw consensus treefiles from phylogenetic analysis of vertebrate claudin protein sequences (viewable in *TreeView*). (**A**) *Poisson* model analysis. (**B**) *Blosum62* model analysis.(**C**) *WAG* model analysis. (**D**) *Equalin* model analysis.

C

(Hs_CLDN4:0.075642,Mm_Cldn4:0.094737,(((((((Dr_47871:0.172695,Tr_Cldn27c:0.118910):0.093262,Tr_Cldn27a:0.264098):0.075541,(((Tr_Cldn28a:0.117337,DrCLDN_E:0.138130):0.032480,Tr_Cldn28b:0.115880):0.088826,((Dr_L796314:0.396238,Tr_Cldn28c:0.151570):0.266715,((DrCLDN_F:0.244099,Tr_Cldn27b:0.218156):0.262479,Tr_Cldn27d:0.667069):0.258090):0.120792):0.058794):0.039391,((Dr_112437:0.255649,Tr_Cldn29b:0.216301):0.076508,(DrCLDN_D:0.168525,Tr_Cldn29a:0.124696):0.093895):0.066152,((DrCLDN_A:0.185764,DrCLDN_B:0.162332):0.083135,Tr_Cldn30a:0.162607,Tr_Cldn30c:0.167477,(Tr_Cldn30b:0.170485,(Tr_Cldn30d:0.320425,Dr_Z136892:0.432551):0.187851):0.223054):0.092224):0.077385,(((((Dr_0151512:0.161269,Tr_Cldn5c:0.238537):0.241745,(((DrCLDN_5a:0.116044,Tr_Cldn5a:0.084506):0.048313,(DrCLDN_5b:0.180021,Tr_Cldn5b:0.164997):0.060324):0.129566,((Hs_CLDN5v1:0.035227,Mm_Cldn5:0.067276):0.323824,Xt_CLDN5:0.145244):0.143044):0.153811):0.077691,((Hs_CLDN6:0.056690,Mm_Cldn6:0.079390):0.184226,(Hs_CLDN9:0.012467,Mm_Cldn9:0.025874):0.145333):0.144809,DrCLDN_G:0.334129,(((DrCLDN_K:0.134911,Tr_Cldn31:0.100111):0.138005,Dr_LOC4771:0.630314):0.258608,((Dr_L570842:0.042719,Tr_Cldn32b:0.079686):0.366742,(((((((Dr_ZG92192:0.100256,Tr_Cldn7b:0.099910):0.104335,Tr_Cldn7a:0.104730):0.068854,DrCLDN_7:0.131696):0.156043,Xt_MG75689:0.162095):0.123781,(Hs_CLDN7:0.048080,Mm_Cldn7:0.043199):0.176696,(((Hs_CLDN1:0.024239,Mm_Cldn1:0.084553):0.172669,Xt_CLDN1:0.237523):0.068650,(DrCLDN_1:0.290413,Tr_Cldn1:0.177639):0.252886):0.117177):0.085436,(((Tr_Cldn19:0.074049,DrCLDN_19:0.134189):0.065804,Xt_CLDN19:0.041624):0.131397,(Hs_CLDN19i:0.033414,Mm_Cldn19i:0.022551):0.154463):0.330535):0.111970,(((((((Dr_L556021:0.289301,Tr_Cldn10e:0.291935):0.441107,Dr_CLD10L2:0.381301):0.329070,(Tr_Cldn10c:0.273711,(Tr_Cldn10d:0.245270,Dr_dZ228E2:0.477297):0.137602):0.287287):0.158204,(((Dr_LOC4456:0.183143,Tr_Cldn10b:0.138331):0.071614,(Xt_CLDN10:0.150402,(((Hs_CLDN10_:0.045433,Mm_Cldn10A:0.007592):0.289879,Mm_Cld10Ab:0.013813):0.057550,Hs_CLD10ib:0.008555):0.188067):0.087534):0.066689,(DrCLDN_10:0.122115,Tr_Cldn10a:0.117612):0.134491):0.161440):0.246256,((Tr_Cldn15a:0.110351,(Tr_Cldn15b:0.155145,DrCLDN_15:0.209263):0.039149,Dr_ZGC1367:0.423931):0.219116,((Hs_CLDN15:0.095643,Mm_Cldn15:0.168572):0.245937,Xt_CLD15_1:0.331304):0.136209):0.157611):0.137113,((DrCLD10L1a:0.217085,Tr_Cldn25:0.492352):0.184287,(DrCLD10L1b:0.171203,Tr_Cldn26:0.421429):0.245336):0.317238):0.301106,((Dr_L557209:0.638108,(Tr_Cldn18:0.450468,((((Dr_CH21121:0.233928,Tr_CldnD1:0.261788):0.179959,((Hs_CLDND1v:0.047610,Mm_Cldnd1:0.049695):0.186843,Xt_CLDND1:0.358415):0.136534):0.989675,((Hs_TMEM204:0.147222,Xt_TMEM204:0.113924):0.139179,Tr_TMEM204:0.171635):1.393471):0.384526,((((Dr_PMP22a:0.268852,Tr_Pmp22_1:0.252201):0.220612,(((Hs_PMP22:0.061358,Mm_Pmp22:0.093957):0.087280,Xt_MG69407:0.135279):0.208594,Dr_PMP22b:0.136493):0.079797):0.218867,Tr_Pmp22_2:0.340965):0.661878,(Hs_CLDND2:0.215292,Mm_Cldnd2:0.162698):0.651059):0.227354):0.744765):0.155246):0.280236,((Hs_CLD18i2:0.069443,Xt_CLDN18:0.184211):0.053472,Mm_Cldn18:0.090666):0.355111):0.476798,(((((Dr_ZG92247:0.146349,Tr_Cldn11a:0.277604):0.082017,DrCLDN_11:0.420120):0.075041,Tr_Cldn11b:0.476656):0.108677,((Hs_CLDN11:0.048250,Mm_Cldn11:0.021989):0.178959,Xt_CLDN11:0.214301):0.157444):0.662254,(((Hs_CLDN16:0.031064,Mm_Cldn16:0.063227):0.152183,Xt_CLDN16:0.123062):1.192865,Dr_L793915:0.775015):0.221806):0.158793):0.153546):0.105668,((((DrCLDN_20:0.089016,Tr_Cldn20a:0.055839):0.097001,(Dr_L151228:0.224362,Tr_Cldn20b:0.439903):0.069545):0.267156,(Hs_CLDN20:0.114993,Mm_Cldn20:0.186751):0.205073):0.408527,((((Hs_CLDN14v:0.056646,Mm_Cldn14v:0.022751):0.169150,Tr_Cldn14a:0.815944):0.108018,Xt_CLDN14:0.249844):0.185779,((DrCLDN_2:0.259703,Tr_Cldn2:0.342697):0.235369,((Hs_CLDN2:0.046467,Mm_Cldn2:0.051450):0.204171,Xt_CLDN2:0.327506):0.241495):0.134353):0.133549):0.224667,(DR_L568833:0.515429,Tr_Cldn14b:0.329302):1.168361,(((Dr_DKEY98F:0.361155,Tr_Cldn33c:0.262260):0.372212,((((Hs_CLDN22:0.088786,Hs_CLDN24:0.063503):0.065741,((Mm_L039801:0.004442,Mm_LO45502:0.004637):0.050488,Mm_Cldn22:0.079587):0.160398):0.154954,(Hs_CLDN25:0.159738,Mm_Cldn25:0.116738):0.431125):0.169662):0.278148,((((Dr_LOC2327:0.386934,Tr_Cldn33a:0.498789):0.120414,Dr_Z153311:0.478101):0.133796,Tr_Cldn33b:0.332110):0.261288,Xt_CLDN22v:0.796810):0.193583):0.414095,(((((Dr_L553515:0.323256,Tr_Cldn23a:0.285822):0.132254,Dr_L567620:0.385601):0.445984,(Hs_CLDN23:0.142708,Mm_Cldn23:0.118232):0.545610):0.262399,(Dr_L794676:0.140313,Tr_Cldn23b:0.148462):0.878851):0.611552,(((DrCLDN_12:0.145334,Tr_Cldn12:0.245799):0.152569,((Hs_CLDN12:0.052328,Mm_Cldn12:0.046528):0.120710,Xt_CLDN12:0.252833):0.287218):1.330733,Dr_ZG63990:1.522410):0.252159):0.309884,Tr_Cldn13:1.230760):0.142947):0.100943):0.072654,((((Dr_792492:0.120291,Tr_Cldn3a:0.111742):0.076103,((DrCLDN_C:0.158094,Tr_Cldn3d:0.158889):0.085334,Tr_Cldn3b:0.266764):0.126293):0.050828,(DrCLDN_H:0.137741,Tr_Cldn3c:0.155218):0.079664):0.060451,((Hs_CLDN3:0.047123,Mm_Cldn3:0.052288):0.178257,(Xt_CLDN3:0.083405,((DrCLDN_J:0.172298,Tr_Cldn6:0.248086):0.294857,(((Dr_LOC6193:0.379838,Tr_Cldn8a:0.364827):0.158807,((Dr_Z110333:0.208161,Tr_Cldn8d:0.166216):0.321821,((DrCLDN_8:0.225394,Tr_Cldn8b:0.130369):0.136275,(Tr_Cldn8c:0.286709,DrCLDN_17:0.474082):0.153532):0.130868):0.159253):0.165847,(((Hs_CLDN17:0.084109,Mm_Cldn17:0.130365):0.397762,(Hs_CLDN8:0.072002,Mm_Cldn8:0.118661):0.118791):0.156436,((Xt_CLDN8:0.037060,Xt_0145356:0.036224):0.024158,Xt_CLDN17:0.054646):0.191217):0.130365):0.213128):0.181920):0.071607):0.042210):0.058380,(DrCLDN_I:0.137753,Tr_Cldn32a:0.172543):0.389466):0.066397,(Xt_CLDN6.1:0.049790,Xt_CLDN6SK:0.034463):0.163465):0.056477):0.050998,Xt_CLDN4:0.128239):0.103460,Mm_Cldn13:1.028370):0.056306);

D

(Hs_CLDN4:0.073198,Mm_Cldn4:0.106936,Xt_CLDN4:0.124309,Mm_Cldn13:0.683337,Tr_Cldn13:0.885689,Dr_ZG63990:1.203651,(Xt_CLDN6.1:0.051808,Xt_CLDN6SK:0.032519):0.157117,(DrCLDN_J:0.154631,Tr_Cldn6:0.238672):0.344073,((DrCLDN_12:0.129339,Tr_Cldn12:0.241318):0.195869,((Hs_CLDN12:0.051589,Mm_Cldn12:0.042919):0.129984,Xt_CLDN12:0.231866):0.182957):0.922625,(Dr_L570842:0.057364,Tr_Cldn32b:0.062281):0.351116,(DrCLDN_I:0.144067,Tr_Cldn32a:0.162230):0.307878,(DR_L568833:0.410569,Tr_Cldn14b:0.334996):0.847263,((Hs_CLDN6:0.052423,Mm_Cldn6:0.080220):0.155915,(Hs_CLDN9:0.010801,Mm_Cldn9:0.024862):0.135875):0.121446,((((Dr_L553515:0.310883,Tr_Cldn23a:0.254012):0.140124,Dr_L567620:0.311091):0.385826,(Hs_CLDN23:0.116822,Mm_Cldn23:0.125507):0.377204):0.169794,(Dr_L794676:0.144226,Tr_Cldn23b:0.121057):0.698079):0.478929,(((Dr_0151512:0.161935,Tr_Cldn5c:0.214891):0.219021,(((DrCLDN_5a:0.113046,Tr_Cldn5a:0.087837):0.056275,(DrCLDN_5b:0.174830,Tr_Cldn5b:0.159006):0.045781):0.136870,((Hs_CLDN5v1:0.036878,Mm_Cldn5:0.057631):0.270197,Xt_CLDN5:0.147110):0.126408):0.120485):0.073363,(DrCLDN_G:0.272688,((DrCLDN_K:0.122514,Tr_Cldn31:0.101467):0.115412,Dr_LOC4771:0.511476):0.246473):0.086416):0.053353,((((Dr_L557209:0.672449,Tr_Cldn18:0.449283):0.260623,((Hs_CLD18i2:0.067075,Xt_CLDN18:0.201213):0.056276,Mm_Cldn18:0.066881):0.280819):0.198029,(((((Dr_CH21121:0.207257,Tr_CldnD1:0.230239):0.200192,(Hs_CLDND1v:0.051422,Mm_Cldnd1:0.040007):0.186526):0.127768,Xt_CLDND1:0.265807):0.713655,((Hs_TMEM204:0.124145,Xt_TMEM204:0.108999):0.144590,Tr_TMEM204:0.159570):1.001278):0.211792,((((Dr_PMP22a:0.277133,Tr_Pmp22_1:0.182264):0.207594,(((Hs_PMP22:0.075911,Mm_Pmp22:0.078967):0.065728,Xt_MG69407:0.147599):0.196452,Dr_PMP22b:0.136404):0.083313):0.186043,Tr_Pmp22_2:0.249766):0.469670,(Hs_CLDND2:0.214655,Mm_Cldnd2:0.134006):0.600782):0.160177):0.448393):0.247915,((((Dr_DKEY98F:0.322796,Tr_Cldn33c:0.239232):0.376588,((Hs_CLDN22:0.081520,Hs_CLDN24:0.055932):0.064629,((Mm_L039801:0.004229,Mm_LO45502:0.004183):0.045644,Mm_Cldn22:0.072512):0.144078):0.128826):0.168858,(Hs_CLDN25:0.152599,Mm_Cldn25:0.103248):0.249078):0.210097,((((Dr_LOC2327:0.340873,Dr_Z153311:0.432897):0.080156,Tr_Cldn33a:0.423048):0.107823,Tr_Cldn33b:0.274711):0.186020,Xt_CLDN22v:0.688631):0.223265):0.221790):0.173101,(((DrCLDN_20:0.061039,(Tr_Cldn20a:0.053810,(Dr_L151228:0.218898,Tr_Cldn20b:0.394338):0.109089):0.064183):0.239312,(Hs_CLDN20:0.116984,Mm_Cldn20:0.177959):0.204020):0.349293,((((Hs_CLDN14v:0.058577,Mm_Cldn14v:0.016789):0.169308,Tr_Cldn14a:0.660430):0.075514,Xt_CLDN14:0.263205):0.159987,((DrCLDN_2:0.252074,Tr_Cldn2:0.298740):0.205216,((Hs_CLDN2:0.041528,Mm_Cldn2:0.055805):0.195586,Xt_CLDN2:0.312740):0.195296):0.146118):0.105772):0.153992,(((((((Dr_ZG92192:0.098217,Tr_Cldn7b:0.093258):0.114709,Tr_Cldn7a:0.095623):0.065877,DrCLDN_7:0.136792):0.122168,Xt_MG75689:0.159524):0.125286,(Hs_CLDN7:0.045531,Mm_Cldn7:0.045946):0.162867):0.060207,(((Hs_CLDN1:0.025339,Mm_Cldn1:0.080336):0.126642,(DrCLDN_1:0.268224,Tr_Cldn1:0.165192):0.238902):0.091292,Xt_CLDN1:0.198011):0.122990):0.087505,(((Tr_Cldn19:0.075758,DrCLDN_19:0.131263):0.054203,Xt_CLDN19:0.046873):0.130137,(Hs_CLDN19i:0.033598,Mm_Cldn19i:0.018715):0.132438):0.280779):0.132778,(((((((Dr_L556021:0.264738,Tr_Cldn10e:0.276886):0.338597,Dr_CLD10L2:0.317795):0.292196,(Tr_Cldn10c:0.251347,(Tr_Cldn10d:0.181714,Dr_dZ228E2:0.448198):0.128541):0.226099):0.167305,((Dr_LOC4456:0.182620,((Xt_CLDN10:0.131617,(((Hs_CLDN10_:0.042818,Mm_Cldn10A:0.009332):0.266439,Mm_Cld10Ab:0.011836):0.055349,Hs_CLD10ib:0.010315):0.195858):0.080031,(DrCLDN_10:0.128258,Tr_Cldn10a:0.107318):0.156801):0.071567):0.091328,Tr_Cldn10b:0.073280):0.168646):0.221673,((((Tr_Cldn15a:0.116165,DrCLDN_15:0.199703):0.049456,Tr_Cldn15b:0.146149):0.052513,Dr_ZGC1367:0.345115):0.192339,((Hs_CLDN15:0.086545,Mm_Cldn15:0.161507):0.226840,Xt_CLD15_1:0.290698):0.133077):0.123781):0.087458,((DrCLD10L1a:0.236211,Tr_Cldn25:0.390883):0.129780,(DrCLD10L1b:0.179739,Tr_Cldn26:0.385382):0.225944):0.245303):0.240169,((((((Dr_ZG92247:0.145496,Tr_Cldn11a:0.262420):0.067250,DrCLDN_11:0.394737):0.074158,Tr_Cldn11b:0.387050):0.117106,((Hs_CLDN11:0.037005,Mm_Cldn11:0.028909):0.175862,Xt_CLDN11:0.187642):0.128596):0.509567,Dr_L793915:0.674327):0.142288,((Hs_CLDN16:0.025844,Mm_Cldn16:0.060215):0.101532,Xt_CLDN16:0.146378):0.828680):0.141275):0.151500):0.078656,(((((Dr_47871:0.157846,Tr_Cldn27c:0.120943):0.072528,Tr_Cldn27a:0.262302):0.062201,(((Tr_Cldn28a:0.101941,DrCLDN_E:0.137316):0.042228,Tr_Cldn28b:0.097932):0.072772,((Dr_L796314:0.363111,Tr_Cldn28c:0.160430):0.245641,((DrCLDN_F:0.209584,Tr_Cldn27b:0.218019):0.231971,Tr_Cldn27d:0.614246):0.195488):0.115076):0.079745):0.051177,((Dr_112437:0.235736,Tr_Cldn29b:0.187028):0.084178,(DrCLDN_D:0.182039,Tr_Cldn29a:0.113889):0.083059):0.048664):0.029428,(((DrCLDN_A:0.167872,DrCLDN_B:0.152800):0.076804,(Tr_Cldn30b:0.168562,(Tr_Cldn30d:0.303981,Dr_Z136892:0.397806):0.158523):0.197574):0.060529,(Tr_Cldn30a:0.151958,Tr_Cldn30c:0.158829):0.058264):0.088370):0.063824,(((Dr_792492:0.113521,Tr_Cldn3a:0.115582):0.078465,(DrCLDN_H:0.132852,Tr_Cldn3c:0.147680):0.082312):0.056814,((Hs_CLDN3:0.043737,Mm_Cldn3:0.052181):0.156687,Xt_CLDN3:0.132805):0.045018,((DrCLDN_C:0.153448,Tr_Cldn3d:0.167059):0.086614,Tr_Cldn3b:0.258812):0.107661):0.057231,(((Dr_LOC6193:0.330561,Tr_Cldn8a:0.341705):0.135959,((Dr_Z110333:0.223770,Tr_Cldn8d:0.122396):0.292313,((DrCLDN_8:0.217555,Tr_Cldn8b:0.124853):0.121828,(Tr_Cldn8c:0.270877,DrCLDN_17:0.419866):0.103857):0.127807):0.164385):0.148118,((Hs_CLDN17:0.093729,Mm_Cldn17:0.113874):0.278603,((Hs_CLDN8:0.101525,Mm_Cldn8:0.094497):0.141237,((Xt_CLDN8:0.033549,Xt_CLDN17:0.065852):0.030035,Xt_0145356:0.016250):0.225831):0.110569):0.086671):0.186438);

Figure B1 Continued.

Figure B2. Genomic synteny of claudin groups 6, 9,11a-b, 18, 22 and 24. (**A**) Claudins 22 and 24 are paralog genes restricted to tetrapods, (**B**) Claudin 6 and 9 are putative paralogs in tetrapods,(**C**) confirmation of correct paralog identity for zebrafish *cldn11a* and *cldn11b*, (**D**) chromosomal rearrangement at the zebrafish claudin 18 loci gives equivocal evidence for homology. Annotation follows proposed interim reclassification schema. When different, the current gene name is provided in parenthesis. *Ensembl* assembly versions used: human (*GRCh37*), mouse (*NCBI m37*), zebrafish (*Zv9*), and Fugu (*v4*). *Symbols*: empty box, claudin gene (group ortholog); hatched box, genes with no observable ortholog in compared regions; black box, orthologous genes across loci; shaded box, homologous genes giving alternate evidence for paralog identity; rc, reverse complement. Gene and inter-gene distances depicted are for illustrative purposes only and are not to scale.

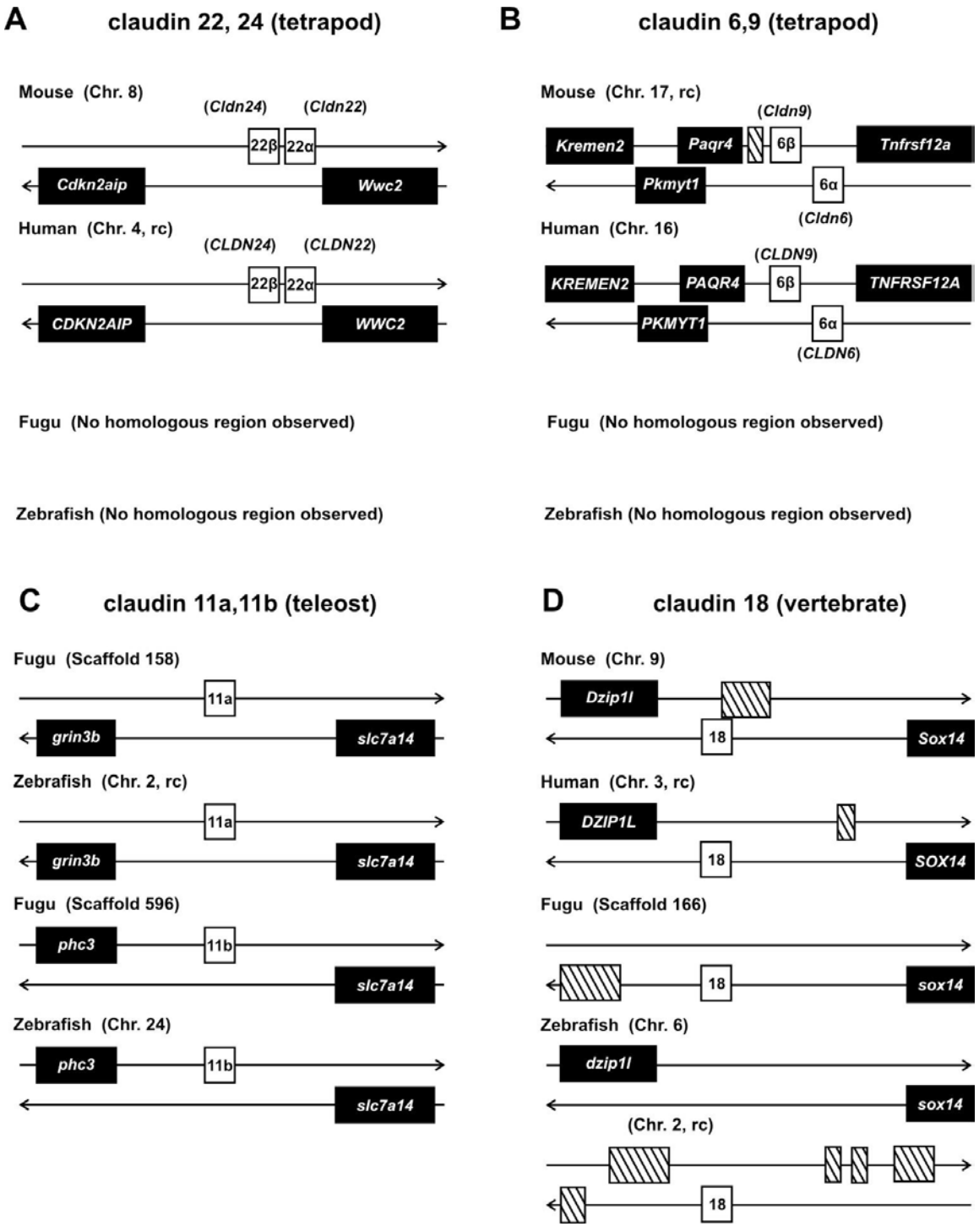
A
claudin 22, 24 (tetrapod)
Mouse (Chr. 8)
(Cldn24)
(Cldn22)
22β
22α
Cdkn2aip
Wwc2
Human (Chr. 4, rc)
(CLDN24)
(CLDN22)
22β
22α
CDKN2AIP
WWC2
Fugu (No homologous region observed)
Zebrafish (No homologous region observed)
B
claudin 6,9 (tetrapod)
Mouse (Chr. 17, rc)
(Cldn9)
Kremen2
Paqr4
6β
Tnfrsf12a
Pkmyt1
6α
(Cldn6)
Human (Chr. 16)
(CLDN9)
KREMEN2
PAQR4
6β
TNFRSF12A
PKMYT1
6α
(CLDN6)
Fugu (No homologous region observed)
Zebrafish (No homologous region observed)
C
claudin 11a,11b (teleost)
Fugu (Scaffold 158)
11a
grin3b
slc7a14
Zebrafish (Chr. 2, rc)
11a
grin3b
slc7a14
Fugu (Scaffold 596)
phc3
11b
slc7a14
Zebrafish (Chr. 24)
phc3
11b
slc7a14
D
claudin 18 (vertebrate)
Mouse (Chr. 9)
Dzip1l
18
Sox14
Human (Chr. 3, rc)
DZIP1L
18
SOX14
Fugu (Scaffold 166)
18
sox14
Zebrafish (Chr. 6)
dzip1l
sox14
(Chr. 2, rc)
18

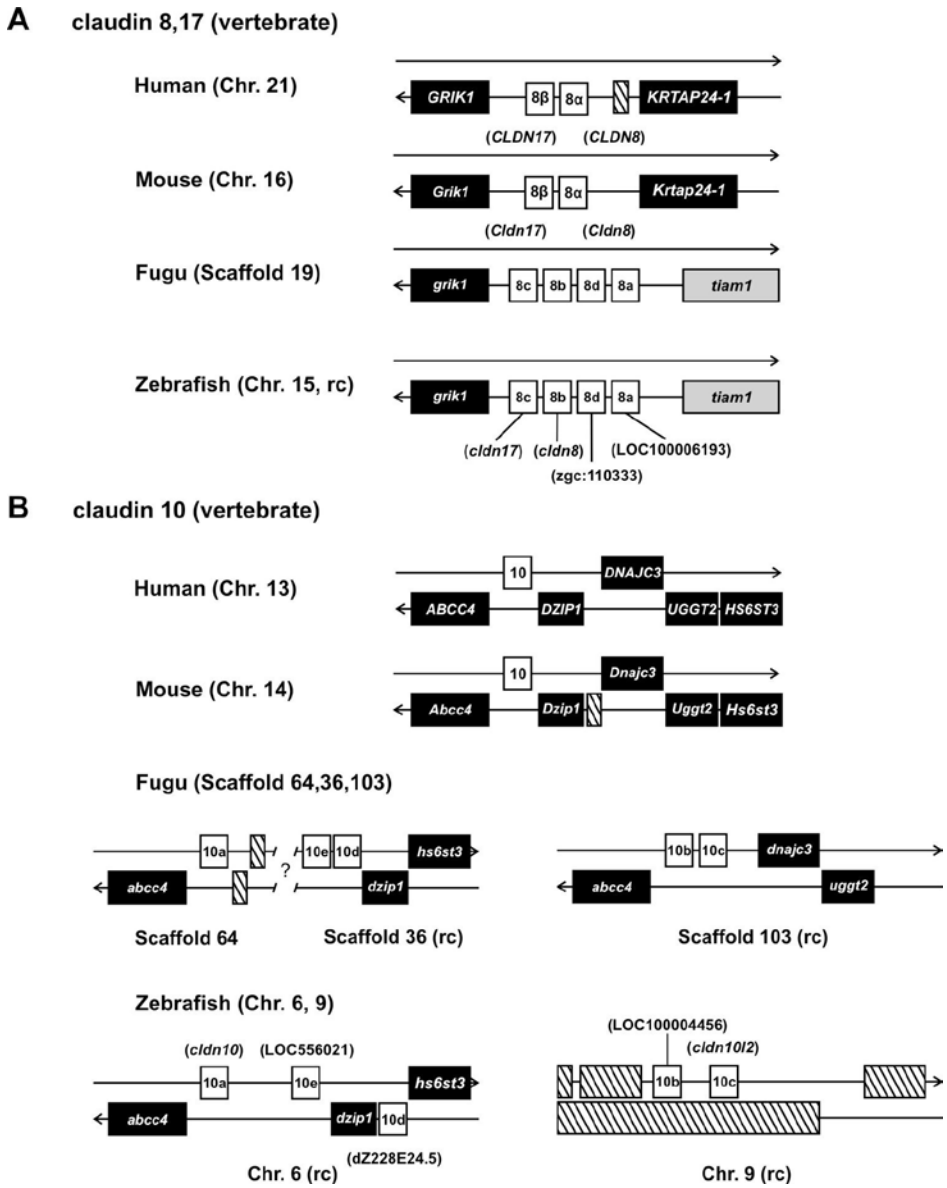

Figure B3.Genomic synteny of claudin groups 8, 10, and 17 (**A**) Claudins 8 and 17 are paralogous genes in mammals. In ray-finned fishes, this group has expanded to 4 identifiable paralogs (*cldn8a-d*). (**B**) A single claudin 10 homolog is present in mammals, however combined evolutionary analysis suggests the presence of 5 discrete homologs in teleost fishes (*cldn10a-e*). Annotation follows proposed interim reclassification schema. When different, the current gene name is provided in parenthesis. *Ensembl* assembly versions used: human (*GRCh37*), mouse (*NCBI m37*), zebrafish (*Zv9*), and Fugu (*v4*). *Symbols*: empty box, claudin gene (group ortholog); hatched box, genes with no observable ortholog in compared regions; black box, orthologous genes across loci; shaded box, homologous genes giving alternate evidence for paralog identity; rc, reverse complement. Gene and inter-gene distances depicted are for illustrative purposes only and are not to scale.

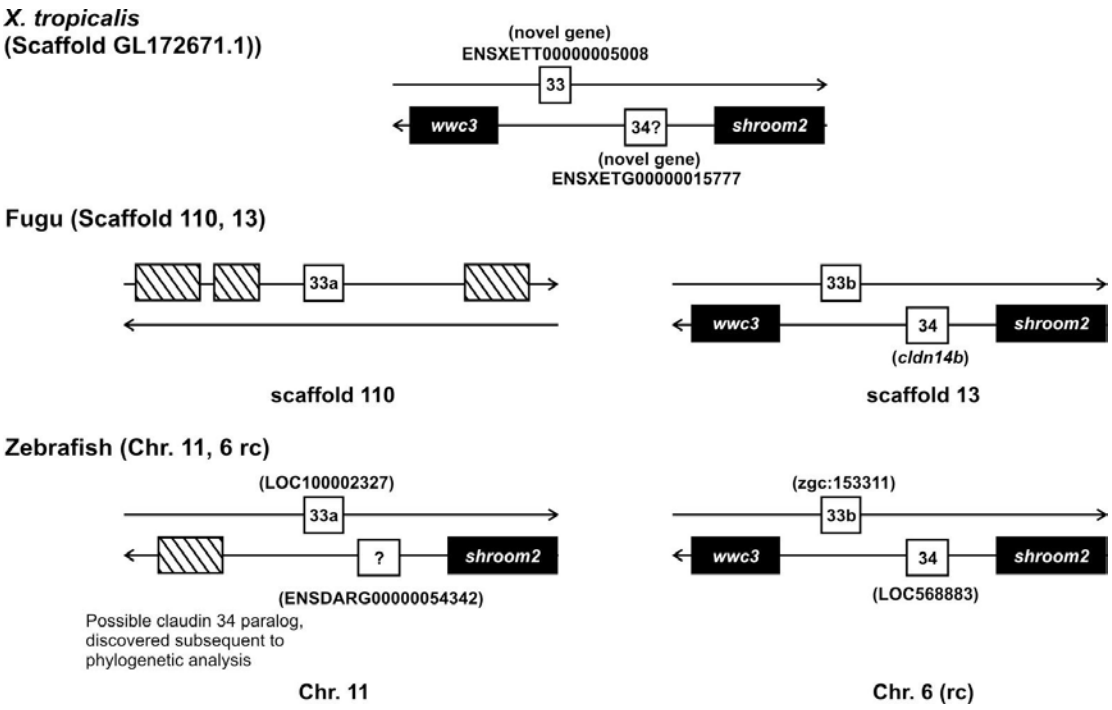

Figure B4. Genomic synteny of claudin groups 33 and 34**.** Two zebrafish claudin 33 paralogs were identified by comparison to homologous loci in the frog (*Xenopus tropicalis*) and Fugu genomes. A single zebrafish claudin 34 homolog was originally identified, but an additional claudin, possibly a paralog of *cldn34*, was discovered after new revisions to the genome assembly (*Zv9*). Annotation follows proposed interim reclassification schema. When different, the current gene name is provided in parenthesis. *Ensembl* assembly versions used: *X. tropicalis* (*JGI v4.2*), zebrafish (*Zv9*), and Fugu (*v4*). *Symbols*: empty box, claudin gene (group ortholog); hatched box, genes with no observable ortholog in compared regions; black box, orthologous genes across loci; shaded box, homologous genes giving alternate evidence for paralog identity; rc, reverse complement. Gene and inter-gene distances depicted are for illustrative purposes only and are not to scale.

Figure B5. Genomic synteny of claudin groups 3, 4, 5c, 8-like, 28, 29, 30, 36, and 37. With the possible exception of claudin 5c and 36, all teleost claudin groups appear to be distant homologs of tetrapod claudins 3 and 4, indicating significant genomic expansion of this locus. An additional zebrafish claudin, *cldn36*, was discovered after new revisions to the zebrafish genomic assembly (Zv9). Annotation follows proposed interim reclassification schema. When different, the current gene name is provided in parenthesis. *Ensembl* assembly versions used: human (*GRCh37*), mouse (*NCBI m37*), zebrafish (*Zv9*), and Fugu (*v4*). *Symbols*: empty box, claudin gene (group ortholog); hatched box, genes with no observable ortholog in compared regions; black box, orthologous genes across loci; shaded box, homologous genes giving alternate evidence for paralog identity; rc, reverse complement. Gene and inter-gene distances depicted are for illustrative purposes only and are not to scale

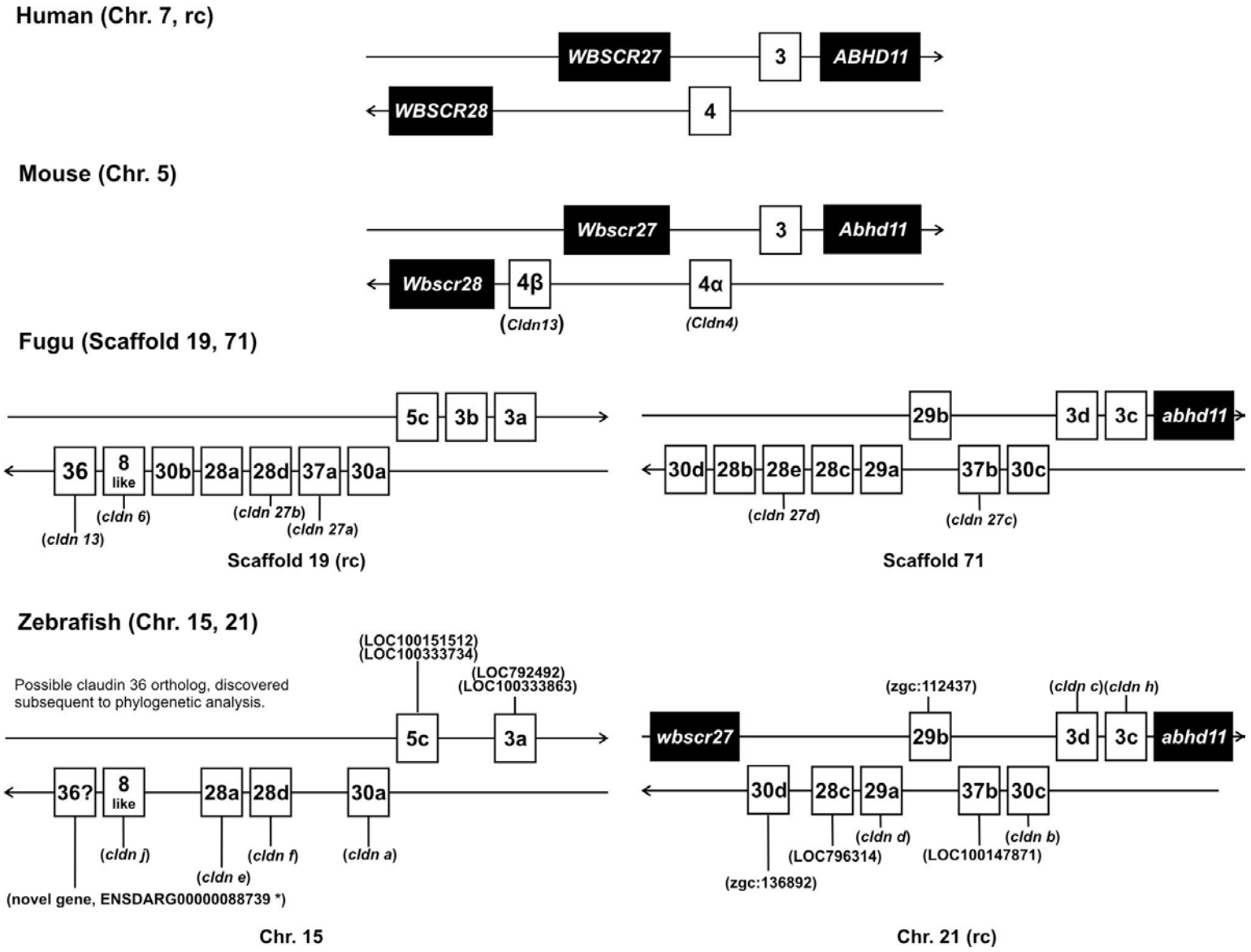
Human (Chr. 7, rc)
WBSCR27
3
ABHD11
WBSCR28
4
Mouse (Chr. 5)
Wbscr27
3
Abhd11
Wbscr28
4β
4α
(Cldn13)
(Cldn4)
Fugu (Scaffold 19, 71)
5c
3b
3a
36
8 like
30b
28a
28d
37a
30a
(cldn 13)
(cldn 6)
(cldn 27b)
(cldn 27a)
Scaffold 19 (rc)
29b
3d
3c
abhd11
30d
28b
28e
28c
29a
37b
30c
(cldn 27d)
(cldn 27c)
Scaffold 71
Zebrafish (Chr. 15, 21)
Possible claudin 36 ortholog, discovered subsequent to phylogenetic analysis.
(LOC100151512)
(LOC100333734)
(LOC792492)
(LOC100333863)
5c
3a
36?
8 like
28a
28d
30a
(cldn j)
(cldn e)
(cldn f)
(cldn a)
(novel gene, ENSDARG00000088739 *)
Chr. 15
(zgc:112437)
(cldn c)(cldn h)
wbscr27
29b
3d
3c
abhd11
30d
28c
29a
37b
30c
(cldn d)
(LOC796314)
(zgc:136892)
(LOC100147871)
(cldn b)
Chr. 21 (rc)

Appendix C

Chapter Four Supplemental Information

Table C1. List of PCR primer pairs used for qPCR expression analysis.

Gene (*symbol*)	Primer Sequence (5' to 3')	*Genbank Acc. No.* (NCBI)	Notes
β-actin 1 (*bactin1*)	(For) GAA ATC GCC GCA CTG GTT (Rev) CGA ATC CGG CCT TGC A	*AB037865*	nucleotide position (*nt*) 91...145
glucose transporter 1 (*slc2a1, glut1*)	(For) CAG AGA GCC CCC GAT TCC (Rev) GCA CGG ATT TGG CCT TGT T	*XM_003453669*	*nt* 1052...1111
glucose transporter 4-like (*slc2a4l, glut4l*)	(For) AGC CCC CGA TTC CTC TAC A (Rev) GGC CAC TCT TGG CAT GGT	*XM_003458705*	*nt* 643...697
glycogen phosphorylase (*pyg*)	(For) GGC TCG CCC CGA GTA CAT (Rev) CGT TTC CTC CAC TCG TCC AT	*DQ010415*	*nt* 623...677
hormone sensitive lipase (*hsl*)	(For) GCG CAT GCT ACA TGA CAA CAG (Rev) CCC GCT TTC ATC CTG GAA	*FJ601660*	*nt* 99...153
leptin a (*lepa*)	(For) GGG TCT CCC AGA TCA AGT ACG A (Rev) TGC CGC CAC AGA TGA ATG	*KC354702*	*nt* 335...395
leptin receptor (*lepr*)	(For) AAA TTC ACC GGA AGC AAA CCT (Rev) TGC AGC CGG GAC TGT GT	*KC354703*	*nt* 475...530
lipoprotein lipase (*lpl*)	(For) CGG AGA CCT TAC CAA CCA CAA (Rev) GCC GGC GGG ATC CA	*FJ623077*	*nt* 334...388
Na^+, K^+-ATPase α1a (*atpa1a*)	(For) AAC TGA TTT GGT CCC TGC AA (Rev) ATG CAT TTC TGG GCT GTC TC	*GR645170*	FW type, *nt* 231...310, Tipsmark *et al.*, 2011
Na^+, K^+-ATPase α1b (*atpa1b*)	(For) GGA GCG TGT GCT TCA TCA CT (Rev) ATC CAT GCT TTG TGG GGT TA	*U82549*	SW type, *nt* 3238...3327, Tipsmark *et al.*, 2011

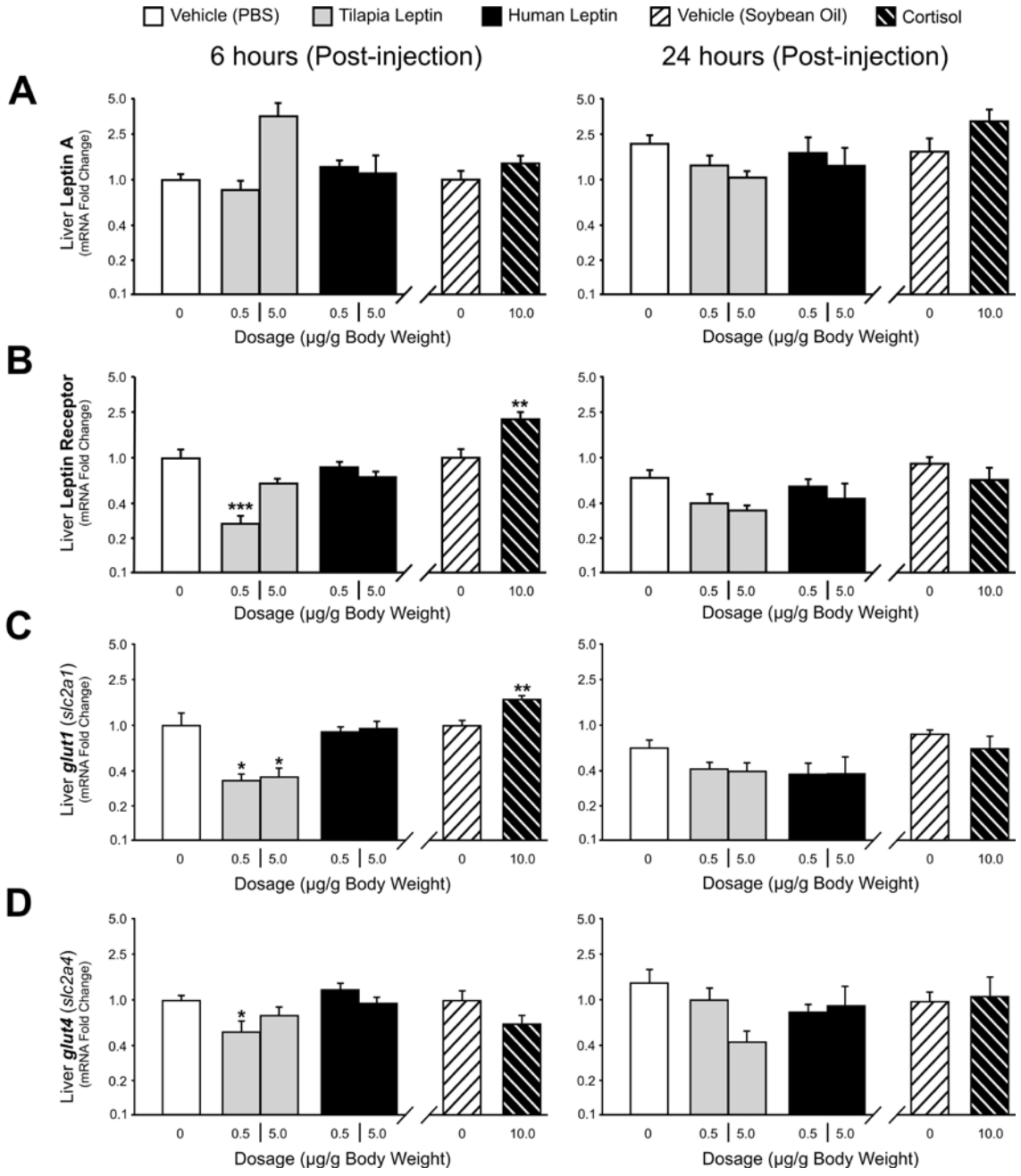

Figure C1. Effect of leptin or cortisol injection (6 and 24 hours) on liver mRNA expression of *lepa*, *lepr*, and glucose transporters (*glut1*, *glut4-l*). *Leptin* – intraperitoneal (IP) injection of tilapia or human leptin (0.5 and 5.0 µg/ g BW) or sham (PBS; phosphate buffered saline). *Cortisol* –IP injection of 10 µg/ g BW or sham (soybean oil). **(A)** leptin (*lepa*) mRNA. (**B**) leptin receptor (*lepr*) mRNA. (**C**) *glut1* (*slc2a1*) mRNA. (**D**) *glut4-l* (*slc2a4-l*) mRNA. *Symbols*: asterisks denote significant effects against sham at a given time *** $p < 0.001$, ** $p < 0.01$, * $p < 0.05$. All mRNA data are expressed as fold change relative to the 6-hour sham groups. Values represent the group mean ± SEM (n = 5-8).

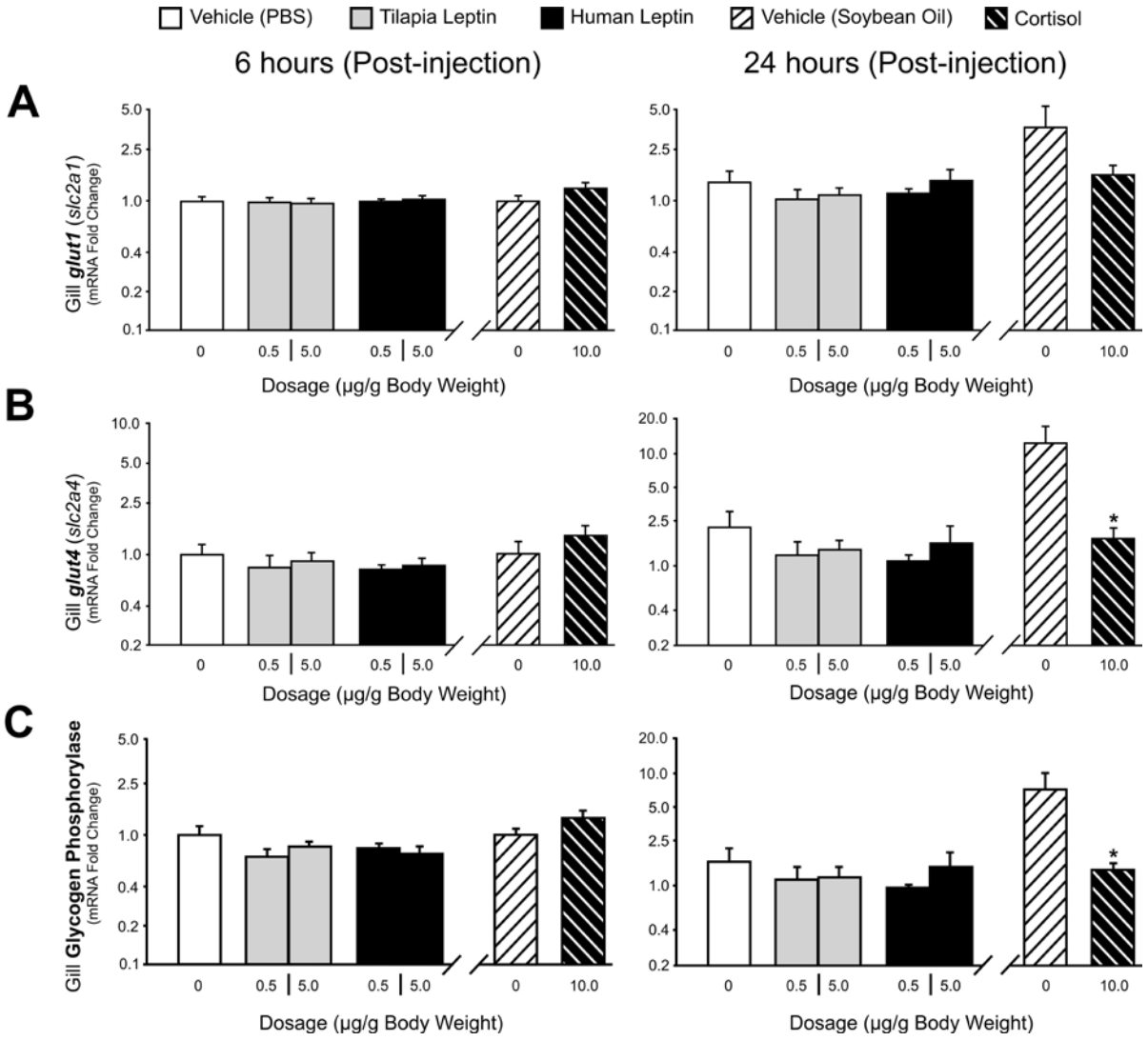

Figure C2. Effect of leptin or cortisol injection (6 and 24 hours) on gill mRNA expression of glucose transporters (*glut1*, *glut4-l*) and glycogen phosphorylase (*gyp*). *Leptin* – intraperitoneal (IP) injection of tilapia or human leptin (0.5 and 5.0 µg/ g BW) or sham (PBS; phosphate buffered saline). *Cortisol* –IP injection of 10 µg/ g BW or sham (soybean oil). **(A)** *glut1* (*slc2a1*) mRNA (**B**) *glut4-l* (*slc2a4-l*) mRNA. (**C**) glycogen phosphorylase (*gyp*) mRNA. *Symbols*: asterisks denote significant effects against sham at a given time *** $p < 0.001$, ** $p < 0.01$, * $p < 0.05$. All mRNA data are expressed as fold change relative to the 6-hour sham groups. Values represent the group mean ± SEM (n = 5-8).

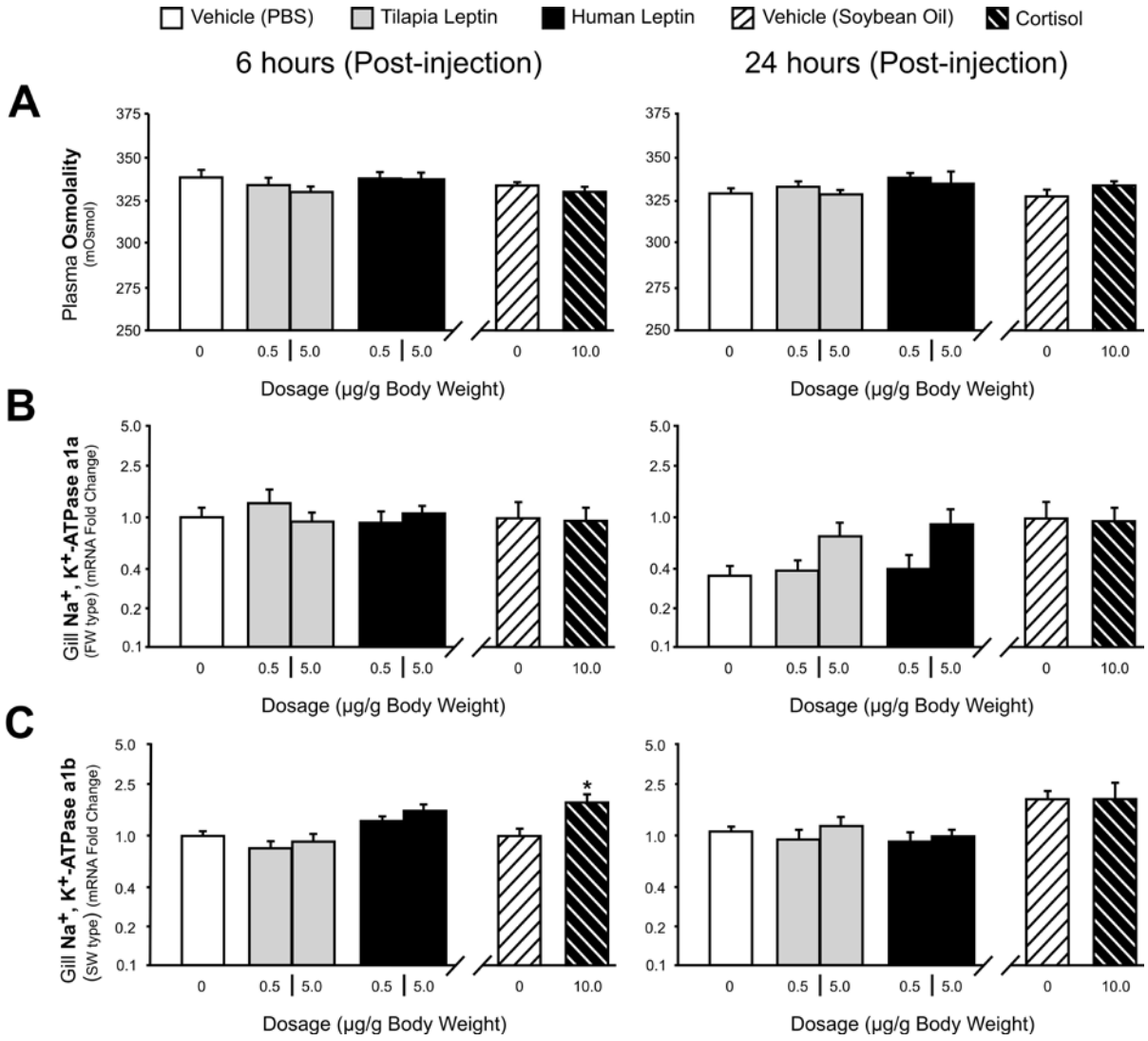

Figure C3. Effect of leptin or cortisol injection (6 and 24 hours) on plasma osmolality and gill mRNA expression of Na^+, K^+-ATPase alpha subunits (*atpa1a*, *atpa1b*). *Leptin* – intraperitoneal (IP) injection of tilapia or human leptin (0.5 and 5.0 µg/ g BW) or sham (PBS; phosphate buffered saline). *Cortisol* –IP injection of 10 µg/ g BW or sham (soybean oil). **(A)** plasma osmolality (mOsmol) (**B**) *atpa1a* mRNA (Freshwater isoform). (**C**) *atpa1b* mRNA (Seawater isoform). *Symbols*: asterisks denote significant effects against sham at a given time *** $p < 0.001$, ** $p < 0.01$, * $p < 0.05$. All mRNA data are expressed as fold change relative to the 6-hour sham groups. Values represent the group mean ± SEM (n = 5-8).